

# Green Chemistry

Cutting-edge research for a greener sustainable future

[www.rsc.org/greenchem](http://www.rsc.org/greenchem)

Volume 9 | Number 1 | January 2007 | Pages 1–100



Downloaded on 11 November 2014  
Published on 01 January 2007. <http://pubs.rsc.org> | doi:10.1039/B610051H

ISSN 1463-9262

RSC Publishing

Harmer *et al.*  
Synthesis and applications of  
superacids

Hempel  
The DBU: promoting sustainable  
chemistry

Venkataramanan *et al.*  
Green synthesis of titania nanowire  
composites

He *et al.*  
Electrosynthesis of  
phenyl-2-propanone derivatives



1463-9262(2007)9:1;1-B



# Journal of Environmental Monitoring

Comprehensive, high quality coverage of multidisciplinary, international research relating to the measurement, pathways, impact and management of contaminants in all environments.

- Dedicated to the analytical measurement of environmental pollution
- Assessing exposure and associated health risks
- Fast times to publication
- Impact factor: 1.578
- High visibility - cited in MEDLINE



# Green Chemistry

Cutting-edge research for a greener sustainable future

[www.rsc.org/greenchem](http://www.rsc.org/greenchem)

RSC Publishing is a not-for-profit publisher and a division of the Royal Society of Chemistry. Any surplus made is used to support charitable activities aimed at advancing the chemical sciences. Full details are available from [www.rsc.org](http://www.rsc.org)

## IN THIS ISSUE

ISSN 1463-9262 CODEN GRCHFJ 9(1) 1-100 (2007)



### Cover

A superacid, TFESA, and a supported version, have been developed with all the benefits of traditional superacids but much easier to handle, a wider processing window and simple to follow using  $^1\text{H}$  NMR. These strong acid catalysts can enhance and make many chemical processes more efficient. Image reproduced by permission of Mark Harmer, from *Green Chem.*, 2007, 9(1), 30.

## CHEMICAL TECHNOLOGY

T1

Chemical Technology highlights the latest applications and technological aspects of research across the chemical sciences.

## Chemical Technology

January 2007/Volume 4/Issue 1

[www.rsc.org/chemicaltechnology](http://www.rsc.org/chemicaltechnology)

## EDITORIAL

13

### Happy New Year from Green Chemistry

Reflecting on last year and looking ahead to the developments for *Green Chemistry*.



## EDITORIAL STAFF

**Editor**

Sarah Ruthven

**Publishing assistant**

Emma Hacking

**Team leader, serials production**

Stephen Wilkes

**Technical editor**

Edward Morgan

**Administration coordinator**

Sonya Spring

**Editorial secretaries**

Donna Fordham, Jill Segev, Julie Thompson

**Publisher**

Emma Wilson

Green Chemistry (print: ISSN 1463-9262; electronic: ISSN 1463-9270) is published 12 times a year by the Royal Society of Chemistry, Thomas Graham House, Science Park, Milton Road, Cambridge, UK CB4 0WF.

All orders, with cheques made payable to the Royal Society of Chemistry, should be sent to RSC Distribution Services, c/o Portland Customer Services, Commerce Way, Colchester, Essex, UK CO2 8HP. Tel +44 (0) 1206 226050; E-mail sales@rscdistribution.org

2007 Annual (print + electronic) subscription price: £902; US\$1705. 2007 Annual (electronic) subscription price: £812; US\$1534. Customers in Canada will be subject to a surcharge to cover GST. Customers in the EU subscribing to the electronic version only will be charged VAT.

If you take an institutional subscription to any RSC journal you are entitled to free, site-wide web access to that journal. You can arrange access via Internet Protocol (IP) address at [www.rsc.org/ip](http://www.rsc.org/ip). Customers should make payments by cheque in sterling payable on a UK clearing bank or in US dollars payable on a US clearing bank. Periodicals postage paid at Rahway, NJ, USA and at additional mailing offices. Airfreight and mailing in the USA by Mercury Airfreight International Ltd., 365 Blair Road, Avenel, NJ 07001, USA.

US Postmaster: send address changes to Green Chemistry, c/o Mercury Airfreight International Ltd., 365 Blair Road, Avenel, NJ 07001. All despatches outside the UK by Consolidated Airfreight.

PRINTED IN THE UK

**Advertisement sales:** Tel +44 (0) 1223 432246; Fax +44 (0) 1223 426017; E-mail [advertising@rsc.org](mailto:advertising@rsc.org)

# Green Chemistry

Cutting-edge research for a greener sustainable future

[www.rsc.org/greenchem](http://www.rsc.org/greenchem)

Green Chemistry focuses on cutting-edge research that attempts to reduce the environmental impact of the chemical enterprise by developing a technology base that is inherently non-toxic to living things and the environment.

## EDITORIAL BOARD

**Chair**

Professor Martyn Poliakoff  
Nottingham, UK

**Scientific Editor**

Professor Walter Leitner  
RWTH-Aachen, Germany

**Associate Editors**

Professor C. J. Li  
McGill University, Canada  
Professor Kyoko Nozaki  
Kyoto University, Japan

**Members**

Professor Paul Anastas  
Yale University, USA  
Professor Joan Brennecke  
University of Notre Dame, USA  
Professor Mike Green  
Sasol, South Africa  
Professor Buxing Han  
Chinese Academy of Sciences,  
China  
Professor Roshan Jachuck  
Clarkson University, USA

Dr Alexei Lapkin  
Bath University, UK  
Dr Janet Scott  
Unilever, UK  
Professor Tom Welton  
Imperial College, UK

## INTERNATIONAL ADVISORY EDITORIAL BOARD

James Clark, York, UK  
Avelino Corma, Universidad  
Politécnica de Valencia, Spain  
Mark Harmer, DuPont Central  
R&D, USA  
Herbert Hugl, Lanxess Fine  
Chemicals, Germany  
Makato Misono, Kogakuin  
University, Japan  
Colin Raston,  
University of Western Australia,  
Australia

Robin D. Rogers, Centre for Green  
Manufacturing, USA  
Kenneth Seddon, Queen's  
University, Belfast, UK  
Roger Sheldon, Delft University of  
Technology, The Netherlands  
Gary Sheldrake, Queen's  
University, Belfast, UK  
Pietro Tundo, Università ca  
Foscari di Venezia, Italy

## INFORMATION FOR AUTHORS

Full details of how to submit material for publication in Green Chemistry are given in the Instructions for Authors (available from <http://www.rsc.org/authors>). Submissions should be sent via ReSource: <http://www.rsc.org/resource>.

Authors may reproduce/republish portions of their published contribution without seeking permission from the RSC, provided that any such republication is accompanied by an acknowledgement in the form: (Original citation) – Reproduced by permission of the Royal Society of Chemistry.

© The Royal Society of Chemistry 2007. Apart from fair dealing for the purposes of research or private study for non-commercial purposes, or criticism or review, as permitted under the Copyright, Designs and Patents Act 1988 and the Copyright and Related Rights Regulations 2003, this publication may only be reproduced, stored or transmitted, in any form or by any means, with the prior permission in writing of the Publishers or in the case of reprographic reproduction in accordance with the terms of licences issued by the Copyright Licensing Agency in the UK. US copyright law is applicable to users in the USA.

The Royal Society of Chemistry takes reasonable care in the preparation of this publication but does not accept liability for the consequences of any errors or omissions.

Ⓢ The paper used in this publication meets the requirements of ANSI/NISO Z39.48-1992 (Permanence of Paper).

Royal Society of Chemistry: Registered Charity No. 207890

## PERSPECTIVE

15

**The DBU: promoting sustainable chemistry**

Maximilian Hempel

The Deutsche Bundesstiftung Umwelt (DBU) is among the world's largest environmental foundations. Actual fields of promotion and some results of successfully completed projects are summarized.



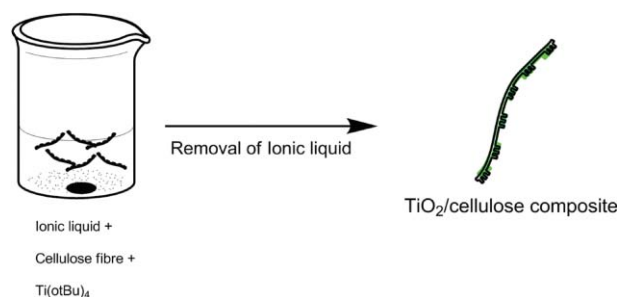
## COMMUNICATIONS

18

**Green synthesis of titania nanowire composites on natural cellulose fibers**

Natarajan Sathiyamoorthy Venkataramanan, Keitaro Matsui, Hajime Kawanami and Yutaka Ikushima\*

A simple, efficient and environmentally benign approach for the synthesis of titania nanowire is achieved by using natural fibres as templates and ionic liquids as solvent.

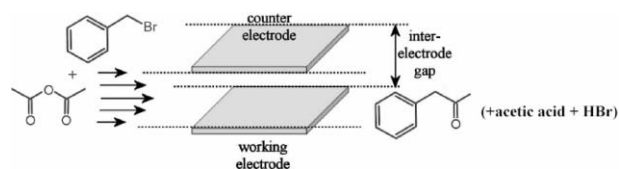


20

**Electrosynthesis of phenyl-2-propanone derivatives from benzyl bromides and acetic anhydride in an unsupported micro-flow cell electrolysis process**

Ping He, Paul Watts, Frank Marken and Stephen J. Haswell\*

The synthesis of P2P performed by direct electroreductive coupling of benzyl bromides and acetic anhydride in a micro-flow electrolysis cell equipped with micro-gap Pt electrodes.

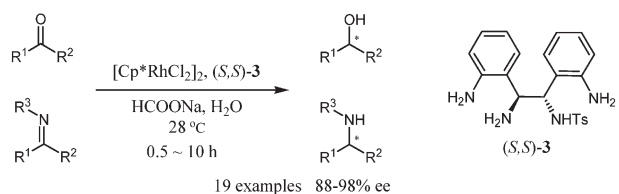


23

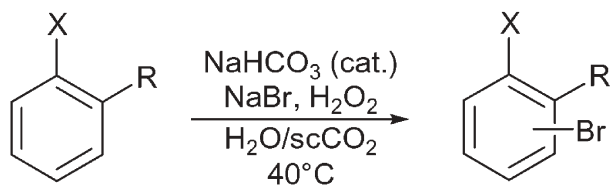
**Asymmetric transfer hydrogenation of ketones and imines with novel water-soluble chiral diamine as ligand in neat water**

Li Li, Jiashou Wu, Fei Wang, Jian Liao, Hua Zhang, Chunxia Lian, Jin Zhu\* and Jingen Deng\*

A novel water-soluble rhodium(III) catalyst was efficient for the asymmetric transfer hydrogenation of ketones and imines in neat water with high reactivity and excellent enantioselectivity.



26

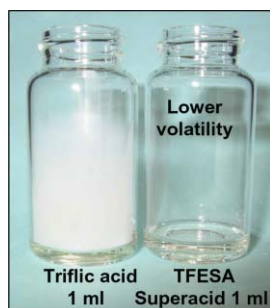
X=OH, NH<sub>2</sub> or NHMeR=H, Me, *i*Bu...

### Oxybromination of phenol and aniline derivatives in H<sub>2</sub>O/scCO<sub>2</sub> biphasic media

Benjamin Ganchegui and Walter Leitner\*

The oxybromination of aniline and phenol derivatives is performed, with high conversions and selectivities, in H<sub>2</sub>O/scCO<sub>2</sub> exploiting the intrinsic reactivity of the biphasic system.

30



### Synthesis and applications of superacids. 1,1,2,2-Tetrafluoroethanesulfonic acid, supported on silica

Mark A. Harmer,\* Christopher Junk, Vsevolod Rostovtsev, Liane G. Carcani, Jemma Vickery and Zoe Schnepf

The improved synthesis and catalytic use of a number of low volatility superacids is highlighted (compared to triflic acid). These materials have been optimized for reactions of key industrial importance.

38

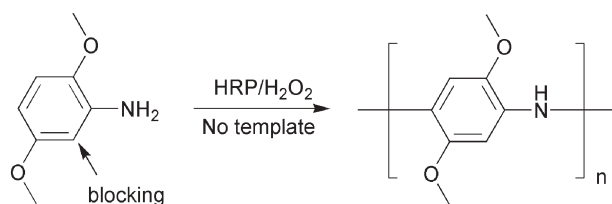


### Novel chemical recycling of polycarbonate (PC) waste into bis-hydroxyalkyl ethers of bisphenol A for use as PU raw materials

Chao-Hsing Lin, Hsing-Yo Lin, Wei-Zhi Liao and Shenghong A. Dai\*

From waste PC to new PU.

44



### Synthesis of polyaniline derivatives via biocatalysis

Seong-Cheol Kim, Pilho Huh, Jayant Kumar,\* Bongsoo Kim, Jang-Oo Lee, Ferdinando F. Bruno and Lynne A. Samuelson\*

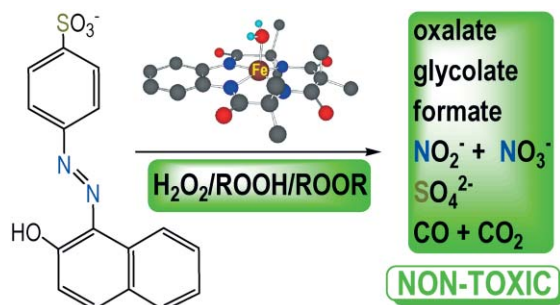
Three structurally different aniline monomers have been polymerized with horseradish peroxidase without the use of templates.

49

### Fe<sup>III</sup>-TAML-catalyzed green oxidative degradation of the azo dye Orange II by H<sub>2</sub>O<sub>2</sub> and organic peroxides: products, toxicity, kinetics, and mechanisms

Naima Chahbane, Delia-Laura Popescu, Douglas A. Mitchell, Arani Chanda, Dieter Lenoir,\* Alexander D. Ryabov,\* Karl-Werner Schramm and Terrence J. Collins\*

Orange II oxidation by peroxides catalyzed by Fe<sup>III</sup>-TAMLs at pH 9–11 leads to CO<sub>2</sub>, CO, phthalic and smaller aliphatic acids as non-toxic major mineralization products.

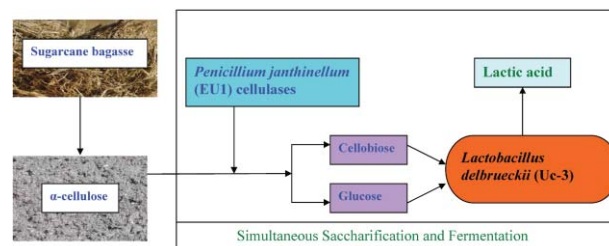


58

### Lactic acid production from waste sugarcane bagasse derived cellulose

Mukund G. Adsul, Anjani J. Varma and Digambar V. Gokhale\*

This study deals with the simultaneous saccharification and fermentation (SSF) of sugarcane bagasse cellulose to lactic acid using cellulase preparations of *Penicillium janthinellum* mutant EU1 and cellobiose utilizing *Lactobacillus delbrueckii* mutant Uc3 isolated in our laboratory.

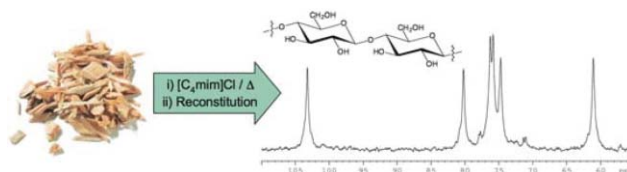


63

### Can ionic liquids dissolve wood? Processing and analysis of lignocellulosic materials with 1-*n*-butyl-3-methylimidazolium chloride

Diego A. Fort, Richard C. Remsing, Richard P. Swatloski, Patrick Moyna,\* Guillermo Moyna\* and Robin D. Rogers\*

We show that solvents based on the ionic liquid 1-*n*-butyl-3-methylimidazolium chloride can partially dissolve wood, and demonstrate that celluloses virtually free of lignin and hemicellulose can be recovered from the resulting wood extracts.

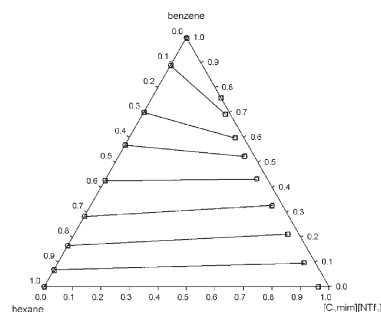


70

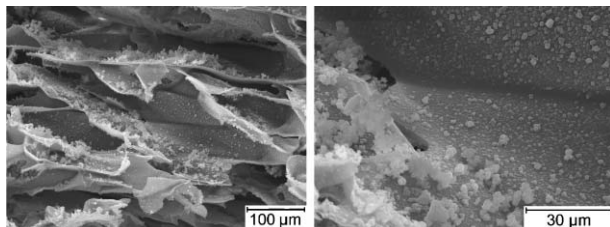
### Separation of aromatic hydrocarbons from alkanes using the ionic liquid 1-ethyl-3-methylimidazolium bis{(trifluoromethyl) sulfonyl}amide

Alberto Arce, Martyn J. Earle,\* Héctor Rodríguez and Kenneth R. Seddon

The ionic liquid 1-ethyl-3-methylimidazolium bis{(trifluoromethyl) sulfonyl}amide can selectively remove benzene from its mixtures with hexane: it may be suitable as an alternative solvent in liquid extraction processes.



75

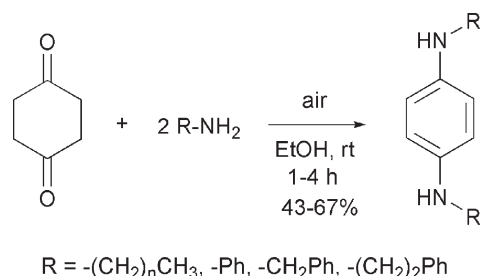


### Green synthesis of a temperature sensitive hydrogel

Márcio Temtem, Teresa Casimiro, João F. Mano\* and Ana Aguiar-Ricardo\*

A thermoresponsive hydrogel, poly(*N*-isopropylacrylamide), PNIPAAm, with possible applications in drug delivery, tissue engineering and as smart membranes with tuned permeability, was synthesised in supercritical carbon dioxide. A strategy of solvent-free impregnation/coating of polymeric surfaces with PNIPAAm is also suggested.

80

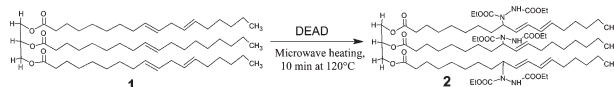


### One-step synthesis of *N,N'*-dialkyl-*p*-phenylenediamines

Luke T. Higham, Katsuya Konno, Janet L. Scott, Christopher R. Strauss\* and Tatsuaki Yamaguchi

Condensation of 1,4-cyclohexanedione with primary alkylamines occurred at room temperature in air and were complete within a few hours, with high atom economy and with water as the major by-product.

85

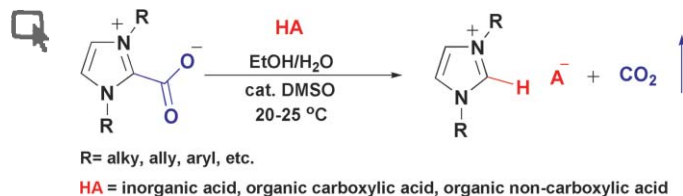


### Novel modified soybean oil containing hydrazino-ester: synthesis and characterization

Atanu Biswas,\* Brajendra K. Sharma, J. L. Willet, K. Vermillion, Sevim Z. Erhan and H. N. Cheng\*

A novel synthetic approach for chemical modification of vegetable oils is presented. The structural modification is carried out using diethyl azodicarboxylate (DEAD) in the absence of catalyst and solvent.

90



### Ionic liquids *via* reaction of the zwitterionic 1,3-dimethylimidazolium-2-carboxylate with protic acids. Overcoming synthetic limitations and establishing new halide free protocols for the formation of ILs

Marcin Smiglak, John D. Holbrey, Scott T. Griffin, W. Matthew Reichert, Richard P. Swatloski, Alan R. Katritzky,\* Hongfang Yang, Dazhi Zhang, Kostyantyn Kirichenko and Robin D. Rogers\*

An improved protocol for the synthesis of ILs *via* a one-pot, halide-free, process is discussed.



## AUTHOR INDEX

- Adsul, Mukund G., 58  
 Aguiar-Ricardo, Ana, 75  
 Arce, Alberto, 70  
 Biswas, Atanu, 85  
 Bruno, Ferdinando F., 44  
 Carcani, Liane G., 30  
 Casimiro, Teresa, 75  
 Chahbane, Naima, 49  
 Chanda, Arani, 49  
 Cheng, H. N., 85  
 Collins, Terrence J., 49  
 Dai, Shenghong A., 38  
 Deng, Jingen, 23  
 Earle, Martyn J., 70  
 Erhan, Sevim Z., 85  
 Fort, Diego A., 63  
 Ganchequi, Benjamin, 26  
 Gokhale, Digambar V., 58  
 Griffin, Scott T., 90  
 Harmer, Mark A., 30  
 Haswell, Stephen J., 20
- He, Ping, 20  
 Hempel, Maximilian, 15  
 Higham, Luke T., 80  
 Holbrey, John D., 90  
 Huh, Pilho, 44  
 Ikushima, Yutaka, 18  
 Junk, Christopher, 30  
 Katritzky, Alan R., 90  
 Kawanami, Hajime, 18  
 Kim, Bongsoo, 44  
 Kim, Seong-Cheol, 44  
 Kirichenko, Kostyantyn, 90  
 Konno, Katsuya, 80  
 Kumar, Jayant, 44  
 Lee, Jang-Oo, 44  
 Leitner, Walter, 26  
 Lenoir, Dieter, 49  
 Li, Li, 23  
 Lian, Chunxia, 23  
 Liao, Jian, 23  
 Liao, Wei-Zhi, 38
- Lin, Chao-Hsing, 38  
 Lin, Hsing-Yo, 38  
 Mano, João F., 75  
 Marken, Frank, 20  
 Matsui, Keitaro, 18  
 Mitchell, Douglas A., 49  
 Moyna, Guillermo, 63  
 Moyna, Patrick, 63  
 Popescu, Delia-Laura, 49  
 Reichert, W. Matthew, 90  
 Remsing, Richard C., 63  
 Rodríguez, Héctor, 70  
 Rogers, Robin D., 63, 90  
 Rostovtsev, Vsevolod, 30  
 Ryabov, Alexander D., 49  
 Samuelson, Lynne A., 44  
 Schnepp, Zoe, 30  
 Schramm, Karl-Werner, 49  
 Scott, Janet L., 80  
 Seddon, Kenneth R., 70  
 Sharma, Brajendra K., 85
- Smiglak, Marcin, 90  
 Strauss, Christopher R., 80  
 Swatloski, Richard P., 63, 90  
 Temtem, Márcio, 75  
 Varma, Anjani J., 58  
 Venkataramanan, Natarajan Sathiyamoorthy, 18  
 Vermillion, K., 85  
 Vickery, Jemma, 30  
 Wang, Fei, 23  
 Watts, Paul, 20  
 Willet, J. L., 85  
 Wu, Jiashou, 23  
 Yamaguchi, Tatsuaki, 80  
 Yang, Hongfang, 90  
 Zhang, Dazhi, 90  
 Zhang, Hua, 23  
 Zhu, Jin, 23

## FREE E-MAIL ALERTS AND RSS FEEDS


Contents lists in advance of publication are available on the web *via* [www.rsc.org/greenchem](http://www.rsc.org/greenchem) - or take advantage of our free e-mail alerting service ([www.rsc.org/ej\\_alert](http://www.rsc.org/ej_alert)) to receive notification each time a new list becomes available.

**RSS** Try our RSS feeds for up-to-the-minute news of the latest research. By setting up RSS feeds, preferably using feed reader software, you can be alerted to the latest Advance Articles published on the RSC web site. Visit [www.rsc.org/publishing/technology/rss.asp](http://www.rsc.org/publishing/technology/rss.asp) for details.

## ADVANCE ARTICLES AND ELECTRONIC JOURNAL

Free site-wide access to Advance Articles and the electronic form of this journal is provided with a full-rate institutional subscription. See [www.rsc.org/ejs](http://www.rsc.org/ejs) for more information.

\* Indicates the author for correspondence: see article for details.

 Electronic supplementary information (ESI) is available *via* the online article (see <http://www.rsc.org/esi> for general information about ESI).

# Lust and Love

Is it more than chemistry?

By Gabriele and Rolf Froböse

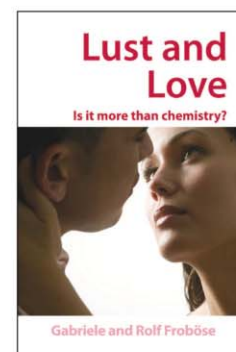
**Why do people fall in love?**

**Why do we find some people attractive?**

**How does our physiology affect the way we feel?**

**Explore the science behind love, sex and passion**

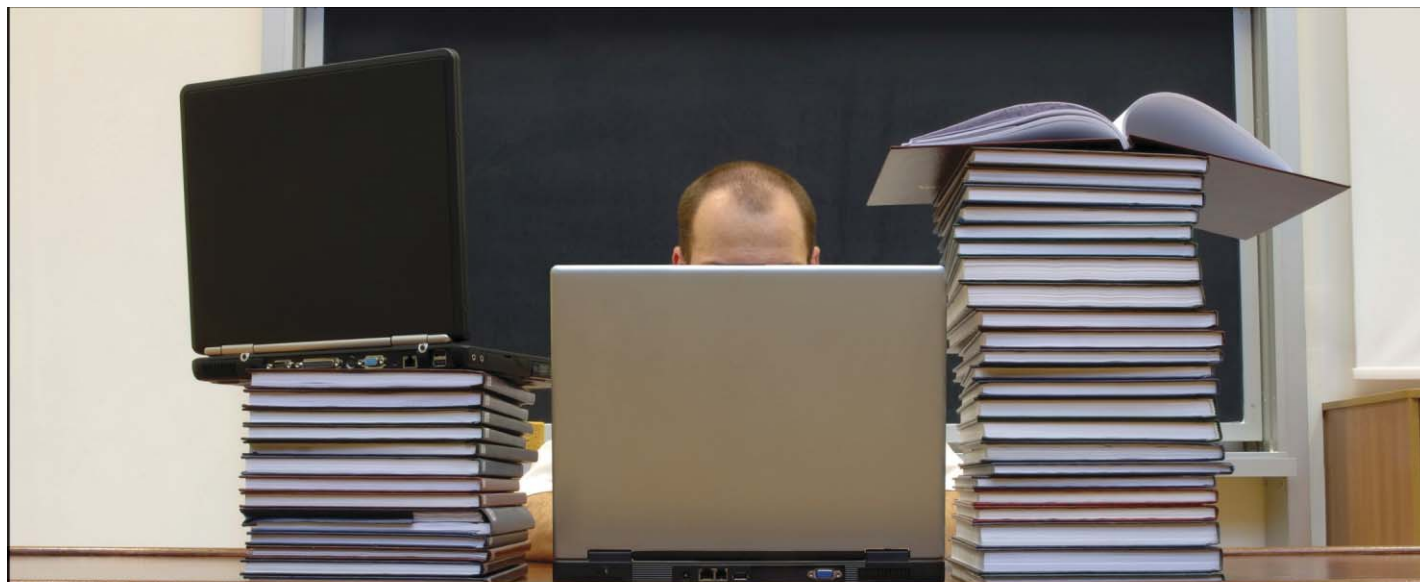
Hardback | 2006 | xii + 170 pages | £24.95 | RSC Member Price £16.50  
 ISBN 10: 0 85404 867 7 | ISBN 13: 978 0 85404 867 0



Registered Charity Number: 207890

RSC Publishing

[www.rsc.org/lustandlove](http://www.rsc.org/lustandlove)



## There is an easier way to keep up with research in your field...

An integral part of managing your career as a scientist is staying on top of the news and developments in your field of research and related areas. A good knowledge of your industry is a key component to your success, but finding the time to keep up with the latest research news can pose the greatest challenge.

**The solution?** By signing up for e-alerts from one of our free news services, you can receive updates about newsworthy and significant research appearing in RSC journals in a quick and easily digestible monthly alert.

**Free access.** From each news item you can link directly to the source research paper, which is completely free to access and download for a limited period.

**New tools to help you.** In addition to research news, our news services also feature

- **Instant insights** – whirlwind tours of exciting research areas you should know about
- **Interviews** – leading scientists share their opinions

**Chemical  
Technology**

[www.rsc.org/chemicaltechnology](http://www.rsc.org/chemicaltechnology)

**Chemical  
Science**

[www.rsc.org/chemicalscience](http://www.rsc.org/chemicalscience)

**Chemical  
Biology**

[www.rsc.org/chembiology](http://www.rsc.org/chembiology)

RSCPublishing

[www.rsc.org/ej\\_alert](http://www.rsc.org/ej_alert)

Registered Charity Number 207890

# Environmental Science Books

## Issues in Environmental Science & Technology

### Series Editors:

*R E Hester and R M Harrison*

Format: **Hardback**

Price: **£45.00**

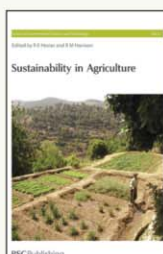
RSC Member Price: **£29.25**

Written by leading experts, this series presents a multidisciplinary approach to pollution and the environment. Focussing on the science and broader issues including economic, legal and political considerations.

### Sustainability in Agriculture Vol. No. 21

Discusses the key factors impacting on global agricultural practices including fair trade, the use of pesticides, GM products and government policy.

2005 | xiv+130 pages | ISBN-10: 0 85404 201 6  
ISBN-13: 978 0 85404 201 2



### Chemicals in the Environment Assessing and Managing Risk Vol. No. 22

Beginning with a review of the current legislation, the book goes on to discuss scientific and technical issues relating to chemicals in the environment and future developments.

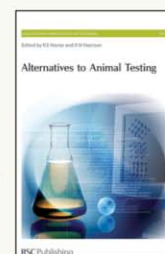
2006 | xvi+158 pages | ISBN-10: 0 85404 206 7  
ISBN-13: 978 0 85404 206 7



### Alternatives to Animal Testing Vol. No. 23

Provides an up-to-date discussion on the development of alternatives to animal testing including; international validation, safety evaluation, alternative tests and the regulatory framework.

2006 | xii+118 pages | ISBN-10: 0 85404 211 3  
ISBN-13: 978 0 85404 211 1



### Practical Environmental Analysis 2nd Edition

By *M Radojevic and V N Bashkin*

A new edition textbook providing an up-to-date guide to practical environmental analysis. Ideal for students and technicians as well as lecturers wishing to teach the subject.

Hardback | 2006 | xxiv+458 pages | £39.95 | RSC member price  
£25.75 | ISBN-10: 0 85404 679 8 | ISBN-13: 978 0 85404 679 9



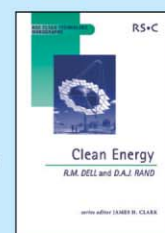
### Clean Energy (RSC Clean Technology Monographs)

By *R M Dell and D A J Rand*

Series Editor *J H Clark*

Covering a broad spectrum of energy problems, this highly accessible book discusses in detail strategies for the world's future energy supply.

Hardback | 2004 | xxxvi+322 pages | £89.95 | RSC Member Price  
£58.25 | ISBN-10: 0 85404 546 5 | ISBN-13: 978 0 85404 546 4



### An Introduction to Pollution Science

By *R M Harrison*

A student textbook looking at pollution and its impact on human health and the environment. Covering a wide range of topics including pollution in the atmosphere, water and soil, and strategies for pollution management.

Hardback | 2006 | ca xii+322 pages | £24.95 | RSC Member Price  
£16.50 | ISBN-10: 0 85404 829 4 | ISBN-13: 978 0 85404 829 8

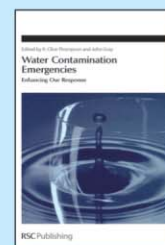


### Water Contamination Emergencies Enhancing Our Response

By *J Gray and K C Thompson*

A look at the impact and response of contaminated water supplies including the threat of chemical, biological, radiological and nuclear (CBRN) events.

Hardback | 2006 | x+372 pages | £99.95 | RSC Member Price  
£64.75 | ISBN-10: 0 85404 658 5 | ISBN-13: 978 0 85404 658 4



# Alternative Fuel Technologies

A series of PCCP special issues guest edited by Joachim Maier (MPI Stuttgart), Dirk Guldi (Universität Erlangen-Nürnberg), and Adriano Zecchina (University of Torino)

Following on from the highly successful nano-themed issues, PCCP presents a series of themed issues on Alternative Fuel Technologies. Published in selected printed issues of PCCP over the coming months and collected online on a dedicated website, these issues feature the very latest research including:

- ▶ fuel cells
- ▶ electrochemical energy conversion
- ▶ supercapacitors and molecular materials
- ▶ hydrogen storage
- ▶ solar energy conversion
- ▶ biohydrogen

Sign up for RSS alerts to have the latest articles delivered directly to your desktop



RSC Publishing

[www.rsc.org/pccp/altfuel](http://www.rsc.org/pccp/altfuel)

Registered Charity Number 207890

# Happy New Year from Green Chemistry

DOI: 10.1039/b617389f

Welcome to the January 2007 issue of *Green Chemistry*, our ninth year of publication, which will see a number of developments for the Journal.

## Editorial board

We welcome two new members onto the board; Mike Green from Sasol in South Africa and Alexei Lapkin from Bath University, whose interests reflect the widening scope of the Journal. Alexei and Mike replace Steve Howdle and Michael Warhurst, who we thank for their input into the Journal during their time on the board.

## Content

As many of you will have already read, the December 2006 Highlights section was the last one to be published. We would like to thank Markus Hölscher, our News Editor, for his regular contribution to the Journal which provided an up-to-date overview of current research.

For peer-reviewed contributions, *Green Chemistry* continues to publish original research papers, communications, perspectives and review articles, and last year the most highly accessed paper was a review of dissolution of cellulose with ionic liquids by Zhu *et al.*, published in the April issue (*Green Chem.*, 2006, **8**, 325–327 (DOI: 10.1039/b601395c)). We have a number of reviews scheduled for 2007 and invite authors to submit their reviews to *Green Chemistry*.

We also have two themed issues planned for this year, the first containing papers from the Green Chemistry for Fuel Synthesis and Processing Symposium at the ACS meeting in San Francisco last September. Another collection of peer-reviewed research papers will be published from the international conference on Green Solvents for Processes held in Friedrichshafen, Germany, from October 8–11 2006.

## Impact factors and immediacy index

The 2005 impact factors, released by ISI<sup>®</sup> in June 2006, showed *Green Chemistry* to remain relatively static at 3.255. Calculated annually, ISI<sup>®</sup> impact factors provide an indication of the quality of a journal—they take into account the number of citations in a given year for all the citeable documents published within a journal in the preceding two years. As well as having a high impact, work published in RSC Journals is also amongst the most topical. The immediacy index measures how topical and urgent papers published in a journal are, by dividing the number of citations in a given year by the number of articles published in the journal that year. The 2005 immediacy index for *Green Chemistry* was 0.631.

The impressive impact factors and immediacy indexes for RSC journals reinforce the RSC's reputation as the home of exciting new research.

## RSC prizes and awards

In 2006 *Green Chemistry* awarded two poster prizes, one at the 1st European Chemistry Congress and the other at the Green Solvents for Processes meeting.

In 2006, RSC Publishing awarded more than 20 prizes and sponsored lectureships to high-profile researchers. The recipients gained financial support to present and discuss their work at events throughout the world, in recognition of their research achievements. More than £15,000 (or \$30,000) was granted to the recipients, in total, to cover travel expenses to sponsored lectureships in countries such as China, Japan, US and UK. In 2007, in addition to the poster prizes, *Green Chemistry* will be sponsoring two lectures, and full details of these events will be confirmed in due course.

## RSC open science

Authors publishing in *Green Chemistry* now have the option of paying a fee in

exchange for making their accepted communication, research paper or review article openly available to all *via* the web, with RSC Open Science. The scheme is only made available to authors once their papers have been accepted for publication, following the normal rigorous peer-review procedures (RSC Open Science operates in parallel with the normal publication route, which remains free to authors). Authors who have published their work in *Green Chemistry* are also able to retrospectively apply for their work to be included in the scheme. Further information can be found at: [www.rsc.org/openscience](http://www.rsc.org/openscience).

## Technological innovation

2006 has seen RSC Publishing invest significantly in technological developments across all of its products. Introduced last year, RSS feeds, or 'really simple syndication', have proved extremely popular with our readers. Subscribers receive alerts as soon as an Advance Article is published in *Green Chemistry*. You can subscribe *via* the *Green Chemistry* homepage.

Subscribers to *Green Chemistry* will now link from the contents lists straight through to the HTML view of selected articles, in just one quick step. Here you can download references to citation managers (such as EndNote, Ref Manager, ProCite and BibTex), sign up for RSS feeds, search for citing articles (otherwise known as 'forward linking'), print the article with just one click and send the article to a friend or colleague.

From 2007, authors publishing in *Green Chemistry* will see their science "come alive" thanks to an exciting new project pioneered by the RSC. Enhanced HTML in RSC articles will allow chemical and biological compounds mentioned in the text to be identified; by clicking on the compound readers will be able to obtain further information about that compound, including a downloadable structure plus a list of relevant subject areas. The RSC is the first publisher to utilise the International Chemical

Identifier (InChI) (a digital equivalent of the IUPAC name for any particular covalent compound where structures are expressed in terms of five layers of information—connectivity, tautomeric, isotopic, stereochemical, and electronic) for a project of this type and scope. The technology will be used to enhance RSS alerts so that future news feeds can include chemical structures and other enhanced information. RSC Publishing intends to evolve this project to match author and reader needs, so tell us what you think: we welcome your feedback on this new functionality and will incorporate your ideas to develop the service further. Find out more at [www.rsc.org/sciencecomealive](http://www.rsc.org/sciencecomealive).

These developments demonstrate the investment in publishing products and services over the past year, and 2007 will see us enhancing our products further.

### What our authors say

We are always happy to receive feedback from authors, especially if it helps us to further improve the publishing experience. Because we believe that RSC Publishing offers the best service of any scientific publisher, we have published a selection of the comments we have

received from authors from around the globe—take a look at [www.rsc.org/authorquotes](http://www.rsc.org/authorquotes).

### Changes and developments to Chemical Science, Chemical Technology and Chemical Biology, and news of Chemistry World

Showcasing hot science from *Green Chemistry* and other RSC Journals in *Chemical Science*, *Chemical Technology* and *Chemical Biology* has proved very popular with readers and authors alike. In fact, the free supplements have become so successful that from January 2007, all issues will be eight pages (in print), contain new article types and come complete with a fresh new look for the front page. Supplementary material will also be available online.

Meanwhile *Chemistry World*, the RSC's award-winning magazine, launched two new web features at the end of 2006. The **Chemistry World Blog** is an interactive forum for news, discussion and opinion, looking at the science hitting the headlines. The **Chemistry World Podcast** interviews high profile scientists about the latest and hottest topics in science, and is free to download at [www.rsc.org/chemistryworld](http://www.rsc.org/chemistryworld).

### Not just journals...

As well as an impressive portfolio of prestigious journals, the RSC has a wide selection of products for anyone with an interest in the chemical sciences. Visit the shop at [www.rsc.org/shop](http://www.rsc.org/shop) to browse over 400 book titles, subscribe to or purchase an individual article from *Green Chemistry* or any other RSC journal, join or renew RSC membership, or register to attend a conference or training event.

In addition, RSC Publishing is pleased to announce the launch of the *RSC eBook Collection*. RSC books are now available online and can be easily downloaded as either chapters or books. The collection is fully searchable and also integrated with RSC Journal content. To search the collection or for further information, visit [www.rsc.org/ebooks](http://www.rsc.org/ebooks).

We would like to thank our readers and authors for their continued support of *Green Chemistry*, and look forward to the year ahead.

Martyn Poliakoff,  
Chair of the Editorial Board  
Walter Leitner, Scientific Editor  
Sarah Ruthven, RSC Editor

# The DBU: promoting sustainable chemistry

Maximilian Hempel

Received 21st August 2006, Accepted 26th September 2006

First published as an Advance Article on the web 26th October 2006

DOI: 10.1039/b612042n

The Deutsche Bundesstiftung Umwelt (DBU) is among the world's largest environmental foundations. Its actual fields of promotion and some of the results of its successfully completed projects are summarized.

## Origin and function

In 1990, the Deutsche Bundesstiftung Umwelt DBU was established by decision of the German Bundestag with the objective of promoting innovative projects in the field of environmental protection. The promotional activities include the fields environmental technology, research and communication. As a non-profit organisation and foundation established according to Civil Law, the DBU's promotional activities are beyond state programmes but can supplement these. The DBU is among the world's largest environmental foundations (Fig. 1); since its establishment nearly 6000 projects have received financial backing totalling approximately €1.1 billion, with particular focus on small and medium-sized enterprises.

The Deutsche Bundesstiftung Umwelt promotes the sustainable model of development. At the United Nations conference in Rio, 179 countries committed themselves to this model by signing an agenda for the 21st century (<http://www.bmu.de/files/pdfs/allgemein/application/pdf/agenda21.pdf>). The concept of 'sustainable development' requires ongoing strategies, e.g. by:

- Minimising consumption rates of transitory resources *via* improvement of efficiency, substitution of transitory resources by renewable ones and by recycling (life cycle assessment).



Fig. 1 Headquarters of the Deutsche Bundesstiftung Umwelt, Osnabrück, Germany.

Deutsche Bundesstiftung Umwelt, An der Bornau 2, 49090, Osnabrück, Germany. E-mail: [m.hempel@dbu.de](mailto:m.hempel@dbu.de); Fax: +49(0)541 9633 193; Tel: +49(0)541 9633 310

- Preventing the consumption rates of renewable materials and energies from exceeding their given rate of reproduction.
- Preventing emissions from exceeding the capacity for regeneration and absorption by environmental media and human beings.

The DBU supports in two ways, by personal subsidy (postgraduate scholarship) and by subsidies for companies and institutes (co-operation projects).

## Postgraduate—Scholarship at German universities

The Deutsche Bundesstiftung Umwelt has established a German scholarship programme to promote promising young scientists in the field of environmental protection. Per annum about 60 scholarships for postgraduates from different disciplines—mostly in chemistry, biology and engineering—are provided.

Scholarship applications can be submitted twice a year, on the 15th February and the 15th August. Besides a brief and a detailed outline of the research project further documents such as recommendation letters are required. Corresponding forms are obtainable from the DBU office or <http://www.dbu.de/stipendien/download.php> (German version).

The application will be assessed by external experts. Afterwards the most promising candidates are invited to present their project in a selection procedure which is held in the DBU office twice a year. The committee consists of about 20 independent external and DBU scientists. Grants are approved shortly after the interviews.

With the Baltic states, the region of Kaliningrad, Poland, the Czech Republic, Hungary, Romania and Bulgaria, the DBU initiated an international scholarship programme, offering an additional qualification for young scientists from those countries through a research stay in Germany.

The partner organisations co-ordinate the application procedure in the respective countries. After the programme has been announced at the foreign universities, a selection of the best candidates for a 6–12 month research stay in Germany takes place once in a year (<http://www.dbu.de/english/international.php>).

## Cooperation projects between institutions and small and medium enterprises (SME)

The DBU particularly encourages co-operation projects between small and medium-sized enterprises and research

institutions. The three main criteria for obtaining a subsidy are:

- Innovation: the project has to promise an advance compared to the state-of-the-art of current research and technology.
- Exemplary and model character: the innovation should be of interest to a broad segment of the actors (*e.g.* a complete industrial sector). It should also be possible to implement the innovation under commercial conditions within a brief time-scale.
- Environmental benefit: the innovation should lead to new, supplementary measures for the protection of the environment.

The actual fields of promotions are laid down in the guidelines with nine special topics. One field of support is Sustainable Chemistry—procedures and products, aiming to promote projects within the following objectives:

- Development of chemical techniques to convert renewable and waste materials to new products and materials.
- Development of new applications of micro- and nano-techniques (*e.g.* micro-reaction for synthesis).
- Development of optimized chemical processes, *e.g.* with new catalysts or separation techniques.

Projects in this field usually include a life cycle assessment or eco-efficiency analysis. The decision to fund largely depends on the concrete contribution of the project towards environmental benefit. Within those projects, the Deutsche Bundesstiftung Umwelt supports additional measures for dissemination and consolidation project results.

### Results of successfully completed projects

The following brief reviews of three successfully completed projects should give an impression of the variety of supported projects within the last three years in the field of sustainable chemistry.

#### Deep desulfurisation of diesel by extraction with ionic liquids

The company Solvent Innovation GmbH in Cologne, the Chair for Chemical Engineering of the Bayreuth University and the Chair for Chemical Reaction Technology of the Erlangen-Nuremberg University jointly developed a new extraction procedure for the desulfurisation of diesel on the basis of ionic liquids.

S compounds in fuels lead to SOX emissions, causing air pollution and acid rain. Thus, great effort is needed to reduce the S content in transportation fuels to 10 ppm and below. Halogen-free ionic liquids like 1-*n*-butyl-3-methylimidazolium octylsulfate ([BMIM][O<sub>8</sub>SO<sub>4</sub>]) are suitable to extract oil refinery streams by liquid-liquid extraction. This concept provides an interesting (supplemental) alternative for deep desulfurisation. The process enables a desulfurisation under moderate conditions—ambient temperature and pressure—without use of additional hydrogen. It can be considered, that especially those sulfur compounds, which are difficult to reduce by conventional hydrodesulfuration (HDS), *e.g.* dibenzothiophene derivatives, are selectively extractable.

The project shows, that ionic solvents are capable to replace the conventional technologies for the desulfurisation of diesel. Compared with usual solvents, ionic liquids exhibit various ecological benefits, *e.g.* they do not evaporate, they are neither combustible nor do they contaminate the atmosphere.<sup>1,2</sup>

#### Micro-reaction technology in the chemical industry and its ecological potential

The characteristic feature of microreactors is their significantly higher specific surface as compared to conventional reactors. Thus, heat transfer coefficients are very high and allow an extremely efficient heat exchange. Microstructured reactors are therefore especially suited for highly exothermic reactions which can be conducted in a practically isothermic manner. High surface-to-volume ratios lead also to higher yields and improved selectivities during the formulation of chemical compounds. In co-operation with the Bayer AG the company CPC Cellular Process Chemistry Systems GmbH, Mainz developed a microreaction system for very exothermic lithium-organic reactions—the two-step synthesis of *m*-anisaldehyde from *m*-bromanisole. Due to the exothermic behavior of this reaction, the production of *m*-anisaldehyde requires significant safety measures.

The Institute for Technical Chemistry and Environmental Chemistry of the Friedrich-Schiller-University Jena performed a life-cycle assessment (LCA) comparing the conventional discontinuous batch process with the newly developed continuous micro-scale set-up.

The life-cycle assessment clearly indicates positive environmental impact for the micro-reaction technology: the lower solvent demand, the reduced number of rinsing and cleaning steps, the drastically decreased amount of waste and energy consumption. Compared to these ecological benefits, the fabrication of the microreactors, thermostats, distillation units *etc.* only plays a minor role. The advantages include also safety features (Fig. 2): microreaction technology reduces the risk of storing and handling dangerous chemicals. The amount of reactants used is much smaller than that in conventional reactors.<sup>3–5</sup>



Fig. 2 One objective of sustainable chemistry is to prevent emissions.



## Sustainability in the organic chemistry lab course (Nachhaltigkeit im organisch-chemischen Praktikum)

This project aims to implement sustainability into the education of chemists. For a long time the most important goal of a chemist was to create a compound in suitable amounts and high purity from available starting materials. The traditional education in chemistry had a strong focus on practical lab techniques and methods for compound purification. In the past, ecological aspects, *e.g.* energy consumption or amount of waste and by-products, were only attached to industrial processes, not to education and laboratory experiments. Although the goal for a chemist, working in organic synthesis, is still the same: synthesizing a compound in good yield and high purity, additional skills must be acquired. In the last 20 years much more attention has been attributed to undesired effects of chemical compounds on the environment. Thus, we have learned one clear lesson: it is much better, less difficult and less expensive to develop processes and compounds which are sustainable from the beginning than to remove dangerous chemicals from the environment by end-of-pipe-techniques. To allow a better coverage of all the issues of sustainability in chemical education a team of seven German universities developed a database, which contains approx. 100 laboratory experiments. Besides a detailed experimental protocol, safety guidelines and analytical data, a variety of additional material is provided concerning the different fields of sustainability. The material can be individually

adapted to any type of organic chemistry teaching lab course or used for projects in and outside the classroom. All materials are available free of charge at the following website: <http://www.oc-praktikum.de/>.<sup>6</sup>

## Acknowledgements

The author would like to thank Dr C. Schneider, Olympus Ireland, for humorous orthographical support.

## References

- 1 J. Eßer, P. Wasserscheid and A. Jess, *Green Chem.*, 2004, **6**, 316–322.
- 2 M. Uerdingen, P. Wasserscheid and A. Jess, *Tiefenschwefelung von Diesöl durch Flüssig-Flüssig-Extraktion mit ionischen Flüssigkeiten—Final Report of the DBU-funded Project AZ 21490*, Solvent Innovation GmbH, Köln, 2006, 79 pp.
- 3 T. Schwalbe, A. Kursawe and J. Sommer, Application Report on Operating Cellular Process Chemistry Plants in Fine Chemical and Contract Manufacturing Industries, *Chem.-Ing.-Tech.*, 2005, **28**, 408–419.
- 4 D. Kralisch and G. Kreisel, *Bewertung der ökologischen Potenziale der Mikroverfahrenstechnik, CIT*, 2005, **77**, 6, 2005, 784–791.
- 5 V. Autze and D. Kralisch, *Mikroreaktionstechnik für umweltgerechtere Produktion in der chemischen Industrie—Final Report of the DBU-funded Project AZ 19348*, Institut für Technische Chemie und Umweltchemie Friedrich-Schiller-Universität Jena, Jena, 2006, 40 pp.
- 6 M. Bahadir, H. Hopf, A. Nijakowski, R. Vogt, B. Jastorff, R. Störmann, J. Ranke, B. Ondruschka, G. Kreisel, M. Nüchter, A. Diehlmann, D. Lenoir, H. Parlar, C. Wattenbach, J. Metzger, U. Biermann, B. König, Ch. Braig and B. Krelle, *Neues und nachhaltigeres organisch-chemisches Praktikum*, Verlag Harri Deutsch, Darmstadt, 2005, 150 pp.

# Green synthesis of titania nanowire composites on natural cellulose fibers†

Natarajan Sathiyamoorthy Venkataramanan, Keitaro Matsui, Hajime Kawanami and Yutaka Ikushima\*

Received 11th July 2006, Accepted 4th October 2006

First published as an Advance Article on the web 13th October 2006

DOI: 10.1039/b609887h

A simple, efficient and environmentally benign approach for the synthesis of titania nanowire is achieved by using natural fibres as templates and ionic liquids as solvent.

Since the discovery of carbon nanotubes, nanotubular materials have received great attention, both on their fundamental and industrial aspects, due to their superior properties and applications.<sup>1</sup> Unfortunately, reports on their synthesis, especially of metal oxides, by environmentally benign approaches are scarce,<sup>2,3</sup> as they are extremely unstable and need organic supports. Among the various metal oxides, titania has attracted much attention, owing to its utility in the photochemical splitting of water,<sup>3</sup> as an electrode material in dye-sensitized solar cells,<sup>4</sup> as a photocatalyst for removal of harmful organic compounds,<sup>5</sup> in UV-protective and self-cleaning coatings<sup>6</sup> and as a catalyst support.<sup>7</sup> Recently, much interest has been paid to the shape-controlled synthesis of anisotropic titania nanorods or nanowires.<sup>8</sup> These nanowires are found to play an important role as both interconnections and active components in fabricating nanoscale electronic, photonic devices and as sensors.<sup>9</sup>

Templating is commonly employed for the controlled production of materials with an ordered structure and with desired properties. In the past, a variety of templates, including aluminium oxide,<sup>10</sup> carbon nanotubes,<sup>11</sup> surfactants,<sup>12</sup> polymer fibers,<sup>13</sup> supramolecular compounds<sup>14</sup> and egg shell membranes<sup>15</sup>, has been widely used. Recently, Kunitake *et al.* have used natural cellulosic substances as templates for the synthesis of titania nanotubes with varying outer diameter, as a replica of the initial cellulose fibers, by a repeated filtration–deposition cycle using a nanocoating technique.<sup>16</sup>

Synthesis of nanomaterials in solvents has the advantage of uniform coating of the materials on the surface of the template. In this context ionic liquids (ILs) are considered to be a green solvent for the synthesis of organic substances. Only in recent years, due to the environmental knowledge, has attention been focused on the synthesis of nanomaterials by the use of ionic liquids as solvents.<sup>17</sup> Hollow TiO<sub>2</sub> microspheres have been prepared in hydrophobic ionic liquids, and it was reported that the size was influenced by the counter ion, the rate of stirring and the reaction temperature.<sup>18</sup> Rogers *et al.* have shown that ILs can be used as non-derivatizing solvents for cellulose, and regeneration of the cellulose fibers can

be achieved by the addition of water or ethanol solution without a change in its morphology.<sup>19</sup> It is important to note that natural cellulose fibers possess surface hydroxyl groups, and can be a suitable binder for immobilization and stabilization of metal oxide nanoparticles.<sup>20</sup> In continuation of the environmentally benign methods for the synthesis of nanoparticles,<sup>3</sup> herein we report a green and simple method for the synthesis of TiO<sub>2</sub> nanowires on cellulose fibre by taking advantage of the dissolution of cellulose in an ionic liquid, and thereby obtaining a uniform TiO<sub>2</sub> layer over cellulose.

The TiO<sub>2</sub>/cellulose composite wires were prepared by the addition of Ti(OBu)<sub>4</sub> (0.5 mg) over a period of 30 min to a dissolved lint free cellulose sheet (0.5 mg) (Adventec, Japan) in 5 ml of 1-butyl-3-methylimidazolium chloride ([C<sub>4</sub>mim]Cl). To this stirred solution, 20 ml of ethanol was added, and centrifuged to remove the IL and the unreacted metal alkoxide. Complete removal of IL was done by washing the TiO<sub>2</sub> composite for several times. Finally, the material was dried in flowing air at ambient temperature.

The field emission scanning electron microscopy (FESEM)† image in Fig. 1(a) shows a network of TiO<sub>2</sub> layered fibers with the morphology of the cellulose template and their replica. Fig. 1(b) shows the individual TiO<sub>2</sub>/cellulose composite nanowires,

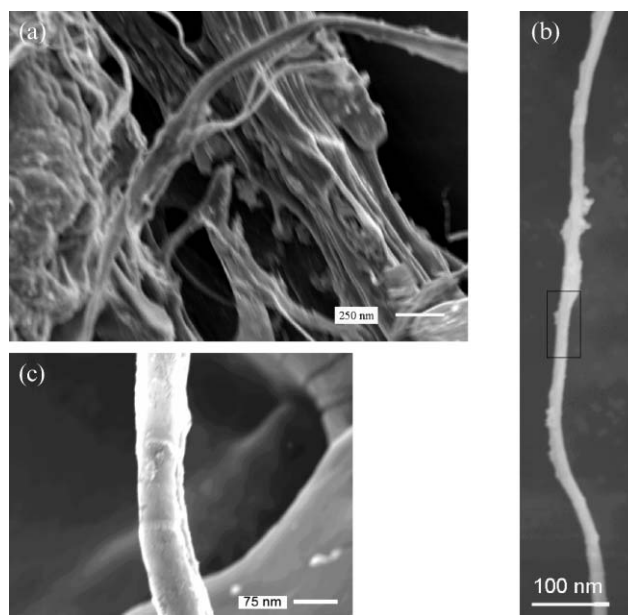


**Fig. 1** FESEM image of TiO<sub>2</sub>/cellulose composite wire. (a) Titania replicas of cellulose, (b) individual nanowires separated from the assembly, (c) FESEM image of the boxed area in (b).

Research Center for Compact Chemical Process, National Institute of Advanced Industrial Science and Technology (AIST), 4-2-1, Nigatake, Miyagino-ku, Sendai, 983-8551, Japan. E-mail: y-ikushima@aist.go.jp; Fax: +81-22-232-7002; Tel: +81-22-237-521

† Electronic supplementary information (ESI) available: A detailed experimental procedure, reflectance spectra, XRD and EDX spectra. See DOI: 10.1039/b609887h

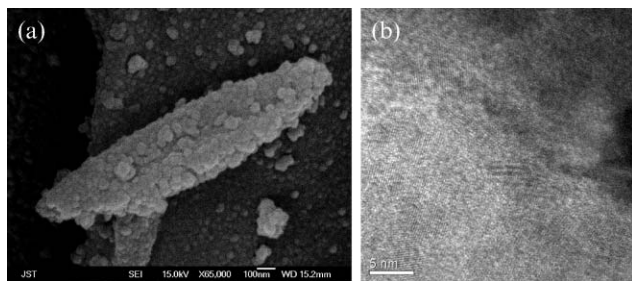


**Fig. 2** (a) FESEM image of the calcined TiO<sub>2</sub>/cellulose composite, (b) HRTEM image of calcined TiO<sub>2</sub> nanowires constituting networks of the cellulose template.

separated from the assembly, which is 100–500 nm in length. It is important to note that the cellulose sheet used in the present study is composed of long uniform cellulose fibers in a network morphology, and the regenerated cellulose fibers will have a uniformity from the interior to the exterior surface.<sup>21</sup> Fig. 1(c) shows the uniform TiO<sub>2</sub> layer, with wall thickness of 30–100 nm. However these nanowires were found to be fragile. The thickness of the TiO<sub>2</sub> layer can be controlled by changing the concentration of the Ti(*t*OBu)<sub>4</sub>.

As expected, the energy dispersive X-ray (EDX)<sup>‡</sup> analysis of TiO<sub>2</sub>/cellulose composite shows that the composition present is C, O and Ti. The X-ray diffraction analysis<sup>‡</sup> of TiO<sub>2</sub>/cellulose composite showed no peaks, indicating that the composite is amorphous. On the other hand, calcined TiO<sub>2</sub> (500 °C, 2 h) displayed crystalline reflection peaks that are characteristic to the anatase TiO<sub>2</sub>.

Fig. 2(a) shows the FESEM image of the calcined nanowires, retaining the morphology of the cellulose sheet, but with a porous crystalline formation due to the higher temperature of calcination. A typical HRTEM<sup>‡</sup> image of the titania nanowires obtained from the calcined TiO<sub>2</sub>/cellulose composite at 500 °C for 2 hours is shown in Fig. 2(b). The image revealed the presence of many crystallites showing clear anatase lattice fringes. The nanotubes consist of anatase nanocrystals, which was further confirmed from the XRD pattern.

The specific surface area was measured by physisorption of nitrogen according to Brunauer–Emmett–Teller (BET), and for the nanotubes obtained after calcination was found to be 14.65 m<sup>2</sup> g<sup>-1</sup>, higher than observed by Su *et al.* for anatase nanoparticles calcined at 700 °C.<sup>22</sup> Reflectance UV–Vis spectroscopic data of the calcined TiO<sub>2</sub> wire shows an absorption edge of 360 nm that corresponds to a size of 3.0 nm for the anatase nanoparticles, which was in agreement with the previous reports.<sup>23</sup>

In conclusion, we demonstrate herein an efficient and green chemical pathway to TiO<sub>2</sub>/cellulose nanowire composites and titania nanotubes by the surface sol-gel process, using an IL as a green solvent medium and cellulosic substances as templates. This method is advantageous as it gives a uniform surface of TiO<sub>2</sub> around the template and the IL can be reused. This approach

may provide a pathway to synthesis of hybrid metal–titania nanotubes and metal nanowires, which is under investigation.

## Notes and references

<sup>‡</sup> FESEM images were recorded on a JEOL JSM-6330FS Fluorescent Emission Scanning Electron Microscope, along with energy dispersion X-ray (EDX) analysis. X-Ray powder diffraction (XRD) patterns were recorded on a Japan Rigaku D/max-c rotation anode X-ray diffractometer, using CuK $\alpha$  radiation ( $l \approx 1.54178 \text{ \AA}$ ), with a scanning rate of  $2^\circ \text{ s}^{-1}$ . HRTEM images were recorded on a Hitachi H-800 TEM at an operating voltage of 200 kV.

- (a) M. Law, J. Goldberger and P. Yang, *Annu. Rev. Mater. Res.*, 2004, **34**, 83; (b) J. Goldberger, R. Fan and P. Yang, *Acc. Chem. Res.*, 2006, **39**, 231.
- (a) Q. Lu, F. Gao and S. Komarneni, *Langmuir*, 2005, **21**, 6002; (b) Q. Y. Lu, F. Gao and S. Komarneni, *Adv. Mater.*, 2004, **16**, 1629; (c) P. Raveendran, J. Fu and S. L. Wallen, *J. Am. Chem. Soc.*, 2003, **125**, 13940; (d) J. C. Liu, P. Raveendran, Z. Shervani and Y. Ikushima, *Chem. Commun.*, 2004, 2582; (e) J. Liu, G. Qin, P. Raveendran and Y. Ikushima, *Chem.–Eur. J.*, 2006, **12**, 2131.
- J. H. Park, S. Kim and A. J. Bard, *Nano Lett.*, 2006, **6**, 24.
- U. Bach, D. Lupo, P. Comte, J. E. Moser, F. Weisso, J. Salbeck, H. Spreitzer and M. Graetzel, *Nature*, 1998, **395**, 583.
- A. Fujishima, T. N. Rao and D. A. Tryk, *J. Photochem. Photobiol.*, 2000, **1**, 1.
- (a) S. Baskaran, L. Song, J. Liu, Y. L. Chen and G. L. Graff, *J. Am. Ceram. Soc.*, 1998, **81**, 401; (b) G. Dagan and M. Tomkiewics, *J. Phys. Chem.*, 1993, **97**, 12651.
- S. Matsuda and A. Kato, *Appl. Catal.*, 1983, **8**, 149.
- (a) X. Jiang, Y. Wang, T. Herricksb and Y. Xia, *J. Mater. Chem.*, 2004, **14**, 695; (b) J. M. Wu, W. T. Wu and H. C. Shih, *J. Electrochem. Soc.*, 2005, **152**, G613–G616; (c) Y. Xiong, B. T. Mayers and Y. Xia, *Chem. Commun.*, 2005, 5013.
- Y. Huang, X. F. Duan and C. M. Lieber, *Small*, 2005, **1**, 142.
- Z. Miao, D. Xu, J. Ouyang, G. Guo, X. Zhao and Y. Tang, *Nano Lett.*, 2002, **2**, 717.
- D. Eder, I. A. Kinloch and A. H. Windle, *Chem. Commun.*, 2006, 1448.
- M. Adachi, Y. Murata, J. Takao, J. Jiu, M. Sakamoto and F. Wang, *J. Am. Chem. Soc.*, 2004, **126**, 14943.
- L. Zhang and M. Wan, *J. Phys. Chem. B*, 2003, **107**, 6748.
- M. N. Tahir, M. Eberhardt, P. Theato, S. Faiß, A. Janshoff, T. Gorelik, U. Kolb and A. Tremel, *Angew. Chem., Int. Ed.*, 2006, **45**, 908.
- D. Yang, L. M. Qi and J. M. Ma, *J. Mater. Chem.*, 2003, **13**, 1119.
- (a) I. Huang, I. Ichinose and T. Kunitake, *Angew. Chem., Int. Ed.*, 2006, **45**, 2883; (b) J. Huang and T. Kunitake, *J. Am. Chem. Soc.*, 2003, **125**, 11834.
- (a) E. R. Cooper, C. D. Andrews, P. S. Wheatley, P. B. Webb, P. Wormald and R. E. Morris, *Nature*, 2004, **430**, 1012; (b) D. S. Jacob, A. Joseph, S. P. Mallenahalli, S. Shanmugam, S. Makhluif, J. Calderon-Moreno, Y. Kolytipin and A. Gedanken, *Angew. Chem., Int. Ed.*, 2005, **44**, 6560.
- T. Nakashima and N. Kimizuka, *J. Am. Chem. Soc.*, 2003, **125**, 6386.
- (a) R. P. Swatloski, S. K. Spear, J. D. Holbrey and R. D. Rogers, *J. Am. Chem. Soc.*, 2002, **124**, 4974; (b) M. B. Turner, S. K. Spear, J. D. Holbrey and R. D. Rogers, *Biomacromolecules*, 2004, **5**, 1379; (c) R. C. Remsing, R. P. Swatloski, R. D. Rogers and G. Moyna, *Chem. Commun.*, 2006, 1271.
- H. Zhang, J. Wu, J. Zhang and J. He, *Macromolecules*, 2005, **38**, 8272.
- J. H. He, T. Kunitake and T. Watanabe, *Chem. Commun.*, 2005, 795.
- C. Su, B. Y. Hong and C. M. Tseng, *Catal. Today*, 2004, **96**, 119.
- A. Furube, T. Asahi, H. Masuhara, H. Yamashita and M. Anpo, *J. Phys. Chem. B*, 1999, **103**, 3120.

# Electrosynthesis of phenyl-2-propanone derivatives from benzyl bromides and acetic anhydride in an unsupported micro-flow cell electrolysis process†

Ping He,<sup>a</sup> Paul Watts,<sup>a</sup> Frank Marken<sup>b</sup> and Stephen J. Haswell<sup>\*a</sup>

Received 20th July 2006, Accepted 26th October 2006

First published as an Advance Article on the web 3rd November 2006

DOI: 10.1039/b610415k

A simple process for the synthesis of phenyl-2-propanone is described based on a one-step electrochemical acylation reaction, involving the direct electroreductive coupling of benzyl bromides and acetic anhydride in a micro-flow electrolysis cell, equipped with micro-gap Pt electrodes. The technique offered yields typically in excess of 80% with corresponding high levels of product selectivity. The electrochemical process was also scaled-up by connecting four identical micro electrochemical cells in parallel to increase product throughput.

Phenyl-2-propanone, commonly referred to as P2P, is probably the most popular intermediate for the manufacture of amphetamine and methamphetamine,<sup>1</sup> and represents a versatile intermediate for the synthesis of pharmaceuticals, agrochemicals and fragrances. Due to the relatively simple structure of the compound and because of its common use,<sup>1</sup> a number of synthetic routes for its production have been developed. Most of these methods require the presence of a catalyst based on organometallic complexes,<sup>2</sup> metal acetates,<sup>3</sup> metal halides,<sup>4</sup> or Grignard reagents<sup>5</sup> to give overall yields of up to 70%. There remains however scope for greener and cleaner methods based, for example, on electrochemical technology to be more effectively exploited. In 1977, Shono<sup>6</sup> described a novel electrosynthesis process based on the reduction of benzyl chlorides in the presence of carboxylic acid chlorides in acetonitrile or *N,N*-dimethylformamide media, and using a conventional two compartment cell with a ceramic diaphragm and 1 M supporting electrolyte. Yields varied between 29 and 73% depending on the starting materials. In 1986, a patent<sup>7a</sup> reported a process for the synthesis of P2P by electrochemical reduction of benzyl chlorides in the presence of acetic anhydride using an undivided electrolysis cell equipped with a sacrificial anode (*i.e.* Mg, Al, Zn), organic solvent (*N,N*-dimethylformamide, acetonitrile, tetrahydrofuran), and supporting electrolyte to give yields of 55% to 64%. In 1994, this process was further modified to use the electrochemical arylation of  $\alpha$ -chloroketones with arylhalides in the presence of a catalytic nickel complex.<sup>7c</sup> All of these cited electrochemically based processes suffer, however, from complicated work up and generate only modest yields.

<sup>a</sup>Department of Chemistry, University of Hull, Hull, UK HU6 7RX.

E-mail: s.j.haswell@hull.ac.uk

<sup>b</sup>Department of Chemistry, University of Bath, Bath, UK BA2 7AY

† Electronic supplementary information (ESI) available: Experimental procedures, P2P syntheses described in literature and characterization. See DOI: 10.1039/b610415k

Micro reactor methodology has been shown to have numerous practical advantages (when compared with batch reactors),<sup>8</sup> including a safe operating environment, good process control, and the capability to scale-up for industrial production. In addition electrosyntheses in micro reactors has been shown to offer higher yields, in the absence of a supporting electrolyte,<sup>9</sup> which reduces costly work up and purification steps.

In this present study we describe a simple and clean process for the synthesis of P2P based on a one-step electrochemical acylation reaction by direct electroreductive coupling of benzyl bromides and acetic anhydride in a micro-flow electrolysis cell equipped with micro-gap Pt electrodes. The reaction occurs in DMF solvent without supporting electrolyte to generate excellent yields of the products when compared with conventional synthetic methods. Notable benefits of this novel electrochemical process include (i) simple operation, (ii) no need for electrolytes, (iii) minimum product work-up, and (iv) high yield and selectivity of products.

Initially, the acylation reaction of benzyl bromide with acetic anhydride was studied by cyclic voltammetry at conventional Pt-disc (diameter 0.5 mm) and micro Pt-disc electrodes (diameter 25  $\mu$ m) to establish the reaction mechanism. The electroreduction of benzyl bromide is chemically irreversible, leading to the formation of either toluene *via* a two-electron reduction<sup>10</sup> or dibenzyl formally *via* a one-electron reduction. Fig. 1 shows cyclic voltammograms obtained in DMF for (i) the reduction of acetic anhydride, (ii) the reduction of benzyl bromide, and (iii) the

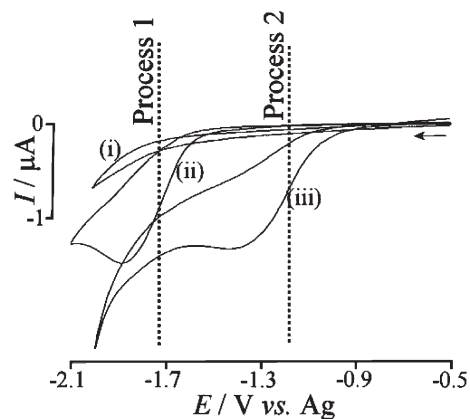


**Fig. 1** Cyclic voltammograms (scan rate of 0.1 V s<sup>-1</sup>) obtained at a 0.5 mm diameter platinum disc electrode immersed in 0.1 M *n*-Bu<sub>4</sub>NBF<sub>4</sub>-DMF for (i) 60 mM acetic anhydride, (ii) 3 mM benzyl bromide, and (iii) 3 mM benzyl bromide in the presence of 60 mM acetic anhydride.

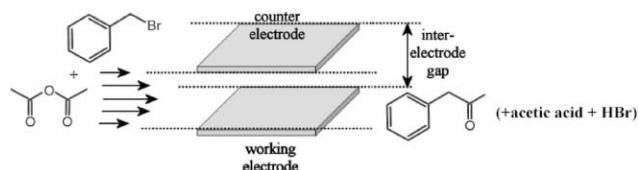


**Fig. 2** Schematic representation of the acylation reaction during micro reactor electrosynthesis. A flow of reagents through a rectangular cavity with working and counter electrode facing each other results in the formation of products.

reduction of benzyl bromide in the presence of excess acetic anhydride.

The irreversible reduction of benzyl bromide (Process 1) occurs as a two-electron process (see ESI†). In the presence of acetic anhydride, a new reductive peak appears (Process 2) at more positive potential position. The peak current for Process 2 increases with increasing amounts of acetic anhydride (for 15 mM to 60 mM) whilst the peak current for Process 1 gradually decreases. The overall mechanism remains a two-electron transfer, with Process 2 being observed only at platinum electrode surfaces and not at glassy carbon or gold (see ESI†). The ratio of peak currents for Processes 1 and 2 is scan rate dependent, consistent with a fast preceding chemical step coupled to electron transfer at the platinum surface. Acetyl from acetic anhydride is likely to act as a “trap” for a benzyl anion intermediate formed at the platinum electrode surface.

Preparative micro reactor electrolysis was conducted in a rectangular cavity micro-flow cell (see Fig. 2) with products being determined off-line by using GC/MS and <sup>1</sup>H-NMR. The reaction medium, containing 5 mM benzyl bromide in DMF with varied amount of acetic anhydride, was continuously pumped through the cell, in which two platinum electrodes with a working area of 45 mm<sup>2</sup> each were positioned with an inter-electrode gap of 160 μm to produce a 7.2 μl cell volume.

The electro-acylation reactions were conducted galvanostatically and product samples were collected for a 30 minute period. Table 1 summarizes the conversion and product distribution for the range of conditions employed in this study.

From Table 1 it can be seen (Entry 1–4) that the conversion and product distribution are dependent on the molar ratio of benzyl

bromide to acetic anhydride and the applied current (or potential). Voltages between 5–5.4 V were required to obtain sufficiently high levels of conversion (>85%) in most cases. The best result obtained was 81% of phenyl-2-propanone with 9% of toluene at a flow rate of 10 μl min<sup>-1</sup> (corresponding to 43 s contact time, see Entry 4). Lower ratios of acetic anhydride to benzyl bromide led to the formation of more toluene (Entry 2–3), and even the formation of the dibenzyl product (Entry 1).

Other benzyl bromide derivatives such as 1-phenylethyl bromide, 4-methylbenzyl bromide, 4-methoxybenzyl bromide, and 4-bromobenzyl bromide were also examined (see Entry 5–8 in Table 1) for the acylation reaction with acetic anhydride. It is noted that the presence of Br<sup>-</sup> and CH<sub>3</sub>O<sup>-</sup> groups on the benzyl bromides promote the formation of the debromination products (see Entry 7–8), compared to CH<sub>3</sub>- and H- groups. In contrast, in the presence of an electron donating group (see Entry 5–6) yields are improved. The formation of bromine due to oxidation of bromide (as a follow up anodic process) was not observed, presumably due to the limited overlap of diffusion layers within the flow cell. The diffusion layer thickness for the process can be estimated based on eqn (1).

$$\delta = \sqrt[3]{\frac{DAh^2}{V_f}} \quad (1)$$

In this equation the diffusion layer thickness is obtained based on the diffusion coefficient  $D$ , the electrode area  $A$ , the half height of the cell  $h$ , and the volume flow rate  $V_f$ . For a diffusion coefficient of 10<sup>-9</sup> m<sup>2</sup> s<sup>-1</sup> and under conditions employed here, the diffusion layer thickness is estimated as  $\delta = 120 \mu\text{m}$ , which is approaching the inter-electrode distance.

Current efficiencies for all processes are typically around 20–25%, consistent with an overall transfer of 4 electrons per benzyl bromide, but background currents in the presence of acetic anhydride are likely to be responsible for the low yield (see Fig. 1). This observation is consistent with literature reports.<sup>7a,b</sup> The electrochemical process was also scaled-up by connecting four identical micro electrochemical cells in parallel. In this case, a similar level of product yield was obtained with a four-fold increase in the quality of the product formation. In summary, micro-flow electrosynthesis offers a surprisingly simple and

**Table 1** Data for preparative electrolysis of benzyl bromides (BB) in the presence of acetic anhydride (AA) in DMF in a micro-flow cell without intentionally added supporting electrolyte<sup>a</sup>

| Entry | Current/mA |                   |                 | AA/BB <sup>b</sup> (mol/mol) | Conv. (%) <sup>c</sup> | Distribution (%) |                  |
|-------|------------|-------------------|-----------------|------------------------------|------------------------|------------------|------------------|
|       |            | R <sub>1</sub>    | R <sub>2</sub>  |                              |                        | P2P <sup>d</sup> | DBr <sup>e</sup> |
| 1     | 0.8        | H                 | H               | 10                           | 87                     | 61               | 26 <sup>f</sup>  |
| 2     | 0.8        | H                 | H               | 20                           | 85                     | 62               | 23               |
| 3     | 1.1        | H                 | H               | 20                           | 92                     | 66               | 26               |
| 4     | 1.1        | H                 | H               | 40                           | 90                     | 81               | 9                |
| 5     | 1.1        | CH <sub>3</sub>   | H               | 40                           | 93                     | 87               | 6                |
| 6     | 1.1        | H                 | CH <sub>3</sub> | 40                           | 98                     | 96               | 2                |
| 7     | 1.3        | CH <sub>3</sub> O | H               | 40                           | 99                     | 83               | 16               |
| 8     | 1.1        | Br                | H               | 40                           | 73                     | 51               | 22               |

<sup>a</sup> 5 mM benzyl bromides, acetic anhydride concentration as shown in the Table, electrode gap is 160 μm, electrode area 45 mm<sup>2</sup>, flow rate 10 μl min<sup>-1</sup> corresponding to 43 s contact time. <sup>b</sup> Molar concentration ratio. <sup>c</sup> The conversion was determined based on the quality of benzyl bromide before and after reaction using *n*-decane as an internal standard. <sup>d</sup> P2P represents P2P or its derivatives. <sup>e</sup> DBr is debromination yield for benzyl bromides. <sup>f</sup> Side products include debromination of benzyl bromide (16%) and dimer formation (10%).

low waste access to phenyl-2-propanone derivatives which is readily optimized and can be scaled-up. It is very likely that in future a wider range of chemical processes will be identified to be suitable for this kind of simple and clean micro-reactor technology.

## Acknowledgements

We thank EPSRC for funding (Project No. GR/S34106)

## Notes and references

- 1 A. C. Allen and T. S. Cantrell, *Synthetic reductions in clandestine amphetamine and methamphetamine laboratories: A Review*, Forensic Science International, Elsevier, 1989, vol. 42, p. 183.
- 2 (a) R. Ballini, *Synthesis*, 1994, 723; (b) S. Inaba and R. D. Rieke, *Tetrahedron Lett.*, 1983, **24**, 2451; (c) S. Inaba and R. D. Rieke, *J. Org. Chem.*, 1985, **50**, 1373.
- 3 (a) M. E. Kurz, V. Baru and P. N. Nguyen, *J. Org. Chem.*, 1984, **49**, 1603; (b) A. C. Allen, M. L. Stevensen, S. M. Nakamura and R. A. Ely, *J. Forensic Sci.*, 1992, **37**, 301.
- 4 (a) K. Lee and D. Y. Oh, *Tetrahedron Lett.*, 1988, **29**, 2977; (b) K. Okabe, T. Ohwada, T. Ohta and K. Shudo, *J. Org. Chem.*, 1989, **54**, 733.
- 5 (a) P. Canonne, G. B. Foscolos and G. Lemay, *Tetrahedron Lett.*, 1980, **21**, 155; (b) K. Okabe, T. Ohwada, T. Ohta and K. Shudo, *J. Org. Chem.*, 1972, **37**, 3369.
- 6 T. Shono, *Chem. Lett.*, 1977, 1021.
- 7 (a) M. D. Moingeon and J. Chaussard, *US Pat.*, 4 629 541, 1986; (b) E. D'Incan, S. Sibille, J. Périchon, M. D. Moingeon and J. Chaussard, *Tetrahedron Lett.*, 1986, **27**, 4175; (c) M. Durandetti, S. Sibille, J.-Y. Nédélec and J. Périchon, *Synth. Commun.*, 1994, **24**, 145.
- 8 (a) S. Taghavi-Moghadam, A. Kleemann and K. G. Golbig, *Org. Process Res. Dev.*, 2001, **5**, 652; (b) T. Kawaguchi, H. Miyata, K. Ataka, K. Mae and J. Yoshida, *Angew. Chem., Int. Ed.*, 2005, **44**, 2413.
- 9 (a) C. A. Paddon, G. J. Pritchard, T. Thiemann and F. Marken, *Electrochem. Commun.*, 2002, **4**, 825; (b) R. Horcajada, M. Okajima, S. Suga and J. Yoshida, *Chem. Commun.*, 2005, 1303; (c) P. He, P. Watts, F. Marken and S. J. Haswell, *Electrochem. Commun.*, 2005, **7**, 918; (d) P. He, P. Watts, F. Marken and S. J. Haswell, *Angew. Chem., Int. Ed.*, 2006, **45**, 4146.
- 10 (a) J. Grimshaw, *Electrochemical Reactions and Mechanisms in Organic Chemistry*, Elsevier, Amsterdam, 2000, pp. 98–103; (b) *Organic Electrochemistry*, ed. H. Lund and O. Hammerich, Marcel Dekker, New York, 2001.

# Asymmetric transfer hydrogenation of ketones and imines with novel water-soluble chiral diamine as ligand in neat water

Li Li,<sup>ab</sup> Jiashou Wu,<sup>a</sup> Fei Wang,<sup>a</sup> Jian Liao,<sup>a</sup> Hua Zhang,<sup>a</sup> Chunxia Lian,<sup>a</sup> Jin Zhu\*<sup>a</sup> and Jingen Deng\*<sup>a</sup>

Received 15th August 2006, Accepted 7th November 2006

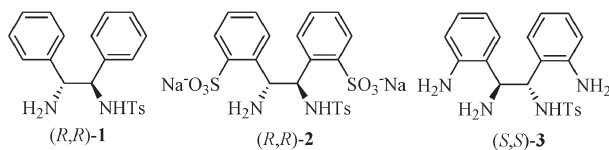
First published as an Advance Article on the web 16th November 2006

DOI: 10.1039/b611809g

A novel water-soluble rhodium(III) catalyst prepared from *o,o'*-aminated *N*-tosyl-1,2-diphenylethylenediamine (*S,S*)-**3** and [Cp\*RhCl<sub>2</sub>]<sub>2</sub>, which was efficient for the asymmetric transfer hydrogenation of ketones and imines in neat water with high reactivity and excellent enantioselectivity, has been developed.

Asymmetric transfer hydrogenation (ATH) of prochiral ketones and imines is a pivotal reaction for the synthesis of chiral alcohols and amines owing to its ease of handling, lower cost and safety.<sup>1</sup> Among the various chiral catalysts reported, the most notable is the ruthenium catalyst Ru-TsDPEN [TsDPEN = *N*-(*p*-toluenesulfonyl)-1,2-diphenylethylenediamine, (*R,R*)-**1**] developed by Noyori and Ikariya.<sup>2</sup> This catalyst has been applied to the asymmetric transfer hydrogenation of both ketone and imine, leading to good to excellent ees with 2-propanol<sup>2</sup> and HCOOH-NEt<sub>3</sub>,<sup>3</sup> respectively, as hydrogen donor as well as solvent.

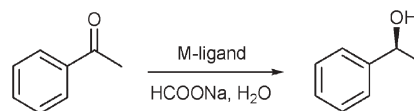
As a consequence of the increasing demand for efficient and environmentally friendly methods, there has been considerable interest in the development of water-soluble catalytic systems which allow catalytic reactions to occur in water.<sup>4</sup> We have reported a water-soluble catalyst based on the Noyori-Ikariya system, which has been successfully used in the asymmetric transfer hydrogenation of ketones and imines in aqueous media.<sup>5</sup> Although the ligand (*R,R*)-**2** in the catalyst can be easily synthesized, its purification was rather difficult. Herein, we report a novel water-soluble catalytic system with chiral vicinal diamine (*S,S*)-**3** as ligand for the ATH of ketones and imines in neat (*i.e.* organic solvent- and surfactant-free) water, which is easily prepared and purified from the nitro-precursor *via* catalytic hydrogenation.<sup>6</sup>



## Results and discussion

We started with the ATH of acetophenone by using transition metal complexes of the ligand, (*S,S*)-**3** as catalysts with HCO<sub>2</sub>Na<sup>7</sup> as hydrogen source in neat water. The precatalyst was generated

by *in situ* reacting (*S,S*)-**3** with [Cp\*RhCl<sub>2</sub>]<sub>2</sub>, [Cp\*IrCl<sub>2</sub>]<sub>2</sub>, and [RuCl<sub>2</sub>(*p*-cymene)]<sub>2</sub>, respectively, in degassed water at 40 °C for 1 h. To our delight, with the water-soluble Rh-(*S,S*)-**3** complex,<sup>8</sup> (*S*)-phenethyl alcohol was obtained after 0.5 h at 28 °C with high conversion and enantioselectivity (97% and 97% ee, Table 1, entry 1). Other types of metal complexes were tested as catalyst precursors and were much less reactive (entries 2 and 3). The Rh-(*R,R*)-**2** exhibited low conversion and the enantioselectivity was inferior (entry 4).



Encouraged by the result obtained with Rh-(*S,S*)-**3**, we then extended this system to a wide range of substituted acetophenones **4–9**, the related ketones **10–13** and the heteroaryl ketone **14**. All the ketones can be transformed to the corresponding secondary alcohols at fast rates in an organic solvent free system under optimization conditions as shown in Fig. 1. A substituent on the *ortho*-site of the acetophenone decreases the enantioselectivity (88% ee for **6**). When the Rh-(*S,S*)-**3** was applied to propiophenone **10**, 2'-acetonaphthone **11**, and cyclic substrates **12** and **13**, 95% to 98% ees were achieved. In the reaction of heteroatom ketone **14**, chiral alcohol was obtained in excellent enantioselectivity (98% ee) with 97% conversion in 1 h.

Optical pure 2-bromo-1-arylethanol were the key intermediates of  $\beta$ -adrenergic receptor agonists, which were usually obtained from the corresponding  $\alpha$ -bromomethylaromatic ketones by reduction employing CBS<sup>9</sup> oxazaborolidine or biocatalysts.<sup>10</sup> In aqueous media,  $\alpha$ -bromomethylaromatic ketones **15–19** can also be converted to corresponding chiral 2-bromo alcohols quickly with high enantioselectivity (90% to 97% ee) by using Rh-(*S,S*)-**3**

**Table 1** Asymmetric transfer hydrogenation of acetophenone in water<sup>a</sup>

| Entry | Ligand                   | Metal complexes                                      | Conv. (%) <sup>b</sup> | ee (%) <sup>b</sup> |
|-------|--------------------------|--|------------------------|---------------------|
| 1     | ( <i>S,S</i> )- <b>3</b> | [Cp*RhCl <sub>2</sub> ] <sub>2</sub>                 | 97                     | 97                  |
| 2     | ( <i>S,S</i> )- <b>3</b> | [Cp*IrCl <sub>2</sub> ] <sub>2</sub>                 | 29                     | 94                  |
| 3     | ( <i>S,S</i> )- <b>3</b> | [RuCl <sub>2</sub> ( <i>p</i> -cymene)] <sub>2</sub> | 33                     | 95                  |
| 4     | ( <i>R,R</i> )- <b>2</b> | [Cp*RhCl <sub>2</sub> ] <sub>2</sub>                 | 9                      | 10                  |

<sup>a</sup> Unless otherwise indicated, the reaction was carried out in 1 mL of water under argon atmosphere at 28 °C for 0.5 h using 0.4 mmol ketone, [M-(*S,S*)-**3**] : [acetophenone] : [HCO<sub>2</sub>Na] = 1 : 100 : 500. The configuration of phenethyl alcohol was determined by comparison of the sign of optical rotation with literature data.<sup>2</sup>

<sup>b</sup> Determined by GC analysis.

<sup>a</sup>Key Laboratory of Asymmetric Synthesis and Chirality of Sichuan Province and Union Laboratory of Asymmetric Synthesis, Chengdu Institute of Organic Chemistry, Chinese Academy of Sciences, Chengdu, 610041, China. E-mail: jgdeng@cioc.ac.cn; Fax: +86 8522 3978  
<sup>b</sup>Graduate School of Chinese Academy of Sciences, Beijing, China

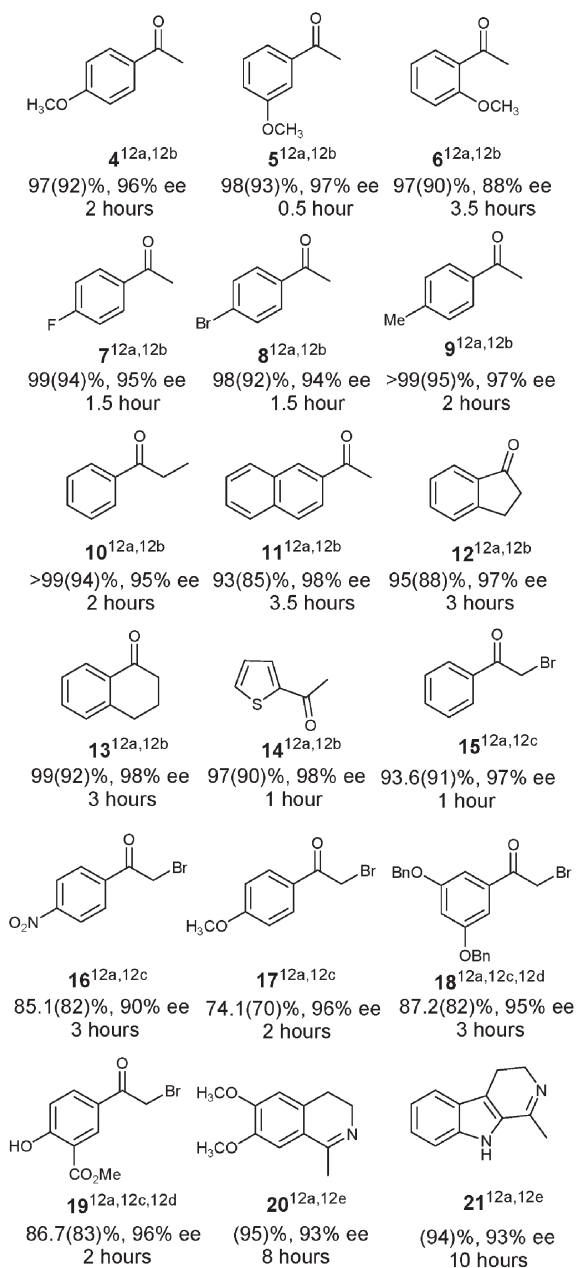


**Fig. 1** ATH of ketones and imines with Rh-(*S,S*)-3 in water.<sup>12</sup>

as catalyst, in which the reduced products of **18** and **19** are the key medicinal intermediates of anti-asthma drugs, terbutaline and salbutamol, respectively.<sup>11</sup> Moreover, high activity and enantioselectivity were observed for the transfer hydrogenation of imines **20** and **21** (93% ee and 95% yield for **20**, 93% ee and 94% yield for **21**).

In conclusion, we have developed a novel water-soluble catalyst prepared from the chiral vicinal diamine, (*S,S*)-3 and [Cp\**Rh*Cl<sub>2</sub>]<sub>2</sub>, which have been shown to be efficient for the catalytic asymmetric transfer hydrogenation of ketones and imines with sodium formate as hydrogen donor in neat water. It is also notable that this catalytic system can catalyze the ATH of  $\alpha$ -bromomethylaromatic ketones and imines besides simple ketones and give high yields and enantioselectivities within a few hours at 28 °C.<sup>5,7</sup>

## Experimental

<sup>1</sup>H NMR spectra was recorded on Bruker (300 MHz) equipment in CDCl<sub>3</sub> with TMS ( $\delta$  0.00) as internal standard. Enantiomeric excess was determined by GC on chiral CP-cyclodextrin B-236 M/CP-Chirasil-DEX columns or HPLC on Chiral OD/OJ columns. The concentration of rhodium in both organic and aqueous layers was determined by ICP-MS analysis. M-(*S,S*)-3 complexes were synthesized following Noyori *et al.*'s procedure.<sup>13</sup> The  $\alpha$ -bromomethylaromatic ketones<sup>14</sup> and imines<sup>15</sup> were prepared as reported in the literature. All other reagents were purchased from commercial sources and were used without further purification.

### Typical procedure for asymmetric transfer hydrogenation of ketones and imines

The mixture of (*S,S*)-3 (1.7 mg, 0.0044 mmol) and [RhCl<sub>2</sub>(Cp\*)]<sub>2</sub> (1.3 mg, 0.002 mmol) was degassed three times. 1 mL of degassed water was added and the mixture was stirred at 40 °C for 1 h. Ketone/imine (0.4 mmol) and HCO<sub>2</sub>Na·2H<sub>2</sub>O (208 mg, 2.0 mmol) were added to the solution. The mixture was degassed three times and was stirred under argon at 28 °C. When the reaction was completed (determined by TLC), the reaction mixture was extracted with CH<sub>2</sub>Cl<sub>2</sub> (5 mL) three times. For ketones, the conversion and enantioselectivity were determined by GC. For  $\alpha$ -bromomethylaromatic ketones, the yield was determined by <sup>1</sup>H-NMR using 1,3,5-trimethylbenzene as an internal standard. Isolated yield was obtained by flash chromatography.

### Acknowledgements

This work was financially supported by the National Natural Science Foundation of China (Nos. 20572108 and 203900507).

### Notes and references

- For a recent review, see: S. Gladiali and E. Alberico, *Chem. Soc. Rev.*, 2006, **35**, 226–236.
- S. Hashiguchi, A. Fujii, J. Takehara, T. Ikariya and R. Noyori, *J. Am. Chem. Soc.*, 1995, **117**, 7562–7563.
- A. Fujii, S. Hashiguchi, N. Uematsu, T. Ikariya and R. Noyori, *J. Am. Chem. Soc.*, 1996, **118**, 2521–2522; N. Uematsu, A. Fujii, S. Hashiguchi, T. Ikariya and R. Noyori, *J. Am. Chem. Soc.*, 1996, **118**, 4916–4917.
- For a comprehensive review, see: D. Sinou, *Adv. Synth. Catal.*, 2002, **344**, 221–237.
- Y. Ma, H. Liu, L. Chen, X. Cui, J. Zhu and J. Deng, *Org. Lett.*, 2003, **5**, 2103–2106; J. Wu, F. Wang, Y. Ma, X. Cui, L. Cun, J. Zhu, J. Deng and B. Yu, *Chem. Commun.*, 2006, 1766–1768.
- D. Xue, Y. C. Chen, X. Cui, Q. W. Wang, J. Zhu and J. G. Deng, *J. Org. Chem.*, 2005, **70**, 3584–3591.
- H. Y. Rhyoo, H. J. Park and Y. K. Chung, *Chem. Commun.*, 2001, 2064–2065; S. Ogo, T. Abura and Y. Watanabe, *Organometallics*, 2002, **21**, 2964–2969; X. Wu, X. Li, W. Hems, F. King and J. Xiao, *Org. Biomol. Chem.*, 2004, **2**, 1818–1821; X. Wu, D. Vinci, T. Ikariya and J. Xiao, *Chem. Commun.*, 2005, 4447–4449.
- After biphasic separation with Et<sub>2</sub>O/AcOEt (1 : 1, v/v), a little catalyst was extracted into the organic layer. For Rh-(*S,S*)-3, the concentration of rhodium in both organic and aqueous layers was 0.85  $\mu\text{g mL}^{-1}$  and 55.1  $\mu\text{g mL}^{-1}$ , respectively.
- E. J. Corey and C. J. Helal, *Angew. Chem., Int. Ed.*, 1998, **37**, 1986–2012.
- A. Goswami, R. L. Bezbaruah, J. Goswami, N. Borthakur, D. Dey and A. K. Hazarika, *Tetrahedron: Asymmetry*, 2000, **11**, 3701–3709.
- F. Wang, H. Liu, L. Cun, J. Zhu, J. Deng and Y. Jiang, *J. Org. Chem.*, 2005, **70**, 9424–9429.



- 12 (a) Reactions were carried out in 1 mL of water under an argon atmosphere at 28 °C by using 0.4 mmol ketone, [Rh-(*S,S*)-3] : [ketone] : [HCO<sub>2</sub>Na] = 1 : 100 : 500; data in parentheses were the isolated yields. (b) The conversion and ee were determined by GC, and the configuration of alcohols was *S*-form. (c) Yield was determined by <sup>1</sup>H NMR, ee was determined by GC or HPLC, and the configuration of alcohols was *R*-form. (d) 0.5 Equivalent of Triton X-100 was used.<sup>11</sup>
- (e) Ee was determined by HPLC, and the configuration of amines was *R*-form.
- 13 K. J. Haack, S. Hashiguchi, A. Fujii, T. Ikariya and R. Noyori, *Angew. Chem., Int. Ed. Engl.*, 1997, **36**, 285–288.
- 14 L. C. King and G. K. Ostrum, *J. Org. Chem.*, 1964, **29**, 3459–3461.
- 15 P. N. Craig, F. P. Nabenhauer, P. M. Williams, E. Macko and J. Joner, *J. Am. Chem. Soc.*, 1952, **74**, 1316–1317.



## Looking for that **special** chemical science research paper?

TRY this free news service:

### Chemical Science

- highlights of newsworthy and significant advances in chemical science from across RSC journals
- free online access
- updated daily
- free access to the original research paper from every online article
- also available as a free print supplement in selected RSC journals.\*

\*A separately issued print subscription is also available.

Registered Charity Number: 207890

22030682

RSCPublishing

[www.rsc.org/chemicalscience](http://www.rsc.org/chemicalscience)

# Oxybromination of phenol and aniline derivatives in H<sub>2</sub>O/scCO<sub>2</sub> biphasic media

Benjamin Ganchegui and Walter Leitner\*

Received 12th July 2006, Accepted 6th September 2006

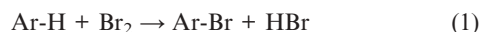
First published as an Advance Article on the web 3rd October 2006

DOI: 10.1039/b609992k

The oxybromination of phenols and anilines was achieved in the benign H<sub>2</sub>O/scCO<sub>2</sub> biphasic system using NaBr–H<sub>2</sub>O<sub>2</sub> as the bromine source without the need for metal catalysts or acidic additives. The reactivity of the system is associated with the intrinsic acidity of the medium and the *in situ* generation of percarbonic acid. High conversions of the starting material were achieved together with very good selectivities under optimized conditions.

## Introduction

Brominated aromatic compounds are widely used as building blocks for fine chemicals.<sup>1</sup> They are also present in the structure of many natural compounds of pharmacological interest.<sup>2</sup> Most of the processes currently operating for the bromination of aryl compounds employ toxic, corrosive, and expensive molecular bromine, resulting in the formation of large amounts of HBr waste (eqn (1)). In view of the wide use of brominated aromatics, it is of interest to develop ecologically benign and economically attractive alternatives to these processes. In this context, oxybromination is safer and greener since it avoids the hazardous Br<sub>2</sub>, replacing it in most cases with a bromide salt in the presence of an oxidant agent under acidic conditions (eqn (2)).



The systems reported for oxybromination so far require strongly acidic conditions, volatile organic solvents (VOCs) and metal or other catalysts (*e.g.* vanadium, copper, zeolites).<sup>3</sup> The oxidizing equivalents are mostly provided by peroxides in the processes,<sup>4</sup> although molecular oxygen could be activated in some instances.<sup>5–7</sup> Kulkrani *et al.* reported a metal free system operating for the oxybromination of aniline and anisole derivatives in acetic acid as solvent.<sup>8</sup> Liang *et al.* recently performed the oxybromination of aromatics in CH<sub>3</sub>CN–aqueous HBr mixtures, mediated by NaNO<sub>2</sub>.<sup>7</sup>

Increasing effort is currently devoted to the replacement of VOCs in modern organic synthesis and scCO<sub>2</sub> is a promising alternative, since it is non-toxic and non-flammable.<sup>9</sup> Moreover, it is cheap and readily available. In this article we describe an effective approach to the oxybromination of phenol and aniline derivatives performed without any metal catalyst or potential toxic/polluting acid addition in a biphasic system consisting of scCO<sub>2</sub> and H<sub>2</sub>O.

Institut für Technische und Makromolekulare Chemie, RWTH Aachen, Worringerweg 1, Aachen, 52074, Germany.  
E-mail: Leitner@itmc.rwth-aachen.de; Fax: +49-(0)241-8022177;  
Tel: +49-(0)241-8026480

## Results and discussion

### Background

The use of an H<sub>2</sub>O/scCO<sub>2</sub> biphasic system holds several potential advantages: in addition to the benign character of both scCO<sub>2</sub> and water, the coexistence of water with scCO<sub>2</sub> results in an intrinsic pH value around 3 of the water phase (Fig. 1). Moreover, the water phase recovers its neutral pH within a few minutes following the depressurization of CO<sub>2</sub>. Thus, this solvent system provides “switchable” acidic conditions without the need for external acid.

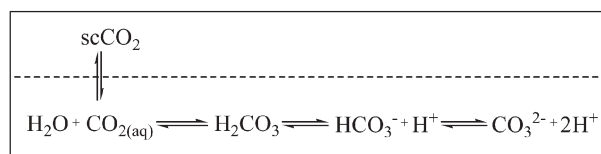
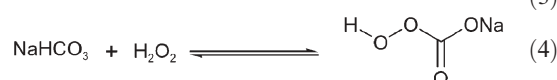
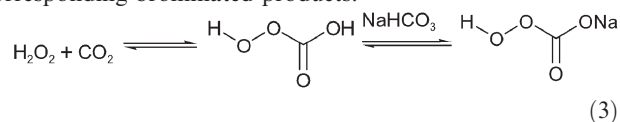


Fig. 1 Intrinsic acidity of H<sub>2</sub>O/scCO<sub>2</sub> biphasic media.

In oxidation processes, the *in situ* generation of percarbonic acid from H<sub>2</sub>O<sub>2</sub> and CO<sub>2</sub> offers an additional possibility to exploit the chemical reactivity of the H<sub>2</sub>O/scCO<sub>2</sub> system (eqn (3)). Eckert *et al.* invoked percarbonic acid to rationalise the rate enhancement observed in the metal free epoxidation of olefins with H<sub>2</sub>O<sub>2</sub> in H<sub>2</sub>O/scCO<sub>2</sub>.<sup>10</sup> Such an activating effect can also be achieved by the addition of NaHCO<sub>3</sub> to an aqueous H<sub>2</sub>O<sub>2</sub> solution.<sup>11</sup> The formation of the sodium carboxylate of percarbonic acid then allows a higher concentration of the overall percarbonic species (eqn (4)). Such a bicarbonate activated hydrogen peroxide (BAP), in the absence of CO<sub>2</sub>, was used by Richardson *et al.* for the metal free epoxidation of olefins<sup>12</sup> and sulfide oxidation<sup>13</sup> in water. We therefore decided to investigate the reactivity of aromatic compounds with bromide salts in the presence of H<sub>2</sub>O<sub>2</sub> using an H<sub>2</sub>O/scCO<sub>2</sub> biphasic reaction medium in order to obtain the corresponding brominated products.



### Screening of reaction conditions

The so called ‘‘oxybromination’’ of an electron rich arene leads to a mixture of *ortho*- and *para*- brominated species, and polybromination is also possible. The use of an *ortho*-substituted substrate reduces the possible combinations to three products. Thus, in order to simplify the analytics, *o*-cresol **1a** was used as model substrate in a first screening for suitable reaction conditions (Table 1).

Submitting *o*-cresol **1a** to NaBr/H<sub>2</sub>O<sub>2</sub> in water at 40 °C resulted in a poor conversion of 12% (entry 1). Using the biphasic H<sub>2</sub>O/scCO<sub>2</sub> system under otherwise identical conditions, the conversion increased to 54% (entry 2 vs. 1). If the reaction was performed in absence of scCO<sub>2</sub> but with a catalytic amount of NaHCO<sub>3</sub>, there was a noticeable enhancement compared to the CO<sub>2</sub>-free system, but conversion was still lower than in the H<sub>2</sub>O/scCO<sub>2</sub> system (entry 3). This supports the involvement of percarbonic species in a BAP-type mechanism. The actual oxidant in this case would be percarbonic acid sodium salt (eqn (4)).<sup>11</sup>

The reason for less improvement with NaHCO<sub>3</sub> than that observed in H<sub>2</sub>O/scCO<sub>2</sub> is assumed to be the absence of acidic conditions necessary to achieve an efficient oxybromination.<sup>3</sup> Indeed, by combining the effects of the biphasic H<sub>2</sub>O/scCO<sub>2</sub> system with the addition of a catalytic amount of NaHCO<sub>3</sub> the conversion could be raised to 91% within 4 hours, while the monobromination selectivity remained high (89%, entry 4). A shorter reaction time (entry 5) or a lower NaBr stoichiometry further improved the monobromo adduct selectivity albeit at the expense of a drop in conversion.

Since oxidation reactions in scCO<sub>2</sub> can be initiated by the reactor walls<sup>14</sup> and the conversion of bromide ions into bromine with hydrogen peroxide is known to be iron catalyzed,<sup>15</sup> it was checked whether the iron-containing steel walls of the autoclave had an influence on the rate of the oxybromination. A test reaction was performed with a glass

liner inside the autoclave. Conversion and selectivities were largely identical to those obtained in absence of the coating (entry 6 vs. 4). This indicates that either the reactor walls are not involved in the overall process or the bromide oxidation step is not rate limiting for this transformation.

Finally several bromide salts were tested (entries 7–9). Both KBr and [NBu<sub>4</sub>]Br exhibited comparable reactivities to NaBr whereas [NH<sub>4</sub>]Br was less effective. Therefore NaBr was kept as the standard bromine source for the rest of this work.

In summary, oxybromination of *o*-cresol could be achieved readily using H<sub>2</sub>O<sub>2</sub>/NaBr as the bromine source in an H<sub>2</sub>O/scCO<sub>2</sub> biphasic system. More than 90% conversion and 90% selectivity for the monobrominated product was achieved. In a preparative scale experiment under the conditions of Table 1, entry 4, a mixture of the *ortho*- and *para*-brominated products (**2a** : **3a** = 40 : 60) was isolated in 78% yield along with 8% of the disubstituted product **4a** by flash chromatography after a classical work up.

### Oxybromination of phenol derivatives

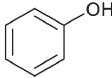
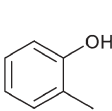
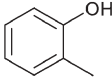
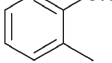
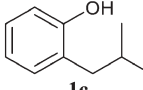
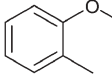
A series of phenol derivatives was submitted to the conditions described above. The results are shown in Table 2. After 3 hours, 98% conversion of phenol **1b** with 88% monobromophenol selectivity was observed (entry 1a). It is assumed that the observed high monobromination selectivity results from two main factors: (i) for electronic reasons, an *ortho*- or *para*-bromination substitution has a deactivating effect toward a further electrophilic bromination of a phenol derivative, (ii) a brominated phenol is less water soluble than phenol itself.<sup>16</sup> Indeed, the orange colour of the water phase indicates that the brominating species is mainly water soluble. Therefore, the partition of substrate, primary product and brominating agent in the biphasic mixture (Fig. 2) is expected to affect the selectivity control.

**Table 1** Oxybromination of *o*-cresol in H<sub>2</sub>O/scCO<sub>2</sub>

| Entry          | MBr : <b>1a</b>    | Equiv. NaHCO <sub>3</sub> | Solvent system                     | Conv. <sup>a</sup> (%) | Selectivity <sup>b</sup> (%)                           |           |
|----------------|--------------------|---------------------------|------------------------------------|------------------------|--|-----------|
|                |                    |                           |                                    |                        | <b>2a</b> + <b>3a</b> <sup>c</sup><br>(isolated yield) | <b>4a</b> |
| 1              | NaBr               | —                         | H <sub>2</sub> O                   | 12                     | 93   | 7         |
| 2              | NaBr               | —                         | H <sub>2</sub> O/scCO <sub>2</sub> | 54                     | 78   | 22        |
| 3              | NaBr               | 0.1                       | H <sub>2</sub> O                   | 32                     | 92   | 8         |
| 4              | NaBr               | 0.1                       | H <sub>2</sub> O/scCO <sub>2</sub> | 91                     | 89 (78)  | 11 (8)    |
| 5 <sup>d</sup> | NaBr               | 0.1                       | H <sub>2</sub> O/scCO <sub>2</sub> | 48                     | 95   | 5         |
| 6 <sup>e</sup> | NaBr               | 0.1                       | H <sub>2</sub> O/scCO <sub>2</sub> | 93                     | 86   | 14        |
| 7              | KBr                | 0.1                       | H <sub>2</sub> O/scCO <sub>2</sub> | 86                     | 91   | 9         |
| 8              | TBAB               | 0.1                       | H <sub>2</sub> O/scCO <sub>2</sub> | 90                     | 89   | 11        |
| 9              | NH <sub>4</sub> Br | 0.1                       | H <sub>2</sub> O/scCO <sub>2</sub> | 60                     | 93   | 7         |

<sup>a</sup> Standard conditions: *o*-cresol : MBr : H<sub>2</sub>O<sub>2</sub> = 1 : 3 : 3, 40 °C, 4 h; GC conversion using octan-1-ol as standard. <sup>b</sup> Selectivity is expressed as the ratio of the GC peak areas; the only detected products are those 3 compounds. <sup>c</sup> Mono-brominated compounds were obtained as a 40 : 60 mixture of *ortho*- and *para*- isomers. <sup>d</sup> Reaction time = 2 h. <sup>e</sup> Reaction with a glass lined autoclave.

**Table 2** Oxybromination of phenol derivatives in H<sub>2</sub>O/scCO<sub>2</sub>

| Entry | Substrate  | Water solubility <sup>a</sup> /g L <sup>-1</sup><br>(at pH = 7) | NaBr (equiv.) | t/h | Conv. <sup>b</sup> (%) | Selectivity <sup>c</sup> (%) |       |        |
|-------|--|---|---------------|-----|------------------------|------------------------------|-------|--------|
|       |  |   |               |     |                        | Mono-Br                      | Di-Br | Tri-Br |
| 1a    |               | 80  | 3             | 3   | 98                     | 88                           | 11    | 1      |
| 1b    | <br><b>1b</b> | 80  | 3             | 6   | 100                    | 52                           | 33    | 15     |
| 1c    |  |   | 1             | 4   | 57                     | 93                           | 7     | 0      |
| 1d    |  |   | 6             | 4   | 100                    | 3                            | 5     | 92     |
| 2a    |               | 20  | 3             | 3   | 74                     | 94                           | 6     | —      |
| 2b    | <br><b>1a</b> | 20  | 3             | 3.5 | 89                     | 93                           | 7     | —      |
| 2c    |  |   | 1             | 4   | 41                     | 98                           | 2     | —      |
| 3a    | <br><b>1c</b> | 1   | 3             | 3   | 38                     | 97                           | 3     | —      |
| 3b    |  |   | 3             | 6   | 58                     | 91                           | 9     | —      |
| 3c    |  |   | 3             | 20  | 75                     | 82                           | 18    | —      |
| 3d    |  |   | 1             | 20  | 35                     | 96                           | 4     | —      |
| 4     | <br><b>1d</b> | 0.5   | 3             | 20  | 0                      | —                            | —     | —      |

<sup>a</sup> Conditions: substrate : NaHCO<sub>3</sub> : NaBr : H<sub>2</sub>O<sub>2</sub> = 1 : 0.1 : 3 : 3, 40 °C; solubilities from Acros Chemicals. <sup>b</sup> GC conversion with octan-1-ol as internal standard. <sup>c</sup> Selectivity is expressed as the ratio of the GC peak areas.

Increasing the reaction time resulted in a further reaction of the monobrominated adducts allowing the formation of di- and tribromophenol (entry 1b). Tuning the NaBr stoichiometry opens a further possibility to regulate the selectivity toward mono- or tribromophenol: a 1 : 1 ratio for **1b** : NaBr led to a good monobromo selectivity (93%), albeit at conversion of only 57% (entry 1c). In the presence of 6 equivalents of NaBr, the reaction led to a full conversion along with 92% tribromophenol selectivity (entry 1d).

The influence of the water solubility of the substrates mentioned above is also evident from the relative reactivities of the substituted phenols **1a–d**. *o*-Cresol **1a** proved less reactive than phenol **1b**, even though it should be electronically more activated. Most significantly, the electronically almost identical substrate **1c** proved far less reactive than **1a**, in parallel to a largely reduced water solubility. Finally, the most hydrophobic substrate **1d** proved unreactive. However, an

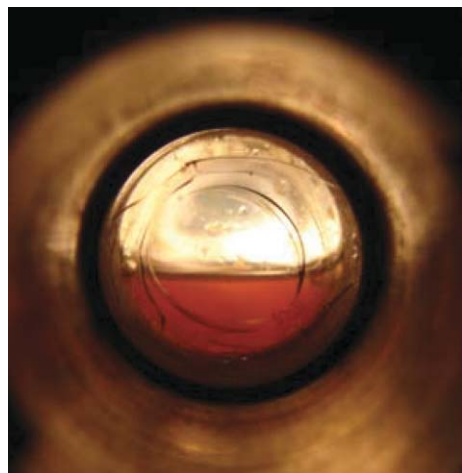
additional deactivation effect by blocking the protic OH can not be excluded in this case.

### Oxybromination of aniline derivatives

Given the successful and straightforward oxybromination of phenol derivatives in the H<sub>2</sub>O/scCO<sub>2</sub> system, amino-substituted aromatics were tested under similar reaction conditions (Table 3). Aniline **5a** reacted smoothly and 98% conversion was achieved after 4 hours (entry 1). In contrast to the situation observed with phenol **1b**, the disubstituted products **7a** were formed with high preference from **5a**. The *o,o'*- and *o,p*-isomers were typically observed in a ratio of 45 : 55. The monosubstituted product **6a** (*ortho* : *para* = 70 : 30) can be obtained with good selectivity at reasonable conversion by reducing the amount of bromine source (entry 1b). Excellent yield for the monobrominated products (*ortho* : *para* = 35 : 65) were also achieved with substrate **5b** (entry 2). The *N*-substituted derivatives **5c** and **5d** were far less reactive, which may again reflect their largely reduced water solubility (entries 3 and 4).

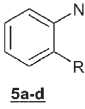
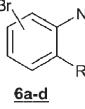
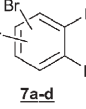
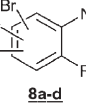
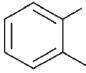
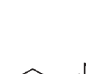
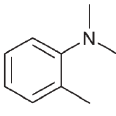
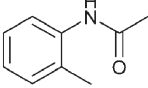
### Conclusion

This work provides a new method for the production of brominated phenol and aniline derivatives using NaBr–H<sub>2</sub>O<sub>2</sub> as a bromine source in the benign H<sub>2</sub>O/scCO<sub>2</sub> biphasic reaction medium. This system is suitable for the reaction of sufficiently water soluble substrates; mono-, di-, or tribrominated products could be obtained with high selectivities under suitable conditions. This new procedure represents an attractive green approach to brominated aromatics for several reasons: (i) it avoids the use and handling of Br<sub>2</sub>; (ii) no VOCs are used as solvents; (iii) the two components of the reaction medium, water and CO<sub>2</sub>, are non-toxic, non-flammable, cheap and readily available; (iv) the intrinsic reactivity of the biphasic system avoids the use of additional acids or metal catalysts.



**Fig. 2** Biphasic H<sub>2</sub>O/scCO<sub>2</sub> system for the oxybromination of cresol using NaBr/H<sub>2</sub>O<sub>2</sub>.

**Table 3** Oxybromination of aniline derivatives in H<sub>2</sub>O/scCO<sub>2</sub>

| Entry | Substrate   | NaBr (equiv.) |   | Time/h | Conv. <sup>a</sup> (%) | Sel. <sup>b</sup> (%)<br>6/7/(8) |
|-------|---|---------------|---|--------|------------------------|----------------------------------|
|       |   | 3             | 1 |        |                        |                                  |
| 1     |  | 3             | 1 | 4      | 98                     | 29/70/(1)                        |
|       |  |               |   | 4      | 65                     | 96/3/(1)                         |
|       |  |               |   |        |                        |                                  |
|       |  |               |   |        |                        |                                  |
| 2     |  | 3             | 1 | 4      | 94                     | 91/9                             |
|       |  |               |   | 4      | 43                     | 98/2                             |
| 3     |  | 3             |   | 20     | 22                     | 99/1                             |
| 4     |  | 3             |   | 20     | 0                      | —                                |

<sup>a</sup> Conditions: substrate : NaHCO<sub>3</sub> : NaBr : H<sub>2</sub>O<sub>2</sub> = 1 : 0.1 : 3 : 3, 40 °C; GC conversion with octan-1-ol as internal standard.

<sup>b</sup> Selectivity is expressed as the ratio of the GC peak areas.

## Experimental

### Safety warning

Experiments using compressed gases must only be conducted in suitable equipment and under appropriate safety precautions.

### Reagents and analytics

Reactants were purchased from Acros and used without further purification. GC analyses were performed on a Hewlett Packard 5890 series II instrument, using octan-1-ol as standard. GC/MS were recorded on a Hewlett Packard 5973 quadrupole-spectrometer (EI, 70 eV). NMR spectra were recorded on a Bruker DPX-300 spectrometer (<sup>1</sup>H: 300 MHz, <sup>13</sup>C: 75 MHz).

### Typical procedure

A 10 mL window-equipped stainless steel autoclave was charged with NaHCO<sub>3</sub> (8.4 mg, 0.1 mmol), NaBr (309 mg, 3 mmol), *o*-cresol (108 mg, 1 mmol), 2 mL water and finally H<sub>2</sub>O<sub>2</sub> (175 μL, 3 mmol). Then, a weighed amount of CO<sub>2</sub> (8 g) was added using a compressor. The reactor was heated to 40 °C, whereby the pressure rose to 100–110 bar. After the given reaction time, the reactor was cooled down to 0 °C and CO<sub>2</sub> was removed through a double cold trap within 20 minutes. The water phase in the reactor and the cold traps were extracted with ether and the combined extracts analysed by GC using octan-1-ol as standard. Products

were identified by GC/MS and <sup>1</sup>H NMR and comparison to authentic samples.

2-bromo-6-methylphenol: <sup>1</sup>H NMR (CDCl<sub>3</sub>, 300 MHz, 298 K): 2.28 (s, 3H, CH<sub>3</sub>); 5.35 (s, 1H, OH); 6.64–6.77 (m, 1H, ArH); 6.95–7.06 (m, 1H, ArH); 7.20–7.32 (m, 1H, ArH); MS (EI, 70 eV): 188, 186 (M<sup>+</sup>, 42); 107 (–Br, 100).

4-bromo-6-methylphenol: <sup>1</sup>H NMR (CDCl<sub>3</sub>, 300 MHz, 298 K): 2.24 (s, 3H, CH<sub>3</sub>); 4.78 (s, 1H, OH); 6.51–6.63 (m, ArH); 7.10–7.19 (m, 1H, ArH); 7.19–7.26 (m, 1H, ArH); MS (EI, 70 eV): 188, 186 (M<sup>+</sup>, 72); 107 (–Br, 100).

2,4-dibromo-6-methylphenol: <sup>1</sup>H NMR (CDCl<sub>3</sub>, 300 MHz, 298 K): 2.28 (s, 3H, CH<sub>3</sub>); 4.92 (s, 1H, OH); 7.02 (s, 1H, ArH); 7.24 (s, 1H, ArH); MS (EI, 70 eV): 268 (52), 266 (100), 264 (53); 187 (70); 185 (70).

## Acknowledgements

Financial support of the German Ministry of Science and Education (bmbf; Lighthouse Project “Sustainable Aromatic Chemistry”) and the Fonds der Chemische Industrie is gratefully acknowledged.

## References

- I. P. Beletskaja and A. V. Cheprakov, *Chem. Rev.*, 2000, **100**, 3009.
- A. Butler and J. V. Walker, *Chem. Rev.*, 1993, **93**, 1937.
- G. Rothenberg and J. H. Clark, *Green Chem.*, 2000, **2**, 248–251 and references therein.
- M. Battacharjee, *Polyhedron*, 1992, **11**, 2817; B. M. Choudary, Y. Udha and P. N. Reddy, *Synlett*, 1994, 450; K. Smith, P. He and A. Taylor, *Green Chem.*, 1999, **1**, 35; U. Bora, G. Bose, M. K. Chaudhuri, S. S. Dhar, R. Gopinath, A. T. Khan and B. K. Patel, *Org. Lett.*, 2000, **2**, 247; G. Rothenberg and J. H. Clark, *Org. Process Res. Dev.*, 2000, **4**, 270; N. Narender, K. V. V. Krishna Mohan, R. Vinod Reddy, P. Srinivasu, S. J. Kulkarni and K. V. Ragavan, *J. Mol. Catal. A: Chem.*, 2003, **192**, 73; J. Salazar and R. Dorta, *Synlett*, 2004, 1318.
- R. Neumann and I. Asael, *J. Chem. Soc., Chem. Commun.*, 1988, 1285; E. J. Pressman, J. Y. Ofori, G. L. Soloveichik, J. L. Male and R. C. Mills, *US Pat.* 01431442004; G. L. Soloveichik, *US Pat.* 0049441, 2005; E. J. Pressman, J. L. Male, R. C. Mills and J. Y. Ofori, *US Pat.* 0059843, 2005; R. C. Mills and J. Y. Ofori, *US Patent* 0049440, 2005.
- R. Raja and P. Ratnasamy, *J. Catal.*, 1997, **170**, 244.
- G. Zhang, R. Liu, Q. Xu, L. Ma and X. Liang, *Adv. Synth. Catal.*, 2006, **348**, 862.
- K. V. V. Krishna Mohan, N. Narender, P. Srinivasu, S. J. Kulkarni and K. V. Rhagavan, *Synth. Commun.*, 2004, **34**, 2143.
- Chemical Synthesis Using Supercritical Fluids*, ed. P. G. Jessop and W. Leitner, Wiley-VCH, Weinheim, 1999; A. Baiker, *Chem. Rev.*, 1999, **99**, 453; P. Licence, J. Ke, M. Sokolova, S. K. Ross and M. Poliakoff, *Green Chem.*, 2003, **5**, 99; W. Leitner, *Acc. Chem. Res.*, 2002, **35**, 746.
- S. A. Nolen, J. Liu, J. S. Brown, P. Pollet, B. C. Eason, K. N. Griffith, R. Gläser, D. Bush, D. R. Lamb, C. L. Liotta and C. A. Eckert, *Ind. Eng. Chem. Res.*, 2002, **41**, 316.
- D. E. Richardson, H. Yao, K. M. Frank and D. A. Bennett, *J. Am. Chem. Soc.*, 2000, **122**, 1729.
- H. Yao and D. E. Richardson, *J. Am. Chem. Soc.*, 2000, **122**, 3220.
- D. A. Bennett, H. Yao and D. E. Richardson, *Inorg. Chem.*, 2001, **40**, 2996.
- N. Theyssen, Z. Hou and W. Leitner, *Chem.-Eur. J.*, 2006, **12**, 3401 and references therein.
- I. V. Zakharov, Y. V. Geletii and V. A. Adamyan, *USSR Pat.*, SU1623947, 1991.
- Solubility of phenol and *p*-bromophenol in water at 25 °C and pH = 7 are 80 g L<sup>-1</sup> and 25 g L<sup>-1</sup> respectively.

# Synthesis and applications of superacids. 1,1,2,2-Tetrafluoroethanesulfonic acid, supported on silica

Mark A. Harmer,<sup>\*a</sup> Christopher Junk,<sup>a</sup> Vsevolod Rostovtsev,<sup>a</sup> Liane G. Carcani,<sup>a</sup> Jemma Vickery<sup>b</sup> and Zoe Schnepf<sup>b</sup>

Received 24th May 2006, Accepted 15th September 2006

First published as an Advance Article on the web 2nd October 2006

DOI: 10.1039/b607428f

In this paper we focus on the synthesis and use of superacids, in particular 1,1,2,2-tetrafluoroethanesulfonic acid (TFESA), and describe how these can be optimized for reactions of key industrial importance. One area of considerable interest is the field of superacid catalysis and, specifically, the development of safer and more cost-effective acid catalysts. We report a new simplified route for preparation of these acids, making these more readily available and opening up a large number of opportunities. Partially fluorinated superacids offer several advantages over the acids commonly used in catalysis (sulfuric, hydrofluoric acid and aluminium chloride): lower loadings, lower reaction temperatures (leading to increased selectivity), fewer by-products, shorter reaction times and higher throughput. TFESA and its longer chain analogs are much less volatile than triflic acid (CF<sub>3</sub>SO<sub>3</sub>H). We tested these superacids in several processes (aromatic alkylation, acylation of arenes, isomerization, oligomerization and the Fries rearrangement). These materials are excellent acid catalysts, comparable to triflic acid, and yet easier to handle. We have also prepared supported versions of these catalysts and introduced the ability to recycle.

## Introduction

Sustainable growth is critical for both highly developed and developing countries. The term 'sustainable growth' is best defined as a way to meet societal needs while reducing our environmental footprint. From an industrial point of view this offers a wide variety of opportunities. These include the development of materials from renewable resources (such as alcohols from corn, and the production of bio-derived polymers), the optimization of industrial processes by catalysis (such as replacing homogeneous catalysts with heterogeneous ones), improvements in atom economy, development of renewable sources of energy, optimization of energy conversion using new technologies such as fuel cells and the continued development of hybrid car engines.<sup>1</sup>

In this paper we focus on the use of Brønsted superacidic catalysts and describe how these can be utilized for a number of acid catalyzed reactions of industrial importance. We also show that supported versions of these acids show superior properties to the free acid. Traditional homogeneous acids such as hydrofluoric (exceptionally hazardous) and sulfuric acids (often has been used in large volumes relative to the reactants) have a number of drawbacks in industrial processes and, furthermore, generate large amounts of waste associated with the separation of the product. Replacing these acids with highly active catalysts (such as superacids) that can be recycled and easily separated reduces waste, reduces energy needs, cuts down the process time and makes the overall process both safer and more economical. Superacidic materials are finding

uses in an increasingly wide range of industrial applications. For example, triflic acid is already employed in fine chemical synthesis, batteries, and ionic liquids (anions). Interest in these materials is growing.<sup>2-4</sup>

A useful starting point in discussion of superacidic materials is the subject of acid strength. Superacids are defined as having a Hammett acidity constant ( $H_0$ ) of greater than  $-12$ . In essence, they are acids that are stronger than 100% H<sub>2</sub>SO<sub>4</sub>.<sup>5</sup> It is exactly this property that gives these materials many advantages over traditional acids such as HF. The higher acid strength means that smaller amounts of acid can often be used. These superacids can also catalyze reactions at temperatures that are lower than those of sulfuric acid-catalyzed processes. In industrial catalysis, this can mean the difference between handling vast quantities of H<sub>2</sub>SO<sub>4</sub>, with all the inherent hazards it entails, compared to a small amount of a highly active alternative. Sulfuric acid is also inherently quite reactive which can, in turn, lead to unwanted by-products. These include sulfonate esters (reactions with alcohols) and also sulfonation of aromatic rings (arising from the oxidizing ability of sulfuric). Sulfate esters have to be removed by additional processing steps that lead to poorer yields (lower atom efficiency), additional work up costs and more waste. Triflic acid and the acids described in this paper do not suffer from the same drawbacks. The anion, TFES, is non-coordinating and the formation of sulfate type esters is not a problem.

This paper focuses on the largely unused classes of superacids of the form RCHF<sub>2</sub>SO<sub>3</sub>H (R = F, Cl or fluoroalkyl). Although our research has included the potential of these materials for various applications, the main focus has been the use of these acids for catalysis. We also emphasize three aspects: the safe delivery of superacids, the effective use of superacids, and acid recycling.

<sup>a</sup>DuPont Central Research and Development, Experimental Station, Wilmington, Delaware, 19880, USA.

E-mail: Mark.A.Harmer@USA.DuPont.Com

<sup>b</sup>School of Chemistry, University of Bristol, UK

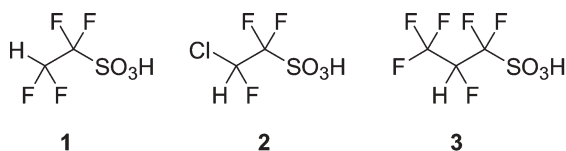
The importance of acid catalysts in industry cannot be overstated. Acid catalysts, are employed in an extensive range of commercial reactions: alkylations, acylations, rearrangements and oligomerizations. Alkylations are common in the commercial production of ethyl benzene, trimethylpentane for the surfactants industry. Traditionally, homogeneous acid catalysts such as  $\text{AlCl}_3$ ,  $\text{FeCl}_3$ ,  $\text{H}_2\text{SO}_4$ ,  $\text{HF}$  and  $\text{BF}_3$ , are employed.<sup>6,7</sup> Isomerization and olefin oligomerization are used in refining and preparation of lubricants.<sup>8</sup> Acylation, a key reaction for the fine chemicals industry, currently utilizes  $\text{AlCl}_3$  or catalytic quantities of hazardous  $\text{HF}$ .<sup>9–11</sup> Fries reaction is used in the production of hydroxyacetophenone, an important precursor for the formation of the painkiller *p*-hydroxyacetanilide, and is promoted by  $\text{BF}_3$ .<sup>11</sup>

There are several problems associated with the traditional acid catalysts described above. The hazards of hydrofluoric acid pose severe dangers to people and the environment during both transportation and usage. Lewis acids such as  $\text{FeCl}_3$  and  $\text{AlCl}_3$  often need to be used in stoichiometric quantities, and subsequently create sizable waste streams. The current drive to use solid acid catalysts solves some of these issues, decreasing waste generation.<sup>11–13</sup> As a result, recyclable materials and reduced waste lead to a more economical processes. However, it is very likely that both liquid and solid acids will be used in the foreseeable future.

Here, we describe the preparation and properties of fluoro-alkylsulfonic acids such as 1,1,2,2-tetrafluoroethanesulfonic (TFESA) and 1,1,2,3,3,3-hexafluoropropanesulfonic (HFPSA) acids. We expect the acidity functions of these acids to be similar to triflic acid ( $\text{CF}_3\text{SO}_3\text{H}$ ). As we discuss below, the catalytic conversions for a range of reactions are comparable to triflic acid. This is usually a reasonable guide for acid strength. The acidity function of  $\text{CF}_3\text{SO}_3\text{H}$  for example is similar to  $\text{CF}_3\text{CF}_2\text{SO}_3\text{H}$  ( $H_0$  of  $-14.1$  and  $-14$  respectively). It is also known that appending a sulfonic acid group to either a  $\text{CF}_2$  or  $\text{CF}_2$  group such as  $\text{CF}_2\text{CF}_2$  does not alter the acidity significantly.<sup>14</sup> A range of applications of these acids as well as supported versions of TFESA will be described.

## Results and discussion

Triflic acid is a well-known and commercially available superacid.<sup>2,11</sup> In this paper we describe the synthesis of three alternate superacids (1–3) and a supported version of one of them (TFESA, 1). This paper will focus mainly on 1,1,2,2-tetrafluoroethanesulfonic acid (1). Compared to triflic, these acids have lower volatility which translates to ease of handling.



- 1, 1,1,2,2-tetrafluoroethanesulfonic acid (TFESA)
- 2, 1,1,2-trifluoro-2-chloroethanesulfonic acid
- 3, 1,1,2,3,3,3-hexafluoropropanesulfonic acid (HFPSA)

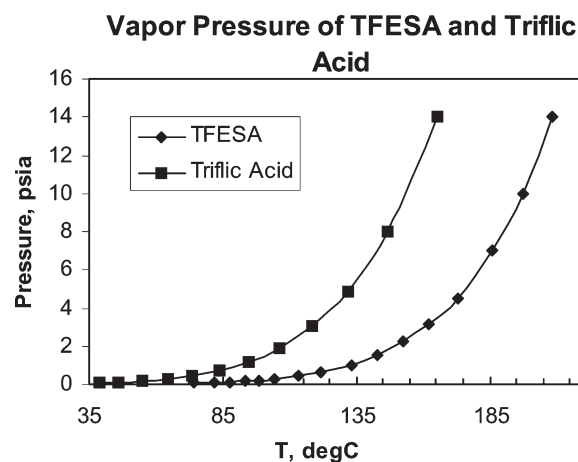


Fig. 1 Vapour pressures of TFESA and triflic acid.

The boiling point of 1 (210 °C) is higher than that of triflic (165 °C) or hydrofluoric (19 °C) acid. Vapour pressures of the two acids are compared in Fig. 1. The lower vapour pressure of TFESA makes handling of the acid easier, improving safety. The higher boiling point also increases the processing window during which these acids may be used. A simple illustration showing the reduced volatility is shown in Fig. 2.

In addition, all compounds under discovery in this article contain a hydrogen on the second carbon which acts as a spectroscopic fingerprint in the proton NMR spectrum, Fig. 3. This feature is especially useful in several ways, one of which is determining any potential contamination of the product with the acid. In biphasic type reactions NMR can also be used to determine distribution coefficients of the acid.

In terms of the synthesis, TFESA was first synthesized by Barrick.<sup>15</sup> Subsequently, we have made a number of improvements in the synthesis.<sup>16</sup> The literature describe the use of free radical initiators to facilitate the addition of the sulfite ion to fluorinated double bonds. We found that the reaction works



Fig. 2 Visual comparison of triflic acid (left vial, 1 g) to TFESA (right vial, 1 g) in air after 1 min.

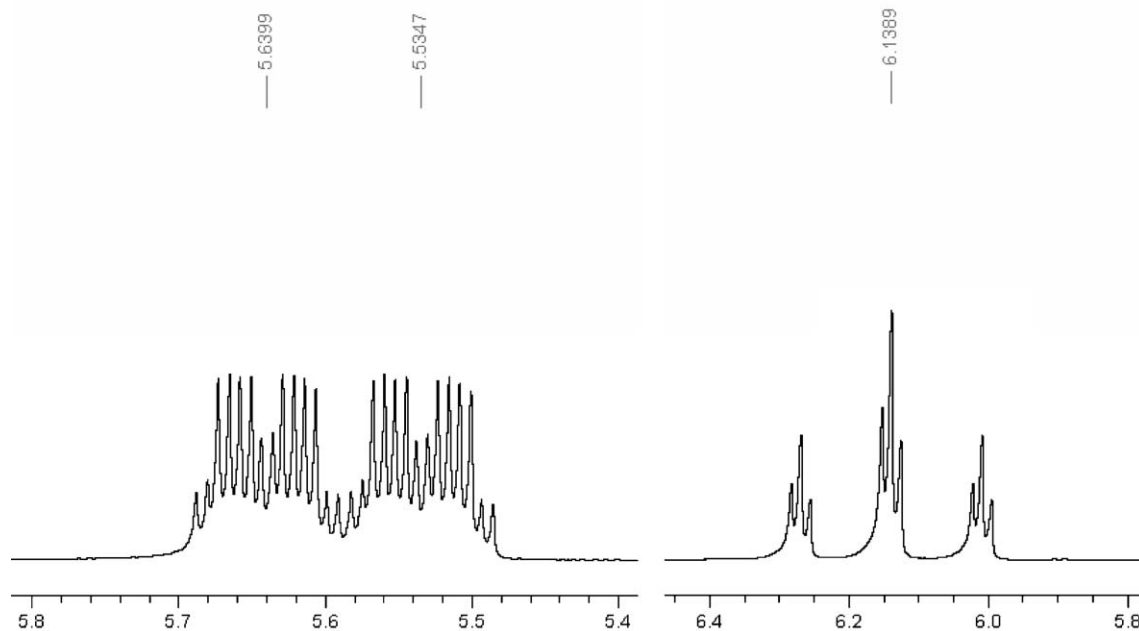
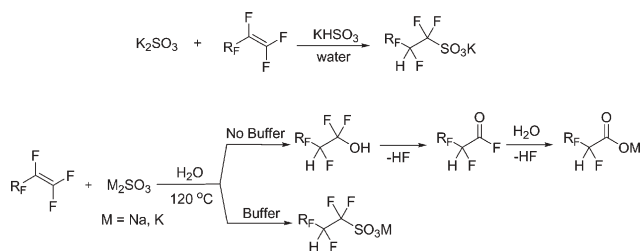


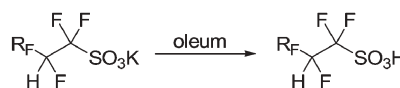
Fig. 3  $^1\text{H}$  NMR of **3** (left) and **1** (right) in  $\text{CDCl}_3$ .

well in the absence of the initiators and that it most likely occurs through a nucleophilic attack by the sulfite. The fluorinated carbanion, which is formed after sulfite addition, is protonated by water. In the absence of a buffer, the result is an increasingly basic solution that promotes hydrolysis of tetrafluoroethylene to the unwanted by-product difluoroacetate ( $\text{HCF}_2\text{COOM}$ ), as well as the desired product. Acidity of the reaction mixture can be conveniently controlled by a buffer solution comprised of sulfite and bisulfite ions. At pH 5–6, fluoroalkylsulfonates were obtained in high yields with little or no difluoroacetate impurities. Careful attention to pH (to prevent formation of the difluoroacetate) leads to better product selectivity (typically >99%).



We have also found that sulfite addition to TFE can also be achieved by using TFE/ $\text{CO}_2$  mixtures. In this case the carbon dioxide acts as an internal buffer, again leading to greater selectivity.

Conversion of dried sulfonates to the corresponding acid is accomplished by distillation from oleum in one step. Alternatively, a two-step procedure can be used. First, acid hydrate is distilled from concentrated sulfuric acid. In the second step, it is dehydrated in thionyl chloride and redistilled again to afford anhydrous superacids. In summary, sulfite addition to TFE proceeds smoothly, with high selectivity, and high yield.



| $\text{R}_\text{F}$ | overall yield |
|---------------------|---------------|
| F                   | 85%           |
| $\text{CF}_3$       | 84%           |

We investigated a number of reactions of industrial importance using the liquid superacids. These include the formation of linear alkyl benzenes (LAB), acylation, the Fries reaction, olefin isomerization and olefin oligomerization (Scheme 1).

High catalytic conversions were obtained demonstrating the utility of these Brønsted acids, except in the case of olefin isomerization and oligomerization, where the immiscibility of these polar acids with the reaction mixture diminished the catalyst's activity. The results are shown below in Table 1.

In alkylation reactions all of the superacids tested show quite high catalytic conversion and in all cases higher conversion was found compared to sulfuric acid. The formation of linear alkyl benzenes has been recently reviewed.<sup>6,7</sup>

These materials, when sulfonated, represent the basis of the detergents industry. In the current commercial process, HF is used as the catalyst and there is an obvious drive to replace this hazardous material. The products of these reactions contain a mixture of alkylbenzenes with the phenyl group attached to different carbon atoms in the linear hydrocarbon chain. The 2-phenyl isomer is the most preferred product. Branched isomers, which are a result of a skeletal isomerization of the linear hydrocarbon chain, are very undesirable due to lower biodegradability. For all of the superacids tested, catalytic conversions of 95–99% were obtained at 100 °C using xylene as the aromatic. The products contain >95% LABs and the rest (<5%) are the branched alkylates derived from the ~4% branched olefins present in the feed, dimers of 1-dodecene and disubstituted benzene. The linearity of the alkylation using 1-dodecene is >99%. Sulfuric acid at a similar loading showed



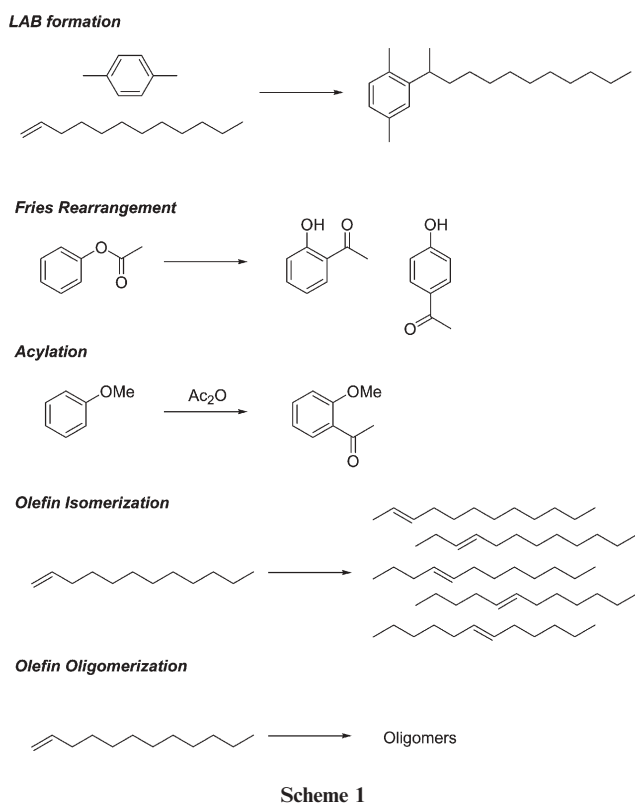


**Table 1** Catalytic activity of superacids and sulfuric acid in the acylation, Fries and alkylation reactions. Numbers shown refer to reactant % conversion (acetic anhydride, phenyl acetate and 1-dodecene, respectively)

| Catalyst type                                      | Acylation <sup>a</sup> | Fries Reaction <sup>b</sup> | Alkylation <sup>c</sup> |
|--|------------------------|-----------------------------|-------------------------|
| HCF <sub>2</sub> CF <sub>2</sub> SO <sub>3</sub> H | 63                     | 71                          | 99                      |
| CF <sub>3</sub> HCF <sub>2</sub> SO <sub>3</sub> H | 59                     | 69                          | 98                      |
| HClCF <sub>2</sub> SO <sub>3</sub> H               | 58                     | 49                          | 95                      |
| CF <sub>3</sub> SO <sub>3</sub> H                  | 61                     | 58                          | 98                      |
| H <sub>2</sub> SO <sub>4</sub>                     | 10                     | —                           | <5                      |

<sup>a</sup> 100 mmol anisole, 100 mmol acetic anhydride at 1 h, 100 °C, 0.5 g of catalyst. <sup>b</sup> 25 g of phenylacetate after 4 h at 140 °C, 0.5 g of catalyst. <sup>c</sup> aromatic alkylation, 15 g of *p*-xylene and 5 g of 1-dodecene after 1 h at 100 °C, 0.5 g of superacid catalyst.

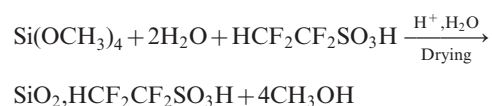
very low activity. Much higher loadings (approx. 20–30 wt% sulfuric) were needed to obtain comparable conversions.

Superacids are also finding increasing uses in fine chemicals synthesis.<sup>2</sup> It is well known that the traditional catalysts used in acylation chemistry and the Fries reaction (used in the manufacture of an ibuprofen intermediate) suffer from several drawbacks, mainly the use of stoichiometric amounts of catalysts (AlCl<sub>3</sub>, BF<sub>3</sub>). This leads to extensive problems with the disposal of the associated waste streams. Again, the above superacids are all active in catalytic amounts and we believe the higher boiling superacids may have the additional advantage of ease of handling due to lower volatility. A number of papers have recently been published on the use of triflic acid and metal triflates, which have been recycled using ionic liquids as a reaction media.<sup>17,18</sup> The ability to recycle is also important in terms of using these acids.

These acids were also investigated in the isomerization and oligomerization of 1-dodecene. The liquid superacids showed

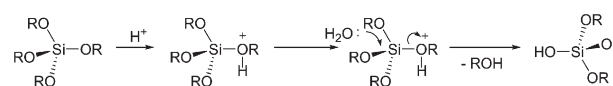
<1% conversion, essentially inactive. This can be explained by the immiscibility in the polar superacids and the non-polar reactant 1-dodecene. This problem was circumvented by developing solid supported versions of these acids. In comparison these show exceptionally high conversion for these same reactions.

Silica supported superacids were prepared using both *in situ* sol-gel method and infiltration into pre-formed porous silica supports. In the case of *in situ* sol-gel, tetramethoxysilane was pre-hydrolysed with an excess of water. TFESA was then added in amounts such that the final loading was between 5 and 75 wt%. Upon addition of the acid a clear homogeneous solution formed, which gelled upon drying in an oven overnight (in nitrogen atmosphere at 80 °C). This procedure gives a hard, glass-like composite with the superacid highly dispersed within and throughout the silica network. Porous particles a few mm in size result.

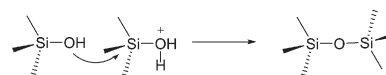


The first step of this process is a hydrolysis of the alkoxides. The mechanism for this hydrolysis (catalysed by a small amount of an acid such as HCl) is well known (below) and results in the formation of polysilicic acid (Si(OH)<sub>4</sub>, not shown).<sup>19</sup> Condensation occurs either by the reaction of two Si-OH groups or reaction of SiOH with SiOR groups leading to the formation of an extended silica network. These two steps occur simultaneously, although in the case of acid-catalyzed reactions hydrolysis occurs rapidly (minutes) followed by slower condensation (hours) at higher temperatures (typically 80 °C) and during the drying stages.

*The acid-catalyzed hydrolysis of a silicon alkoxide*



*Condensation of a neutral silanol group (Si-OH) attacking a silicon centre*



The optimum microstructure (in terms of an acid catalyst) had an acid loading of about 15 to 25 wt% of acid, surface area of about 439 m<sup>2</sup> g<sup>-1</sup>, pore volume 0.74 cc g<sup>-1</sup> and an average pore diameter of about 67 Å. We compared a 5, 25 and 50 wt% containing composite (weight of HCF<sub>2</sub>CF<sub>2</sub>SO<sub>3</sub>H in silica, same moles of acid used in catalysis, in the 1-dodecene alkylation of *p*-xylene). The resulting conversion of the 1-dodecene had values of 50, 82 and 40% respectively (100 °C, 2 hr. reaction time, Table 2). The highest catalytic conversion, had an acid loading within the silica of 25 wt%. A more detailed description will be published separately showing the optimization of the microstructure (in terms of catalyst loading, pore size and surface area). We also found that, in terms of acid stability, the acid does not leach in non-polar solvents such as benzene, hexanes, olefins, toluene and xylenes.

The distribution of the acid in the silica can be inferred by examining pore volume, surface area and pore diameter of the

**Table 2** Catalytic activity of liquid and supported superacid

| Catalyst type   | Alkylation (%) <sup>a</sup> | Isomerization (%) <sup>b</sup> | Oligomerization (%) <sup>c</sup> | Acylation (%) <sup>d</sup> |
|---|-----------------------------|--------------------------------|----------------------------------|----------------------------|
| HCF <sub>2</sub> CF <sub>2</sub> SO <sub>3</sub> H        | 10                          | <2                             | <2                               | 65                         |
| Silica/HCF <sub>2</sub> CF <sub>2</sub> SO <sub>3</sub> H | 82                          | 99                             | 90                               | 68                         |

<sup>a</sup> 15 g of *p*-xylene and 5 g of 1-dodecene after 1 h at 100 °C, 1 g of 25 wt% supported catalyst and 0.25 g of HCF<sub>2</sub>CF<sub>2</sub>SO<sub>3</sub>H. <sup>b</sup> 25 g of 1-dodecene after 30 min at 100° with 1 g of supported acid. <sup>c</sup> 25 g of 1-dodecene after 30 min at 120 °C with 1 g of supported acid. <sup>d</sup> 100 mmol anisole, 100 mmol acetic anhydride after 1 h at 100 °C with 1 g of supported acid.

TFESA/silica network compared to the network where the acid had been leached out (using ethanol). A large increase in pore volume with small increase in pore diameter is consistent with an acid, highly dispersed within and throughout the silica network. The resulting acid-leached silica network had a pore structure (in the case of a 25 wt% containing microstructure as described above) with a surface area of about 540 m<sup>2</sup> g<sup>-1</sup>, pore volume of 0.93 cc g<sup>-1</sup> and a pore diameter of about 70 Å. The higher pore volume is consistent with the removal of the acid and a small increase in pore diameter noted (with no evidence for large pockets of extra pores).

In addition to the *in situ* route, we also found silica/superacid composites could be made by infiltration of pre-formed supports (Fig. 4). The as-received support has a surface area of about 345 m<sup>2</sup> g<sup>-1</sup>, pore volume 1.22 cc g<sup>-1</sup> and a pore diameter of about 141 Å.

This pre-formed spherical support was infiltrated with an diethylether containing TFESA solution. The ether was then removed leaving the silica/TFESA catalyst. Again, the optimum loading was 15–25 wt% of TFESA. Comparison of the silica-supported TFESA prepared by the two approaches revealed that both afforded highly active catalysts for a range of reactions. In non-polar media the TFESA/silica showed higher catalytic conversion in a number of reactions, compared to the TFESA acid.

The silica-supported acids were surprisingly stable in terms of volatility. For example, 1 g of the free acid (TFESA) completely vaporizes when heated to 150 °C under a vacuum (2 h), whereas 85% of the acid in the silica-support was retained (even after 18 h). The TFESA/silica composite was also more stable than the triflic acid/silica composite. A triflic acid containing silica at a similar loading retained about 40 wt% of the original acid after 18 h. From a safety and handling point of view, this feature (very low volatility within

**Fig. 4** Silica supported TFESA (@1.5 mm beads).

the silica) makes these materials especially attractive for use in a wide variety of applications. Another advantage of the increase in stability is catalyst drying. Bronsted acids typically pick up moisture and have to be dried. The TFESA/silica composite can be readily dried with only a small amount of acid loss. The exact nature of the interaction within the support is not known, however the reduced volatility is consistent with hydrogen bonding of the silanols to the acids.

The catalytic conversion of these silica-supported acids was exceptionally high for a number of reactions. Four different types of reactions were investigated to compare the free and the supported acid, (Table 2). In the case of a non-polar reaction mix, very little leaching of the acid occurs. These materials behave as solid acid catalysts (heterogeneous catalysts) with all of the expected advantages compared to homogeneous catalysts. Advantages include ease of product separation, high activity, and the ability to recycle the catalyst. From an industrial point of view, this results in less waste and, inevitably, better economics.

The silica-supported superacids show high conversion in the alkylation of *p*-xylene with 1-dodecene. The conversion is higher than the homogeneous acid itself (Table 2). The product is easy to separate from the catalyst and the catalyst can be easily recycled. At 100 °C, the supported acid shows almost complete conversion after 15 min, in contrast to the liquid TFESA (10% conversion, same molar amounts of acid in each case), Fig. 5. In these studies we reduced the acid loading (essentially 0.25 g vs. 0.5 g of TFESA, see Table 1) to highlight differences. Both the *in situ* sol-gel-derived material and the infiltrated pre-formed material had about the same activity. The extent of leaching was low, with values of about 0.2 to 0.5%, respectively, for a number of alkylation reactions, with about 99.8% of the acid retained within the silica. In a typical study the reaction products were separated from the catalyst and the acid content was determined, both in the organic phase (alkylate phase) and in the silica containing acid phase (see Experimental). We carried out the analogous reaction using a triflic-supported catalyst. The activity was quite low (40% compared to 82% using the TFESA) due to loss of the volatile triflic acid during the supported catalyst preparation and drying stage. The silica-supported TFESA catalyst was recycled twice with a slight decrease in activity (conversions for the 1-dodecene alkylation of *p*-xylene at 1 h of 98, 97, and 94%, three recoveries).

Olefin isomerization was also investigated. The isomerization of long chain olefins is often carried out using large amounts of sulfuric acid, and the isomerized product is subsequently used as a component in lubricants. Olefin isomerization involving *cis-trans*-transformation, or double

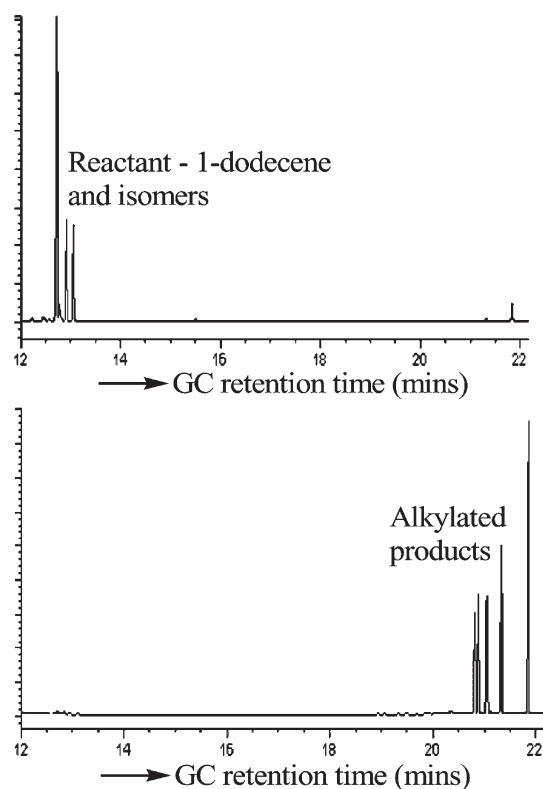


**Fig. 5** GC of the reaction of *p*-xylene (15 g, peaks not shown) with dodecene (5 g, GC retention time 13 min), after 15 min reaction time at 100 °C using liquid TFESA (0.25 g), top, and SiO<sub>2</sub>/TFESA (1 g, 25 wt% loading), bottom, showing higher activity of the supported superacid (*y* axis—*a*/units). Peaks of the alkylated product are found around 21 to 22 min.

bond migration, is relatively easy chemistry.<sup>20</sup> However, many solid acid catalysts quickly deactivate. The olefin isomer products are useful in the formulation of well fluids such as drilling mud, useful for offshore drilling. An Amoco patent by Clarambeau and Steylaerts used Amberlyst<sup>®</sup>, Nafion<sup>®</sup> resin pellets and Nafion<sup>®</sup> resin/silica composites to catalyze the isomerization of terminal olefins with 14 to 20 carbon atoms.<sup>20</sup> The catalysts described herein (impregnation of a pre-formed support) are simpler than the Nafion<sup>®</sup> resin-based systems and may become viable alternatives. Whereas the free acid showed virtually no catalytic activity in this reaction, the supported TFESA catalyst showed equilibrium conversion to the six isomers within about 15 min at 80 °C.

Oligomerization was also found to occur at higher temperatures (120 °C). 1-Dodecene is oligomerized to the dimers and trimers, again with high conversion (>95% of 1-dodecene, Fig. 6). Propylene oligomerization to C<sub>6+</sub> olefins, the famous UOP catalytic condensation process, catalyzed by solid phosphoric acid has been widely used in the petroleum industry for more than 70 years.<sup>12</sup> The oligomerization is typically carried out in a fixed bed reactor at supercritical conditions, *e.g.* ~200 °C and 1000 psig. The products are used as petroleum fuels. There is interest in finding replacements for the currently used catalyst, phosphoric acid, on silica. Both types of pre-formed catalysts (based on *in situ* and pre-formed silica) show high activity for dodecene oligomerization.

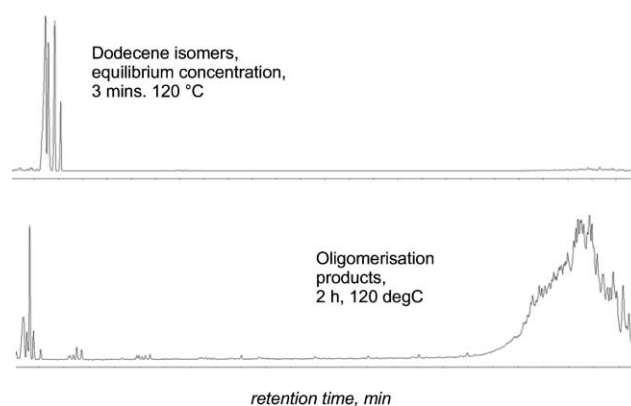


**Fig. 6** GC traces of the reaction of 1-dodecene (20 g) after 3 min (top) and 2 h (bottom) at 120 °C using TFESA/SiO<sub>2</sub> (0.5 g each) showing rapid isomerization followed by oligomerization. (*y* axis—*a*/units).

Therefore, these materials have tremendous potential for use in reactions of industrial importance.

In summary, superacid catalysts based on fluoroalkylsulfonic acids can be produced *via* addition of sulfites to fluorinated olefins in buffered solutions. Catalysts of this type represent an important class of superacid catalysts. New, simplified and high-yielding routes to these compounds open up a wide variety of opportunities. The relatively low volatility and high boiling point translate to safer handling of these materials. Supported versions of these acids enable reactions in non-polar reaction media. The silica supported superacids described in this paper have been found to show high catalytic activity with low leaching in a number of reactions of industrial importance.

## Experimental

### Synthesis of TFESA

A 1-gallon Hastelloy C276 reaction vessel was charged with a solution of 175 g potassium sulfite hydrate (K<sub>2</sub>SO<sub>3</sub>·xH<sub>2</sub>O, 95%, Aldrich), 610g potassium metabisulfite (K<sub>2</sub>S<sub>2</sub>O<sub>5</sub>, 99%, Mallinckrodt) and 1500 mL of deionized water. The vessel was cooled to -35 °C, evacuated and then purged with nitrogen. The evacuate/purge cycle was repeated two more times. The vessel was heated to 120 °C. To the vessel was then added 500 g of tetrafluoroethylene *via* slow addition keeping the pressure below 200 psi. The total reaction time to complete the addition was about 5–6 hours. The reaction was allowed to cool to room temperature before venting excess gases and rinsing the reaction mixture from the shaker tube with deionised water. The water was removed in vacuum and the potassium salt was extracted with acetone. <sup>19</sup>F NMR (D<sub>2</sub>O) δ: -122.0 (dt, <sup>3</sup>J<sub>FH</sub> = 6 Hz, <sup>3</sup>J<sub>FF</sub> = 6 Hz, 2F); -136 (dt, <sup>2</sup>J<sub>FH</sub> = 53 Hz, 2F), consistent with tetrafluoroethanesulfonate (TFES-K). <sup>1</sup>H NMR (D<sub>2</sub>O) δ 6.4 (tt, <sup>2</sup>J<sub>FH</sub> = 53 Hz, <sup>3</sup>J<sub>FH</sub> = 6 Hz, 1H). The acetone layer was removed, filtered, and then dried. This was then added to an excess of sulfuric and followed by addition of thionyl chloride to generate the dehydrated acid, which was purified by distillation (around 110 °C) on a vacuum line. Alternatively, a 100 mL round bottomed flask with a sidearm and equipped with a digital thermometer and magnetic stir bar was placed in an ice bath under positive nitrogen pressure. To the flask was

added 45 g crude TFES-K (potassium and sodium salts can be used interchangeably), 30 g of concentrated sulfuric acid (95–98%) and 78 g oleum (20 wt% SO<sub>3</sub>) while stirring. The amount of oleum was chosen such that there would be a slight excess of SO<sub>3</sub> after the SO<sub>3</sub> reacted with and removed the water in the sulfuric acid and the crude TFES-K. The mixing caused a small exotherm, which was controlled by the ice bath. Once the exotherm was over, a distillation head with a water condenser was placed on the flask, and the flask was heated under nitrogen behind a safety shield. The pressure was slowly reduced using a PTFE membrane vacuum pump (Buchi V-500) in steps of 1.93 psi (100 Torr) in order to avoid foaming. A dry-ice trap was placed between the distillation apparatus and the pump to collect any excess SO<sub>3</sub>. When the pot temperature reached 120 °C and the pressure was held at 0.38 psi (20 Torr) a colorless liquid started to reflux which distilled at 110 °C and 0.57 psi (31 Torr). Proton NMR and analysis showed the product, TFESA, was greater than 99.5% pure with an overall yield of about 85%. Analysis gave the following results: <sup>19</sup>F NMR (CD<sub>3</sub>OD) δ: –125.2 (dt, <sup>3</sup>J<sub>FH</sub> = 6 Hz, <sup>3</sup>J<sub>FF</sub> = 8 Hz, 2F); –137.6 (dt, <sup>2</sup>J<sub>FH</sub> = 53 Hz, 2F). <sup>1</sup>H NMR (CD<sub>3</sub>OD) 6.3 (tt, <sup>3</sup>J<sub>FH</sub> = 6 Hz, <sup>2</sup>J<sub>FH</sub> = 53 Hz, 1H).

#### Synthesis of 1,1,2,3,3,3-hexafluoropropanesulfonic acid (HFPSA):

A 1-litre Hastelloy® C 276 reaction vessel was charged with a solution of anhydrous sodium sulfite (25 g, 0.20 mol), sodium bisulfite 73 g, (0.70 mol) and deionized water (400 ml). The pH of this solution was 5.7. The vessel was cooled to 4 °C, evacuated and then charged with hexafluoropropene (HFP, 120 g, 0.8 mol). The vessel was heated with agitation (1000 rpm) to 120 °C and kept there for 3 hr. The pressure rose to a maximum of 335 psi and then dropped down to 32 psi within 30 minutes. At the end, the vessel was cooled and the remaining HFP was vented, and the reactor was purged with nitrogen. The final solution had a pH of 7.3. The water was removed *in vacuo* on a rotary evaporator to produce a wet solid. The solid was then placed in a vacuum oven 140 degrees C, 48 hr) to produce 219 g of white solid which contained approximately 1 wt% water. The theoretical mass of total solids was 217 g. The crude HFPS-Na can be further purified and isolated by extraction with reagent grade acetone, filtration, and drying. A 100 mL round bottomed flask with a sidearm and equipped with a digital thermometer and magnetic stir bar was placed in an ice bath under positive nitrogen pressure. To the flask was added 50 g crude sodium hexafluoropropanesulfonate (HFPS-Na), 30 g of concentrated sulfuric acid (95–98%) and 58.5 g oleum (20 wt% SO<sub>3</sub>) while stirring. The amount of oleum was chosen such that there would be a slight excess of SO<sub>3</sub> after the SO<sub>3</sub> reacted with and removed the water in the sulfuric acid and the crude HFPSA. The mixing caused a small exotherm, which was controlled by the ice bath. Once the exotherm was over, a distillation head with a water condenser was placed on the flask, and the flask was heated under nitrogen behind a safety shield. The pressure was slowly reduced using a PTFE membrane vacuum pump in steps of 1.93 psi (100 Torr) in order to avoid foaming. A dry-ice trap was placed between the distillation apparatus

and the pump to collect any excess SO<sub>3</sub>. When the pot temperature reached 100 °C and the pressure was held at 0.38 psi (20 Torr) a colorless liquid started to reflux and later distilled at 118 °C and 0.57 psi (23 Torr). A forerun of lower-boiling impurity (1.5 g) was obtained before collecting 36.0 g of the desired acid, hexafluoropropanesulfonic acid (HFPSA). An 84% overall yield from HFP was obtained. <sup>19</sup>F NMR (D<sub>2</sub>O) δ: –74.5 (m, 3F); –113.1, –120.4 (ABq, *J* = 264 Hz, 2F); –211.6 (m, 1F). <sup>1</sup>H NMR (D<sub>2</sub>O): 5.8 (m, <sup>2</sup>J<sub>FH</sub> = 43 Hz, 1H).

#### Synthesis of 1,1,2-trifluoro-2-chloroethanesulfonic acid

The 1,1,2-trifluoro-2-chloroethanesulfonic acid was prepared according to the procedure described for HFPSA, but using 1,1,2-trifluoro-2-chloroethene instead of HFP. Obtained yields were *ca.* 80%.

#### Synthesis of TFESA/Silica

Tetramethylorthosilicate (TMOS, 160 g), water (188 g) and HCl (0.1 M, 1 g) were stirred together for 20 minutes to hydrolyze the tetraalkoxide. HCF<sub>2</sub>CF<sub>2</sub>SO<sub>3</sub>H (20 g) was then added and the mixture left stirring for three hours in an open jar at room temperature. The resulting (still liquid) mixture was placed in a 80 °C oven for 2 days to gel and harden. Drying was completed in a 100 °C vacuum oven for 24 h. Pore diameter and volume were measured by BET method.

#### Catalyst testing

All reagents were reagent grade. The catalyst (solid) was dried at 150 °C overnight before use under vacuum. Acylation: the acid catalyst was added to a dry round bottom flask under a nitrogen atmosphere and anisole 100 mmole and acetic anhydride (freshly distilled) 100 mmole were added. The sealed flask was transferred to a 100 °C oil bath and stirred vigorously. Samples were diluted 1 in 20 in ether for GC analysis. All of the samples were analyzed by a Hewlett Packard 5890 Series II GC equipped with FID detectors. Product identification was carried out with a GC-MS analysis and <sup>1</sup>H NMR. The products were identified by comparison of their spectra and retention time in GC with those of authentic samples (for example para-acetophenone in the acylation reaction studied). In the case of the alkylation reactions (carried out at 100 C with conversion close to 99%), the products contain >95% linear alkylate and the remainder (<5%) are the 4% branched alkylates from the 4% branched olefins (impurity in the feed), and dimers of 1-dodecene. Full details for these reactions has been reported previously<sup>21–24</sup> The Fries reaction, alkylation, oligomerization were all carried out in a similar manner analyzing conversion using gas chromatography. Acid leaching, in the case of 1-dodecene alkylation of *p*-xylene, was measured by first filtering the products from the solid supported acid. The organic mix was then extensively stirred with water to extract the acid (4 times the volume, >48 hrs), and the water containing layer was titrated. Additional water was added to ensure all the acid had been removed. The acid containing water layer was titrated against base to determine the acid content. The filtered solid, containing the bulk of the acid, was also titrated (again

extensive water washing to remove the acid). A good materials balance was obtained with typically greater than 99.5% retention of the acid in the solid (0.5% in the organic product phase).

## Acknowledgements

We would like to thank the invaluable help of Bob Miller, Mike Barker, Keiiche Tanabe, Qun Sun, Ed Howard and Monica Tisack, for help on synthesis and many helpful technical discussions.

## References

- 1 P. T. Anastas and T. C. Williamson, in *Green Chemistry: Frontiers in Benign Chemical Syntheses and Processes*, Oxford University Press, Oxford, 1998.
- 2 J.-P. Simonato, *Chem. Ind.*, 2005, 20.
- 3 E. Marx, *Spec. Chem. Mag.*, 2004, **24**, 24.
- 4 Y. Katsuhara, M. Aramaki, A. Ishii, T. Kume, C. Kawashima and S. Mitsumoto, *J. Fluor. Chem.*, 2006, **127**, 8.
- 5 G. A. Olah, G. K. Surya Prakash and J. Sommer, *Superacids*, Wiley-Interscience, New York, 1985.
- 6 A. de Angelis, C. Flego, P. Ingallina, L. Montanari, M. G. Clerici, C. Carati and C. Perego, *Catal. Today*, 2001, **65**, 363.
- 7 J. A. Kocal, B. V. Vora and T. Imai, *Appl. Catal., A*, 2001, **221**, 295.
- 8 S. J. Miller, *Stud. Surf. Sci. Catal.*, 1994, **84**, 2319.
- 9 G. A. Olah, *Interscience Monographs on Organic Chemistry: Friedel-Crafts Chemistry*, Wiley-Interscience, New York, 1973.
- 10 J. A. Horsley, *Chemtech*, 1997, **27**, 45.
- 11 G. Sartori and R. Maggi, *Chem. Rev.*, 2006, **106**, 1077.
- 12 M. A. Harmer, in *Handbook of Green Chemistry & Technology*, ed. J. Clark and D. MacQuarrie, Blackwell Publishing, Oxford, 2002.
- 13 M. A. Harmer, W. E. Farneth and Q. Sun, *Adv. Mater.*, 1998, **10**, 1255.
- 14 G. A. Olah, in *Acidity and Basicity of Solids*, ed. J. Fraissard and L. Petrakis, Kluwer Academic, Boston, 1994, p. 305–334.
- 15 D. D. Coffman, M. S. Raasch, G. W. Rigby, P. L. Barrick and W. E. Hanford, *J. Org. Chem.*, 1949, **14**, 747.
- 16 M. A. Harmer, C. P. Junk and Z. Schnepf, *US Pat. App.*, filed on 06/07/2005.
- 17 J. Ross and J. Xiao, *Green Chem.*, 2002, **4**, 129.
- 18 V. D. Sarca and K. K. Laali, *Green Chem.*, 2004, **6**, 245.
- 19 G. W. Scherer and C. J. Brinker, *Sol-Gel Science*, Academic, San Diego, 1990.
- 20 M. Clarembeau and P. Steylaerts, *US Pat.* 5 849 974, 1998.
- 21 Q. Sun, M. A. Harmer and W. E. Farneth, *Chem. Commun.*, 1996, 1201.
- 22 A. Heidekum, M. A. Harmer and W. F. Hoelderich, *J. Catal.*, 1999, **188**, 230.
- 23 A. Heidekum, M. A. Harmer and W. F. Hoelderich, *J. Catal.*, 1998, **176**, 260.
- 24 M. A. Harmer, Q. Sun, A. Vega, W. E. Farneth, A. Heidekum and W. F. Hoelderich, *Green Chem.*, 2000, **1**, 7.

# Novel chemical recycling of polycarbonate (PC) waste into bis-hydroxyalkyl ethers of bisphenol A for use as PU raw materials†

Chao-Hsing Lin, Hsing-Yo Lin, Wei-Zhi Liao and Shenghong A. Dai\*

Received 6th July 2006, Accepted 6th September 2006

First published as an Advance Article on the web 26th September 2006

DOI: 10.1039/b609638g

An efficient process for the chemical recycling of polycarbonate (PC) waste into diols of bisphenol A (BPA) for use as raw materials in PU production has been developed. Digestion of PC waste in alkylene glycols, *i.e.*, ethylene glycol (EG) and propylene glycol (PG), with a catalytic amount of sodium carbonate at 180 °C under normal atmospheric pressure afforded partial alkoxylation products of BPA. This initial product mixture was found to consist of BPA (28%) and monohydroxyethyl ether (MHE-BPA, 40%) and bishydroxyethyl ether of bisphenol A (BHE-BPA, 25%) when digested in EG solution. Whereas, in PG digestion solution, the corresponding digestion products consist of monohydroxypropyl ether of BPA (MHP-BPA, 53%) and bishydroxypropyl ether of BPA (BHP-BPA, 21%), with the rest being un-propoxylated BPA. When these digested solutions were further treated with molar excess of urea with a catalytic amount of zinc oxide at 180 °C, BHE from EG or BHP-BPA from PG was produced in high yields. In both digestion processes, cyclic alkylene carbonates, *i.e.* ethylene carbonate (EC) or propylene carbonate (PPC), were observed as the transient intermediates which eventually disappear during the prolonged alkoxylation conditions. ZnO was added to the second step as the catalyst to accelerate urea's trans-esterification process. Both BHE and BHP products have been successfully utilized in making PU polymers with good mechanical properties. This chemical approach thus provides a viable alternative for PC recycling.

## Introduction

Since the 1950s, polycarbonate (PC) has been successfully developed and used as a commodity engineering thermoplastic because of its high-performance properties, such as high transparency, temperature resistance and toughness. More recently, the market consumption of PC has increased even more rapidly due to penetration of its applications into the electronic and media industries. However, PC's commercial success has been marred partially by the problems of its waste at both the post-manufacturing and post-consumer stages. It was estimated that more than 6000 billion discs of PC waste were generated worldwide in 2005 alone which amounted to more than 13 million pounds in one year.<sup>1</sup> In a time of growing concern over environmental protection, reuse of resources has become an important issue for PC also. In addition, the demand for material reuse has become more acute nowadays because of the sharp increase in oil prices. PC plastics were known to be recyclable by means of re-grinding followed by re-extrusion, but the quality of the PC suffered and it generally could not be used in high performance applications.<sup>2</sup> Retro-polymerization or digestion of PC waste into monomeric compounds and reuse in polymer synthesis as raw material has also been touted as another solution to the PC waste problem.

In this way, potentially more avenues of applications could be developed.

One recent approach to the chemical recycling of PC wastes investigated by Oku and his co-workers was to digest them back into BPA and hydroxyethyl ethers of BPA, by treating the PC with ethylene glycol using NaOH (0.1 equiv.) as the promoter.<sup>3,4</sup> In the digestion step, fast de-carboxylation of PC occurred with formation of partial alkoxylation products of BPA. The digestion ended up with formation of a product mixture consisting of BPA, monohydroxyethyl ether of BPA and bishydroxyethyl ether of BPA. In the second step of their process, the digested mixtures were further treated with additional pure ethylene carbonate (EC) to form bishydroxyethyl ether of BPA as the final product. This diol can then be used as a raw material in polymer synthesis.

The industrial feasibility of Oku's process seems to very much hinge upon the availability of EC which is not yet a commodity product despite many inexpensive routes to EC being developed recently. For instance, EC can be made from the reaction of ethylene oxide (EO) and carbon dioxide.<sup>5</sup> In the 1990s, a newer process for the production of alkylene carbonates such as EC from the reaction of the corresponding alkylene glycols and urea, in the presence of metal oxide catalysts<sup>6,7</sup> became known. The latter process can proceed at atmospheric pressure and at a temperature from 130 to 200 °C. This process seems to be safer and more applicable than the pressurized reaction required for the EO and carbon dioxide route.

In view of these studies, we have further advanced Oku's original process by developing a more convenient one-pot

Department of Chemical Engineering, National Chung Hsing University, Taichung, Taiwan. E-mail: shdai@dragon.nchu.edu.tw; Fax: +886-4-2287-4159; Tel: +886-4-2285-1283

† Electronic supplementary information (ESI) available: Fig. S1: Conversion of (A) BHE-BPA and (B) BHP-BPA; Fig. S2: Selectivity of (A) BHE-BPA and (B) BHP-BPA. See DOI: 10.1039/b609638g

atmospheric process of alkoxylation.<sup>3</sup> In the process, the first digestion step is similar to Oku's first digestion step. However, we have adopted the inexpensive urea as our carbonylation agent in glycols in the subsequent step. By doing so, cyclic carbonates were generated *in situ* from ethylene glycol or propylene glycol and were utilized to complete the ethoxylation or propoxylation process in formation of diols of BPA as the final products. We have demonstrated that bisalkoxylated diols of BPA can be formed in one-pot and then be reused in polyurethane as raw materials to form high molecular weight elastomers and plastics.

## Experimental

### Materials and reagents

Poly-bisphenol A carbonate, PC (BPA; analytical grade, Aldrich), waste PC was spent PC from the injection process using LG-Dow (medical grade), bisphenol A (polycarbonate grade, Showa), ethylene glycol (analytical grade, Aldrich), propylene glycol (analytical grade, ARCOS), ethylene carbonate (EC; analytical grade, Lancaster), propylene carbonate (PPC; analytical grade, ARCOS), 4,4'-methylene-bis(phenyl isocyanate) (MDI; analytical grade, Bayer), sodium carbonate (analytical grade, TEDIA), zinc oxide (analytical grade, TEDIA), polytetramethylene glycol, PTMEG (commercial product Terathane 2000, Dupont).

### Instrumentation

Infrared (IR) spectra were recorded with a Perkin Elmer Spectrum One FT-IR spectrometer and the testing samples were cast as potassium bromide pellets. High-performance liquid chromatography (HPLC) spectra were run on a Shimadzu LC-6A using a HYPERSIL-100 C18 column, Thermo Electron Corporation, with a length of 250 mm, and i.d. 4.6 mm through a UV detector with a 254 nm light source. <sup>1</sup>H-NMR spectra were recorded on a Varian Unity Inova FT-NMR (200 MHz) spectrometer. GPCs were run on a Waters Apparatus 515 HPLC pump 717 Autosampler, using a 2410 Refractive Index Detector. Thermal gravimetric analysis (TGA) was performed on a Seiko SII SSC/5200 at a heating rate of 10 °C min<sup>-1</sup>. Differential scanning calorimetry (DSC) was performed on a Seiko SII SSC/5200 at a heating/cooling rate of 10 °C min<sup>-1</sup>. Gas chromatograph (GC) spectra were run on a Finnigan 9001 with a column of QUADREX 007 series methyl silicone (ionization detector, FID). Stress-strain measurements on polymer samples were performed on a Hung Ta HT-8504 tensile tester at an elongation rate of 100% min<sup>-1</sup>. Tensile bars were punched from a solution-cast film of the

polymers. The tensile bars were prepared with the following dimensions: length = 22 mm, width = 5.0 mm, and thickness = 0.50 mm. Hardness measurements were performed on Teclock Durometer GS-702N (Shore D) and GS-709N (Shore A) in compliance with ASTM D2240A.

### One-pot digestion and alkoxylation for converting PC into bis-hydroxyalkyl ether of BPA

**Digestion and ethoxylation of PC waste in EG.** A 250 mL three-necked flask, equipped with a magnetic stirrer, reflux condenser, thermometer, and nitrogen inlet and outlet was charged with polycarbonate (50.8 g; 0.2 mol), ethylene glycol (124.0 g; 2.0 mol) and Na<sub>2</sub>CO<sub>3</sub> (0.4 g) as a catalyst. Then the reaction mixture was heated with a heating mantle to 180 °C under atmospheric pressure and was kept at the same temperature for about 20 minutes. After a small portion of mixture was withdrawn for analysis, the reaction mixture was charged with urea (21.6 g; 0.36 mol) and ZnO (0.2 g). The mixture was heated at 180 °C for an additional 2 h. The solution mixture was then cooled to room temperature. Some solid precipitate formed and was filtered. The excess unreacted ethylene glycol in the reaction mixture was removed by vacuum distillation. The distillate recovered was found to be the unreacted ethylene glycol (88.4 g; 89% recovery). Toluene (50 mL) was poured into the distillation residue for purification by re-crystallization. The white solid was filtered and dried to afford 63.2 g of product for 99% yield. The purified bishydroxyethyl ether of BPA (BHE-BPA) with a melting point of 112.4–113.5 °C (lit.,<sup>8</sup> 112 °C) was identified further by its <sup>1</sup>H-NMR spectrum as shown by the following chemical shifts. The selectivity and conversions were determined by HPLC as shown in Table 1.

BHE-BPA. <sup>1</sup>H-NMR (300 MHz, CDCl<sub>3</sub>)<sup>3</sup> δ 1.63 (s, 6H), 2.03 (t, *J* = 6.3 Hz, 2H), 3.91–3.96 (dt, *J* = 6.3, 4.5 Hz, 4H), 4.06 (t, *J* = 4.5 Hz, 4H), 6.80–7.15 (m, 8H).

**Digestion and propoxylation of PC waste in PG and urea.** The reactor of similar set-up to that indicated in the ethoxylation reaction was charged with waste polycarbonate (30.51 g; 0.12 mol), propylene glycol (91.5 g; 1.2 mol) and Na<sub>2</sub>CO<sub>3</sub> (1.0 g). The reaction mixture was heated to 180 °C under atmospheric pressure and was kept at the same temperature with stirring for about 30 minutes. After withdrawing small portions of the mixture for analysis, the digested mixture was charged with urea (14.4 g; 0.24 mol) and ZnO (0.6 g) as catalyst and the solution was re-heated to 180 °C for an additional 3 h. Then, the reaction solution was cooled to room temperature. The solid precipitates were removed by filtration.

**Table 1** Digestion and alkoxylation of PC pellets and PC wastes

| Process    | Conversion of ethoxylation (%) |         |         |           | Yield (%) | Conversion of propoxylation (%) |         |         |           | Yield (%) |    |
|------------|--------------------------------|---------|---------|-----------|-----------|---------------------------------|---------|---------|-----------|-----------|----|
|            | BPA                            | MHE-BPA | BHE-BPA | Oligomers |           | BPA                             | MHP-BPA | BHP-BPA | Oligomers |           |    |
| PC pellets | R <sup>a</sup>                 | 28      | 40      | 25        | 2         | — <sup>c</sup>                  | 26      | 53      | 21        | 0         | —  |
|            | A <sup>b</sup>                 | 0       | 2       | 91        | 1         | 99                              | 0       | 1       | 97        | 2         | 90 |
| PC wastes  | R                              | 27      | 40      | 23        | 0         | —                               | 23      | 54      | 23        | 0         | —  |
|            | A                              | 0       | 4       | 84        | 5         | 92                              | 0       | 1       | 95        | 3         | 98 |

<sup>a</sup> Retro-polymerization. <sup>b</sup> Alkoxylation. <sup>c</sup> Not observed.

The product mixture was subjected to vacuum distillation to recover unreacted propylene glycol (63.59 g; 87% recovery). The distillation bottom was extracted with aqueous solution in ethyl acetate (50 mL) to remove inorganic salt precipitates. Ethyl acetate was distilled under reduced pressure at room temperature to give a liquid product of 36.81 g by weight or 91% of theory. The isolated products were identified to be the mixture of bishydroxypropyl ethers of BPA (BHP-BPA) by the  $^1\text{H-NMR}$  spectrum. The data were as follows. The yields and conversions were determined by HPLC as shown in Table 1.

**BHP-BPA.**  $^1\text{H-NMR}$  (200 MHz,  $\text{CDCl}_3$ )  $\delta$  1.24–1.36 (m, 6H), 1.63 (s, 6H), 2.33 (s, 2H), 3.69–4.23 (m, 6H), 6.78–7.15 (m, 8H).

### Synthesis of PU polymers with diols prepared

**Polymerization of bis-hydroxyalkyl ether of BPA and MDI to make PU plastics.** A 250 mL resin kettle equipped with a mechanical stirrer, thermometer, and nitrogen inlet–outlet in a heating mantle was charged with purified BHE-BPA (3.16 g; 0.01 mol), freshly distilled MDI (2.5 g; 0.01 mol) and DMF (10 mL) as solvent and was placed under atmosphere. The reaction mixture was stirred and heated to 60 °C for about 4 h. The solvent (DMF) was then removed under vacuum at 70 °C. The isolated polymer was analyzed by GPC and other methods.

**Polymerization of bis-hydroxyalkyl ethers of BPA, PTMEG and MDI to make PU elastomers.** A 250 mL resin kettle equipped with a mechanical stirrer, thermometer, and nitrogen inlet and outlet in a heating mantle was charged with BHE-BPA (10.1 g; 0.032 mol), PEMEG 2000 (16.0 g; 0.008 mol), MDI (10.0 g; 0.04 mol) and DMF (40 mL) as solvent and was placed under atmosphere. The reaction mixture was heated to 75 °C for about 6 h. After cooling, the solvent (DMF) was removed under diminished pressure at 70 °C. The residual polymer solution was then cast by removal of DMF. The isolated polymer was analyzed by GPC, TGA, DSC, durometer and tensile tester.

## Results and discussion

### Digestion of polycarbonate or PC waste by alkylene glycols in the presence of sodium carbonate

In our chemical recycling of polycarbonate (PC) into BPA-diols, two basic reactions, digestion and alkoxylation, were involved and were basically carried out sequentially in tandem. The first step of digestion involved the decarbonylation of PC with action of either ethylene glycol (EG) or propylene glycol (PG) at 180 °C. It was found that alkylene carbonates are generated during the digestion process in the presence of  $\text{Na}_2\text{CO}_3$ , but the cyclic carbonates were found to be quickly consumed to produce the partial alkoxylation products of BPA with concurrent evolution of carbon dioxide. Without addition of any carbonylation reagents at this stage, the digestion product gave only approximately 50% of all phenolic alkoxylation products of BPA. This is because two phenolic groups were generated from PC in formation of only one cyclic carbonate.

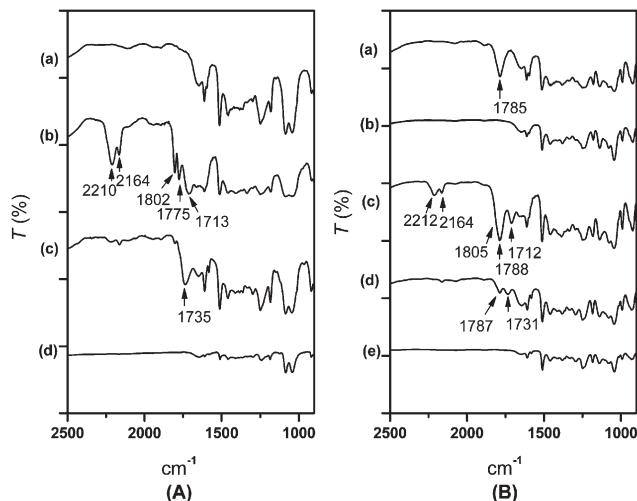


**Fig. 1** IR spectra of PC-EG digestion monitored. (A): (a) Digestion of PC by EG at 180 °C for 20 min, (b) further ethoxylation (urea) at 180 °C for 5 min, (c) 70 min, (d) 90 min. IR spectra of PC-PG reaction monitored. (B): (a) Digestion of PC by PG at 180 °C for 10 min, (b) digestion for 40 min, (c) further propoxylation (urea) at 180 °C for 10 min, (d) 80 min, (e) 120 min.

In the digestion step, the reaction could be best monitored by the disappearing absorption band of the carbonyl group at  $1785\text{ cm}^{-1}$ , Fig. 1 (a), of PC in its IR spectroscopy to signify the complete conversion of PC into alkoxylation products. At 180 °C, this digestion step generally took about 20–30 minutes. The mixtures obtained after digestion with ethylene glycol (EG) were analyzed by HPLC and found to consist of bisphenol A (BPA, 28%), monohydroxyethyl ether of BPA (MHE-BPA, 40%) and bishydroxyethyl ether of BPA (BHE-BPA, 25%). Some intermediate products were also detected in the mixture.

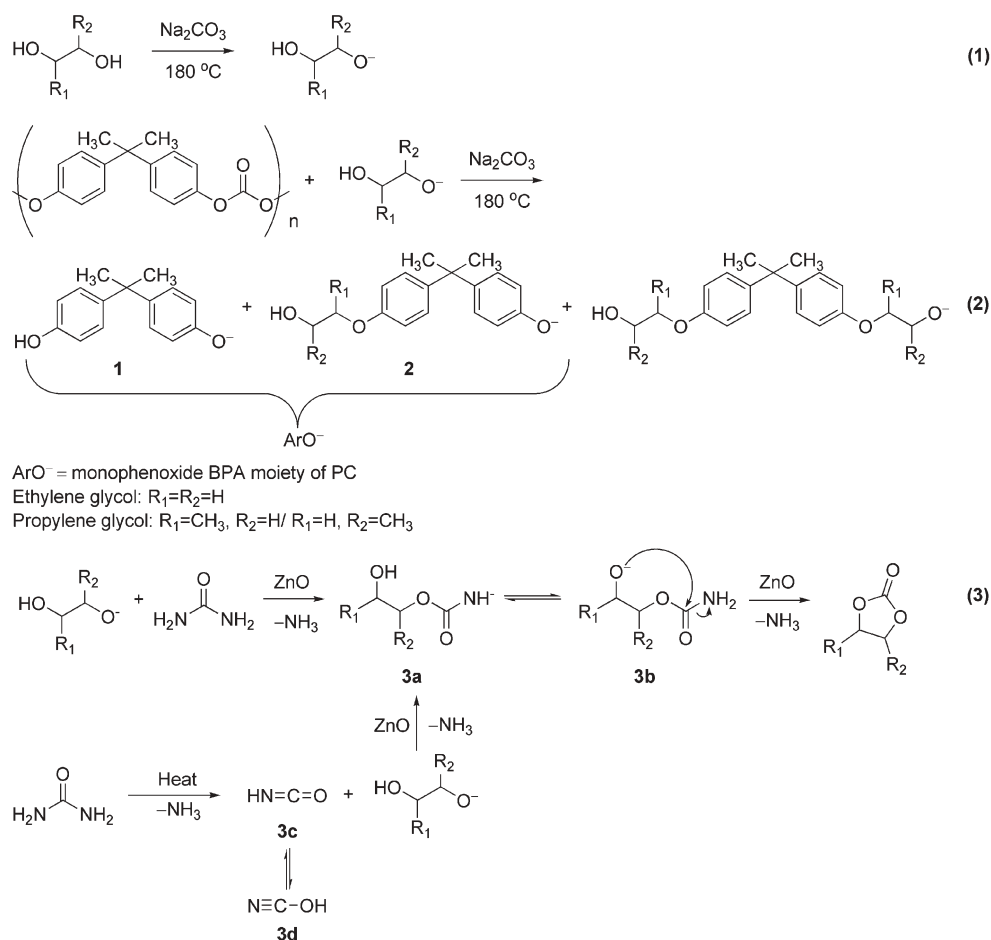
The digestion of PC with propylene glycol (PG) gave three similar major compounds which were analyzed to consist of bisphenol A (BPA, 26%), monohydroxypropyl ether of BPA (MHP-BPA, 53%) and bishydroxypropyl ether of BPA (BHP-BPA, 21%). PC waste digestion by EG or PG gave consistently similar results to that of pure PC as shown in Table 1. The conversions were measured by HPLC.

Complete alkoxylation of phenolic in digested mixtures into bishydroxyalkyl ethers of BPA were accomplished by addition of extra carbonylation reagent, urea (1.8–2.0 equiv.) and  $\text{ZnO}$  (0.05–0.1 equiv.) as a catalyst. In the presence of glycols, urea generated more cyclic alkylene carbonates for alkoxylation. The cyclic alkylene carbonates reacted with BPA and mono-phenolic BPA moiety in the digestion products to produce bishydroxyalkyl ethers of BPA as shown in the reactions indicated in Scheme 1 (Eq. (1) and (2)).

### One-pot alkoxylation by urea-glycol in the presence of zinc oxide

In the alkoxylation of BPA's digested products, urea catalyzed by trace  $\text{ZnO}$  was used as the key carbonylation reagent. Urea would react with the alkylene glycols to generate cyclic alkylene carbonates initially to supplement further alkoxylation. Essentially, this is an extension of Doya's<sup>9</sup> chemistry to





**Scheme 1** Conversion of PC into bishydroxyalkyl ether of BPA with alkylene glycol in the presence of urea.

BPA digestion products without the isolation of pure cyclic carbonates. In our one-pot approach to prepare BPA based diols, this step was generally carried out after the digestion of PC. In the urea-EG case, absorption characteristic of ethylene carbonate (EC) formation could be observed at  $1802\text{ cm}^{-1}$  (Fig. 1 (A) (b)) at the early stage of the reaction. The absorption band characteristic of formation of propylene carbonate (PPC) was observed at  $1785\text{ cm}^{-1}$  by IR (Fig. 1 (B) (c)). Both bands would disappear as the reaction proceeded to completion to form the final BPA diols.

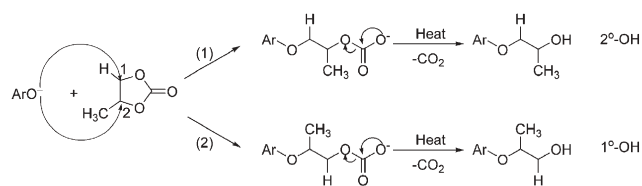
Mechanistically, the formation of cyclic alkylene carbonates from urea and glycols could result from two different pathways as indicated in Scheme 1. One pathway may proceed through attack of glycols at the carbonyl carbon of urea with elimination of  $\text{NH}_3$  to produce intermediate **3a** (Scheme 1, Eq. (3)). The other pathway is directly from thermal decomposition<sup>10</sup> of urea to produce  $\text{NH}_3$  and isocyanic acid (**3c**,  $\text{HNCO}$ )<sup>11,12</sup> as the first step. Spectral evidence from our reaction solutions indicated that both pathways seemed operative. The characteristic absorption bands for  $\text{HNCO}$  could be observed at  $2210/2212\text{ cm}^{-1}$  and its isomer  $\text{HOCN}$  (**3d**) is also detected at  $2164\text{ cm}^{-1}$  by IR spectroscopy (Fig. 1 (A) (b)/(B) (c)).<sup>13</sup> Therefore, the addition of alkylene glycols to  $\text{HNCO}$  is shown to be another route in the production of adduct **3a**. Finally, adduct **3b** would go through an

intramolecular cyclic reaction and eliminate another mole of  $\text{NH}_3$  to produce cyclic alkylene carbonates. In short, BPA alkoxyated diols eventually became the final products of our one-pot process through cyclic carbonates' alkoxylation.

Ethoxylation of BPA with ethylene carbonate under the influence of sodium carbonate is very similar to ethoxylation of BPA with ethylene oxide (EO). In both cases BHE-BPA will become the major product.<sup>14</sup> However, in most of our experiments, only small amounts of oligomeric polyether diol (1%) were detected as impurities in urea-EG ethoxylation. This extended reaction appeared to occur in the case when excess of urea and prolonged reaction time were applied. However, when an appropriate amount of urea was added, a high yield of BHE-BPA (96%) could be achieved. Thus, our results indicate that alkoxylation with cyclic carbonate results in more selectivity than EO for synthesis of mono-ethoxyated products from phenols when the catalyst used is sodium carbonate.

#### Selectivity and steric hindrance effect in propoxylation with urea-PG mixture

Similar to propoxylation with propylene oxide (PO), we have found three major propoxyated diols of BPA<sup>14</sup> in the digestion products, *i.e.*, primary-primary ( $1^\circ, 1^\circ$ ), primary-secondary ( $1^\circ, 2^\circ$ ), and secondary-secondary ( $2^\circ, 2^\circ$ ) in a



**Scheme 2** Diversity of products formation from propoxylation.

relative conversion ratio of 2 : 24 : 70, using our urea–PG one-pot process. These products of propoxylation resulted from the attack of phenate ions of BPA on the unsymmetrical structure of propylene carbonate. When the reaction takes place by route (1), attack on a less-hindered carbon of PC (Scheme 2), it produces products with the secondary hydroxyl group as the major product. In contrast, when  $\text{ArO}^-$  attacks the alkylene carbon (C2) with a methyl group *via* more hindered route (2), the alcohol with a primary hydroxyl group becomes the product. The selectivity of our propoxylation does show a strong steric effect by showing high selectivity of 70–74% for 2°, 2°-diols as the primary product and a low percentage (less than 2%) of 1°, 1°-BPA diol in the propoxylated products. In addition, oligomers formation in the PG–urea reaction catalyzed by sodium carbonate was even lower than in the EG–urea reaction. Therefore, this one-pot synthesis is especially selective for preparing a mono-propylene ether extension for phenols.

### Synthesis of PU with bis-hydroxyalkyl ether of bisphenol A and MDI

Among many potential applications of bis-hydroxyalkyl ethers of bisphenol A, utilization of them as raw materials in production of polyurethane (PU) seems to be one of the most direct. In our study, two types of PUs, plastic and elastomer, were prepared using BHE-BPA and BHP-BPA. For the synthesis of PU plastic, BHE-BPA and BHP-BPA were reacted individually with methylene diphenylene diisocyanate (MDI) in DMF and the products are designated as PU3 and PU4 respectively in Table 2. BHE-BPA and BHP-BPA were also used as the chain-extenders and were reacted with PTMEG-MDI pre-polymer in syntheses of PU elastomers to form PU1 and PU2 respectively. The molecular weight of PU1–4 was measured by means of GPC with DMF as solvent as shown in Table 2. The data indicate that both PU3 and PU4 are high polymers with very limited solubility in tetrahydrofuran solution.

During polymerization, we found that the reactivity of BHE-BPA is far higher than that of BHP-BPA. This phenomenon is consistent with the fact that BHE-BPA is

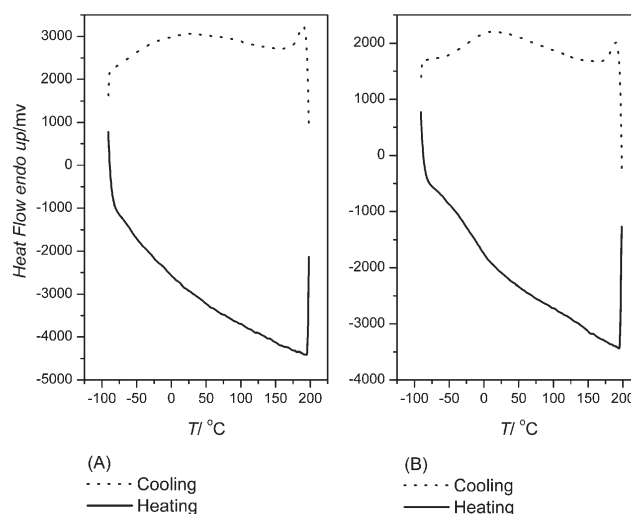


**Fig. 2** DSC traces of PU1 (A) and PU2 (B) at a heating/cooling rate of  $10\text{ }^\circ\text{C min}^{-1}$ .

made entirely of primary hydroxyl groups. This could also explain why the molecular weight of PU4 was found to be only half that of PU3. However, both diols afforded PU of unique mechanical properties as illustrated in the observation below.

### Thermal and mechanical properties of PU prepared

Thermal behavior of PU1 and PU2 was measured by means of TGA and DSC. The temperatures of 5% mass loss for PU1 and PU2 were 291 and 289  $^\circ\text{C}$  respectively in nitrogen as determined by TGA. DSC was used to obtain characteristics of the thermal transitions of PU1 and PU2. The first cooling and second heating traces of PU1 and PU2 are shown in Fig. 2 (A) and (B). The compositions of PU3 and PU4 consist of MDI with BHE-BPA or with BHP-BPA without polyols. The  $T_{g,h}$  of PU3 and PU4 were observed at 81 and 123  $^\circ\text{C}$  respectively (Fig. 3).

For PU1 and PU2, no signs of melting nor crystallization peaks for the hard and soft segments could be discerned. This implies that both PUs are completely amorphous with a phase mixed between hard and soft phases. Chain extenders BHE-BPA and BHP-BPA both have two methyl groups on the methylene bridge in their molecular structures that are different from that of MDI. The steric hindrance caused by dimethyl group substitutions on the methylene bridges of the diols appears to block the tight packing of benzene rings and in turn causes the hard segment of PU in a random orientation. The phenomenon of thermal behavior from DSC seems consistent with these observations.

**Table 2** Thermal and mechanical properties of polyurethane

| Polymer | Compositions (molar ratio)         | Hardness/<br>shore | $T_d^a/^\circ\text{C}$ | $T_{g,h}^b/^\circ\text{C}$ | 100% Young's<br>modulus /MPa | Strength/<br>MPa | Strain at<br>break (%) | Mw/<br>$\text{g mol}^{-1}$ | PDI |
|---------|------------------------------------|--------------------|------------------------|----------------------------|------------------------------|------------------|------------------------|----------------------------|-----|
| PU1     | MDI/BHE-BPA/PTMEG 2000 (1/0.8/0.2) | D 43               | 291                    | — <sup>c</sup>             | —                            | 11               | 48                     | 27590                      | 1.8 |
| PU2     | MDI/BHP-BPA/PTMEG 2000 (1/0.8/0.2) | A 86               | 289                    | —                          | 6.6                          | 15               | 341                    | 64959                      | 3.1 |
| PU3     | MDI/BHE-BPA (1/1)                  | —                  | 285                    | 81                         | —                            | —                | —                      | 188106                     | 1.6 |
| PU4     | MDI/BHP-BPA (1/1)                  | —                  | 279                    | 123                        | —                            | —                | —                      | 45870                      | 1.8 |

<sup>a</sup> Determined at a heating rate of  $10\text{ }^\circ\text{C min}^{-1}$ . <sup>b</sup> h = hard segment. <sup>c</sup> Not observed.

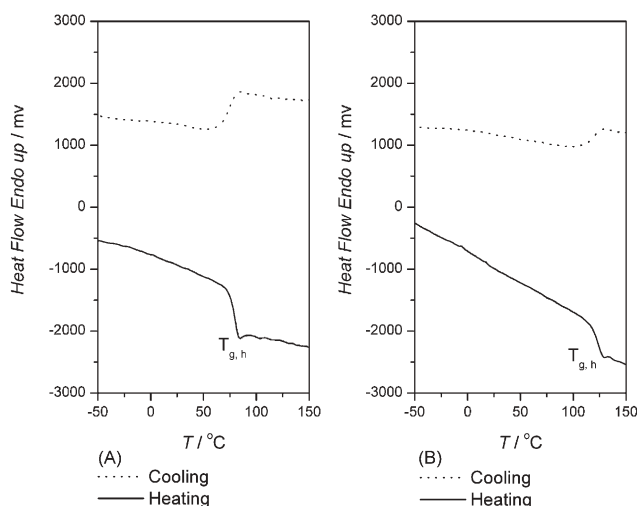


Fig. 3 DSC traces of PU3 (A) and PU4 (B) at a heating/cooling rate of  $10\text{ }^{\circ}\text{C min}^{-1}$ .

Films of PU1 and PU2 were cast from their DMF solutions, and this procedure produced completely transparent, flexible films. Hardnesses of PU1 and PU2 are measured to be D43 and A86 as shown in Table 2. Tensile bars of all PUs were punched from these non-oriented films and measured for their tensile strengths. Table 2 shows the stress-strain behavior of the two materials. Strain at break is expressed as the elongations, in terms of percentage. In PU1, 100% Young's modulus can not be measured, but the data shown for PU2 are totally different. The same formulation but different chain extenders exhibited completely different properties. PU1 behaved as a plastic but PU2 behaved as an elastomer. Again, the most logical reason is the branched methyl groups on the structure of the hydroxyethyl ether group in MHP-BPA. The branched methyl groups not only increase the solubility of bishydroxyalkyl ether of BPA (MHE-BPA is solid and MHP-BPA is liquid at room temperature), but also obstruct the intermolecular packing of the polymer. This result is reflected consistently in the enhanced hardness of PU1 that is D type.

## Conclusions

Both pellets and wastes were converted into the hydroxyalkyl ethers of bisphenol A for use in polyurethane production.

One-pot reactions with PC digestion and alkoxylation of the digested product with urea were developed. The yields of the BPA based diol were accomplished in excess of 90%. The selectivities of these urea-based alkoxylation were analyzed completely. A key use of the alkoxylation is the formation of cyclic alkylene carbonates with alkylene glycols and additional urea from an outside source in the presence of ZnO. This is a unique and economic route to produce different alkoxylation diols of BPA from PC wastes. They can be used as raw materials in the preparation of PU by a one-shot process. We have shown that PU possessing unique mechanical properties can be prepared from these recycled diols. We feel that PU3, PU4 and PU1 appear to possess properties which might make them strong candidates to replace PVC in the market. The detailed information on further endeavor on this green technology along this line of development is forthcoming.

## Acknowledgements

Financial assistance from Kuo-Ching Company of Taichung and from the Green Chemistry Team of the Center for Advanced Industry Technology and Precision Processing, NCHU of Taichung, Taiwan is gratefully acknowledged.

## References

- W. Y. Chen, *Master's Thesis*, Chaoyang University of Technology, 2005.
- G. Witt, *US Pat.*, 5 619 898, 1997; H.-J. Buysch, *US Pat.*, 5 652 275, 1997.
- A. Oku, S. Tanaka and S. Hata, *Polymer*, 2000, **41**, 6749–6753.
- L. C. Hu, A. Oku and E. Yamada, *Polymer*, 1998, **39**, 3841–3845.
- J. T. Dunn and C. W. Va, *US Pat.*, 2 773 881, 1956; C. H. McMullen, J. R. Nelson, B. C. Ream and J. A. Sims, Jr., *US Pat.*, 4 314 945, 1982.
- W. Y. Su and G. P. Speranza, *US Pat.*, 5 003 084, 1991.
- M. Doya, Y. Kanbara, K. Kimizuka and T. Okawa, *US Pat.*, 5 440 004, 1995.
- R. Michel and L. Jacques, *Fr. Pat.*, 1 366 067, 1964.
- M. Doya, T. Ohkawa, Y. Kanbara, A. Okamoto and K. Kimizuka, *US Pat.*, 5 349 077, 1994.
- B. Mavis and M. A. Kinc, *J. Am. Ceram. Soc.*, 2006, **89**, 471–477.
- O. Krocher, M. Elsener and M. Koebel, *Anal. Chim. Acta*, 2005, **537**, 393–400.
- M. U. Alzueta, R. Bilbao, A. Millera, M. Oliva and J. C. Ibanez, *Energy Fuels*, 2000, **14**, 509–510.
- C. Wentrup and H. Bornemann, *Eur. J. Org. Chem.*, 2005, 4521–4524.
- S. Nobuyuki and T. Masahide, *Jap. Pat.*, 2000 128 979, 2000.

# Synthesis of polyaniline derivatives *via* biocatalysis†

Seong-Cheol Kim,<sup>a</sup> Pilho Huh,<sup>a</sup> Jayant Kumar,<sup>\*a</sup> Bongsoo Kim,<sup>b</sup> Jang-Oo Lee,<sup>b</sup> Ferdinando F. Bruno<sup>c</sup> and Lynne A. Samuelson<sup>\*c</sup>

Received 15th May 2006, Accepted 14th September 2006

First published as an Advance Article on the web 9th October 2006

DOI: 10.1039/b606839a

Three structurally different aniline monomers, which can not be polymerized by chemical methods, have been polymerized with horseradish peroxidase. Enzymatic synthesis of linear polyaniline requires template molecules to minimize branching in the polyaniline backbone. Monomers having methoxy and methyl blocking groups at the *ortho* or *meta* position could induce the conducting form of *para*-linked polyaniline without the use of an anionic template, such as SPS. A new mild peroxide, peroxyacetic acid, was identified and used to oxidize horseradish peroxidase in water.

## Introduction

In recent years there have been extensive studies in the use of conducting polyanilines because of their wide range of electrical, electrochemical, and optical properties as well as their good stability.<sup>1–5</sup> Polyaniline is commonly synthesized by oxidizing aniline monomers using electrochemical or chemical methods.<sup>6–10</sup> This polymer can be doped either by a protonic acid or charge-transfer agents. In addition, the electronic and optical properties can be controlled reversibly by varying the doping level.<sup>11,12</sup>

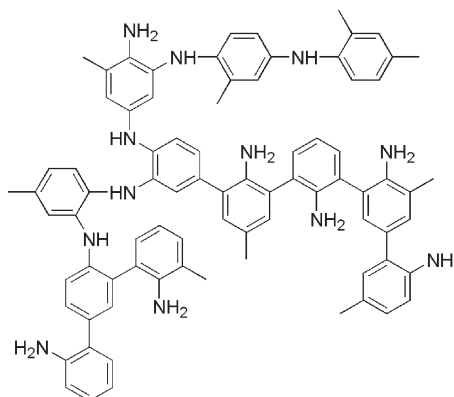
Synthesis of polyaniline *via* biocatalysis with an anionic template has been shown to enhance the water solubility and the stability of the final polyaniline-template complex, and is a more environmentally benign route.<sup>13–17</sup> Using enzymes as a catalyst for the synthesis of polyaniline could also improve the toxic chemical process conditions to a mild and environmentally benign route.

A major drawback of enzymatic polymerization without a template was the precipitation of highly branched low MW polyaniline. Non-conducting forms of branched polymers (oligomers) were formed due to the various resonance structure of aniline radical.<sup>18,19</sup>

Several types of anionic templates have been studied to synthesize the *para*-linked conducting form of polyaniline, such as polyacrylic acid, sulfonated polystyrene, polyvinyl phosphate, lignin sulfonate, RNA and DNA.<sup>13–17</sup> Here the anionic polyelectrolytes serve three critical functions. First, they preferentially align the aniline monomers and promote a more ordered *para*-linked reaction. Furthermore, they provide

counterions for doping of the synthesized polyaniline. Finally, they maintain water solubility, consequently, increasing processability of the final polymer.

Although template assisted polymerization of polyaniline has many advantages, there are still limitations which need to be addressed. Generally template molecules are not suitable dopants for polyanilines, and thus the conductivities of corresponding anionic template/polyaniline complexes are relatively low compared with camphorsulfonic acid-doped polymers. Even though polyaniline shows increased water-solubility due to the anionic template, the wettability of the polyaniline/template solution is poor because most of the substrate is hydrophobic. Once the polyaniline complex is coated and dried on the substrate, it does not dissolve again, which is advantageous for permanent processing but limits the recyclability of the materials. In addition, the removal of the anionic template by ion exchange is quite difficult and time-consuming. Therefore, the complexed polyaniline is hard to modify or to functionalize for certain applications. In this article, we present the enzymatic synthesis of polyaniline derivatives without using templates. Furthermore, we will demonstrate that peroxyacetic acid successfully activates horseradish peroxidase in aqueous solution.



Scheme 1

<sup>a</sup>The Center for Advanced Materials, Polymer Science Program, Departments of Chemistry and Physics, University of Massachusetts, Lowell, MA, 01854, USA. E-mail: Jayant\_Kumar@uml.edu; Fax: +1-978-458-9571; Tel: +1-978-934-3687

<sup>b</sup>Department of Polymer Sci. & Eng., Pusan National University, Pusan, 609-735, Korea. Fax: +82-51-513-7720; Tel: +82-51-510-3637

<sup>c</sup>U. S. Army RDECOM, Natick Soldier Center, Natick, Massachusetts, 01760. E-mail: Lynne\_Samuelson@natick.army.mil; Fax: +1-978-458-9571; Tel: +1-978-934-3972

† Electronic supplementary information (ESI) available: UV-Vis spectra of poly(2-methyl-5-methoxyaniline) with and without templates. See DOI: 10.1039/b606839a

## Results and discussion

The aniline radical has several intermediate resonance structures. These intermediates generate parasitic branches, disrupting, consequently, polyaniline conjugation. The monomer is expected to be primarily positively charged at pHs lower than 4.5, since aniline has a  $pK_a$  of 4.63.<sup>15</sup> The solubility of monomers and oligomers are not high in aqueous solution. To increase the solubility of monomer, at mild acidic conditions, various polar organic solvents have been mixed up to 40 vol%. Methyl and methoxy groups reduce the oxidation potential and can increase the solubility of the corresponding polyaniline in common organic solvents.<sup>20</sup> 2,5-Dimethoxyaniline has two methoxy groups in the *ortho* and *meta* positions. 2-Methyl-5-methoxyaniline and 2-methoxy-5-methylaniline may have a higher chance of *ortho* linkage than 2,5-dimethoxyaniline due to reduced steric hindrance generating a non-conducting form of the polyaniline, as shown before.

Fig. 1 shows the UV-Vis spectra of the substituted polyanilines synthesized in 10 vol% ethanol. As no template was used, several minutes are necessary to generate a polaron transition peak at 800 nm due to a relatively slow reaction. No significant change of intensity of the polaron peak was observed in two hours for 2,5-dimethoxyaniline and 2-methyl-5-methoxyaniline and 2 days for 2-methoxy-5-methylaniline. As expected, 2,5-dimethoxyaniline shows the strongest intensity of polaron transition and 2-methyl-5-methoxyaniline shows a very weak polaron peak after two hours. However, although the polaron transition at 900 nm appeared in two days, 2-methoxy-5-methylaniline does not generate a polaron after a similar time. Poly(2-methoxy-5-methylaniline) also generates an excitonic transition peak at 520 nm, which is assigned to branched low molecular weight polyaniline. This

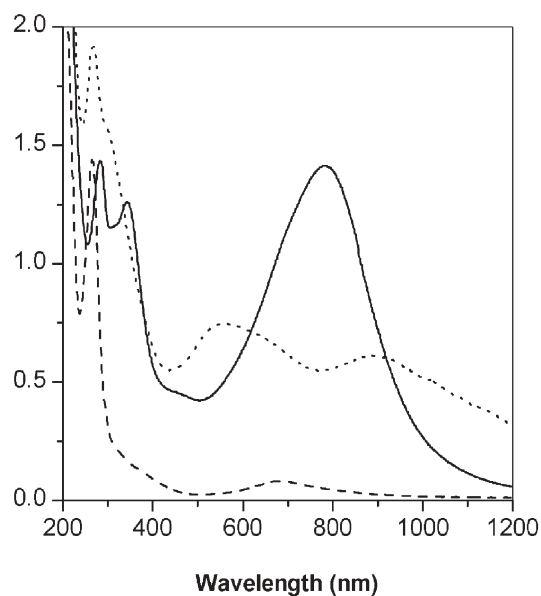
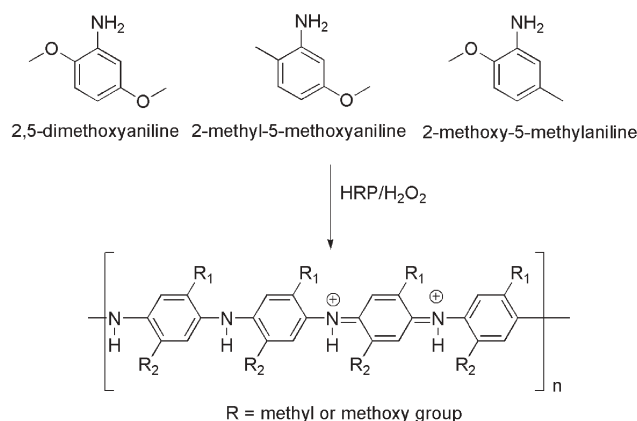


**Fig. 1** UV-Vis spectra of polyanilines in a mixed solvent system; pH 3; reaction time: 2,5-dimethoxyaniline and 2-methyl-5-methoxyaniline (2 hours), 2-methoxy-5-methylaniline (2 days); dopant: HCl; solid line (—): poly(2,5-dimethoxyaniline), broken line (---): poly(2-methyl-5-methoxyaniline), dashed line (---): poly(2-methoxy-5-methylaniline).



**Scheme 2**

difference in the intensity of each polaron peak is expected, and attributed to the pendent groups of aniline monomers. The 2,5-dimethoxyaniline structure provides better solubility and steric hindrance to minimize *ortho* coupling. Thus, the *para* directed reaction can proceed, as indicated by the strong absorption near 800 nm. The other two monomers, 2-methyl-5-methoxyaniline and 2-methoxy-5-methylaniline, however, are less soluble and more prone to *ortho* coupling. Therefore, this figure proves that the limitation of enzyme-catalyzed polyaniline synthesis can be overcome by a careful design of monomers.

Scheme 2 shows the possible emeraldine salt forms of the polymers.<sup>11,12</sup> The conductivity of substituted polyanilines was measured by four point probe method in two days of a reaction. The measured conductivity of the substituted polyanilines was  $0.3 \text{ S cm}^{-1}$  for poly(2,5-dimethoxyaniline) after additional doping with HCl vapor. An order of decrease in conductivity of poly(2,5-dimethoxyaniline) compared to unsubstituted polyaniline could be due to the decreased conjugation caused by two pendent methoxy groups. The intensity of the polaron transition and, consequently, the conductivity, can be modulated by changing the dopant counter ions. Camphorsulfonic acid is known as a stronger dopant than hydrochloric acid.<sup>21</sup> Therefore, the higher intensity of a polaron transition was observed when poly(2-methyl-5-methoxyaniline) was doped with camphorsulfonic acid (see ESI†).

To find the best solvent composition for the enzymatic polymerization, the polymerization reaction was performed at different vol% of ethanol. As the content of organic solvent increases, the solubility of monomers and oligomers increases. However, the activity of horseradish peroxidase decreases because the suitable molecular conformation of an enzyme may change with increasing organic solvent composition. No measurable intensity of a polaron peak at 750 nm was detected in several days when more than 50 vol% of ethanol was added in water. The optimum conditions for polymerization was found at a concentration of 15 vol% ethanol solution. Other polar organic solvents such as DMF, DMSO, 1,4-dioxane and methanol, have similar trends. The enzyme loses its activity gradually with increasing amounts of organic solvent, while the solubility of aniline derivatives increases with the ratio of organic solvent.<sup>22</sup> These two opposing effects give rise to optimum conditions at 15 vol% of organic co-solvent.

*In situ* polymerizations of these anilines were monitored by a UV-vis spectrometer. Real-time monitoring shows that the monomers are slightly soluble in the ethanol–water co-solvent. However, the solubility of the oligomers generated during the reaction increases with reaction time due to the positive charges generated in oligoaniline intermediates by proton doping. At the beginning of the polymerization the  $\pi$ - $\pi^*$  transition peak at 330 nm increases due to the increased solubility of undoped oligo(2,5-dimethoxyaniline).<sup>14,15</sup> As the polymerization proceeds, a gradual increase of the polaron peaks of poly(2,5-dimethoxyaniline) is observed at 750 nm with a decrease of the  $\pi$ - $\pi^*$  transition peak at 330 nm. When the acid-doped polyaniline is generated, its solubility in water gradually increases and it becomes fully soluble after polymerization. It was found that the peak maximum of the polaron transition in poly(2,5-dimethoxyaniline) shifted from 750 to 805 nm in two days, which suggests that the reaction might have continued gradually as time went on.

To determine the reversible redox behavior of the poly(2,5-dimethoxyaniline), the absorption spectra of a product prepared at pH 3 was investigated by varying pH. UV-Vis spectra, as shown in Fig. 4, show the peak shift in absorption spectra of poly(2,5-dimethoxyaniline) with increasing pH from pH 3 to 12.5 by titration with 1 M NaOH (aq). As the pH increases, the intensity of a polaron peak at 750 nm gradually decreases and a new excitation peak at 560 nm appears with a strong  $\pi$ - $\pi^*$  transition peak at 330 nm. At pH 11, the polymer solution changes to a purple color from the original dark green, which indicates that the poly(2,5-dimethoxyaniline) is fully dedoped by NaOH (aq).<sup>14–16</sup> The titration from pH 12.5 to pH 1 shows the opposite behavior.

An interesting and unexpected phenomenon was observed during the enzymatic polymerization of anilines with polar organic solvents. Hydrogen peroxide has been widely used to oxidize the monomer in the presence of an enzyme,

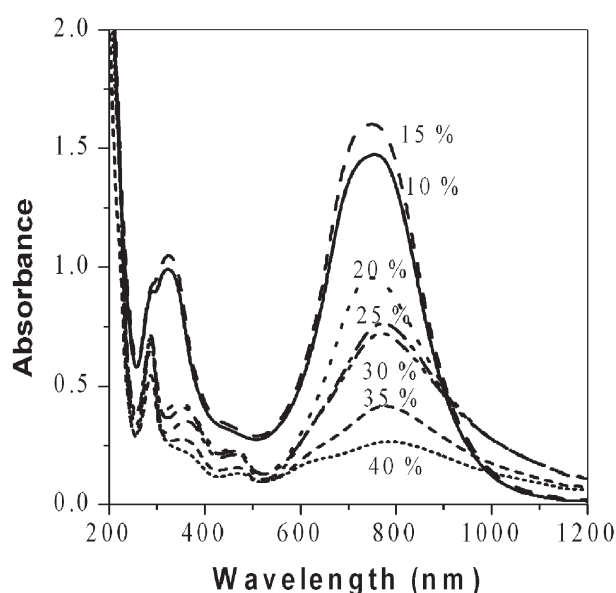


**Fig. 2** UV-Vis spectra of poly(2,5-dimethoxyaniline) as a function of %-ethanol. Polaron peak shows the highest intensity at 15 vol% of organic solvent in two hours.

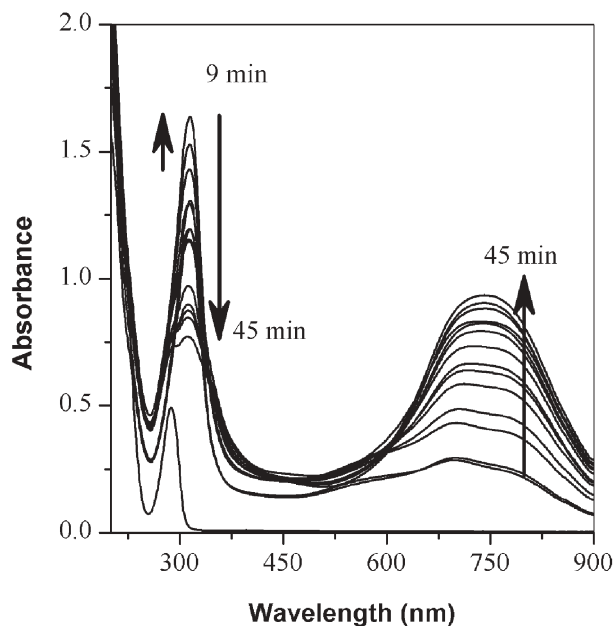


**Fig. 3** UV-Vis spectral change of poly(2,5-dimethoxyaniline) as function of time. Monomer shows a weak  $\pi$ - $\pi^*$  transition at 280 nm due to partial solubility in mixed solvent system.

horseradish peroxidase. Methyl peroxide, ethyl peroxide and hydrogen peroxide are the only known peroxides that can bind to horseradish peroxidase in water.<sup>23,24</sup> However, in these reactions, it was found that when 1,4-dioxane was used as the co-solvent, the polymerization of aniline could proceed without the addition of hydrogen peroxide. It was determined that acetyl acetal in dioxane, used as a stabilizer,<sup>25</sup> is transformed to peroxyacetic acid which in turn could initiate

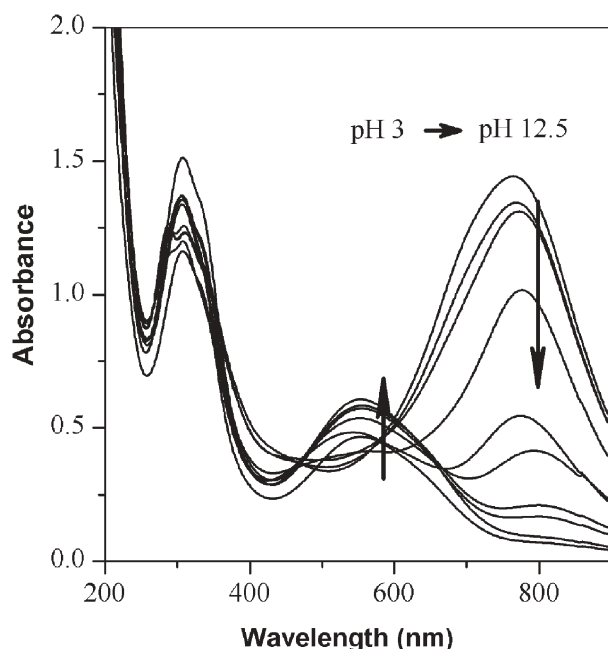
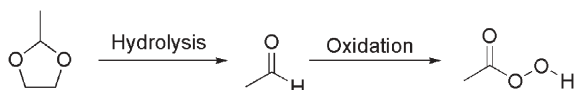


**Fig. 4** UV-Vis spectral change of poly(2,5-dimethoxyaniline) during titration by 1 M NaOH solution. The pH ranged from 3 to 12.5. The pH was monitored by a pH meter during titration.



the polymerization as shown in Scheme 3. To determine the oxidizing power of peroxyacetic acid, it was used as an oxidant instead of  $\text{H}_2\text{O}_2$ . Fig. 5 shows the UV-vis spectra of poly(2,5-dimethoxyaniline) with different oxidizing agents. It is well known that  $\text{H}_2\text{O}_2$  can inactivate the heme structure of horseradish peroxidase due to over oxidation. Therefore, the injection of  $\text{H}_2\text{O}_2$  into an enzymatic reaction cannot be done in high concentrations due to the slow oxidation reaction of monomers. This can often be time consuming and difficult to control. In this case, the peroxyacetic acid may be mild enough to allow a more convenient and easier control of the peroxide addition.

The electrochemical behavior of the polyaniline derivatives were characterized in *N,N*-dimethylformamide with 0.1 M tetrabutylammonium hexafluorophosphate. Incorporation of an alkoxy group at the *ortho* position is known to decrease the oxidation potential of the aniline.<sup>26</sup> Poly(2,5-dimethoxyaniline), poly(2-methyl-5-methoxyaniline) and poly(2-methoxy-5-methylaniline) showed one distinct quasi-reversible redox process at negative potential, which is similar to unsubstituted polyaniline.<sup>20</sup> However, the second redox process is not so clear. Typically, two sets of redox peaks are observed with electrochemically grown and chemically prepared polyaniline.<sup>27</sup> The absence of the second redox peak may be related to the exceptional resistance of the polyaniline derivatives to oxidation to the pernigraniline state.<sup>25</sup> The shoulder in the cyclic voltammogram may be related to irregular couplings, degradation, and oligomer formations.<sup>28–30</sup>

To determine the oxidation state of doped and dedoped poly(2,5-dimethoxyaniline), FT-IR spectra of the

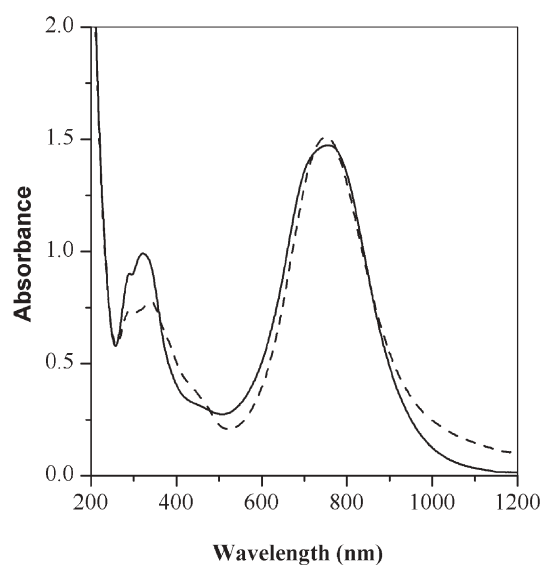


**Fig. 5** The polaron transition of poly(2,5-dimethoxyaniline) with different oxidants; solid line (—): with drop-wise addition of hydrogen peroxide, broken line (---): immediate addition of peroxyacetic acid.

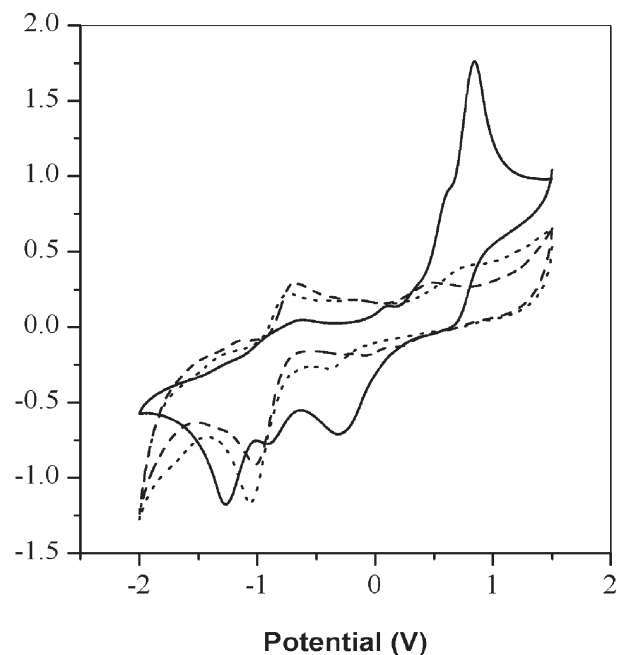


**Fig. 6** Cyclic voltammograms of polyanilines; scan rate: ( $100 \text{ mV s}^{-1}$ ); solid line (—): poly(2,5-dimethoxyaniline), broken line (---): poly(2-methyl-5-methoxyaniline), dashed line (---): poly(2-methoxy-5-methylaniline).

poly(2,5-dimethoxyaniline) were monitored. Fig. 7 shows the FT-IR spectra of poly(2,5-dimethoxyaniline) with different doping states. Two primary NH stretching peaks merge to make a broad secondary NH stretching peaks at  $3400 \text{ cm}^{-1}$  after the polymerization of 2,5-dimethoxyaniline. The poly(2,5-dimethoxyaniline) dedoped with ammonium hydroxide has no C=N stretch at  $1670 \text{ cm}^{-1}$ , which suggests that the dedoped form of poly(2,5-dimethoxyaniline) is in the

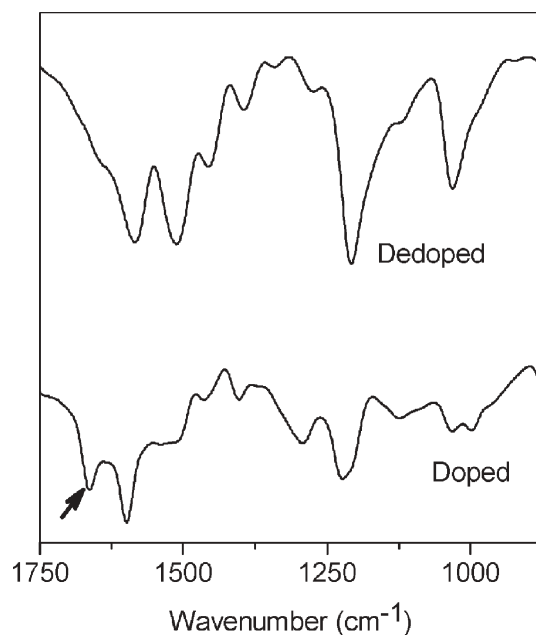


**Fig. 7** FT-IR spectra of poly(2,5-dimethoxyaniline) at different doping states.

leucoemeraldine insulating form.<sup>31</sup> Two correlated bands of  $-\text{OCH}_3$  appear at 1203 and 1042  $\text{cm}^{-1}$  with medium intensity. The intensity of these two peaks decreases at the doped state of the emeraldine salt form, probably due to restricted asymmetric C–O–C deformation. As expected, the doped form of poly(2,5-dimethoxyaniline) shows the double bond character of C=N stretch peak at 1669  $\text{cm}^{-1}$  with the doping by HCl.

The polaron transition peak of poly(2-methyl-5-methoxyaniline) synthesized without templates was different from that obtained from template polymerization. Sulfonated polystyrene and sodium dodecylbenzene sulfonate can align 2-methyl-5-methoxyaniline along the negatively charged template surface, which guide a *para* linkage reaction for the polymerization of poly(2-methyl-5-methoxyaniline). The shoulder at 550 nm may be related with the branching during the polymerization. However, poly(2,5-dimethoxyaniline) shows only one sharp polaron transition at 800 nm, which demonstrates that two methoxy groups can prevent *ortho* coupling successfully without templates.

## Conclusions

A new biological route for the synthesis of conducting polyaniline was presented. This approach has significant importance because conducting polyaniline was synthesized with horseradish peroxidase without any template by careful selection of aniline monomers. The *ortho* branching of polyaniline could be reduced significantly by introducing methyl or methoxy groups on the *ortho* position. The solubility of oligomers as well as the activity of horseradish peroxidase in a mixed solvent system had a significant role in the polymerization of substituted anilines. The synthesized polyanilines having methyl and methoxy groups had increased solubility in water and organic solvents such as DMF, ethanol and DMSO. These soluble homo-polyanilines may be further functionalized at the available *ortho* and *meta* position. Peroxyacetic acid, an oxidized form of a stabilizer found in 1,4-dioxane, proved to serve as a promising mild oxidant under certain reaction conditions and demonstrated a novel way to optimize enzymatic polymerizations. FT-IR spectra showed that the dedoped form of poly(2,5-dimethoxyaniline) is in the leucoemeraldine insulating state not in the emeraldine base form.

## Experimental

Horseradish peroxidase (EC 1.11.1.7) was purchased from Sigma Chemical Co. A stock solution of 10 mg  $\text{mL}^{-1}$  in pH 6.0, 50 mM phosphate buffer was prepared. Aniline monomers were obtained from Aldrich Chemical Co., Inc. All other chemicals and solvents used were also commercially available and used as received. The enzymatic polymerizations were typically carried out at room temperature in a 10 mL buffer solution of pH 3.0 which contained aniline monomer (concentration 0.1 mmol). To the solution, 0.1 mL of horseradish peroxidase stock solution was then added. The reaction was initiated by the addition of a stoichiometric amount of  $\text{H}_2\text{O}_2$  or other peroxide, such as peroxyacetic acid, under vigorous stirring. To avoid the inhibition of horseradish

peroxidase due to the excess amount of peroxide, diluted peroxide (0.3 wt%) was added drop wise.

UV-Vis spectra were recorded on a Perkin–Elmer Lambda-9 UV/Vis/near-infrared spectrophotometer. FT-IR measurements were carried out on a Perkin–Elmer 1760X FT-IR spectrometer. The electrochemical characterization of polyaniline was carried out on an EG&G potentiostat/galvanostat model 263. Cyclic voltammograms were recorded by using a three-electrode cell in 1 M HCl. The conductivity of the synthesized polyaniline was measured by a typical four-probe method. The polyaniline was ground to fine powder and dried in a vacuum at 50 °C for 24 h prior to the measurements.

## References

- 1 A. G. MacDiarmid, *Synth. Met.*, 1997, **84**, 27.
- 2 A. G. MacDiarmid, J. C. Chiang, A. F. Richer and A. J. Epstein, *Synth. Met.*, 1987, **18**, 285.
- 3 Y. Cao, S. Li, Z. Xue and D. Guo, *Synth. Met.*, 1986, **16**, 305.
- 4 R. Noufi, A. J. Nozik, J. White and L. F. Warren, *J. Electrochem. Soc.*, 1982, **129**, 2261.
- 5 W. Westerweele, P. Smith and A. J. Heeger, *Adv. Mater.*, 1995, **7**, 788.
- 6 A. F. Diaz and J. A. Logan, *J. Electroanal. Chem.*, 1980, **111**, 111.
- 7 A. Watanabe, K. Mori, A. Iwabuchi, Y. Iwasaki, Y. Nakamura and O. Ito, *Macromolecules*, 1989, **22**, 3521.
- 8 W. W. Focke, G. E. Wnek and Y. Wei, *J. Phys. Chem.*, 1987, **91**, 5813.
- 9 C.-G. Wu and J.-Y. Chen, *Chem. Mater.*, 1997, **9**, 399.
- 10 G. Liu and M. S. Freund, *Macromolecules*, 1997, **30**, 5660.
- 11 J. C. Chiang and A. G. MacDiarmid, *Synth. Met.*, 1986, **13**, 193.
- 12 M. T. Nguyen, P. Kasai, J. L. Miller and A. F. Diaz, *Macromolecules*, 1994, **27**, 3625.
- 13 L. A. Samuelson, A. Anagnostopoulos, K. S. Alva, J. Kumar and S. K. Tripathy, *Macromolecules*, 1998, **31**, 4376.
- 14 W. Liu, A. L. Cholli, R. Nagarajan, J. Kumar, S. Tripathy, F. F. Bruno and L. A. Samuelson, *J. Am. Chem. Soc.*, 1999, **121**, 11345.
- 15 W. Liu, J. Kumar, S. Tripathy, K. J. Senecal and L. A. Samuelson, *J. Am. Chem. Soc.*, 1999, **121**, 71.
- 16 W. Liu, J. Kumar, S. Tripathy and L. A. Samuelson, *Langmuir*, 2002, **18**, 9696.
- 17 R. Nagarajan, W. Liu, J. Kumar and S. K. Tripathy, *Macromolecules*, 2001, **34**, 3921.
- 18 B. C. Saunders, A. G. Holmes-Siedle and B. P. Stark, in *Peroxidase*, Butterworths, London, 1964.
- 19 P. Wang and J. S. Dordick, *Macromolecules*, 1998, **31**, 941.
- 20 G. D'Aprano and M. Leclerc, *Chem. Mater.*, 1995, **7**, 33.
- 21 M. Thiyagrajan, L. A. Samuelson, J. Kumar and A. L. Cholli, *J. Am. Chem. Soc.*, 2003, **125**, 11502.
- 22 A. M. Klivanov, *Trends Biotechnol.*, 1997, **15**, 97.
- 23 H. B. Dunford, in *Peroxidases in Chemistry and Biology*, ed. J. Everse, K. E. Everse and M. B. Grisham, CRC Press, Boca Raton, FL, USA, 1991; vol. 2, pp. 1–24.
- 24 A. C. Maehly and B. Chance, The assay of catalases and peroxidases, in *Methods of Biochemical Analysis*, 1954, vol. 1, p. 357.
- 25 A. I. Vogel, A. R. Tatchell, B. S. Furnis, A. J. Hannaford and P. W. G. Smith, in *Text Book of Practical Organic Chemistry*, Prentice Hall, New York, 5th edn, 1989, p. 407.
- 26 E. M. Genies and C. Tsintavis, *J. Electroanal. Chem.*, 1985, **195**, 109.
- 27 Y. Wei, W. W. Focke, G. E. Wnek, A. Ray and A. G. MacDiarmid, *J. Phys. Chem.*, 1989, **93**, 495.
- 28 L. T. Yu, M. S. Borredon, M. Jozefowicz, G. Belorgey and R. Buvet, *J. Polym. Sci. Polym. Symp.*, 1967, **10**, 2931.
- 29 R. L. Hand and R. F. Nelson, *J. Am. Chem. Soc.*, 1974, **96**, 850.
- 30 T. Kobayashi, H. Yneyma and H. Tamara, *J. Electroanal. Chem.*, 1984, **177**, 293.
- 31 M. G. Mikhael, A. B. Padias and H. K. Hall, Jr., *J. Polym. Sci., Part A: Polym. Chem.*, 1997, **35**, 1673.



# Fe<sup>III</sup>-TAML-catalyzed green oxidative degradation of the azo dye Orange II by H<sub>2</sub>O<sub>2</sub> and organic peroxides: products, toxicity, kinetics, and mechanisms†

Naima Chahbane,<sup>a</sup> Delia-Laura Popescu,<sup>b</sup> Douglas A. Mitchell,<sup>b</sup> Arani Chanda,<sup>b</sup> Dieter Lenoir,<sup>\*a</sup> Alexander D. Ryabov,<sup>\*b</sup> Karl-Werner Schramm<sup>a</sup> and Terrence J. Collins<sup>\*b</sup>

Received 6th April 2006, Accepted 4th October 2006

First published as an Advance Article on the web 17th October 2006

DOI: 10.1039/b604990g

Oxidation of Orange II ([4-(2-hydroxynaphthyl)azo]benzenesulfonic acid), sodium salt) by hydrogen peroxide catalyzed by iron(III) complexed to tetra amido macrocyclic ligands (Fe<sup>III</sup>-TAML activators) in aqueous solutions at pH 9–11 leads to CO<sub>2</sub>, CO, phthalic acid and smaller aliphatic carboxylic acids as major mineralization products. The products are non-toxic according to the *Daphnia magna* test. Several organic intermediates have been identified by HPLC and GC-MS that allowed the detailed description of Orange II degradation. The catalytic oxidation can also be performed by organic oxidants such as benzoyl peroxide, *tert*-butyl and cumyl hydroperoxides. Kinetic studies of the catalyzed oxidation indicated that Fe<sup>III</sup>-TAML activators react first with ROOR' to form an oxidized catalyst ( $k_1$ ), which then oxidizes Orange II ( $k_{II}$ ). Neglecting the reversibility of the first step, the rate equation is rate =  $k_1 k_{II} [Fe^{III}][ROOR'] [Dye] / (k_1 [ROOR'] + k_{II} [Dye])$ ; here Fe<sup>III</sup> and ROOR' represent the catalyst and peroxide, respectively. The rate constant  $k_1$  equals  $(74 \pm 3) \times 10^3$ ,  $(1.4 \pm 0.1) \times 10^3$ ,  $24 \pm 2$ , and  $11 \pm 1 \text{ M}^{-1} \text{ s}^{-1}$  for benzoyl peroxide, H<sub>2</sub>O<sub>2</sub>, *t*-BuOOH, and cumyl hydroperoxide at pH 9 and 25 °C, respectively. An average value of  $k_{II}$  equals  $(3.1 \pm 0.9) \times 10^4 \text{ M}^{-1} \text{ s}^{-1}$  under the same conditions. The unraveling of the kinetic mechanism allows the comprehension of the robust reactivity, and this is discussed in detail using the representative results of DFT calculations.

## Introduction

Effluents containing textile dyes discharged by dye manufacturing and textile wet processing industries present significant environmental problems. In 1978, 9000 tons (2%) of the 450 000 tons of dyes produced worldwide was discharged in effluents from textile dyeing industries.<sup>1</sup> The total amount of dyes discharged was about 50 000 tons.<sup>1</sup> With the worldwide growth in fiber consumption, the use of dyes and their discharge is likely to continue to rise. Modern textile dyes are chemically stable and resistant to degradation by sunlight, water, soap, bleach, and perspiration.<sup>2</sup> They are difficult to degrade in textile wastewaters under the aerobic conditions that prevail in biological treatment plants.<sup>3,4</sup> Dyes in wastewater create aesthetic problems, limit the possible uses of the water, and reduce the efficacy of microbiological wastewater treatment because they may be toxic to microorganisms.<sup>5</sup> Dyes absorb and scatter the sunlight essential for the algae growth. The products of dye degradation can be mutagenic,

carcinogenic, or teratogenic<sup>6</sup> and cause long-term health concerns.<sup>7</sup> Azo dyes that incorporate the –N=N– moiety account for up to 70% of all textile dyestuffs produced.<sup>2</sup>

The degradation of organic dyes has therefore attracted much attention. New technologies for wastewater decolorization are especially needed. Modern chemical methods include TiO<sub>2</sub>-mediated photodegradation,<sup>8–11</sup> Fenton systems,<sup>12</sup> and soluble transition metal catalysts in combination with various oxidizing agents.<sup>13–23</sup> Several research groups have studied the catalyzed decolorization of dyes by H<sub>2</sub>O<sub>2</sub>.<sup>24,25</sup> Tosik and Wiktorowski have reported on the decolorization by ozone and H<sub>2</sub>O<sub>2</sub> with Fenton reagent.<sup>26</sup> Ozone degrades practically all dyes, reacting rapidly with both C–N and N=N bonds. The reactions are slow at lower temperatures and require higher catalyst and H<sub>2</sub>O<sub>2</sub> doses. Segal *et al.* have studied the oxidation of pinacyanol chloride by H<sub>2</sub>O<sub>2</sub> in the presence of several catalysts in aqueous alkaline solution at room temperature.<sup>27</sup> The catalysts known as octahedral molecular sieves are the most active when doped with Fe<sup>III</sup>, Cr<sup>III</sup>, and Co<sup>II</sup>. Fourteen

<sup>a</sup>Institute of Ecological Chemistry, GSF – National Research Center for Environment and Health, Postfach 1129, Neuherberg, D-85778, Germany. E-mail: lenoir@gsf.de

<sup>b</sup>Department of Chemistry, Carnegie Mellon University, 4400 Fifth Avenue, Pittsburgh, PA, 15213, USA. E-mail: ryabov@andrew.cmu.edu; tc1u@andrew.cmu.edu; Fax: +1-412-268-1061; Tel: +1-412-268-6177

† Electronic supplementary information (ESI) available: Initial rates of **1c**-catalyzed bleaching of Orange II at pH 5–11 as a function of [Ic] and [Orange II]; spectral changes during **1a**-catalyzed oxidation of Orange II by benzoyl peroxide. See DOI: 10.1039/b604990g

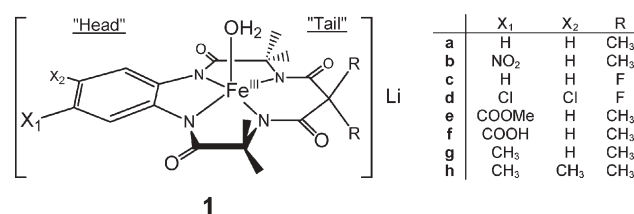
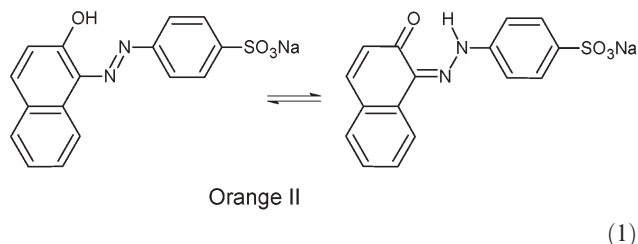


Chart 1 Iron(III)-TAML activators used in this work.

different catalysts have been compared. The deepest bleaching (65%) was accomplished in a matter of 30 min.

We have long been interested in developing green methodologies for decomposing pollutants in effluent streams and have synthesized highly active catalysts, called Fe–TAML activators (Fe<sup>III</sup> complexes of tetra amido macrocyclic ligands, **1**), that exhibit the capacity to marshal hydrogen peroxide to destroy pollutants in various effluent streams.<sup>28–30</sup> Fe<sup>III</sup>–TAML activators and their degradation products tested to date appear not to present toxicity concerns.<sup>29</sup> Here we describe the beginnings of a detailed investigation of the use of Fe–TAML catalysts for the oxidative degradation of Orange II by H<sub>2</sub>O<sub>2</sub> and organic peroxides. In aqueous solution, Orange II predominately exists as a keto tautomer (eqn (1)).<sup>31</sup>



The reactivity of Fe–TAML activators is comparable to that of H<sub>2</sub>O<sub>2</sub>-activating enzymes.<sup>32</sup> Therefore, it has been of interest to evaluate the relative catalytic features of Fe<sup>III</sup>–TAML activators and enzymes in oxidation of the dye. Reports on the horseradish peroxidase-catalyzed oxidation of Orange II are conflicting. According to Stiborová *et al.* horseradish peroxidase does not catalyze the oxidation of Orange II by H<sub>2</sub>O<sub>2</sub> at pH 4.7–8.4.<sup>33</sup> Morita *et al.* and Zhu *et al.* claim that this oxidation occurs.<sup>34,35</sup> Stoddart *et al.* have reported that microsomal cytochrome P450 readily catalyzes the oxidation of Orange II with a maximum activity observed at pH 7.<sup>36</sup> Chivukula and coworkers have described the lignin peroxidase-catalyzed oxidation of Orange II into 1,2-naphthoquinone and 4-sulfophenyl hydroperoxide.<sup>37</sup> López *et al.* have reported that manganese peroxidase also degrades the dye and have identified the degradation products by <sup>1</sup>H NMR and electrospray ionization-ion trap mass spectrometry.<sup>38</sup>

## Experimental

### Materials

Fe<sup>III</sup>–TAML<sup>®</sup> complexes **1a–h** were synthesized at Carnegie Mellon University by published methods.<sup>39</sup> Hydrogen peroxide (30% w/w) was purchased from Fluka. Orange II, which is also called Acid Orange 7, ([4-[(2-hydroxynaphthyl)azo] benzenesulfonic acid], sodium salt) was from Aldrich. It

was used without further purification (87%) for TOC measurements and studies of products of its catalytic degradation. For kinetic investigations, Orange II was purified by passing through a column filled with SMT Bulk-C18 (Separation Methods Technologies Inc., Newark) with water as the eluent. Catalase from *Aspergillus niger* was a Merck preparation. All other reagents and solvents (at least ACS reagent grade) were obtained from commercial sources (Aldrich, Fisher, Acros, Fluka) and used as received or, if necessary, after purification as described elsewhere.<sup>40</sup>

### General procedure for degradation of Orange II by Fe<sup>III</sup>–TAML–H<sub>2</sub>O<sub>2</sub>

Orange II and **1** were combined in a buffered solution and stirred under isothermal conditions (thermostatted with a temperature precision of  $\pm 0.5$  °C). Various amounts of 30% H<sub>2</sub>O<sub>2</sub> were then added to achieve the final concentration of H<sub>2</sub>O<sub>2</sub> of 0.01 M (Table 1). A decrease in the Orange II absorption band at the maximum (485 nm) was monitored during the reaction using a Cary 1 UV-Vis spectrophotometer. The mixture was quenched by a method appropriate to the analysis. In every experiment, the concentration of H<sub>2</sub>O<sub>2</sub> was high enough not to constitute a limiting factor.

### Analysis of degradation products by ion-chromatography

For analysis of small organic acids and ions the reaction was performed as described above and was quenched with 1.5  $\mu$ L catalase (5000 U mg<sup>-1</sup>). The analysis was performed with a Dionex IonPac IC-AS50 column (250  $\times$  2 mm) with a pre-column AG11-HC (2  $\times$  50 mm) and a CD-25 electrochemical detector operated in a conductivity mode.

### Determination of TOC

The Orange II degradation was performed as described above. The reaction was quenched with 40  $\mu$ L concentrated HCl and then the solution was diluted to 5 mL with water. The sample was injected into a TOC analyzer (Schimadzu 5000) and the results for the total organic carbon in the sample (mg L<sup>-1</sup>) were obtained. Blank measurements were also performed. Blank samples consisted of 1 mL buffer, the **1a** catalyst, and 40  $\mu$ L HCl; the volume was then made to 5 mL with water.

### Toxicity measurements

The toxicity of the dye and its degradation products were tested using 24 h born *Daphnia magna* at different dilutions as described in the standard operating protocol.<sup>41</sup> Daphnids were grown in the laboratory and were fed *Scenedesmus subspicatus*

**Table 1** Mass balance (in %) after treatment of Orange II (10<sup>-4</sup> M) by Fe<sup>III</sup>–TAML (**1a**) (2  $\times$  10<sup>-7</sup> M), H<sub>2</sub>O<sub>2</sub> (10<sup>-2</sup> M) at 25 °C, pH 10 (carbonate buffer)

| Prod-uct | Phthalic acid | Oxalic acid                         | Glycolic acid                       | Formic acid        | NO <sub>2</sub> <sup>-</sup> | NO <sub>3</sub> <sup>-</sup> | SO <sub>4</sub> <sup>2-</sup> | CO + CO <sub>2</sub> | Total |
|----------|---------------|-------------------------------------|-------------------------------------|--------------------|------------------------------|------------------------------|-------------------------------|----------------------|-------|
| Buffer   |               | HO <sub>2</sub> C–CO <sub>2</sub> H | HOCH <sub>2</sub> CO <sub>2</sub> H | HCO <sub>2</sub> H |                              |                              |                               |                      |       |
| 0.02 M   | 12.2          | 2.1                                 | 0.7                                 | 3.4                | 1                            | 2.2                          | 4.3                           | 32                   | 57    |
| 0.2 M    | 10.4          | 2.2                                 | 2.7                                 | 3.2                | —                            | —                            | 6.2                           | 35                   | 61    |

chodat. All solutions were prepared in doubly distilled water. Room temperature was kept at  $20 \pm 2$  °C. Toxicity experiments were carried out with 10 daphnids in each test beaker with 50 mL of final volume. Results were evaluated on the basis of immobilization percentage obtained by dividing the number of immobilized animals by total animals. The toxicity of wastewater samples was referred to as toxic when the immobilization percent was higher than 50%.<sup>41</sup>

### Kinetic studies of the catalyzed bleaching of Orange II by H<sub>2</sub>O<sub>2</sub> and organic peroxides

All kinetic measurements were performed at 298 K using a Hewlett Packard Diode Array spectrophotometer (model 8453) equipped with a thermostatted cell holder and an automatic 8-cell positioner. Stock solutions of **1** (*ca.*  $1 \times 10^{-3}$  M) and Orange II ( $1-8 \times 10^{-4}$  M) were prepared in HPLC grade water. Solutions of hydrogen peroxide were standardized by measuring the absorbance at 230 nm ( $\epsilon = 72.8 \text{ M}^{-1} \text{ cm}^{-1}$ )<sup>42</sup> or by titration as described elsewhere.<sup>43</sup> Stock solutions of other oxidizing agents were freshly prepared daily. The pH was measured using a Corning 220 pH meter, which was calibrated with standard buffer solutions at pH 4, 7, and 10. All oxidation reactions were carried out in 0.01 M phosphate buffer at pH ranging from 5 to 11. Initial rates of Orange II oxidation were calculated from the linear absorbance *versus* time plots using the extinction coefficients for Orange II of 17 800, 23 000, and 19 400  $\text{M}^{-1} \text{ cm}^{-1}$  at pH 5–7, 9 and 11, respectively, when the conversion of the dye did not exceed 10–20%. A typical kinetic run was performed as follows. The phosphate buffer was added to a cuvette with a stopper. Appropriate amounts of the stock solutions of Orange II and activator were then added. The reaction was initiated by addition of an aliquot of the stock solution of oxidizing agent. All initial rates reported are the mean values of at least three determinations. Calculations of the rate constants were carried out using a Sigma Plot 2001 package (Version 7.0).

### DFT calculations

Density functional calculations were performed using Becke's three parameter hybrid functional (B3LYP) provided by the Gaussian 03 (release B.05) software package.<sup>44</sup> The basis set 6–31G was used for geometry optimizations and Mulliken charge analysis. All calculations were carried out in vacuum (in the absence of any solvent). Mulliken population analysis was employed to monitor electron distribution. The self-consistent field calculations were terminated upon reaching tight convergence criteria ( $10^{-6}$  root mean square deviation in the density matrix and  $10^{-8}$  atomic unit maximum deviation in energy). The calculations for benzoyl peroxide activation mechanism were performed using acetyl peroxide as a model.

## Results and discussion

### General observations

Electronic spectroscopy is a rational technique for monitoring the oxidation of Orange II. The dye has an intense absorption band with a maximum at 485 nm in water. Hydrogen peroxide

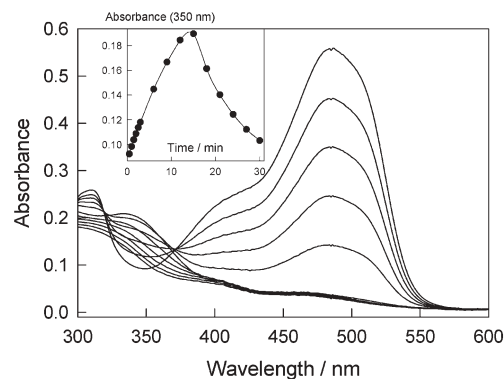


**Fig. 1** Spectral changes that accompany the catalytic oxidation of Orange II by H<sub>2</sub>O<sub>2</sub> in the presence of **1a**. Conditions: [**1a**]  $2.6 \times 10^{-7}$  M, [Orange II]  $2.7 \times 10^{-5}$  M, [H<sub>2</sub>O<sub>2</sub>]  $4.4 \times 10^{-4}$  M, pH 9 (0.01 M phosphate), 25 °C; spectra recorded with 3 min interval. Inset shows changes of absorbance at 350 nm with time; see text for details.

itself oxidizes Orange II very slowly. Fe<sup>III</sup>–TAML activators increase the rate immensely; the spectral changes observed during **1a**-catalyzed oxidation of Orange II are presented in Fig. 1. The major oxidation trend is a gradual decrease in the maximum intensity at 485 nm. The collapse of the 485 nm chromophore is due to the lost conjugation in the dye leading to colorless oxidation products. The inset to Fig. 1 shows that absorbance at 350 nm first increases and then decreases. This bi-phasic behavior, which is also observed for **1c** but the maximum of the 350 nm band is developed faster than in the case of **1a**, is obviously due to the formation and collapse of an intermediate under the catalytic conditions. The catalytic degradation performed at [H<sub>2</sub>O<sub>2</sub>] =  $3.3 \times 10^{-4}$  M and [**1**] =  $2 \times 10^{-7}$  M (pH 9–11, 25 °C) is usually complete within 10–30 min. Control experiments with Fe<sup>III</sup>–TAML activators in the absence of H<sub>2</sub>O<sub>2</sub>, or with H<sub>2</sub>O<sub>2</sub> in the absence of the catalyst, or with the catalase enzyme from *Aspergillus niger* in the presence of H<sub>2</sub>O<sub>2</sub>, all indicated no degradation of Orange II under these experimental conditions.

Catalysts **1a** and **1c** differ in terms of number of equivalents of H<sub>2</sub>O<sub>2</sub> needed for the bleaching of one equivalent of the color of Orange II, *i.e.* the number of equivalents of H<sub>2</sub>O<sub>2</sub> needed for degradation of Orange II, if its concentration is associated exclusively with the absorbance at 485 nm. Thus, a decrease of the absorbance at 485 nm has been measured after several consecutive additions of known aliquots of H<sub>2</sub>O<sub>2</sub>. Using the extinction coefficient of Orange II at 485 nm, the number of bleached equivalents has been calculated and is shown in Fig. 2. Note again that this is only the *color removing stoichiometry*, not the stoichiometry of complete oxidative degradation. Curiously, the **1a** catalyst needs only one half equivalent of H<sub>2</sub>O<sub>2</sub> (1 oxidation equivalent) whereas **1c** needs one equivalent (2 oxidation equivalents). Hence, if only the color bleaching is at issue, the **1a** catalyst is more economical because it needs half the amount of H<sub>2</sub>O<sub>2</sub> compared to **1c**. This observation may be explained if primary, non-absorbing products are oxidized slower by **1a** than by **1c**. Therefore, more hydrogen peroxide is used by **1c** due to “spectrally invisible” oxidations (see below).

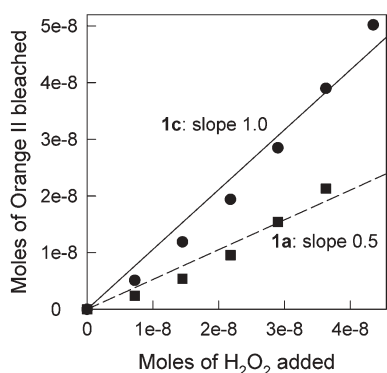


**Fig. 2** Number of moles of Orange II bleached against number of moles of  $\text{H}_2\text{O}_2$  added when catalyzed by **1a** (■) and **1c** (●). Conditions: [**1a**]  $9.9 \times 10^{-7}$  M, [**1c**]  $1.24 \times 10^{-7}$  M, pH 9.0 (0.01 M phosphate),  $25^\circ\text{C}$ . See text for details.

### Identification of products of degradation of Orange II

The formation of small organic acids and inorganic ions as mineralization products was anticipated. Phthalic acid was quantified using GC-MS. Formic, glycolic, and oxalic acids were detected by ion-chromatography; the data is summarized in Table 1. These breakdown molecules, known as ultimate organic products during the aromatic ring-opening,<sup>45</sup> are non-toxic and biodegradable.<sup>46</sup> The mineralization products are nitrite, nitrate, sulfate, and  $\text{CO}_2$  (Table 1). Nitrite and nitrate are produced from nitrogens of the azo group of Orange II. The ions  $\text{NO}_2^-$  and  $\text{NO}_3^-$  could not be reliably measured due to interference from carbonate (0.2 M). Sulfate originates from the sulfonyl group. The level of mineralization equals 35% from determining the total organic carbon.

The data in Table 1 indicates that more than 61% of Orange II was degraded under these conditions, yielding products shown in Table 1. There may be other products, which are difficult to detect by the techniques employed. Phthalic acid, the major degradation product, is stable under the experimental conditions. It is formed from the naphthalene ring of Orange II.<sup>46,47</sup> The presence of phthalic acid was also confirmed by GC-MS analysis (data not shown). A control test with the dye before the catalytic degradation shows no presence of this compound.

The toxicity of the solution has been evaluated before and after degradation. The data is shown in Fig. 3. The degradation products are non-toxic. The initial toxicity of Orange II decreased after the treatment by a factor of *ca.* 3 (see Fig. 3). Due to the protocol of the method,<sup>41</sup> the value of mL of tested sample is a measure for toxicity. The larger this number the smaller is the toxicity. Zero points of immobilization of *Daphnia magna* in the control tubes were confirmed. A maximum toxicity of 20% was observed in both experiments. Zero mortality of *Daphnia magna* in the control tubes has been confirmed. This result demonstrates that the  $\text{Fe}^{\text{III}}$ -TAML-catalyzed degradation of Orange II by  $\text{H}_2\text{O}_2$  is safe and free from the formation of toxic oxidation products. It should be mentioned that other research groups studying peroxide catalysts employing Fenton chemistry would encounter major toxicity issues.

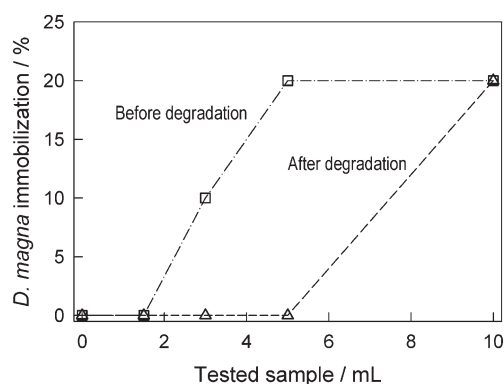


**Fig. 3** Effects of Orange II (□) and its degradation products (△) on immobilization of *Daphnia magna*. Conditions: [Orange II]  $10^{-4}$  M, [**1a**]  $2 \times 10^{-7}$  M, [ $\text{H}_2\text{O}_2$ ]  $10^{-2}$  M,  $25^\circ\text{C}$ , pH 10 (0.02 M carbonate).

### Kinetics of 1a-catalyzed bleaching of Orange II by $\text{H}_2\text{O}_2$

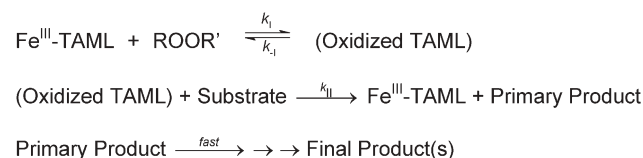
The kinetic data reported in this work has been interpreted in terms of the general mechanism shown in Scheme 1. The  $\text{Fe}^{\text{III}}$ -TAML activator reacts reversibly with a primary oxidizing agent to form an oxidized catalyst ( $k_1$ ,  $k_{-1}$ ), which then oxidizes a substrate ( $k_{\text{II}}$ ) followed by several fast steps.

The initial rate for the consumption of Orange II is given by eqn (2), which has been derived applying the steady-state approximation to (Oxidized TAML) and using the mass balance equation for the catalyst:  $[\text{Fe}^{\text{III}}]_{\text{T}} = [\text{Fe}^{\text{III}}] + [\text{Oxidized TAML}]$ . Correspondingly, the rate of bleaching should be proportional to the amount of catalyst and may level off with increasing both Orange II and oxidant concentrations. In general, these features hold for both **1a** and **1c** catalysts.

$$-\frac{d[\text{Orange II}]}{dt} = \frac{k_1 k_{\text{II}} [\text{Fe}^{\text{III}}]_{\text{T}} [\text{ROOR}'] [\text{Orange II}]}{k_{-1} + k_1 [\text{ROOR}'] + k_{\text{II}} [\text{Orange II}]} \quad (2)$$

The initial rate method<sup>48</sup> is the optimal kinetic technique for studying the catalytic activity of  $\text{Fe}^{\text{III}}$ -TAML activators because **1a-h** are fragile and undergo intramolecular inactivation under the operating conditions.<sup>49</sup> This phenomenon does not compromise the catalysis but explains why, as in the case of enzymes, the kinetic curves are more difficult to analyze in their entirety, and dealing with initial rates is preferred.

The initial rate of Orange II bleaching by  $\text{H}_2\text{O}_2$  is proportional to the concentration of **1a** and the rate is notably higher at pH 11 than at pH 9 (Fig. 4). Minor intercepts could be attributed to the “background” non-catalytic oxidation by hydrogen peroxide. Dependencies of the initial rates on Orange II and  $\text{H}_2\text{O}_2$  concentrations at pH 9 and 11 are presented in Fig. 5. It is interesting to note that at pH 11,



**Scheme 1** General mechanism for catalysis by  $\text{Fe}^{\text{III}}$ -TAMLS.

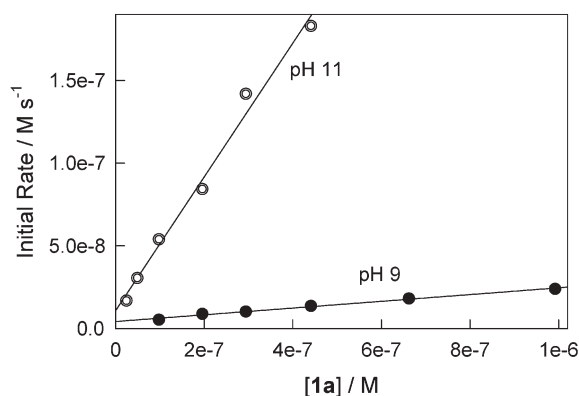


**Fig. 4** Initial rates of **1a**-catalyzed bleaching of Orange II by  $\text{H}_2\text{O}_2$  as a function of  $[\mathbf{1a}]$  at pH 9 and 11. Conditions:  $[\text{Orange II}] 4.5 \times 10^{-5} \text{ M}$ ,  $[\text{H}_2\text{O}_2] 3.3 \times 10^{-4} \text{ M}$ ,  $25^\circ\text{C}$ .

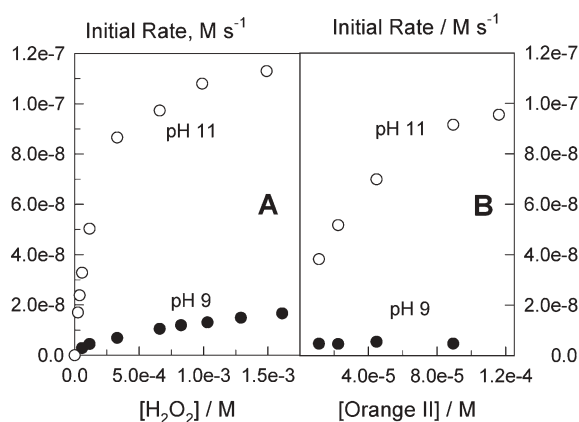


**Fig. 5** Initial rates of **1a**-catalyzed bleaching of Orange II by  $\text{H}_2\text{O}_2$  as a function of  $[\text{H}_2\text{O}_2]$  (A) and  $[\text{Orange II}]$  (B). Conditions:  $25^\circ\text{C}$ ,  $[\mathbf{1a}] 2 \times 10^{-7} \text{ M}$ , when  $[\text{Orange II}]_{\text{fixed}} 4.5 \times 10^{-4} \text{ M}$ ,  $[\text{H}_2\text{O}_2]_{\text{fixed}} 3.3 \times 10^{-4} \text{ M}$ .

where the bleaching is faster, there are Michaelis type dependencies in the concentrations of Orange II and  $\text{H}_2\text{O}_2$ . The inverse rates have linear dependence on inverse concentrations of the both reagents (graphs not shown) supporting eqn (2) and suggesting that  $k_{-1}$  is negligible under these conditions. The case at pH 9 is slightly different. The initial rate is less curved when plotted against  $[\text{H}_2\text{O}_2]$  and practically independent of the Orange II concentration. To ensure that eqn (2) holds, a more detailed kinetic investigation has been performed at pH 11. The initial rates as a function of  $[\text{H}_2\text{O}_2]$  have been measured at different concentrations of Orange II covering at least a ten-fold concentration range. These data are shown as a three dimensional (3D) graph in Fig. 6.

All data in Fig. 6 have been fitted to eqn (2) on the assumption that  $k_{-1} \sim 0$  to obtain the rate constants  $k_1$  and  $k_{\text{II}}$  of  $(1.9 \pm 0.2) \times 10^3$  and  $(4.5 \pm 0.5) \times 10^4 \text{ M}^{-1} \text{ s}^{-1}$ , respectively. The 3D mesh in Fig. 6 has been generated using the best-fit rate constants; the black circles are the experimentally measured initial rates. Data in Fig. 6 agree with those in Fig. 5 and illustrate the catalytic dye bleaching by  $\text{Fe}^{\text{III}}$ -TAML activators. When the concentration of  $\text{H}_2\text{O}_2$  is low, the formation of the oxidized TAML is rate-limiting and the initial

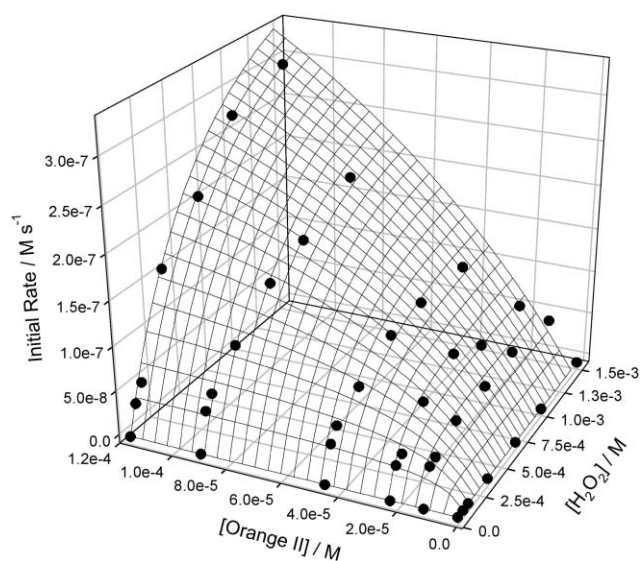


**Fig. 6** 3D-Plot showing the dependence of initial rates of **1a**-catalyzed bleaching of Orange II by  $\text{H}_2\text{O}_2$  as a function of  $[\text{H}_2\text{O}_2]$  and  $[\text{Orange II}]$ . Conditions:  $[\mathbf{1a}] 2 \times 10^{-7} \text{ M}$ , pH 11,  $25^\circ\text{C}$ .

rates are independent of  $[\text{Orange II}]$ . Speeding up the formation of oxidized TAML by increasing  $[\text{H}_2\text{O}_2]$  moves the bleaching into a different kinetic regime, where the step driven by  $k_{\text{II}}$  is the slowest and hence the rate is almost proportional to the Orange II concentration. Such 3D plots are observed when numerical values of the products  $k_1[\text{H}_2\text{O}_2]$  and  $k_{\text{II}}[\text{Dye}]$  are comparable.<sup>50</sup>

#### Substituent (Hammett) effects on the rate constants $k_1$ and $k_{\text{II}}$

Using a series of  $\text{Fe}^{\text{III}}$ -TAML activators with the same  $\text{R} = \text{Me}$  but different ring substituents X, *i.e.* complexes **1a,b,e-h**, electronic effects on the rate constants  $k_1$  and  $k_{\text{II}}$  have been investigated. The values of  $k_1$  and  $k_{\text{II}}$  have been calculated from the rates of Orange II bleaching catalyzed by **1a,b,e-h** measured at  $\text{H}_2\text{O}_2$  concentrations in the range  $(0.3\text{--}12) \times 10^{-3} \text{ M}$  at pH 9 and  $25^\circ\text{C}$  (Table 2). Two corresponding Hammett plots are shown in Fig. 7. As seen, the electron-withdrawing groups at the aromatic ring favor both  $k_1$  and  $k_{\text{II}}$ , the effect on  $k_1$  being stronger. The positive  $\rho$  values equal 0.4 and 0.2 for  $k_1$  and  $k_{\text{II}}$ , respectively. The value of 0.4 agrees well with that previously found (0.3) using an easy-to-oxidize  $\text{Ru}^{\text{II}}$  dye, for which the relation  $k_1[\text{H}_2\text{O}_2] \ll k_{\text{II}}[\text{Dye}]$  holds always.<sup>32</sup> Rather surprisingly, the sensitivity of  $\text{Fe}^{\text{III}}$ -TAML activators

**Table 2** The rate constants  $k_1$  and  $k_{\text{II}}$  (in  $\text{M}^{-1} \text{ s}^{-1}$ ) for the **1**-catalyzed oxidation of Orange II at pH 9 and  $25^\circ\text{C}$

| Catalyst (X)                 | Peroxide               | $10^{-3} \times k_1$ | $10^{-4} \times k_{\text{II}}$ |
|------------------------------|------------------------|----------------------|--------------------------------|
| <b>1a</b> (H)                | $\text{H}_2\text{O}_2$ | $1.40 \pm 0.01$      | $3.8 \pm 0.3$                  |
| <b>1g</b> (Me)               | $\text{H}_2\text{O}_2$ | $0.27 \pm 0.04$      | $1.2 \pm 0.4$                  |
| <b>1h</b> (Me <sub>2</sub> ) | $\text{H}_2\text{O}_2$ | $0.26 \pm 0.02$      | $1.4 \pm 0.7$                  |
| <b>1f</b> (COOH)             | $\text{H}_2\text{O}_2$ | $0.29 \pm 0.01$      | $1.3 \pm 0.4$                  |
| <b>1e</b> (COOMe)            | $\text{H}_2\text{O}_2$ | $0.68 \pm 0.03$      | $1.6 \pm 0.4$                  |
| <b>1b</b> (NO <sub>2</sub> ) | $\text{H}_2\text{O}_2$ | $1.58 \pm 0.03$      | $3.22 \pm 0.04$                |
| <b>1a</b> (H)                | Benzoyl peroxide       | $74 \pm 3$           | $3.7 \pm 0.9$                  |
| <b>1a</b> (H)                | <i>t</i> -BuOOH        | $0.024 \pm 0.002$    | $3.2 \pm 1.5$                  |
| <b>1a</b> (H)                | Cumyl hydroperoxide    | $0.011 \pm 0.001$    | $1.8 \pm 0.8$                  |

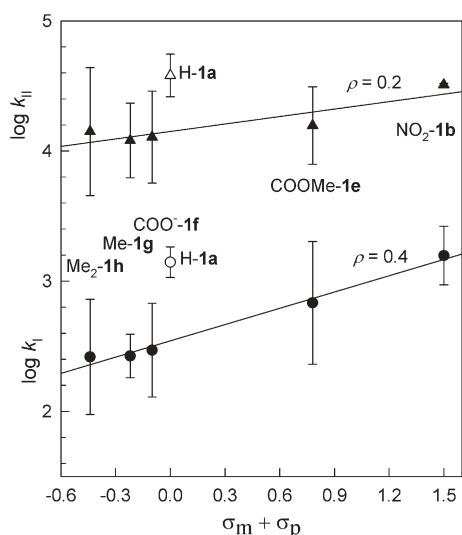


**Fig. 7** Hammett plots for the rate constants  $k_I$  and  $k_{II}$ . The data for the **1a** activator (Table 2) was ignored in linear regressions, the analytic expressions for which are  $\log k_I = (2.5 \pm 0.02) + (0.42 \pm 0.03)(\sigma_m + \sigma_p)$ ,  $\log k_{II} = (4.2 \pm 0.04) + (0.19 \pm 0.06)(\sigma_m + \sigma_p)$ . Doubled value of  $(\sigma_m + \sigma_p)$  was used for **1h**. All values of  $\sigma$  are taken from the review of Hansch, Leo, and Taft.<sup>57</sup>

to the electronic effects in the aromatic ring is exceptionally low for both  $k_I$  and  $k_{II}$  processes. The information for  $k_{II}$  has not been reported before. The slope of 0.2 indicates no dependence. This may reflect the fact that the keto form of Orange II undergoes oxidation. If the hydroxy form would be oxidized at pH 9, much stronger electronic effects could be anticipated due to involvement of the deprotonated naphthol fragment. It is interesting to note that the data for **1a** are somewhat higher than anticipated on the basis of Hammett correlations. The open circle and triangle were ignored here in the linear regressions. Similar behavior for **1a** has been noted previously.<sup>49</sup> A rather speculative explanation of this is that the less-substituted **1a** catalyst has less steric restrictions when it interacts with both oxidants and electron donors.

#### Kinetics of **1c**-catalyzed bleaching of Orange II by $H_2O_2$

As mentioned above, the catalysis by **1a** and **1c** is slightly different. The kinetic features of these activators have therefore been compared. There is a satisfactory first order kinetics in **1c** in bleaching of Orange II by  $H_2O_2$  at pH 5–11 (Fig. 1S in ESI†). At this point, **1a** and **1c** behave similarly. The rate is strongly pH-dependent and the highest activity is observed at pH 9–11. Variation in kinetic performance of **1a** and **1c** is revealed in Fig. 8 where the initial rate is shown as a function of  $[H_2O_2]$ . The rate is almost directly proportional to the peroxide concentration. The transition state is thus made of **1c** and  $H_2O_2$  implying that the rate should be independent of Orange II concentration. The data in Fig. 2S (see ESI†) confirms this. The activation of  $H_2O_2$  by **1c** is thus slower than the subsequent reaction of the oxidized TAML with Orange II, *i.e.*  $k_{II}[\text{Orange II}] \gg k_I[H_2O_2]$ . In other words, in just bleaching, catalyst **1c** is much more powerful than **1a**. This also explains the different stoichiometries observed for **1a** and **1c**. The catalyst **1c** is more robust and performs a higher

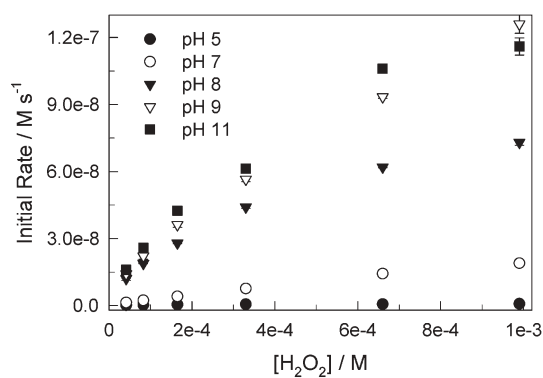


**Fig. 8** Initial rates of **1c**-catalyzed bleaching of Orange II by  $H_2O_2$  at different pH. Conditions: [Orange II]  $4.47 \times 10^{-5}$  M, [**1c**]  $2.5 \times 10^{-7}$  M, 25 °C.

number of “invisible” turnovers using extra equivalents of  $H_2O_2$ . Data for **1c** has been used to construct pH dependence of its catalytic activity, which is actually the pH profile for the rate constant  $k_I$ . The highest activities at pH 9–11 (Fig. 9) agree with our previous findings using the easiest-to-oxidize dyes and single turnover stopped-flow measurements.<sup>32,51</sup> The behavior of **1d** is similar to that of **1c**.

#### Kinetics of **1a**-catalyzed bleaching of Orange II by organic peroxides

In addition to  $H_2O_2$ , the **1a**  $Fe^{III}$ -TAML activator catalyzes the oxidation of Orange II by organic peroxides, *i.e.* *tert*-butyl hydroperoxide, cumyl hydroperoxide, and benzoyl peroxide. The kinetics of **1a**-catalyzed bleaching by organic peroxide has been followed as above by monitoring a decrease in the Orange II concentration at 485 nm (pH 9, 25 °C). If the mechanism in Scheme 1 is true for these oxidants, the rate expression eqn (2) should hold. The initial rate of Orange II bleaching is directly proportional to [**1a**] in the range  $(0.1\text{--}1.0) \times 10^{-6}$  M, but levels off with increasing concentrations of Orange II and three organic peroxides. Data for benzoyl peroxide is shown in Fig. 10. The corresponding double reciprocal plot, *i.e.* inverse rate *versus* inverse concentration, is linear (inset to Fig. 10). The data for other peroxides have been analyzed in a similar

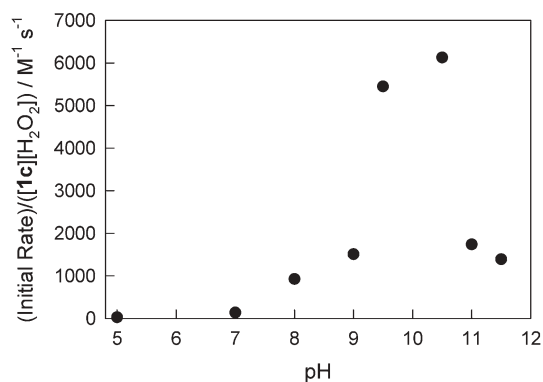


**Fig. 9** Normalized initial rates of the **1c**-catalyzed bleaching of Orange II measured at lower concentrations of  $H_2O_2$ . For conditions, see legend to Fig. 8.

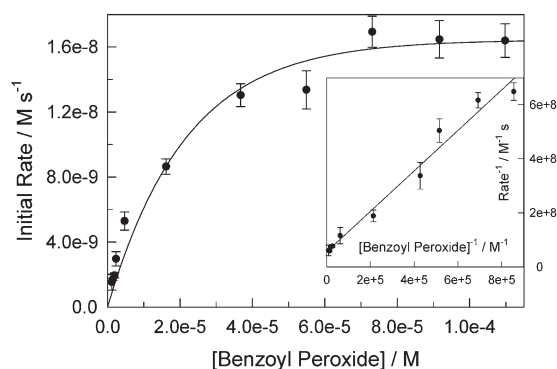


**Fig. 10** Initial rate of **1a**-catalyzed bleaching of Orange II as a function of benzoyl peroxide concentration. Inset shows linear double reciprocal plot used for calculation of  $k_1$  and  $k_{II}$ . Conditions: [Orange II]  $2.7 \times 10^{-5}$  M, [**1a**]  $1.8 \times 10^{-8}$  M, pH 9, 25 °C.

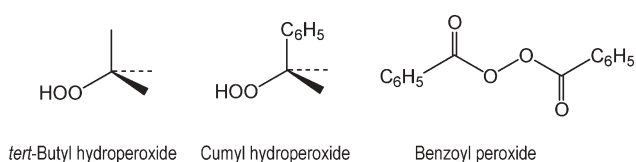


**Chart 2** Organic peroxides used in this study.

way. Straight lines have a common intercept giving similar values of  $k_{II}$ , as expected if the reactions between **1** and all peroxides afford the common oxidized TAML species. The calculated rate constants  $k_1$  and  $k_{II}$  (Table 2) confirm that the rate constants  $k_1$  are lower than  $k_{II}$  for all oxidants but benzoyl peroxide, for which the value of  $k_1$  is exceptionally large. It is higher by a factor of 53 than that for  $\text{H}_2\text{O}_2$ , the most reactive oxidizing agent used with  $\text{Fe}^{\text{III}}$ -TAML activators so far. It should be mentioned that the Orange II bleaching by benzoyl peroxide is a clean process without induction period (Fig. 3S). There are no inflection points on the absorbance *versus* time plots. The reactivity of all peroxides in terms of  $k_1$  decreases in the series benzoyl peroxide ( $6.8 \times 10^3$ ) >  $\text{H}_2\text{O}_2$  (130) > *t*-BuOOH (2) > cumyl hydroperoxide (1).

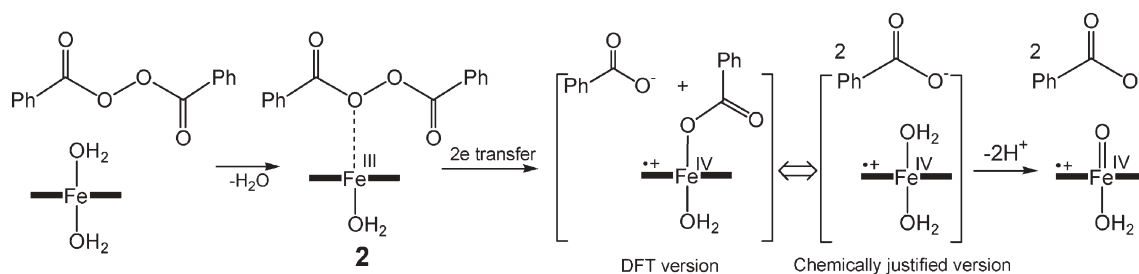
### Mechanistic conclusions and implications

The mechanistic picture of  $\text{Fe}^{\text{III}}$ -TAML-catalyzed bleaching of Orange II by a series of oxidants has two aspects. Suggested by Scheme 1 and eqn (2); these two are the intermediate formation and its performance in the dye oxidation. The steps are characterized by the rate constants  $k_1$  and  $k_{II}$ , respectively.

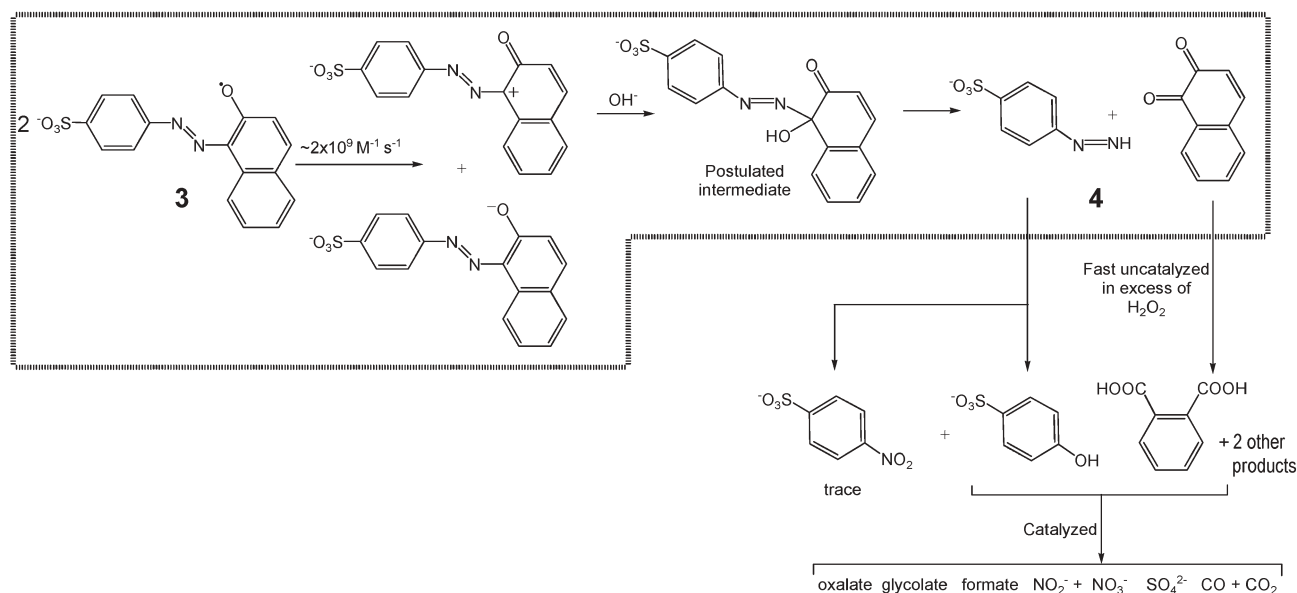
The first unexpected aspect is the highest rate constant  $k_1$  for benzoyl peroxide. This molecule is significantly larger than  $\text{H}_2\text{O}_2$ , but the steric effect does not seem to be a factor. Assuming that the activation of hydroperoxides by  $\text{Fe}^{\text{III}}$ -TAMs **1a-h** occurs as it has been suggested for peroxidases, *i.e.* involving the formation of the  $\text{Fe}^{\text{III}}$ -O-OR intermediate followed by the heterolytic cleavage of the O-O bond,<sup>52,53</sup> the reaction of benzoyl peroxide differs (Scheme 2). Benzoyl peroxide does not have an H-O fragment and therefore its coordination to iron(III) should involve either carbonyl or peroxy oxygen. The DFT calculations suggest that both oxygen atoms may coordinate to iron(III) because their effective negative charges are similar, *i.e.*  $-0.38$  and  $-0.30$  for carbonyl and peroxy oxygen, respectively. The peroxy oxygen (intermediate **2** in Scheme 2) seems to be a better candidate because the  $\sigma^*$  orbital of the O-O fragment is thus much closer to the reducing  $\text{Fe}^{\text{III}}$  center. The DFT calculations (in vacuum) support this mechanistic hypothesis. These have been done by the example of acetyl peroxide instead of benzoyl peroxide. If the carbonyl oxygen is a donor center, the complexation between **1** and benzoyl peroxide is a dead-end pathway, which does not result in the O-O bond cleavage. In contrast, the binding to form intermediate **2** is on the reaction coordinate and the following energy minimum is found for the system consisting of free benzoate and benzoate coordinated to formally  $\text{Fe}^{\text{V}}$  (or  $^+\text{Fe}^{\text{IV}}$ ). Benzoate coordination to iron of TAML does not appear to occur in the aqueous solution because axial ligands are known to undergo ready hydrolysis.<sup>54</sup> Ligation of iron of TAMs by anionic ligands is difficult to achieve in water, and therefore benzoate coordination is improbable. If formed, it will be rapidly hydrolyzed. A more realistic mechanism should involve two free benzoates and oxidized iron (Scheme 2). The formation of two benzoate anions requires two electrons. Two electrons could be moved concertedly or stepwise. The net result is the oxidation of  $\text{Fe}^{\text{III}}$ -TAML and generation of two benzoate anions.

The major feature of the second aspect is the absolute value of the rate constants  $k_{II}$ . The average *measured* value for  $k_{II}$  in the case of **1a** from Table 2 equals  $3.1 \times 10^4 \text{ M}^{-1} \text{ s}^{-1}$  at 25 °C and pH 9 (or  $4.5 \times 10^4 \text{ M}^{-1} \text{ s}^{-1}$  at pH 11). Oakes and Gratton reported the value of  $0.08 \text{ M}^{-1} \text{ s}^{-1}$  for the oxidation of Orange II by *p*-sulfonated perbenzoic acid under the same conditions.<sup>55</sup> The difference is a factor of *ca.*  $4 \times 10^5$ ! This offers a convincing illustration of the power of  $\text{Fe}^{\text{III}}$ -TAML catalysts.

An intriguing (and perhaps general) mechanism for the decolorization of dyes by one-electron oxidizing agents has



**Scheme 2** Plausible mechanism for activation of benzoyl peroxide by  $\text{Fe}^{\text{III}}$ -TAMs. For details, see text.



**Scheme 3** Plausible scheme of 1-catalyzed oxidative degradation of Orange II. Steps in the dotted box were suggested previously.<sup>56</sup>

been proposed after studying Orange II bleaching by pulse radiolysis.<sup>56</sup> It involves diffusion-controlled disproportionation of two primary dye-radicals formed after the initial, rate-limiting electron transfer. The diffusion-controlled disproportionation affords a starting dye and the product of its 2-electron oxidation, which is further involved in a series of transformations. Early steps of this mechanism are shown in Scheme 3.<sup>56</sup> This mechanism is useful for describing the results of catalysis by 1 assuming that the oxidized catalysts 1 generate the primary radical 3 shown in Scheme 3 in a pathway described by the rate constant  $k_{11}$ .

We did not detect 4-diazenylbenzenesulfonate (4) and 1,2-naphthoquinone by HPLC under our catalytic conditions. The probable reason that the quinone was not detected is that under these conditions 1,2-naphthoquinone is rapidly oxidized into phthalic acid plus two additional products just by  $\text{H}_2\text{O}_2$  without participation of 1. 4-Diazenylbenzenesulfonate should be unstable as well. A formation of 4-nitrobenzo- and 4-hydroxybenzenesulfonate detected by HPLC could presumably result from the oxidation of 4-diazenylbenzenesulfonate. Phthalic acid and 4-hydroxybenzenesulfonate undergo the catalyzed oxidation by  $\text{H}_2\text{O}_2$  giving a variety of small biodegradable, non-toxic organic products with substantial mineralization.

In conclusion, the  $\text{Fe}^{\text{III}}\text{-TAML-H}_2\text{O}_2$  system efficiently degrades Orange II into small biodegradable and non-toxic organic products. Substantial mineralization has been observed. The oxidation occurs rapidly compared to biological and other chemical systems that have been previously studied. Furthermore, the ecotoxicological examination suggests that the described technique is an environmentally safe process. With current concerns regarding the treatment of textile dyes, a green process for degrading pollutants is greatly needed; this is especially true for textile dyes. The  $\text{Fe-TAML-H}_2\text{O}_2$  systems show considerable promise to provide such a technology.

## Acknowledgements

Support from Eden-Hall Foundation, NSF (9612990), EPA (Grant RD83), and the Institute for Green Oxidation Chemistry is gratefully acknowledged.

## References

- 1 *Pollution Prevention and Abatement Handbook*, World Bank Group, Washington, D.C., 1998, ISBN 0-8213-3638-X.
- 2 H. Zollinger, *Color Chemistry: Syntheses, Properties and Applications of Organic Dyes and Pigments*, Wiley, Weinheim, 3rd edn, 2003.
- 3 J. R. Easton, in *The dye maker's view of color in dye house effluent*, ed. P. Cooper, Woodhead Publishing Ltd, Bradford, UK, 1995.
- 4 A. Gottlieb, C. Shaw, A. Smith, A. Wheatley and S. Forsythe, *J. Biotechnol.*, 2003, **101**, 49.
- 5 K. Hunger, *Chimia*, 1994, **48**, 520; K. Hunger, *Rev. Prog. Color. Relat. Top.*, 2005, **35**, 76.
- 6 C. Jakopitsch, G. Regelsberger, P. G. Furtmueller, F. Rueker, G. A. Peschek and C. Obinger, *Biochem. Biophys. Res. Commun.*, 2001, **287**, 682.
- 7 M. A. Brown and S. C. DeVito, *Crit. Rev. Environ. Sci. Technol.*, 1993, **23**, 249.
- 8 C. Lagrasta, I. R. Bellobono and M. Bonardi, *J. Photochem. Photobiol. A*, 1997, **110**, 201.
- 9 C. A. K. Gouvea, F. Wypych, S. G. Moraes, N. Duran, N. Nagata and P. Peralta-Zamora, *Chemosphere*, 1999, **40**, 433.
- 10 B. Neppolian, S. Sakthivel, B. Arabindoo, M. Palanichamy and V. Murugesan, *J. Environ. Sci. Health, Part A*, 1999, **A34**, 1829.
- 11 B. Neppolian, H. C. Choi, S. Sakthivel, B. Arabindoo and V. Murugesan, *Chemosphere*, 2002, **46**, 1173.
- 12 B. Utset, J. Garcia, J. Casado, X. Domenech and J. Peral, *Chemosphere*, 2000, **41**, 1187.
- 13 J. Oakes, P. Gratton and I. Weil, *J. Chem. Soc., Dalton Trans.*, 1997, 3805.
- 14 J. Oakes, G. Welch and P. Gratton, *J. Chem. Soc., Dalton Trans.*, 1997, 3811.
- 15 J. Oakes and P. Gratton, *J. Chem. Soc., Perkin Trans. 2*, 1998, 2563.
- 16 J. Oakes, P. Gratton, R. Clark and I. Wilkes, *J. Chem. Soc., Perkin Trans. 2*, 1998, 2569.
- 17 G. R. Hodges, J. R. Lindsay Smith and J. Oakes, *J. Chem. Soc., Perkin Trans. 2*, 1998, 617.



- 18 G. R. Hodges, J. R. Lindsay Smith and J. Oakes, *J. Chem. Soc., Perkin Trans. 2*, 1999, 1943.
- 19 I. Arslan and I. A. Balcioglu, *Dyes Pigm.*, 1999, **43**, 95.
- 20 J. Oakes, P. Gratton and T. Gordon-Smith, *Dyes Pigm.*, 2000, **46**, 169.
- 21 B. C. Gilbert, J. R. L. Smith, M. S. Newton, J. Oakes and R. Pons i Prats, *Org. Biomol. Chem.*, 2003, **1**, 1568.
- 22 R. A. Sheldon and G. Papadogianakis, in *Aqueous-Phase Organometallic Catalysis*, ed. B. Cornils and W. A. Herrmann, Wiley-VCH Verlag, Weinheim, 2nd edn, 2004, pp. 473–480.
- 23 R. Hage and A. Lienke, *Angew. Chem., Int. Ed.*, 2006, **45**, 206.
- 24 D. M. Gould, W. P. Griffith and M. Spiro, *J. Mol. Catal. A: Chem.*, 2001, **175**, 289.
- 25 P. Verma, P. Baldrian and F. Nerud, *Chemosphere*, 2003, **50**, 975.
- 26 R. Tosik and S. Wiktorowski, *Ozone: Sci. Eng.*, 2001, **23**, 295.
- 27 S. R. Segal, S. L. Suib and L. Foland, *Chem. Mater.*, 1997, **9**, 2526.
- 28 T. J. Collins and C. P. Horwitz, *TAPPI Pulping Conference*, Orlando, FL, Oct. 31–Nov. 4, 1999, p. 703.
- 29 S. Sen Gupta, M. Stadler, C. A. Noser, A. Ghosh, B. Steinhoff, D. Lenoir, C. P. Horwitz, K.-W. Schramm and T. J. Collins, *Science*, 2002, **296**, 326.
- 30 T. J. Collins, *Acc. Chem. Res.*, 2002, **35**, 782.
- 31 L. C. Abbott, S. N. Batchelor, J. Oakes, B. C. Gilbert, A. C. Whitwood, J. R. L. Smith and J. N. Moore, *J. Phys. Chem.*, 2005, **109**, 2894.
- 32 A. Ghosh, D. A. Mitchell, A. D. Ryabov, D. L. Popescu, A. Chanda and T. J. Collins, manuscript in preparation.
- 33 M. Stiborova, B. Asfaw, E. Frei and H. H. Schmeiser, *Collect. Czech. Chem. Commun.*, 1996, **61**, 962.
- 34 M. Morita, E. Yamaguchi, E. Komatsu, R. Ito, T. Kamidate and H. Watanabe, *Nihon Yukagakkaishi*, 1999, **48**, 793.
- 35 M. Zhu, X.-M. Huang and H.-X. Shen, *Chin. J. Chem.*, 1999, **17**, 356.
- 36 A. M. Stoddart and W. G. Levine, *Biochem. Pharmacol.*, 1992, **43**, 2227.
- 37 M. Chivukula, J. T. Spadaro and V. Renganathan, *Biochemistry*, 1995, **34**, 7765.
- 38 C. López, A.-G. Valade, B. Combourieu, I. Mielgo, B. Bouchon and J. M. Lema, *Anal. Biochem.*, 2004, **335**, 135.
- 39 Website: <http://www.chem.cmu.edu/groups/collins/awardpatpub/patents/index.html>.
- 40 D. D. Perrin and W. L. F. Armarego, *Purification of Laboratory Chemicals*, Pergamon Press, 1988.
- 41 *DIN EN ISO/IEC 17025, General Requirements of the Authority of Test and Calibration Laboratories*. Version in German, English, French, CEN/CENELEC, Brussels, Belgium, 2000; Normausschuss Wasserwesen (NAW) beim Deutschen Institut für Normung e.V. (DIN). Arbeitsgruppe Biotest: Testverfahren mit Wasserorganismen (Gruppe L): (a) Bestimmung der Wirkung von Wasserinhaltsstoffen auf Kleinkrebse, Prüfungsvorschrift DIN 38 412 Teil 11; (b) Allgemeine Hinweise zur Planung, Durchführung und Auswertung biologischer Testverfahren, Prüfungsvorschrift DIN 38 412 Teil 1. OECD 202 Guideline for Testing of Chemicals 202. *Daphnia* sp., Acute Immobilisation Test and Reproduction Test, OECD, Paris 1984.
- 42 P. George, *Biochem. J.*, 1953, **54**, 267.
- 43 V. N. Goral, M. I. Nelen and A. D. Ryabov, *Anal. Lett.*, 1995, **28**, 2139.
- 44 M. J. Frisch, G. W. Trucks, H. B. Schlegel, G. E. Scuseria, M. A. Robb, J. R. Cheeseman, J. A. Montgomery, Jr., T. Vreven, K. N. Kudin, J. C. Burant, J. M. Millam, S. S. Iyengar, J. Tomasi, V. Barone, B. Mennucci, M. Cossi, G. Scalmani, N. Rega, G. A. Petersson, H. Nakatsuji, M. Hada, M. Ehara, K. Toyota, R. Fukuda, J. Hasegawa, M. Ishida, T. Nakajima, Y. Honda, O. Kitao, H. Nakai, M. Klene, X. Li, J. E. Knox, H. P. Hratchian, J. B. Cross, V. Bakken, C. Adamo, J. Jaramillo, R. Gomperts, R. E. Stratmann, O. Yazyev, A. J. Austin, R. Cammi, C. Pomelli, J. Ochterski, P. Y. Ayala, K. Morokuma, G. A. Voth, P. Salvador, J. J. Dannenberg, V. G. Zakrzewski, S. Dapprich, A. D. Daniels, M. C. Strain, O. Farkas, D. K. Malick, A. D. Rabuck, K. Raghavachari, J. B. Foresman, J. V. Ortiz, Q. Cui, A. G. Baboul, S. Clifford, J. Cioslowski, B. B. Stefanov, G. Liu, A. Liashenko, P. Piskorz, I. Komaromi, R. L. Martin, D. J. Fox, T. Keith, M. A. Al-Laham, C. Y. Peng, A. Nanayakkara, M. Challacombe, P. M. W. Gill, B. G. Johnson, W. Chen, M. W. Wong, C. Gonzalez and J. A. Pople, *GAUSSIAN 03 (Revision B.05)*, Gaussian, Inc., Wallingford, CT, 2004.
- 45 J. Bandara and J. Kiwi, *New J. Chem.*, 1999, **23**, 717.
- 46 M. F. Coughlin, B. K. Kinkle and P. L. Bishop, *Chemosphere*, 2002, **46**, 11.
- 47 V. Nadochenko and J. Kiwi, *J. Chem. Soc., Faraday Trans.*, 1997, **93**, 2373.
- 48 J. H. Espenson, *Chemical Kinetics and Reaction Mechanisms*, McGraw-Hill, Inc., New York, 1995.
- 49 A. Chanda, A. D. Ryabov, S. Mondal, L. Alexandrova, A. Ghosh, Y. Hangun-Balkir, C. P. Horwitz and T. J. Collins, *Chem.–Eur. J.*, 2006, DOI: 10.1002/chem.200600630.
- 50 A. D. Ryabov, V. S. Sukharev, L. Alexandrova, R. Le Lagadec and M. Pfeffer, *Inorg. Chem.*, 2001, **40**, 6529.
- 51 D.-L. Popescu, A. D. Ryabov and T. J. Collins, Abstracts of Papers, 231st ACS National Meeting, Atlanta, GA, US, March 26–30, 2006, p. IEC-052.
- 52 H. B. Dunford, *Adv. Inorg. Biochem.*, 1982, **4**, 41.
- 53 H. B. Dunford, *Heme Peroxidases*, Wiley-VCH, New York, 1999.
- 54 A. Ghosh, A. D. Ryabov, S. M. Mayer, D. C. Horner, D. E. Prasuhn, Jr., S. Sen Gupta, L. Vuocolo, C. Culver, M. P. Hendrich, C. E. F. Rickard, R. E. Norman, C. P. Horwitz and T. J. Collins, *J. Am. Chem. Soc.*, 2003, **125**, 12378.
- 55 J. Oakes and P. Gratton, *J. Chem. Soc., Perkin Trans. 2*, 1998, 1857.
- 56 J. J. F. Coen, A. T. Smith, L. P. Candéias and J. Oakes, *J. Chem. Soc., Perkin Trans. 2*, 2001, 2125.
- 57 C. Hansch, A. Leo and R. W. Taft, *Chem. Rev.*, 1991, **91**, 165.

# Lactic acid production from waste sugarcane bagasse derived cellulose

Mukund G. Adsul,<sup>a</sup> Anjani J. Varma<sup>b</sup> and Digambar V. Gokhale\*<sup>a</sup>

Received 24th April 2006, Accepted 4th October 2006

First published as an Advance Article on the web 17th October 2006

DOI: 10.1039/b605839f

Production of L(+)lactic acid from sugarcane bagasse cellulose, one of the abundant biomass materials available in India, was studied. The bagasse was chemically treated to obtain a purified bagasse cellulose sample, which is much more amenable to cellulase enzyme attack than bagasse itself. This sample, at high concentration (10%), was hydrolyzed by cellulase enzyme preparations (10 FPU g<sup>-1</sup> cellulose) derived from mutants generated in our own laboratory. We obtained maximum hydrolysis (72%), yielding glucose and cellobiose as the main end products. Lactic acid was produced from this bagasse cellulose sample by simultaneous saccharification and fermentation (SSF) in a media containing a cellulase enzyme preparation derived from *Penicillium janthinellum* mutant EU1 and cellobiose utilizing *Lactobacillus delbrueckii* mutant Uc-3. A maximum lactic acid concentration of 67 g l<sup>-1</sup> was produced from a concentration of 80 g l<sup>-1</sup> of bagasse cellulose, the highest productivity and yield being 0.93 g l<sup>-1</sup> h<sup>-1</sup> and 0.83 g g<sup>-1</sup>, respectively. The mutant Uc-3 was found to utilize high concentrations of cellobiose (50 g l<sup>-1</sup>) and convert it into lactic acid in a homo-fermentative way. Considering that bagasse is a waste material available in abundance, we propose to valorize this biomass to produce cellulose and then sugars, which can be fermented to products such as ethanol and lactic acid.

## Introduction

Lactic acid and its derivatives have been widely used in food, pharmaceutical, cosmetic and industrial applications.<sup>1</sup> It has also been receiving great attention as a feedstock for manufacture of polylactic acid (PLA), a biodegradable polymer used as environmentally friendly biodegradable plastic. Lactic acid is produced commercially either by chemical synthesis or by microbial fermentation. Approximately 90% of the total lactic acid produced worldwide is made by bacterial fermentation and the rest is produced synthetically by the hydrolysis of lactonitrile. The chemical synthesis of lactic acid always results in a racemic mixture of lactic acid, which is a major disadvantage. Fermentative production of lactic acid offers the advantages in both utilization of renewable carbohydrates and production of optically pure L- or D-lactic acid, depending on the strain selected.

Lignocellulosic substances are abundantly available resources, which can be utilized as a feedstock for producing a number of bulk chemicals like ethanol or lactic acid through fermentation processes. The possible lignocellulosic substances include sugarcane bagasse, waste paper and agricultural wastes. These resources are seen as an interesting energy sources for several reasons. The application of lignocellulosic residues in bioprocesses not only provides alternative substrates but also helps solve their disposal problems, and with the advent of biotechnological innovations, mainly in the area of enzyme and fermentation technology, many new avenues

have opened up for their proper utilization as value added products. Several chemical or physical pretreatments followed by enzymatic hydrolysis of pretreated lignocellulosic materials are necessary to produce fermentable sugars, which can be diverted to ethanol or lactic acid. Currently, optically pure lactic acid is produced mainly from cornstarch. However, utilization of lignocellulosic agricultural waste by-products for lactic acid production appears to be more attractive because of their low cost; further, they do not impact the food chain for humans. In fact, an attempt to produce lactic acid from cellulosic materials was first reported by Wang *et al.*<sup>2</sup> Since then, several reports appeared on the production of lactic acid from cellulosic materials.<sup>3–9</sup> Recently, Patel *et al.*<sup>10</sup> reported *Bacillus* sp. Strain 36D1 capable of converting lignocellulosic biomass into lactate with high product yield.

India is one of the largest sugar cane growing countries, producing approximately 200 million tons per year, which generate about 45 million tons of bagasse on dry weight basis. We have generated several bagasse samples with decreasing content of lignin, which were used to produce cellulase with high productivities.<sup>11</sup> These bagasse samples were also evaluated as a source for the production of sugars (glucose, xylose, arabinose) using enzymes that were produced by treating delignified bagasse samples with a mutant of *Penicillium janthinellum* NCIM 1171 obtained in our own laboratory,<sup>12,13</sup> thus completing the full cycle of enzyme generation and monosaccharide generation from the same bagasse cellulose broth. This strategy gives the most suitable enzyme for hydrolysis of the bagasse cellulose. In this paper, production of lactic acid by a mutant of *Lactobacillus delbrueckii* NCIM 2365, isolated in our laboratory, was investigated with bagasse derived cellulose sample as a carbon source.

<sup>a</sup>Scientist In-Charge, NCIM, National Chemical laboratory, Pune, 411 008, Maharashtra, India. E-mail: dv.gokhale@ncl.res.in; Fax: +91-20-25902671; Tel: +91-20-25902670

<sup>b</sup>Polymer Science and Engineering Division, National Chemical Laboratory, Dr Homi Bhabha Road, Pune, 411 008, Maharashtra, India

## Experimental

### Chemicals

Cellulose powder-123 (CP-123) was obtained from Carl Schleicher and Schull Co., Dassel, FRG. *p*-Nitrophenyl  $\beta$ -D-glucopyranoside (pNPG), carboxymethylcellulose (CMC) 3,5-dinitrosalysilic acid were obtained from Sigma–Aldrich Co., St Louis, MO, USA. Sodium azide was obtained from S.D.Fine-Chem (India). Avicel PH-101 was obtained from Fluka Chemie GmbH. The  $\alpha$ -cellulose with 0.18% lignin and 98% cellulose was prepared from sugarcane bagasse in our laboratory.

### Preparation of sugarcane bagasse cellulose

Sugarcane bagasse was obtained from Tamil Nadu Pulp and Paper Mills, Chennai, India. This bagasse contains about 43% cellulose, 30% xylan, and 20% lignin, in addition to some silica and other constituents. It was cut into small shreds of 1–3 mm size and then pre-treated with steam and alkali by a proprietary process (under patenting) to remove the xylan, lignin, and other impurities. The final product consisted of 93.5%  $\alpha$ -cellulose, 5.3%  $\beta$ -cellulose (low molecular weight cellulose and traces of hemicellulose), 1.02%  $\gamma$ -cellulose, and 0.18% lignin.

### Strain information and cellulase production

*Penicillium janthinellum* NCIM 1171 was obtained from NCIM Resource Center, Pune, India. Mutants (EMS-UV-8, EU1, EU2D21) of *P. janthinellum* were generated by exposing conidia of the parent strain to UV-irradiation. The mutant EMS-UV-8 is selected on the basis of hydrolysis of phosphoric acid swollen cellulose. EU1 mutant was selected on the basis of Avicel hydrolysis and EU2D-21 is selected on the basis of phosphoric acid swollen cellulose in presence of 2-deoxy-glucose (1.5%). The procedure of generation of these mutants and their crude enzyme mixtures have already been reported earlier.<sup>13</sup> These cultures were maintained on potato dextrose agar (PDA) and sub-cultured once every three months. PDA contained (per litre) extract from 200 g of potatoes, glucose (20.0 g), yeast extract (1.0 g), and agar (20.0 g). Enzyme production was carried out in a 250 ml Erlenmeyer flask, with 70 ml of production medium containing 1% (w/v) cellulose-123 powder and 2.5% wheat bran.<sup>13</sup> *Lactobacillus delbrueckii* mutant Uc-3 producing L(+)lactic acid with high productivity was isolated as described earlier.<sup>14</sup> It was maintained in liquid MRS medium supplemented with 0.1% CaCO<sub>3</sub>.

### Enzymatic hydrolysis of Avicel and sugarcane bagasse cellulose

The saccharification experiments were carried out in a 50 ml conical flask with 25 ml citrate buffer (pH 4.5, 50 mM), 1.25 g or 2.5 g of either bagasse cellulose or Avicel, 2.5 mg sodium azide and crude enzyme preparations from *P. janthinellum* NCIM 1171 or its mutants (EMS-UV-8, EU1, EU2D21). This mixture was incubated at 50 °C with shaking at 150 rpm. The samples were analyzed for the reducing sugars after suitable time intervals.

### Simultaneous saccharification and fermentation (SSF)

SSF was carried out in a 250 ml screw cap conical flask with the production medium consisting of bagasse sample (10.0 g), CaCO<sub>3</sub> (5.0 g), yeast extract (1.0 g) in 125 ml citrate buffer (pH 4.5, 50 mM). The production medium was sterilized at 121 °C for 20 min, the crude enzyme preparation was added, and *Lactobacillus delbrueckii* Uc-3 mutant cells (5%) grown in sucrose based medium<sup>14</sup> were inoculated. The flasks were incubated at 42 °C with shaking at 150 rpm. All the SSF experiments were performed for 72 h in media containing 10 filter paper units (FPU) g<sup>-1</sup> of substrate. The initial pH of the fermentation medium was 6.0. The samples harvested at various time intervals were centrifuged at 5000 rpm for 20 min to separate the cells. The supernatant was acidified by adding an equal volume of 1 N HCl, where free acid is liberated and analyzed by HPLC for lactic acid.

### Analytical methods

The reducing sugar content was estimated as the glucose equivalent by the dinitrosalicylic acid (DNS) method.<sup>15</sup> Cell growth was monitored by visible spectral peak absorbances (UV–VIS Spectrometer–117, Systronics, Mumbai, India) at a wavelength of 660 nm. The glucose, cellobiose and lactic acid in the samples were determined using a high performance liquid chromatography (HPLC) system (Dionex India Limited) equipped with UV- or RI-detectors. An ion exclusion column (Aminex HPX-87H, Biorad, Hercules, CA) was used at a temperature of 30 °C, with 0.008 N H<sub>2</sub>SO<sub>4</sub> as a mobile phase at a flow rate of 0.6 ml min<sup>-1</sup>. The injection volume of the sample was 50  $\mu$ l.

## Results and discussions

Initially, experiments were carried out to evaluate the potential of cellulase enzyme preparations derived from mutants EMS-UV-8, EU1 and EU2D21 towards the hydrolysis of sugarcane bagasse cellulose (lignin content 0.18) and Avicel. Hydrolysis was carried out at two different substrate concentrations (5% and 10%) using 5 FPU g<sup>-1</sup> and 10 FPU g<sup>-1</sup> of the cellulose substrate. It was found that all mutant enzyme preparations gave higher bagasse cellulose/Avicel hydrolysis than that obtained with parent enzyme preparation (Table 1). However, hydrolysis of the most crystalline substrate, Avicel, was always lower than that of bagasse sample irrespective of enzyme preparations used. The mutant enzyme preparations derived from EU1 and EU2D-21 yielded maximum hydrolysis at both 5% and 10% bagasse sample. With the same preparations, the Avicel hydrolysis (at 10% concentration) was only 38%, which was better than that obtained with the parental strain (21%). The rate of hydrolysis of both Avicel and bagasse cellulose sample with the mutant enzyme was faster than with the parental enzyme in spite of very low amounts (10 times less) of  $\beta$ -glucosidase in the mutant enzyme preparation compared to the parent enzyme (Fig. 1). The lower hydrolysis (40%) of Avicel could be due to its micro-crystalline structure, which prevents an easy access to enzymes. We got approximately 84% hydrolysis (at 5% bagasse cellulose concentration) and 72% hydrolysis (at 10% bagasse cellulose

**Table 1** Saccharification of Avicel and sugarcane bagasse cellulose with enzyme preparations derived from parent and mutant strain

| Strains  | Enzyme activities/g of substrate |                      |                     | % Hydrolysis after 96 h |              |                      |                       |
|----------|----------------------------------|----------------------|---------------------|-------------------------|--------------|----------------------|-----------------------|
|          | FPU <sup>a</sup>                 | $\beta$ -glucosidase | CMCase <sup>b</sup> | Avicel (5%)             | Avicel (10%) | BS <sup>c</sup> (5%) | BS <sup>c</sup> (10%) |
| Parent   | 5.0                              | 45.0                 | 210                 | 21                      | 21           | 46                   | 39                    |
| EMS-UV-8 | 5.0                              | 6.5                  | 140                 | 32                      | 33           | 48                   | 45                    |
| EU-1     | 5.0                              | 9.0                  | 175                 | 41                      | 41           | 63                   | 62                    |
| EU2D-21  | 5.0                              | 3.8                  | 170                 | 39                      | 38           | 52                   | 51                    |
| Parent   | 10.0                             | 90.0                 | 420                 | 26                      | 25           | 64                   | 57                    |
| EMS-UV-8 | 10.0                             | 13.0                 | 280                 | 39                      | 32           | 70                   | 56                    |
| EU-1     | 10.0                             | 18.0                 | 350                 | 46                      | 36           | 84                   | 72                    |
| EU2D-21  | 10.0                             | 7.6                  | 340                 | 44                      | 37           | 80                   | 60                    |

<sup>a</sup> FPU—filter paper cellulase units. <sup>b</sup> CMCase—carboxymethylcellulase activity. <sup>c</sup> BS—sugarcane bagasse cellulose sample.

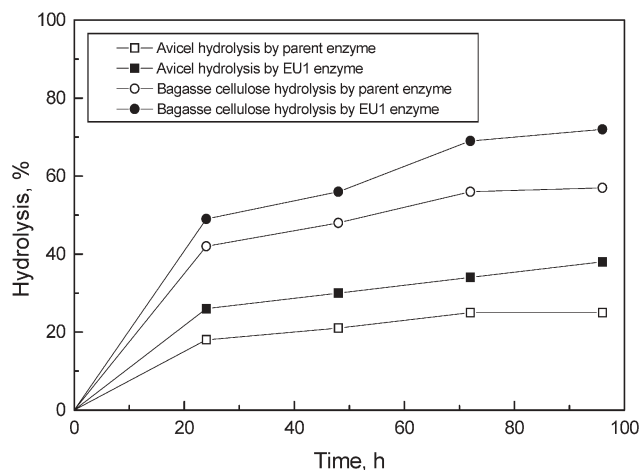


**Fig. 1** Profile of hydrolysis of Avicel and bagasse cellulose by parent and mutant (EU1) enzyme preparations. The hydrolysis was carried out using Avicel and sugarcane bagasse cellulose at 10% with parent and mutant enzyme preparations (10 FPU g<sup>-1</sup>).

concentration) with EU1 enzyme preparation (10 FPU g<sup>-1</sup> bagasse).

The hydrolysis of bagasse cellulose sample with parent enzyme preparation resulted in production of glucose as the only end product, probably due to the presence of very high amounts of  $\beta$ -glucosidase. On the other hand, the hydrolysis broth derived from the treatment of bagasse cellulose with mutant enzyme preparations contained both glucose and cellobiose as end products (Table 2). The amount of xylose

detected was insignificant, indicating a much lower amount of hemicellulose present in sugarcane bagasse cellulose. The mutants produced high levels of glucose because they are selected on the basis of hydrolysis in the presence of 2-deoxyglucose. The presence of cellobiose in the mutant hydrolysate is due to a lower amount of  $\beta$ -glucosidase in the crude enzyme mixture (Table 1). The presence of both glucose and cellobiose in the broth may hinder the further hydrolysis to glucose because they are strong inhibitors of cellulases. However, this drawback can be overcome by SSF methodology to produce lactic acid from bagasse cellulose sample using cellobiose utilizing microbes. Considering the inexpensive nature of bagasse samples, there is no doubt about their high potential as substrates for commercial production of glucose and further fermentation of glucose to other platform chemicals by SSF.

SSF experiments were carried out under the selected conditions (42 °C and pH 6.5) because the organism used in this fermentation is a mutant of *L. delbrueckii* (Uc-3) and cannot grow at temperatures more than 42 °C or at pH less than 5.5. We carried out the SSF at pH 6.5, where the cellulases used were active, with retention of 50% activity. The mutant (Uc-3) used in this study produces lactic acid with very high productivity.<sup>14</sup> SSF experiments were performed in production media containing cellulases (10 FPU g<sup>-1</sup> of substrate). The pH of the fermentation broth also dropped to 5.3 within 24 h (Fig. 2), which is the pH at which the enzymes are most active. There was no cellobiose accumulation during the fermentation at any time. Cellobiose was either converted to glucose by  $\beta$ -glucosidase present in the cellulase

**Table 2** End product analysis of saccharification of Avicel and sugarcane bagasse cellulose sample using different enzyme preparations

| Substrates                          | Enzyme   | Enzyme activity used            |            |                                  |            |
|-------------------------------------|----------|---------------------------------|------------|----------------------------------|------------|
|                                     |          | 5 FPU g <sup>-1</sup> substrate |            | 10 FPU g <sup>-1</sup> substrate |            |
|                                     |          | Cellobiose/mg                   | Glucose/mg | Cellobiose/mg                    | Glucose/mg |
| Avicel (2.5 g)                      | Parent   | 3.0                             | 520.0      | 6.1                              | 610.0      |
|                                     | EMS-UV-8 | 14.0                            | 805.0      | 33.0                             | 780.0      |
|                                     | EU1      | 33.0                            | 1000.0     | 20.0                             | 870.0      |
|                                     | EU2D-21  | 31.0                            | 940.0      | 20.0                             | 900.0      |
| Sugarcane bagasse cellulose (2.5 g) | Parent   | ND <sup>a</sup>                 | 970.0      | ND <sup>a</sup>                  | 1420.0     |
|                                     | EMS-UV-8 | 35.0                            | 1090.0     | 47.6                             | 1345.0     |
|                                     | EU1      | 84.0                            | 1460.0     | 48.5                             | 1740.0     |
|                                     | EU2D-21  | 93.0                            | 1200.0     | 65.0                             | 1420.0     |

<sup>a</sup> ND not detected.

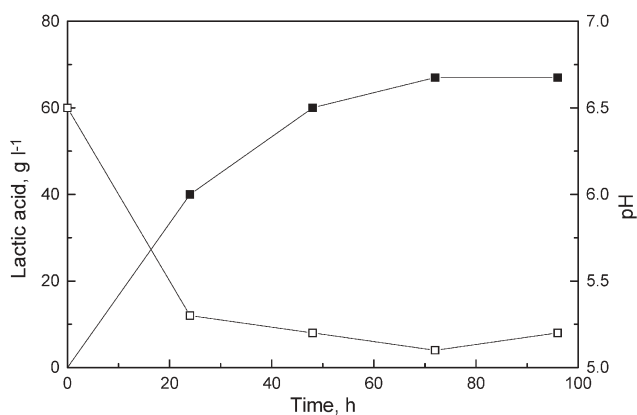


**Fig. 2** Course of lactic acid production (■) and pH (□) during SSF of sugarcane bagasse cellulose ( $80 \text{ g l}^{-1}$ ) using mutant enzyme preparation (EU1,  $10 \text{ FPU g}^{-1}$ ).

preparations or utilized by the mutant strain to produce lactic acid. The presence of higher cellobiose concentration could result in significant inhibition, which could be removed by supplementation of the media with additional cellobiase, leading to a remarkable improvement in lactic acid production in fed batch SSF.<sup>6</sup> However, in simple batch operations with cellulase from *T. reesei* and *L. delbrueckii*, supplementation of media with fresh cellobiase did not improve the overall process.<sup>16</sup> We obtained  $67 \text{ g l}^{-1}$  of lactic acid from  $80 \text{ g l}^{-1}$  of bagasse cellulose sample when we used EU1 enzyme preparations for hydrolysis. The yield ( $\text{g g}^{-1}$ ) and productivity ( $\text{g l}^{-1} \text{ h}^{-1}$ ) of lactic acid were 0.83 and 0.93, respectively. In comparison to other reports in the literature (Table 3), this is the highest yield and productivity of lactic acid reported so far in spite of using less cellulase enzyme ( $10 \text{ FPU g}^{-1}$  of the substrate) with low amounts of  $\beta$ -glucosidase in batch SSF. There is one report on maximum lactic acid production ( $108 \text{ g l}^{-1}$ ), which was achieved by combining multiple substrate addition, supplementation with fresh nutrients and enzymes and removal of lactic acid.<sup>6</sup>

Since there was no cellobiose detected during SSF, we wanted to know the potentiality of the mutant *L. delbrueckii* Uc-3 to utilize cellobiose and convert it into lactic acid. The fermentation experiments were carried out in production medium (initial pH 6.5) containing  $50 \text{ g l}^{-1}$  of cellobiose. The mutant produced  $42 \text{ g l}^{-1}$  of lactic acid within 48 h with 84% yield and  $1.0 \text{ g l}^{-1} \text{ h}^{-1}$  productivity (Fig. 3). The results

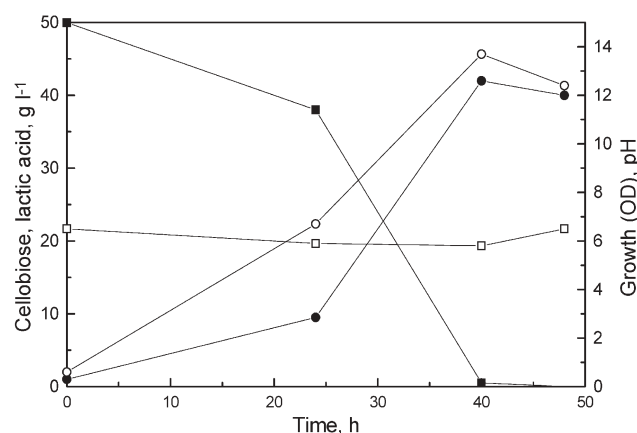


**Fig. 3** Profile of growth (○), pH (□), lactic acid production (●) and cellobiose utilization (■) during fermentation by *L. delbrueckii* mutant, Uc-3. The fermentation was carried out in a medium containing cellobiose ( $50 \text{ g l}^{-1}$ ).

suggested that mutant is capable of utilizing cellobiose at concentrations as high as  $50.0 \text{ g l}^{-1}$ .

## Conclusion

Batch experiments were conducted for conversion of bagasse sample to lactic acid by simultaneous saccharification and fermentation using a cellulase preparation derived from a mutant of *P. janthinellum* (EU1) and *L. delbrueckii* mutant Uc-3. Saccharification experiments were also carried out using mutant enzymes to characterize the cellulose degradation. *L. delbrueckii* mutant Uc-3 was capable of utilizing high concentrations of cellobiose, producing lactic acid with high yield ( $0.9 \text{ g lactic acid per g cellobiose}$ ). Batch SSF yielded  $67 \text{ g l}^{-1}$  of lactic acid from  $80 \text{ g l}^{-1}$  of bagasse sample with yield and productivity of  $0.83 \text{ g g}^{-1}$  of cellulose substrate and  $0.93 \text{ g l}^{-1} \text{ h}^{-1}$ . Applying SSF to lactic acid production has more advantage than SS since we could operate the SSF at conditions suitable and optimum for both cellulose hydrolysis and growth of *L. delbrueckii* mutant. The further improvements in batch SSF to make it cost effective are necessary, as this work indicates great advantages from the industrial viewpoint. The work on utilization of other biomass materials with proper pretreatment and proper integrated saccharification and fermentation processes may lead to bio-recycling of biomass to produce value added chemicals. We are currently

**Table 3** Comparison on recent data with present work on SSF production of lactic acid from cellulosic substrates

| Substrate/ $\text{g l}^{-1}$     | Microorganism                    | Enzyme/ $\text{FPU g}^{-1}$       | F. T. <sup>a</sup> | $C_{\text{max}}$ <sup>b</sup> | $Y_{\text{p/s}}$ <sup>c</sup> | $Q_{\text{p}}$ <sup>d</sup> | Reference |
|----------------------------------|----------------------------------|-----------------------------------|--------------------|-------------------------------|-------------------------------|-----------------------------|-----------|
| $\alpha$ -cellulose              | <i>L. delbrueckii</i> NRRL-B445  | —                                 | —                  | 75                            | 62                            | 0.34                        | 19        |
| Defatted rice bran (100)         | <i>L. delbrueckii</i> IFO 3202   | Cellulase-Y-NC                    | 36                 | 28                            | 28                            | 0.77                        | 9         |
| Filter paper (33)                | <i>L. coryniformi</i> ATCC 25600 | Celluclast and Novozyme (28)      | 48                 | 25                            | 75                            | 0.5                         | 17        |
| Solka Flocc (60)                 | <i>Bacillus sp.</i> Strain 36D1  | Spezyme (10)                      | 192                | 40                            | 65                            | 0.22                        | 10        |
| Solka Flocc (20)                 | <i>B. coagulans</i> strain 36D1  | Genecore International GC220 (10) | 24                 | 13.5                          | 67                            | 0.63                        | 20        |
| Preated cardboard (41)           | <i>L. coryniformi</i> ATCC 25600 | Celluclast & Novozyme (22.8)      | 48                 | 23                            | 56                            | 0.49                        | 8         |
| Paper mill sludge (23.4)         | <i>L. paracasei</i>              | Meicelase MCB8-6 (46)             | 72                 | 17                            | 72                            | 0.23                        | 18        |
| Sugarcane bagasse cellulose (80) | <i>L. delbrueckii</i> Uc-3       | <i>P. janthinellum</i> EU1 (10)   | 72                 | 67                            | 83                            | 0.93                        | This work |

<sup>a</sup> F.T.—Fermentation time (h). <sup>b</sup>  $C_{\text{max}}$ —Maximum lactic acid concentration ( $\text{g l}^{-1}$ ). <sup>c</sup>  $Y_{\text{p/s}}$ —% Product yield ( $\text{g g}^{-1}$ ). <sup>d</sup>  $Q_{\text{p}}$ —Lactic acid productivity ( $\text{g l}^{-1} \text{ h}^{-1}$ ).

working on improving the techno-economic efficiency of the sugarcane bagasse derived cellulose process, so as to obtain an optimum and inexpensive bagasse constitution (cellulose, xylan, and lignin) more amenable to enzyme/microbial attack and further fermentation to lactic acid and other feedstock chemicals that can take place in a facile manner.

## Acknowledgements

The authors gratefully acknowledge the financial support from Department of Biotechnology (DBT), New Delhi and TNBD (NMITLI) Division, CSIR, New Delhi.

## References

- 1 T. B. Vickroy, *Comprehensive Biotechnology*, ed. M. Moo-Young, Pergamon Press, New York, 1985, vol 3, pp. 761–776.
- 2 D. I. C. Wang, C. L. Cooney, A. L. Demain, R. F. Gomez and A. J. Sinskey, *Springfield: National Information Service Report*, COO-4198-4, 1977, pp. 106–123.
- 3 S. Abe and M. Takagi, *Biotechnol. Bioeng.*, 1991, **37**, 93–96.
- 4 K. V. Venkatesh, *Bioresour. Technol.*, 1997, **62**, 91–98.
- 5 S. Thomas, *Appl. Biochem. Biotechnol.*, 2000, **84–86**, 455–468.
- 6 A. B. Moldes, J. L. Alonso and J. C. Parajo, *J. Chem. Technol. Biotechnol.*, 2001, **76**, 279–284.
- 7 G. Bustos, A. B. Moldes, J. M. Cruz and J. M. Dominguez, *Biotechnol. Prog.*, 2005, **21**, 793–798.
- 8 R. Yanez, J. L. Alonso and J. C. Parajo, *J. Chem. Technol. Biotechnol.*, 2005, **80**, 76–84.
- 9 T. Tanaka, M. Hoshina, S. Tanabe, K. Sakai, S. Ohtsubo and M. Taniguchi, *Bioresour. Technol.*, 2006, **97**, 211–217.
- 10 M. A. Patel, M. S. Ou, L. O. Ingram and K. T. Shanmugam, *Biotechnol. Prog.*, 2005, **21**, 1453–1460.
- 11 M. G. Adsul, J. E. Ghule, R. Singh, H. Shaikh, K. B. Bastawde, D. V. Gokhale and A. J. Varma, *Carbohydr. Polym.*, 2004, **54**, 67–72.
- 12 M. G. Adsul, J. E. Ghule, R. Singh, H. Shaikh, K. B. Bastawde, D. V. Gokhale and A. J. Varma, *Carbohydr. Polym.*, 2005, **62**, 6–10.
- 13 M. G. Adsul, K. B. Bastawde, A. J. Varma and D. V. Gokhale, *Bioresour. Technol.*, 2006, DOI: 10.1016/j.biortech.2006.02.036.
- 14 S. R. Kadam, S. S. Patil, K. B. Bastawde, J. M. Khire and D. V. Gokhale, *Process Biochem.*, 2006, **41**, 120–126.
- 15 E. H. Fischer and E. A. Stein, *Biochem. Prep.*, 1961, **8**, 27–32.
- 16 J. C. Parajo, J. L. Alonso and A. B. Moldes, *Food Biotechnol.*, 1997, **11**, 45–58.
- 17 R. Yanez, A. B. Moldes, J. L. Alonso and J. C. Parajo, *Biotechnol. Lett.*, 2003, **25**, 1161–1164.
- 18 K. Nakasaki, N. Akakura, T. Adachi and T. Akiyama, *Environ. Sci. Technol.*, 1999, **33**, 198–200.
- 19 V. P. Iyer and Y. Y. Lee, *Biotechnol. Lett.*, 1999, **21**, 371–373.
- 20 M. A. Patel, M. S. Ou, R. Harbrucker, H. C. Aldrich, M. L. Buszko, L. O. Ingram and K. T. Shanmugam, *Appl. Environ. Microbiol.*, 2006, **72**, 3228–3235.

# Can ionic liquids dissolve wood? Processing and analysis of lignocellulosic materials with 1-*n*-butyl-3-methylimidazolium chloride

Diego A. Fort,<sup>a</sup> Richard C. Remsing,<sup>b</sup> Richard P. Swatloski,<sup>cd</sup> Patrick Moyna,<sup>\*a</sup> Guillermo Moyna<sup>\*b</sup> and Robin D. Rogers<sup>\*c</sup>

Received 30th May 2006, Accepted 19th September 2006

First published as an Advance Article on the web 17th October 2006

DOI: 10.1039/b607614a

The bulk of the cellulose currently employed by industry is isolated from wood through Kraft pulping, a process which traditionally involves a barrage of environmentally detrimental chemicals and is undeniably 'non-green.' In this report we present a simple and novel alternative approach for the processing of lignocellulosic materials that relies on their solubility in solvent systems based on the ionic liquid (IL) 1-*n*-butyl-3-methylimidazolium chloride ([C<sub>4</sub>mim]Cl). Dissolution profiles for woods of different hardness are presented, making emphasis on the direct analysis of the cellulosic material and lignin content in the resulting liquors by means of conventional <sup>13</sup>C NMR techniques. We also show that cellulose can be readily reconstituted from the IL-based wood liquors in fair yields by the addition of a variety of precipitating solvents. Spectroscopic and thermogravimetric studies indicate that the polysaccharide obtained in this manner is virtually free of lignin and hemicellulose and has characteristics that are comparable to those of pure cellulose samples subjected to similar processing conditions.

## Introduction

Wood is one of the most important biorenewable resources available to Man, with well-known uses as fuel, building, and manufacturing material.<sup>1,2</sup> In addition, it is the primary source of cellulose for use in the paper, fiber, paint, membrane, and polymer industries. Among the different approaches currently employed in the production of cellulose from wood, Kraft pulping methods are by far the most heavily used.<sup>3,4</sup> Briefly, the process involves the semi-selective chemical degradation of the lignin/hemicellulose matrix in wood by treatment with solutions of sodium hydroxide and sodium sulfide at high temperatures and pressures. This selectivity results in high yields of cellulose fibers that are stronger and require less bleaching than those obtained by other comparable methods. Despite its popularity and efficiency, Kraft pulping involves the use of a variety of toxic and hazardous chemicals and generates large amounts of air and water pollutants.<sup>3,4</sup> In view of the fact that the annual production of wood pulp nears 200 million tons worldwide,<sup>2</sup> roughly half of which comes from North America,<sup>2,4</sup> the environmental impact of the paper, pulp, and associated industries has become a major global concern. A number of improvements to traditional pulping methods, together with elemental chlorine free (ECF) and totally chlorine free (TCF) bleaching protocols introduced in the 1990s,<sup>3,4</sup> have considerably reduced pollution levels

generated by modern Kraft pulp mills. In addition, cleaner and more efficient pulp delignification strategies based on aqueous biphasic extraction systems, such as the clean fractionation process and methods relying on organosolv or polyethylene glycol (PEG),<sup>5-7</sup> have been demonstrated in recent years. Notwithstanding these advances, the constant tightening of policies affecting this sector and industry self-regulation initiatives have made the search for 'greener' wood processing technologies a never ending endeavor.

The enormous promise of ionic liquids (ILs) as environmentally-friendly materials is now well known, and their numerous applications have been extensively documented.<sup>8,9</sup> ILs have tunable physicochemical properties, usually negligible vapor pressures and, in general, thermal stability over a wide range of temperatures. As a result, they have been used successfully to replace traditional solvents employed in a variety of synthetic and manufacturing processes, and have the potential to reduce the current dependency of industry on volatile organic compounds (VOCs).<sup>8,9</sup> In addition to their role as alternative reaction and extraction media, we and others have shown that certain ILs can dissolve polysaccharides and other biopolymers very efficiently.<sup>10-15</sup> Perhaps the most salient results in this regard have been those obtained with 1-*n*-butyl-3-methylimidazolium chloride ([C<sub>4</sub>mim]Cl, Fig. 1a). This IL dissolves cellulose with no prior derivatization in concentrations of up to 300 g L<sup>-1</sup>, thus facilitating the development of 'greener' technologies for the production of cellulose-based materials.<sup>10,16</sup> As we have recently reported, the solvation of carbohydrates in [C<sub>4</sub>mim]Cl involves the formation of hydrogen bonds between the non-hydrated chloride ions of the IL and the sugar hydroxyl protons in a 1:1 stoichiometry.<sup>17</sup> In the case of cellulose, these interactions disrupt the extensive hydrogen bonding network of the polymer and lead to its dissolution. Additionally, we have shown that following

<sup>a</sup>Facultad de Química, Universidad de la República, Avenida General Flores 2124, Montevideo 11800, Uruguay. E-mail: pmoyna@fq.edu.uy

<sup>b</sup>Department of Chemistry & Biochemistry, University of the Sciences in Philadelphia, 600 South 43rd Street, Philadelphia, PA 19104, USA.

E-mail: g.moyna@usip.edu

<sup>c</sup>Center for Green Manufacturing and Department of Chemistry, The University of Alabama, Tuscaloosa, AL 35487, USA.

E-mail: rdrogers@bama.ua.edu

<sup>d</sup>525 Solutions, Inc., P.O. Box 861395, Tuscaloosa, AL 35486, USA

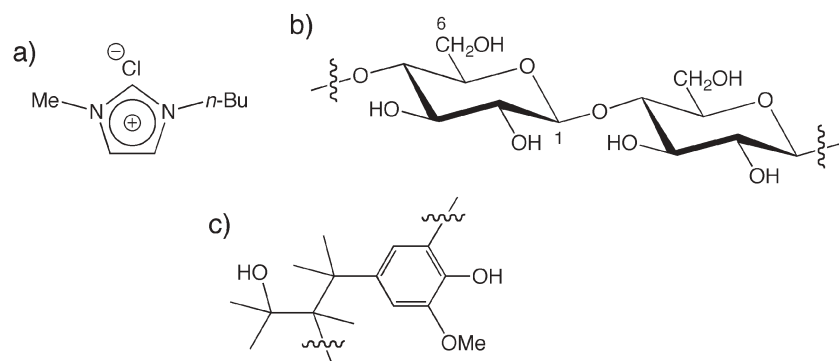


Fig. 1 Structures of [C<sub>4</sub>mim]Cl (a), cellulose (b), and lignin (c).

minimal sample preparation [C<sub>4</sub>mim]Cl is capable of fully dissolving structured polysaccharide-based natural matrices, such as those found in fruits and grains, allowing for their composing carbohydrates to be readily extracted and analyzed.<sup>18</sup> Taking its unique properties as a cellulose solvent also into account, these latter findings prompted us to explore the use of this IL in the development of much needed alternative methods for the extraction and processing of polysaccharides from wood and other forms of lignocellulosic biomass.<sup>19</sup>

As discussed herein, our results indicate that solvent systems based on [C<sub>4</sub>mim]Cl are indeed capable of partially dissolving wood. In addition, we demonstrate that celluloses which are virtually free of lignin and hemicellulose can be easily reconstituted from the resulting IL-based wood extracts, and show that the physicochemical properties of the recovered materials are comparable to those of pure cellulose samples subjected to similar processing conditions.

## Results and discussion

The dissolution in [C<sub>4</sub>mim]Cl of woods of varying hardness, including pine, poplar, eucalyptus, and oak, was studied using an approach based on previously reported methods.<sup>18,20</sup> For each sample, 5 wt% suspensions of dried and finely divided wood chips in a solution of the IL and 15 wt% DMSO-*d*<sub>6</sub> were stirred at 100 °C for periods ranging from 2 to 24 h. As we have shown, the use of small amounts of DMSO-*d*<sub>6</sub> as a co-solvent has no noticeable effect on the solubility of carbohydrates in [C<sub>4</sub>mim]Cl, reduces the viscosity of the mixtures, and, more importantly, allows for the resulting solubilized materials to be analyzed directly with conventional <sup>13</sup>C NMR techniques.<sup>18,20</sup> In all cases, swelling of the wood particles was observed immediately after they came in contact with the IL-based solvent. As time progressed, the coloration and viscosity of the solutions increased and the suspended particles became smaller, indicating that dissolution was taking place. However, none of the samples dissolved completely even after extended periods of time. This is not surprising in view of the fact that the structural matrix of the cell walls of higher plants, made up primarily of tightly associated cellulose and lignin chains (Fig. 1),<sup>1</sup> is significantly more complex than that of the amyloplasts from fruits and grains that were considered in our earlier studies. Following the removal of undissolved particulate matter, the

compositions of the resulting wood extracts, or wood liquors, were inspected using <sup>13</sup>C NMR spectroscopy.<sup>18,20</sup>

The <sup>13</sup>C spectrum of the liquor obtained after dissolving pine wood for 6 h in [C<sub>4</sub>mim]Cl/DMSO-*d*<sub>6</sub>, presented in Fig. 2a, serves to illustrate the most salient aspects of our analyses. Comparison with the spectrum of microcrystalline cellulose (MCC) recorded under identical conditions reveals clearly that this polysaccharide is present in the IL-based wood liquor (Fig. 2b). Of note are the signals at 103.1, 80.1, 76.2, 75.9, 74.7, and 61.0 ppm, all of which are well-resolved and correspond, respectively, to the resonances of the C-1, C-4, C-5, C-3, C-2, and C-6 carbons of cellulose.<sup>20</sup> Similarly, the signal at 57.2 ppm in the spectrum of the liquor correlates with the aromatic OMe <sup>13</sup>C resonance observed in [C<sub>4</sub>mim]Cl/DMSO-*d*<sub>6</sub> solution for Indulin AT (Fig. 2c), a desalted lignin preparation that closely represents the naturally-occurring phenylpropanoid polymer. Though less significant, signals at 103.6, 97.7, 93.0, 80.7, 77.8, 71.4, and 61.9 ppm can be attributed to low molecular weight cellulose oligomers (*i.e.*,  $\gamma$ -celluloses),<sup>20</sup> and indicate that minor degradation of the polysaccharide occurs under these conditions. Finally, considerably weaker signals are also observed at  $\sim$ 170 and  $\sim$ 22 ppm (data not shown). Albeit tentatively, these can be assigned to the carbonyl and methyl carbons of acetate groups present in hemicelluloses by comparison with <sup>13</sup>C CP/MAS NMR data reported for these heteropolysaccharides.<sup>21</sup> Overall, the data presented above prove conclusively that there is partial dissolution of the wood samples in the IL-based solvent system.

The next step in our study involved the estimation of the cellulosic material and lignin extraction levels as a function of dissolution time, or dissolution profiles, for the various types of wood examined. As was stated earlier, the IL-based wood liquors become more viscous and their coloration intensifies with time, a qualitative observation which can be rationalized by an increase in the concentration of polymeric materials in solution.<sup>10</sup> This assumption can be confirmed by cursory inspection of the <sup>13</sup>C NMR spectra of [C<sub>4</sub>mim]Cl/DMSO-*d*<sub>6</sub> liquors obtained at different dissolution times, such as those shown in Fig. 3 for poplar wood extracts. Since these spectra were recorded under analogous experimental conditions, the progressive improvement in the signal-to-noise ratio of the cellulose and lignin resonances is a direct reflection of the increase in the concentration of these polymers in the liquor as



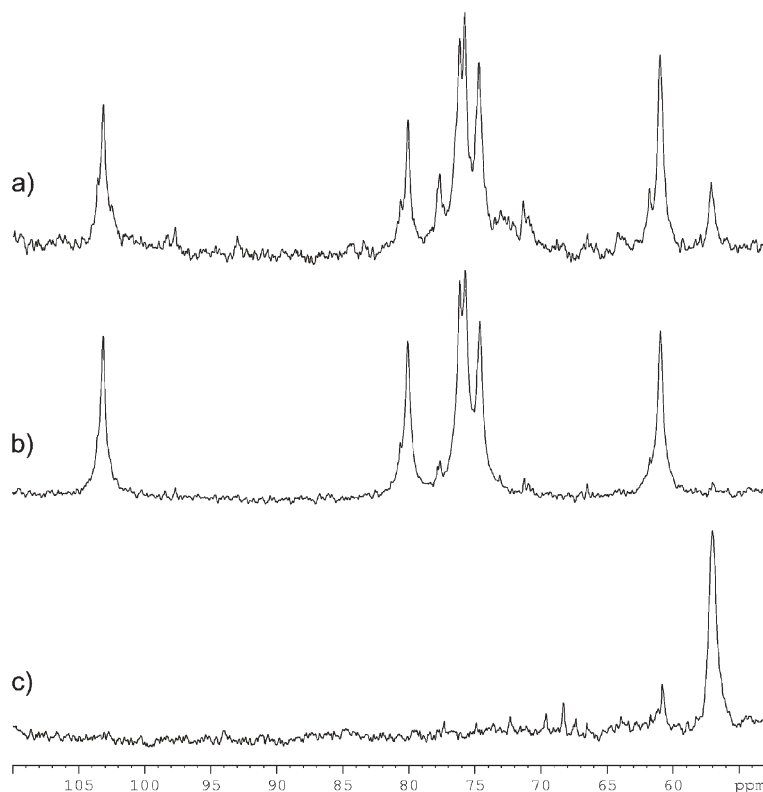


**Fig. 2**  $^{13}\text{C}$  NMR spectra of the extract obtained after dissolving pine wood in  $[\text{C}_4\text{mim}]\text{Cl}/\text{DMSO-}d_6$  for 6 h at  $100\text{ }^\circ\text{C}$  (a), and of 5 wt% solutions of MCC (b) and Indulin AT (c) in the same solvent system.

a function of dissolution time. Further analysis of the data shown in Fig. 3 also reveals that the levels of  $\gamma$ -celluloses grow with time, and although they are still minor components of the solution after 24 h their concentration becomes non-negligible. The remaining types of wood considered in the study followed similar dissolution trends to the one discussed here for poplar.

In order to quantitate cellulosic material and lignin extraction levels, the average of the integrals of the cellulose and cellulose oligomers C-1 and C-6 signals in the 105–92 and 63–59 ppm range, respectively, and the integral of the lignin aromatic OMe  $^{13}\text{C}$  resonance at  $\sim 57$  ppm, were computed for each wood liquor spectrum. These values were then divided by the integrals of the corresponding signals observed in 5 wt% solutions of MCC and Indulin AT in  $[\text{C}_4\text{mim}]/\text{DMSO-}d_6$ , using the areas of the IL  $^{13}\text{C}$  signals in each spectrum as internal normalization factors. Since the initial concentration of wood used in all dissolution experiments was the same as that of the cellulose and lignin reference solutions, these ratios represent the cellulosic material and lignin wt% extraction levels achieved for each sample. This approach was therefore employed to generate dissolution profiles in the IL-based solvent system as a function of time for the four types of wood investigated (Fig. 4). It is important to point out that the poor to modest signal-to-noise ratio observed in the  $^{13}\text{C}$  NMR spectra of the extracts can lead to sizable integration errors, and as a result the extraction levels estimated in this manner have uncertainties of up to  $\pm 5$  wt%.

Analysis of the profiles shown in Fig. 4 yields valuable information regarding the wood dissolution process. First, and

in agreement with the differences in morphological properties and complexity of their lignocellulosic matrices, extraction levels for hardwoods are lower than for softwoods. For example, 44 wt% of the cellulosic materials present in pine wood can be extracted by the IL-based solvent in 12 h, but extraction levels reach only 35 wt% for oak in the same time period. In addition, the cellulosic material to lignin wt% ratio across the dissolution profiles is largely constant and roughly 2:1. This figure correlates well with the reported chemical composition of wood,<sup>1</sup> and suggests that the  $[\text{C}_4\text{mim}]\text{Cl}/\text{DMSO-}d_6$  mixture extracts the two polymers from the wood fibers at approximately equal rates. Finally, the cellulosic material extraction levels after 24 h are, on average, 45 wt%. If this value is again compared with the wt% chemical make-up of wood,<sup>1</sup> our results indicate that the IL-based solvent system is capable of extracting the majority of the cellulose present in the samples. Indeed, we found that continuing the dissolution process for longer periods does not lead to an increase in the concentration of cellulosic materials or lignin in the liquors. On the other hand, and as evidenced by a noticeable increase in the intensities of resonances corresponding to  $\gamma$ -celluloses, contact times beyond 24 h lead to substantial polymer degradation.

Cellulose recovery from the IL-based wood liquors was then investigated. We have previously shown that the polysaccharide can be reconstituted from  $[\text{C}_4\text{mim}]\text{Cl}$  solutions by the addition of precipitating solvents and solvent mixtures miscible with the IL,<sup>10,16</sup> and the suitability of methods based on these techniques was explored. Analysis of the dissolution

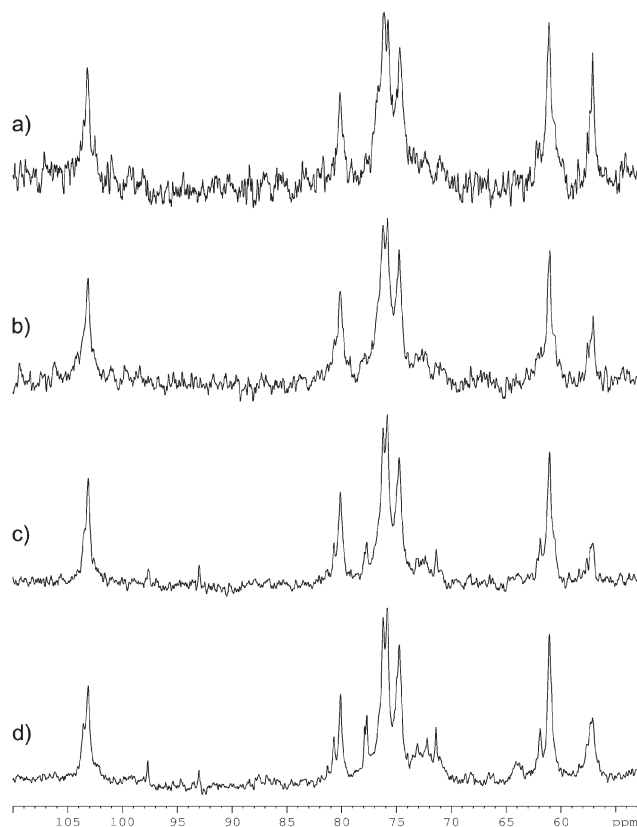


**Fig. 3**  $^{13}\text{C}$  NMR spectra of the extracts obtained after dissolving poplar wood in  $[\text{C}_4\text{mim}]\text{Cl}/\text{DMSO}-d_6$  for periods of 2 (a), 6 (b), 12 (c), and 24 (d) h at  $100\text{ }^\circ\text{C}$ . Vertical scalings were adjusted to make signal intensities comparable among all spectra.

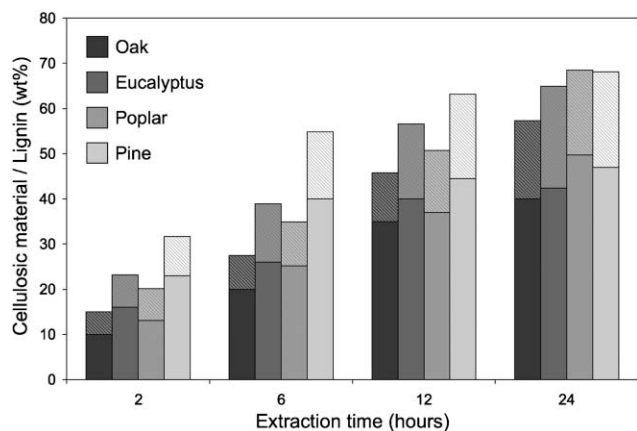


**Fig. 4** Cellulosic material (solid bars) and lignin (dashed bars) extraction profiles in  $[\text{C}_4\text{mim}]\text{Cl}/\text{DMSO}-d_6$  at  $100\text{ }^\circ\text{C}$  for the different wood samples considered as a function of time.

profiles for softwoods presented above indicates that good levels of cellulosic material extraction can be achieved with minimal degradation between 12 and 24 h. Thus, solutions for cellulose reconstitution studies were prepared by dissolving, or pulping, pine wood in the  $[\text{C}_4\text{mim}]\text{Cl}/\text{DMSO}$  mixture for 16 h at  $100\text{ }^\circ\text{C}$ . In order to resemble more closely non-ideal conditions encountered in an industrial setting, the pulping experiments were carried out on a multi-gram scale and using

coarse wood shavings with no preconditioning. Barring an initial evolution of steam from the heterogeneous slurries, the dissolution of the untreated wood fibers proceeded as described earlier, and clear amber colored liquors were obtained after removal of insoluble particles. The reconstitution of the cellulosic materials was achieved through the addition and vigorous mixing of one to two volumes of the precipitating solvents, which included 1:1 acetone–water solutions, dichloromethane or acetonitrile. In all cases, off-white powdery flocs formed shortly after the coagulant mixed with the wood liquors. The solids were recovered by filtration and washed repeatedly with water and acetone to completely remove  $[\text{C}_4\text{mim}]\text{Cl}$  and DMSO. Based on the initial concentration of the wood suspensions and the average cellulose content in wood,<sup>1</sup> the yields of the reconstitution experiments ranged from 30 to 60 wt%.

As expected, the recovered materials were insoluble in traditional laboratory solvents. On the other hand, they dissolved readily in neat  $[\text{C}_4\text{mim}]\text{Cl}$  or  $[\text{C}_4\text{mim}]\text{Cl}/\text{DMSO}-d_6$ , and 5 wt% solutions suitable for NMR spectroscopy could be prepared in all cases. Comparison of the  $^{13}\text{C}$  spectra of the reconstituted samples with that of MCC recorded under identical conditions reveals that they are celluloses of fair purity (Fig. 5). Although  $\gamma$ -cellulose resonances are discernible in all cases, their intensities are considerably lower than in the spectra of the original wood liquors (*i.e.*, Fig. 3d). Furthermore, similar signals are present in the spectrum of

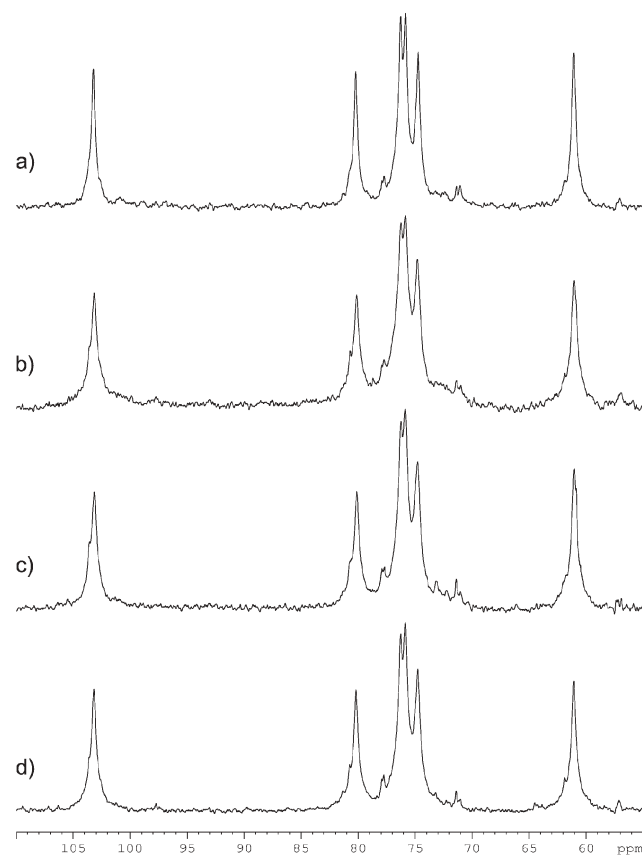


**Fig. 5**  $^{13}\text{C}$  NMR spectra of 5 wt% solutions in  $[\text{C}_4\text{mim}]\text{Cl}/\text{DMSO}-d_6$  of celluloses reconstituted from pine wood liquors using acetone–water (a), dichloromethane (b), and acetonitrile (c), and of MCC (d).

MCC, suggesting that these low molecular weight oligomers are the result of minor decomposition of the polysaccharide occurring during sample preparation. Perhaps the most salient feature of the spectra is their lack of signals at  $\sim 57$  ppm or  $\sim 170$  and  $\sim 22$  ppm that could be attributed, respectively, to lignin aromatic OMe or hemicellulose acetate groups. This indicates that these polymers are not present in significant concentrations in the reconstituted cellulose samples. Since lignins and hemicelluloses were observed in the IL-based wood liquors prior to the cellulose precipitation step, both must remain in the coagulation filtrates. While no effort was made to recover these polymers, their presence in the supernatants was confirmed by  $^{13}\text{C}$  NMR (data not shown). Similar conclusions regarding the purity of the recovered materials can be reached by comparison of their IR spectra, all of which lack absorption bands that characterize lignin and hemicellulose,<sup>22</sup> with that of pure MCC (Fig. 6).

The thermal decomposition profiles of the recovered celluloses were then determined using thermogravimetric analysis (TGA). Neglecting small initial drops in weight occurring near  $100^\circ\text{C}$  due to evaporation of retained moisture, a single pronounced decomposition event followed by slow loss of mass was observed in all cases. The decomposition onset and maximum decomposition rate temperatures computed from the TGA traces of the different samples,  $T_{\text{dec}}$  and  $T_{\text{max}}$ , were in the  $257\text{--}301^\circ\text{C}$  and  $276\text{--}320^\circ\text{C}$  range, respectively, and their residual char yields above  $500^\circ\text{C}$  were between 12.8 and 21.6 wt%. This range of thermal decomposition parameters is comparable to that determined for MCC samples before and after dissolution in  $[\text{C}_4\text{mim}]\text{Cl}/\text{DMSO}$  and reconstitution with acetone–water (Fig. 7), which had  $T_{\text{dec}}$  and  $T_{\text{max}}$  values of  $307$  and  $324^\circ\text{C}$  and  $257$  and  $269^\circ\text{C}$ , respectively. While qualitatively, this indicates that the variations in the morphology and degree of polymerization (DP) of the celluloses recovered from the IL-based wood liquors are within those of pure and  $[\text{C}_4\text{mim}]\text{Cl}$ -processed MCC.<sup>23</sup>

As a final assessment of their physical properties, we explored the use of the regenerated samples in the preparation of cellulose-based membranes following methods described earlier by us.<sup>24</sup> Briefly, 5 wt% solutions of the reconstituted

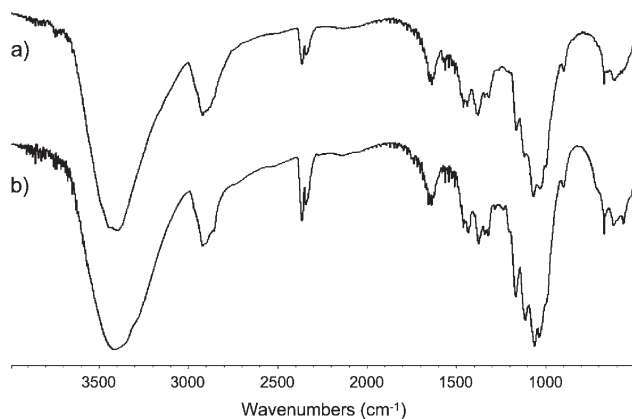


**Fig. 6** IR spectra of cellulose reconstituted from IL based pine wood liquors by the addition of acetonitrile (a) and of MCC (b).

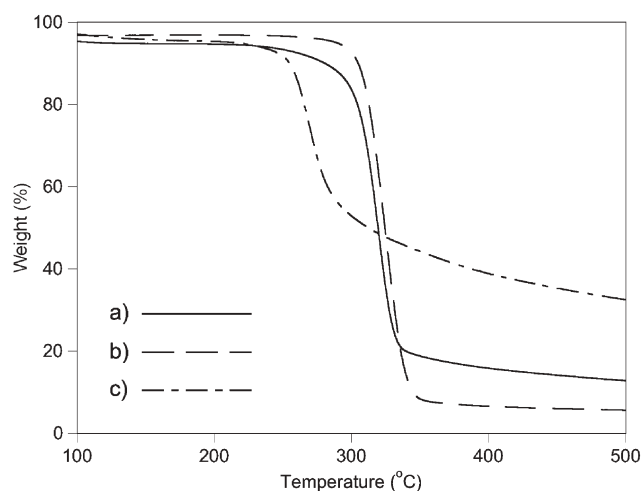


**Fig. 7** Thermal decomposition profiles of cellulose reconstituted from IL based pine wood liquors by the addition of dichloromethane (a), and of samples of MCC before (b) and after (c) dissolution in  $[\text{C}_4\text{mim}]\text{Cl}/\text{DMSO}$  and regeneration with acetone–water.

celluloses redissolved in  $[\text{C}_4\text{mim}]\text{Cl}$  were prepared, cast onto glass plates as thin films, and perfused extensively with water. In all cases, highly flexible membranes identical in all respects to those prepared analogously using pure MCC were obtained. In contrast, all attempts to cast membranes directly from the IL-based wood extracts proved unsuccessful, suggesting that the presence of lignins and/or hemicelluloses inhibits the formation of structured cellulose hydrogels.

## Conclusions

The results discussed above demonstrate that solvent systems based on  $[\text{C}_4\text{mim}]\text{Cl}$  are capable of partially dissolving untreated wood, and show that celluloses with purities, physical properties, and processing characteristics comparable to those of pure cellulose samples subjected to similar treatment can be easily recovered from the resulting solutions. In contrast to wood delignification methods that rely on the insolubility of cellulose, the IL has the ability to dissolve lignin and polysaccharides simultaneously. Thus, the intricate network of non-covalent interactions between these polymers is effectively disrupted after dissolution, leading to celluloses which are devoid of lignin and hemicellulose upon regeneration. Furthermore, the fact that the wood components are in  $[\text{C}_4\text{mim}]\text{Cl}$  solution should, in principle, allow for their *in situ* derivatization. For example, cellulose could be acylated or carbanilated directly in the IL-based wood liquors following recently reported procedures,<sup>11,25</sup> drastically reducing the number of steps currently required to produce these derivatives from raw materials.

While our findings are encouraging, several aspects of the novel methodology described here need to be addressed before it can be considered as an alternative ‘green’ strategy for the extraction of cellulose from lignocellulosic materials. First, the effects of dissolution time and temperature on the crystallinity and DP of the celluloses obtained through this approach were not studied, and these should be rigorously quantitated. In addition,  $[\text{C}_4\text{mim}]\text{Cl}$  has been shown to display moderate

toxicity,<sup>26</sup> and use of this IL on large scales must be combined with efficient recycling protocols.<sup>27</sup> The suitability as wood solvents of [C<sub>2</sub>mim]Cl, an IL with a slightly higher melting point but significantly less toxicity than [C<sub>4</sub>mim]Cl, and other imidazolium chlorides known to solubilize cellulose, could be evaluated as well.<sup>11,25</sup> Similarly, the use of DMSO as a dissolution co-solvent should be minimized or avoided. In our case, DMSO-*d*<sub>6</sub> and DMSO were employed solely to reduce the viscosity of the IL-based wood liquors and facilitate their handling and analysis. Preliminary results indicate that similar reductions in viscosity can be achieved with PEG, a solvent which we have successfully used in the development of cleaner methods for the delignification of wood pulps.<sup>7</sup> Finally, the energy requirements of the process need to be determined and compared with those of established cellulose extraction and purification protocols. Work on these areas is well under way, and the results from our ongoing investigations will be reported in due course.

## Experimental

### Materials

Pine (*Pinus* spp.), poplar (*Populus* spp.), eucalyptus (*Eucalyptus* spp.), and oak (*Quercus* spp.) wood shavings were procured from local woodshops. With the exception of the materials employed in pulping/reconstitution experiments, the samples were finely divided with a mortar and pestle and dried to constant weight under vacuum before use. The [C<sub>4</sub>mim]Cl used in all the studies was prepared following reported procedures.<sup>28</sup> Samples of Indulin AT were obtained from Westvaco (Charleston, SC, USA). DMSO-*d*<sub>6</sub> (99.9% D) was purchased from Cambridge Isotope Laboratories (Cambridge, MA, USA). All other solvents and reagents were obtained from Sigma–Aldrich (St. Louis, MO, USA).

### Wood dissolution profiles

5 wt% suspensions of wood chips in IL–DMSO-*d*<sub>6</sub> were prepared by combining 100 mg of the different samples, 1.6 g of [C<sub>4</sub>mim]Cl, and 300 mg of DMSO-*d*<sub>6</sub> in test tubes followed by thorough vortexing. The heterogeneous mixtures were then heated at 100 °C for periods of either 2, 6, 12, or 24 h with constant stirring, and subsequently filtered through glass wool to remove undissolved material. The resulting clear liquors were transferred to 5 mm NMR tubes and used in the determination of wood dissolution profiles, as detailed above.

### Wood pulping and cellulose reconstitution experiments

1 g of untreated pine wood shavings (~5 mm × 5 mm in size, 5–10 wt% moisture content) were suspended in 19 g of a [C<sub>4</sub>mim]Cl/DMSO solution (84:16 wt%), and pulped at 100 °C for 16 h with the aid of a magnetic stirrer. The mixture was then filtered through a heated Büchner funnel fitted with a 20 µm Magna<sup>®</sup> nylon membrane (Osmonics/MSI, Westborough, MA, USA) to remove undissolved solids. Cellulose samples were reconstituted from the resulting clear, amber-colored, viscous liquor as flocs by rapid mixing with ~50 mL of either 1:1 acetone–water, dichloromethane, or acetonitrile. The powdery off-white solids were then filtered,

washed repeatedly with acetone and water, and dried overnight in a vacuum oven at 100 °C prior to their use in <sup>13</sup>C NMR, IR, and TGA experiments.

### NMR and IR spectroscopy

Samples used in the determination of wood dissolution profiles were obtained as described in the previous section. The 5 wt% solutions of MCC, Indulin AT, and reconstituted cellulose samples in [C<sub>4</sub>mim]/DMSO-*d*<sub>6</sub> used in NMR experiments were prepared as reported earlier.<sup>18,20</sup> Proton-decoupled <sup>13</sup>C spectra were collected at 90 °C on a Bruker AVANCE 400 NMR spectrometer equipped with a 5 mm BBO probe operating at a <sup>13</sup>C frequency of 100.61 MHz. A total of 20 000 scans were collected in all cases, and spectra were processed with a 10 Hz line-broadening factor.

IR spectra of the cellulose samples were recorded on a Thermo-Electron Nicolet Avatar 370 DTGS FT-IR spectrophotometer using KBr pellets.

### Thermogravimetric analysis

The thermal decomposition profiles of the reconstituted cellulosic materials were determined using a TA Instruments 2950 thermogravimetric analyzer (New Castle, DE, USA). Each sample was analyzed in a platinum pan with nitrogen as the purge gas. In all experiments the temperature was increased from 30 to 700 °C at a constant rate of 10 °C min<sup>-1</sup>.

### Acknowledgements

Funding from the NSF CCLI-A&I program (Grant DUE-9952264), the Camille and Henry Dreyfus Foundation, and DHC Analysis is acknowledged (GM, RCR, DAF, and PM). RDR and RPS recognize support from BASF Corporation.

### References

- 1 *Kirk-Othmer Encyclopedia of Chemical Technology*, John Wiley & Sons, New York, 4th edn., 1998, vol. 25, pp. 627–664.
- 2 *FAO Yearbook of Forest Products 2003*, FAO Forestry Series No. 38 and Statistics Series No. 185, Food and Agriculture Organization of the United Nations, Rome, Italy, 2005.
- 3 *Kirk-Othmer Encyclopedia of Chemical Technology*, John Wiley & Sons, New York, 4th edn., 1996, vol. 20, pp. 494–582.
- 4 *Profile of the Pulp and Paper Industry*, EPA Office of Compliance Sector Notebook EPA/310-R-02-002, US Environmental Protection Agency, Washington, DC, 2nd edn., 2002.
- 5 S. K. Black, B. R. Hames and M. D. Myers, *US Pat.*, 5 730 837, 1998.
- 6 T. J. McDonough, *Tappi J.*, 1993, **76**, 186–193.
- 7 H. D. Willauer, J. G. Huddleston, M. Li and R. D. Rogers, *J. Chromatogr., B: Biomed. Appl.*, 2000, **743**, 127–135.
- 8 R. D. Rogers and K. R. Seddon, *Science*, 2003, **302**, 792–793.
- 9 *Ionic Liquids IIIA/B: Fundamentals, Progress, Challenges, and Opportunities*, ed. R. D. Rogers and K. R. Seddon, *ACS Symp. Ser. 901/902*, American Chemical Society, Washington, DC, 2005.
- 10 R. P. Swatloski, S. K. Spear, J. D. Holbrey and R. D. Rogers, *J. Am. Chem. Soc.*, 2002, **124**, 4974–4975.
- 11 J. Wu, J. Zhang, H. Zhang, J. He, Q. Re and M. Guo, *Biomacromolecules*, 2004, **5**, 266–268.
- 12 Q. Liu, M. H. A. Janssen, F. van Rantwijk and R. A. Sheldon, *Green Chem.*, 2005, **7**, 39–42.
- 13 D. M. Phillips, L. F. Drummy, D. G. Conrady, D. M. Fox, R. R. Naik, M. O. Stone, P. C. Trulove, H. C. De Long and R. A. Mantz, *J. Am. Chem. Soc.*, 2004, **126**, 14350–14351.
- 14 H. Xie, S. Li and S. Zhang, *Green Chem.*, 2005, **7**, 606–608.

- 15 H. Xie, S. Zhang and S. Li, *Green Chem.*, 2006, **8**, 630–633.
- 16 R. P. Swatloski, R. D. Rogers and J. D. Holbrey, *US Pat.*, 6824599, 2004.
- 17 R. C. Remsing, R. P. Swatloski, R. D. Rogers and G. Moyna, *Chem. Commun.*, 2006, 1271–1273.
- 18 D. A. Fort, R. P. Swatloski, P. Moyna, R. D. Rogers and G. Moyna, *Chem. Commun.*, 2006, 714–716.
- 19 A. J. Ragauskas, C. K. Williams, B. H. Davison, G. Britovsek, J. Cairney, C. A. Eckert, W. J. Frederick, Jr., J. P. Hallett, D. J. Leak, C. L. Liotta, J. R. Mielenz, R. Murphy, R. Templer and T. Tschaplinski, *Science*, 2006, **311**, 484–489.
- 20 J. S. Moulthrop, R. P. Swatloski, G. Moyna and R. D. Rogers, *Chem. Commun.*, 2005, 1557–1559.
- 21 W. Kolodziejewski, J. S. Frye and G. E. Maciel, *Anal. Chem.*, 1982, **54**, 1419–1424.
- 22 T. P. Abbott, D. M. Palmer, S. H. Gordon and M. O. Bagby, *J. Wood Chem. Technol.*, 1988, **8**, 1–28.
- 23 M. E. Calahorra, M. Cortázar, J. I. Eguiazábal and G. M. Guzmán, *J. Appl. Polym. Sci.*, 1989, **37**, 3305–3314.
- 24 (a) J. D. Holbrey, S. K. Spear, M. B. Turner, R. P. Swatloski and R. D. Rogers, *US Pat.*, 6808557, 2004; (b) M. B. Turner, S. K. Spear, J. D. Holbrey and R. D. Rogers, *Biomacromolecules*, 2004, **5**, 1379–1384; (c) M. B. Turner, S. K. Spear, J. D. Holbrey, D. T. Daly and R. D. Rogers, *Biomacromolecules*, 2005, **6**, 2497–2502.
- 25 S. Barthel and T. Heinze, *Green Chem.*, 2006, **8**, 301–306.
- 26 R. P. Swatloski, J. D. Holbrey, S. B. Memon, G. A. Caldwell, K. A. Caldwell and R. D. Rogers, *Chem. Commun.*, 2004, 668–669.
- 27 K. E. Gutowski, G. A. Broker, H. D. Willauer, J. G. Huddleston, R. P. Swatloski, J. D. Holbrey and R. D. Rogers, *J. Am. Chem. Soc.*, 2003, **125**, 6632–6633.
- 28 J. G. Huddleston, A. E. Visser, W. M. Reichert, H. D. Willauer, G. A. Broker and R. D. Rogers, *Green Chem.*, 2001, **3**, 156–164.



## Looking for that **special** chemical biology research paper?

TRY this free news service:

### Chemical Biology

- highlights of newsworthy and significant advances in chemical biology from across RSC journals
- free online access
- updated daily
- free access to the original research paper from every online article
- also available as a free print supplement in selected RSC journals.\*

\*A separately issued print subscription is also available.

Registered Charity Number: 207890

RSCPublishing

[www.rsc.org/chembiology](http://www.rsc.org/chembiology)

18040681

# Separation of aromatic hydrocarbons from alkanes using the ionic liquid 1-ethyl-3-methylimidazolium bis{(trifluoromethyl) sulfonyl}amide<sup>†</sup>

Alberto Arce,<sup>a</sup> Martyn J. Earle,<sup>\*b</sup> Héctor Rodríguez<sup>a</sup> and Kenneth R. Seddon<sup>b</sup>

Received 17th July 2006, Accepted 5th October 2006

First published as an Advance Article on the web 25th October 2006

DOI: 10.1039/b610207g

The liquid–liquid equilibrium for the ternary system formed by hexane, benzene and the ionic liquid 1-ethyl-3-methylimidazolium bis{(trifluoromethyl)sulfonyl}amide, [C<sub>2</sub>mim][NTf<sub>2</sub>], has been experimentally determined at 25 °C and 40 °C. The results show that the [C<sub>2</sub>mim][NTf<sub>2</sub>] can selectively remove benzene from its mixtures with hexane, suggesting that this ionic liquid can be used as an alternative solvent in liquid extraction processes for the removal of aromatic compounds from their mixtures with alkanes.

## Introduction

Separation of aromatic and non-aromatic compounds has traditionally been one of the most challenging tasks in refinery processes.<sup>1</sup> Their boiling points are often rather close, making it difficult to perform the separation by simple distillation under economically acceptable conditions. In addition, the formation of azeotropes may occasionally complicate the operation even more.<sup>2</sup>

The common processes usually chosen by industry to deal with such separations are liquid extraction, extractive distillation and azeotropic distillation.<sup>2,3</sup> Each of these techniques is suitable for the treatment of feeds within different ranges of aromatic contents. Typically this ranges from 20 to 100 wt%, with none of them showing favourable economics to manage feeds below 20 wt% of aromatics.<sup>3</sup> Liquid extraction is currently the most interesting alternative to process hydrocarbon streams, with an aromatic content in the range 20 to 65 wt%. Compared to both extractive and azeotropic distillation techniques, liquid extraction has a low energetic demand, so it would be valuable to extend the range in which extraction might be profitably used.

An inherent problem to all the three techniques cited above is related to use of a solvent, which is mixed with the feed and comes out of the extractor, or the column, accompanying the raffinate and extract streams. Typical solvents in these processes are organic compounds such as sulfolane (conventionally the principal one), ethylene glycols, dimethylsulfoxide, *N*-methylpyrrolidone, *N*-formylmorpholine or carbonate derivatives, among some others.<sup>2–4</sup> The recovery of these solvents from the extract and raffinate streams must be carried out by distillation, thus resulting in an additional increase in the installation and operational costs of the processes.

Apart from the thermodynamically favourable behaviour for the extraction, desirable attributes for the solvents are:

chemical stability, low toxicity, non-corrosivity, low cost, and ease in their recovery from the extract.<sup>5</sup> Considering this list, ionic liquids might constitute an alternative option for conventional solvents in liquid extraction.<sup>6,7</sup> Room temperature ionic liquids have received increasing attention by the scientific community, particularly since the late 1990s.<sup>8</sup> They have a negligible vapour pressure at ambient temperatures and pressures,<sup>9</sup> which would open the possibility of using simpler techniques, such as flash distillation, in the recovery of the ionic liquids from the raffinate and extract streams.<sup>‡</sup> In addition, and despite several exceptions, there is a wide variety of chemically stable, non-corrosive ionic liquids, with most of them possessing a large liquid range. Their current problems could be the high price and the relatively unknown toxicity,<sup>10</sup> the former being expected to dramatically decrease as a result of their implementation in industrial processes, and their production at large scale, and the later requiring further research to establish standard assessments.<sup>11</sup>

Several groups have already explored the application of ionic liquids to liquid extraction,<sup>12</sup> with the separation of aromatic and non-aromatic hydrocarbons being a key focus. However, only a few papers report the liquid–liquid equilibrium (LLE) data of the systems studied.<sup>7,13–15</sup>

Here we present the LLE data of the ternary system (hexane + benzene + [C<sub>2</sub>mim][NTf<sub>2</sub>]) at two different temperatures, 25 °C and 40 °C, in the classical range of temperatures in which extraction at atmospheric pressure has a practical application. Hexane and benzene have been chosen as representatives of aliphatic and aromatic compounds. The ionic liquid has been preliminary selected according to its low melting point (well below room temperatures), its relatively low viscosity (thus facilitating fluid flow and mass transfer), and the fact that the anion [NTf<sub>2</sub>]<sup>−</sup> does not decompose to give HF under conditions normally used for liquid–liquid extractions, as some other typical anions in ionic liquids chemistry do.<sup>16</sup>

<sup>‡</sup> Although it is known that ionic liquids can be distilled at high temperature and low pressure,<sup>9</sup> under the conditions envisaged here they may be considered as essentially non-volatile.

<sup>a</sup>Department of Chemical Engineering, University of Santiago de Compostela, E-15782, Santiago de Compostela, Spain

<sup>b</sup>The QUILL Research Centre, The Queen's University of Belfast, Belfast, BT9 5AG, UK. E-mail: quill@qub.ac.uk

<sup>†</sup> Electronic supplementary information (ESI) available: Calculation of compositions of phases at equilibrium. See DOI: 10.1039/b610207g

## Experimental

Benzene with a nominal purity of 99.0% was purchased from LabScan. Hexane with a nominal purity of 97.0% was supplied by BDH. Both hydrocarbons were used as received, without further purification. The ionic liquid [C<sub>2</sub>mim][NTf<sub>2</sub>] was prepared by a metathetic reaction of [C<sub>2</sub>mim]Cl and Li[NTf<sub>2</sub>], following an analogous procedure to that described elsewhere;<sup>17</sup> the water content of the final product was found to be <100 ppm, quantified by Karl-Fischer titration.<sup>18</sup>

The feasibility of [C<sub>2</sub>mim][NTf<sub>2</sub>] as solvent for the liquid-liquid extraction of benzene from its mixture with hexane was analyzed by determining experimental tie-lines covering the whole immiscibility region of the ternary system (hexane + benzene + [C<sub>2</sub>mim][NTf<sub>2</sub>]). Mixtures of all the three compounds (or just two, in the cases of the two immiscible pairs of the system) with a global composition being in the immiscibility region, were prepared. These mixtures were placed inside a glass cell, sealed, and thermostatically controlled at 25.0 °C or 40.0 °C. The mixtures were vigorously stirred for not less than 1 h, followed by a settling period of several hours to ensure that the thermodynamic equilibrium was reached. Next a sample was taken from each equilibrium phase into which the system had split: a top (hydrocarbon-rich) phase and a bottom (ionic liquid-rich) phase, and the compositional analyses were performed as indicated below.

The determination of the composition of the samples was carried out by means of <sup>1</sup>H NMR spectroscopy. Details of the specific method, already applied in the study of LLE ternary systems with ionic liquids, can be found elsewhere.<sup>19</sup> This technique combines simplicity and sufficient accuracy for practical purposes. To assess the precision of the method in this particular case, homogeneous probe vials with overall compositions in the proximities of the binodal curve, and covering the whole range of compositions, were prepared by weight using a Metler Toledo AT261 balance, precise to within ±10<sup>-4</sup> g. After dissolving the samples in deuterated solvent and running them in a Bruker Avance DPX-500 spectrometer, selected peaks for each component were integrated to calculate the molar fractions. The measured results were found to be in good agreement with the actual compositions. Calibration lines with standard deviations of 0.006 or less for each compound were obtained. The maximum absolute deviation was found to be 0.009 in mole fractions. Thus, the technique was validated and used within the equilibrium experiments.

## Results and discussion

The measured compositions of the experimental tie-line ends of the ternary system (hexane + benzene + [C<sub>2</sub>mim][NTf<sub>2</sub>]) at 25 °C are reported in Table 1; the data corresponding to a temperature of 40 °C are shown in Table 2.

The feasibility of using the ionic liquid as a solvent to perform the extraction of benzene from a mixture with hexane was evaluated by classic parameters such as the solute distribution ratio ( $\beta$ ) and the selectivity ( $S$ ), calculated from

**Table 1** Composition of the experimental tie-line ends, and values of the solute distribution ratio ( $\beta$ ) and selectivity ( $S$ ) for the ternary system (hexane + benzene + [C<sub>2</sub>mim][NTf<sub>2</sub>]) at 25 °C. The mole fractions of hexane, benzene and [C<sub>2</sub>mim][NTf<sub>2</sub>] are represented by  $x_1$ ,  $x_2$  and  $x_3$ , respectively

| Hydrocarbon-rich phase |       |       | Ionic liquid-rich phase |       |       | $\beta$ | $S$   |
|------------------------|-------|-------|-------------------------|-------|-------|---------|-------|
| $x_1$                  | $x_2$ | $x_3$ | $x_1$                   | $x_2$ | $x_3$ |         |       |
| 1.000                  | 0.000 | 0.000 | 0.039                   | 0.000 | 0.961 | —       | —     |
| 0.930                  | 0.070 | 0.000 | 0.038                   | 0.096 | 0.866 | 1.37    | 33.56 |
| 0.834                  | 0.166 | 0.000 | 0.038                   | 0.211 | 0.751 | 1.27    | 27.90 |
| 0.717                  | 0.283 | 0.000 | 0.035                   | 0.327 | 0.638 | 1.16    | 23.67 |
| 0.573                  | 0.427 | 0.000 | 0.039                   | 0.432 | 0.529 | 1.01    | 14.86 |
| 0.431                  | 0.569 | 0.000 | 0.034                   | 0.523 | 0.443 | 0.92    | 11.65 |
| 0.300                  | 0.700 | 0.000 | 0.031                   | 0.597 | 0.372 | 0.85    | 8.25  |
| 0.112                  | 0.888 | 0.000 | 0.018                   | 0.692 | 0.290 | 0.78    | 4.85  |
| 0.000                  | 1.000 | 0.000 | 0.000                   | 0.757 | 0.243 | 0.76    | —     |

**Table 2** Composition of the experimental tie-line ends, and values of the solute distribution ratio ( $\beta$ ) and selectivity ( $S$ ) for the ternary system (hexane + benzene + [C<sub>2</sub>mim][NTf<sub>2</sub>]) at 40 °C. The mole fractions of hexane, benzene and [C<sub>2</sub>mim][NTf<sub>2</sub>] are represented by  $x_1$ ,  $x_2$  and  $x_3$ , respectively

| Hydrocarbon-rich phase |       |       | Ionic liquid-rich phase |       |       | $\beta$ | $S$   |
|------------------------|-------|-------|-------------------------|-------|-------|---------|-------|
| $x_1$                  | $x_2$ | $x_3$ | $x_1$                   | $x_2$ | $x_3$ |         |       |
| 1.000                  | 0.000 | 0.000 | 0.041                   | 0.000 | 0.959 | —       | —     |
| 0.877                  | 0.123 | 0.000 | 0.038                   | 0.148 | 0.814 | 1.20    | 27.77 |
| 0.733                  | 0.267 | 0.000 | 0.039                   | 0.291 | 0.670 | 1.09    | 20.48 |
| 0.590                  | 0.410 | 0.000 | 0.038                   | 0.419 | 0.543 | 1.02    | 15.87 |
| 0.449                  | 0.551 | 0.000 | 0.036                   | 0.503 | 0.461 | 0.91    | 11.39 |
| 0.303                  | 0.697 | 0.000 | 0.032                   | 0.578 | 0.390 | 0.83    | 7.85  |
| 0.233                  | 0.767 | 0.000 | 0.030                   | 0.618 | 0.352 | 0.81    | 6.26  |
| 0.106                  | 0.894 | 0.000 | 0.018                   | 0.699 | 0.283 | 0.78    | 4.60  |
| 0.000                  | 1.000 | 0.000 | 0.000                   | 0.764 | 0.236 | 0.76    | —     |

the experimental data. These parameters are defined by the following expressions:

$$\beta = \frac{x_2^{\text{II}}}{x_2^{\text{I}}} \quad (1)$$

$$S = \frac{x_2^{\text{II}} x_1^{\text{I}}}{x_2^{\text{I}} x_1^{\text{II}}} \quad (2)$$

where  $x$  is the molar fraction; superscripts I and II refer to the hydrocarbon-rich and ionic liquid-rich phase, and subscripts 1 and 2 to hexane (inert) and benzene (solute), respectively. The values of  $\beta$  and  $S$  are shown in Table 1 and Table 2, together with the experimental equilibrium data.

Fig. 1(a) and (b) show graphical representations of the tie-lines of the ternary systems at 25 °C and 40 °C, respectively, in a triangular diagram. As it can be seen (Tables 1 and 2), the effect of the temperature is rather small, with the characterising parameters of the extraction actually being slightly better for the lower temperature. Therefore, the quality of the process is maximised by working at room temperature, thus avoiding the consumption of energy required to heat the extracting unit.

By inspection of the LLE data (or the triangular diagrams), another significant aspect is the fact that the ionic liquid does not enter the equilibrium hydrocarbon-rich phase. At least, the presence of [C<sub>2</sub>mim][NTf<sub>2</sub>] was not detected in the upper phase by NMR. In an attempt to measure presence of traces of

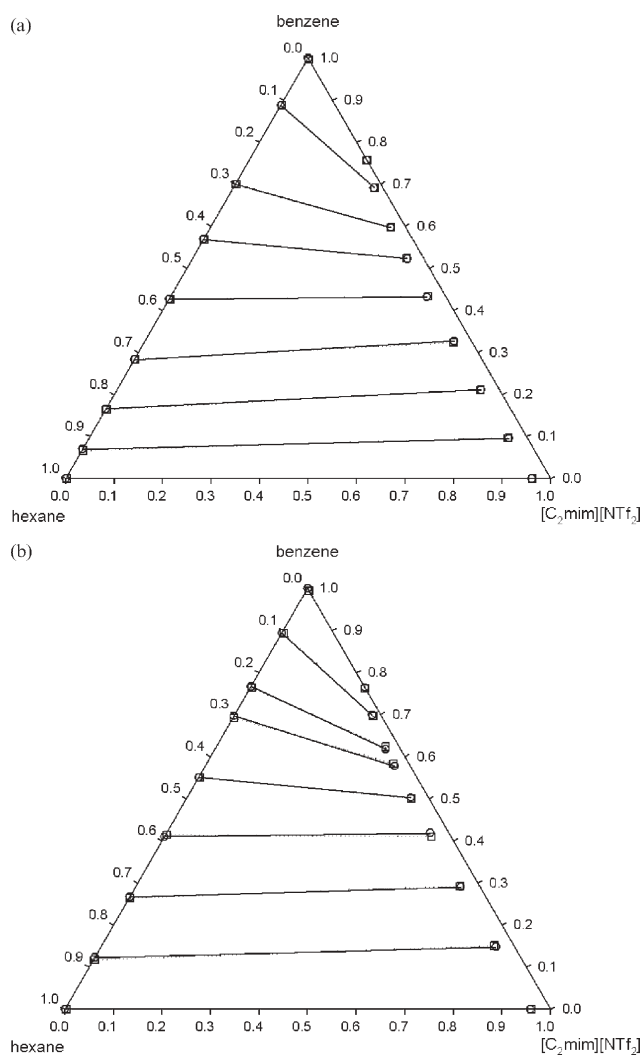


**Fig. 1** (a) Experimental tie-lines (○, solid line) for the LLE of the ternary system (hexane + benzene + [C<sub>2</sub>mim][NTf<sub>2</sub>]) at 25 °C. The corresponding tie-lines correlated by means of the NRTL equation are also plotted (□, dotted line). (b) Experimental tie-lines (○, solid line) for the LLE of the ternary system (hexane + benzene + [C<sub>2</sub>mim][NTf<sub>2</sub>]) at 40 °C. The corresponding tie-lines correlated by means of the NRTL equation are also plotted (□, dotted line).

[C<sub>2</sub>mim][NTf<sub>2</sub>] in the raffinate stream, two mixtures of [C<sub>2</sub>mim][NTf<sub>2</sub>] with either hexane (250 cm<sup>3</sup>) or a 15% benzene/85% hexane mixture (250 cm<sup>3</sup>) were prepared and after equilibrating at 25 °C, the [C<sub>2</sub>mim][NTf<sub>2</sub>] layer was separated. The solvent was evaporated and the residues were weighed. The hexane layer contained no measurable ionic liquid (<0.1 ppm) and the 15% benzene/85% hexane mixture was found to contain 1.4 ppm ionic liquid. This showed that a post-extraction treatment of the raffinate to recover the solvent and turn it back to the extraction unit, may be necessary if the benzene content of the raffinate was high.

The graphical representation of the solute distribution ratio, at 25 °C, as a function of the solute mole fraction in the hydrocarbon-rich phase is shown in Fig. 2. A comparison with data in literature<sup>20</sup> for the ternary system (hexane + benzene + sulfolane {2,3,4,5-tetrahydrothiophene-1,1-dioxide}) at the

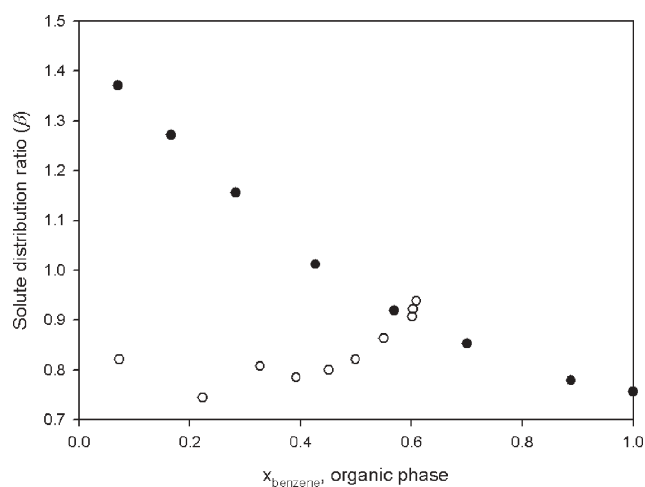


**Fig. 2** Solute distribution ratio for the ternary systems (hexane + benzene + [C<sub>2</sub>mim][NTf<sub>2</sub>]) (●) and (hexane + benzene + sulfolane) (○), at 25 °C, as a function of the mole fraction of benzene in the hydrocarbon-rich phase.

same temperature is made. At present sulfolane is the most widely recognised solvent in industrial processes for the separation of aromatic and aliphatic hydrocarbons by liquid extraction. The values of  $\beta$  in the comparable zone are clearly higher when using the ionic liquid, thus indicating a clear preference of the ionic liquid for the benzene in the mixture of hydrocarbons, and also meaning a reduction in the amount of solvent required to carry out the treatment of a given feed stream.

As the solute distribution ratios with the ionic liquid decrease from values above the unity to values below it (equivalently, there is a change in the sign of the tie-lines slope), the system presents solutropy.<sup>21</sup> The solutrope corresponds to the horizontal tie-line for which  $\beta = 1$ ; in this case, it happens for immiscible mixtures with an overall mole fraction of benzene somewhere in the range 0.40–0.50. To date, there are only a few values of the solute distribution ratio above unity reported in literature, for the separation of aromatic and aliphatic hydrocarbons.

Selectivity for the data at 25 °C was also plotted as a function of the mole fraction of solute in the organic phase, and compared to the system with sulfolane as solvent.<sup>20</sup> The results are shown in Fig. 3. The selectivity for the sulfolane system is higher at the lowest values of aromatic hydrocarbon content, then decreasing faster than the selectivity with the ionic liquid as the mole fraction of benzene in the system increases. Thus, the sulfolane's only advantage over the [C<sub>2</sub>mim][NTf<sub>2</sub>] is in a narrow range. Nevertheless, as it was stated in the introductory section of this paper, at such low levels of aromatic hydrocarbon content, the extraction process is not viable from an economical point of view when using volatile compounds such as sulfolane, due to the cost of the post-extraction stages for the recovery of the solvent. The problem might be avoided by using the ionic liquid, as its negligible vapour pressure makes it easier to recover. Therefore, from this perspective, [C<sub>2</sub>mim][NTf<sub>2</sub>] is also more advantageous than sulfolane in practical processes.



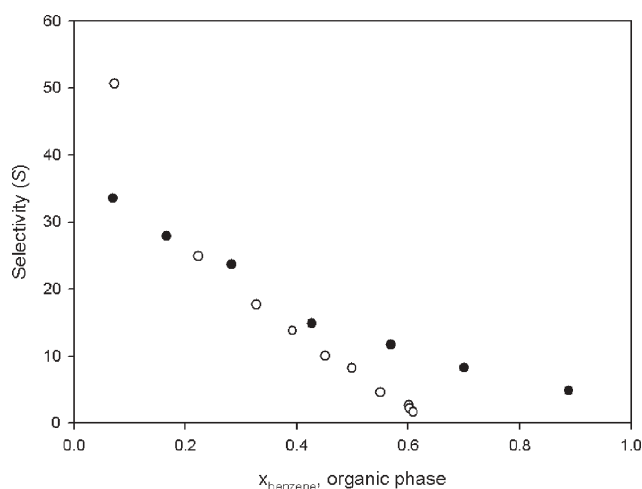


**Fig. 3** Selectivity for the ternary systems (hexane + benzene + [C<sub>2</sub>mim][NTf<sub>2</sub>]) (●) and (hexane + benzene + sulfolane) (○), at 25 °C, as a function of the mole fraction of benzene in the hydrocarbon-rich phase.

### Data correlation

The correlation of the LLE data is interesting as it permits a computational treatment and opens the possibility of designing simulation software. Thus, in this case, the non-random two-liquid (NRTL) equation<sup>22</sup> was used to correlate the experimental data. In spite of being a model initially developed for non-electrolytes, previous works<sup>13–15,19</sup> demonstrate that the original NRTL equation can successfully correlate LLE data of ternary systems involving ionic liquids.

A computer program by Sørensen<sup>23</sup> was used to calculate the binary interaction parameters of the NRTL equation. A summary of how this program calculates the binary interaction parameters of the model can be found elsewhere.<sup>19</sup> The capability of the correlation was evaluated by means of the residual function  $F$  and the mean error of the solute distribution ratio  $\Delta\beta$ , defined as:

$$F = 100 \left[ \sum_k \min_i \sum_j \left( \frac{x_{ijk} - \hat{x}_{ijk}}{6M} \right)^2 \right]^{0.5} \quad (3)$$

$$\Delta\beta = 100 \left[ \frac{1}{M} \sum_k \left( \frac{\beta_k - \hat{\beta}_k}{\beta_k} \right)^2 \right]^{0.5} \quad (4)$$

where subscript  $i$  refers to the components (1, 2, or 3), subscript  $j$  to the phases ( $j = \text{I, II}$ ), and subscript  $k$  to the tie-lines ( $k \in [1, M]$ , where  $M$  is the total number of experimental tie-lines); ‘min’ refers to the minimum value obtained by the Nelder–Mead method;  $x$  is the mole fraction;  $\beta$  is the solute distribution ratio; and the symbol ^ on top indicates a calculated value.

The non-randomness parameter of the model,  $\alpha$ , was set to different values between 0.10 and 0.40, the best results being found for the correlation with  $\alpha$  equal to 0.32, both at 25 °C and at 40 °C.<sup>22</sup> The binary interaction parameters, as well as the values of the corresponding residuals, are reported in Table 3. As expected, the difference between the parameters

**Table 3** Binary interaction parameters ( $\Delta g_{ij}$ ,  $\Delta g_{ji}$ ) for the correlation of the experimental LLE data by the NRTL equation ( $\alpha = 0.32$ ) at 25 °C and 40 °C, and the corresponding residuals  $F$  and  $\Delta\beta$ . (Components legend: 1, hexane; 2, benzene; and 3, [C<sub>2</sub>mim][NTf<sub>2</sub>])

| $T/^\circ\text{C}$ | Compounds $i-j$ | Binary interaction parameters ( $\alpha = 0.32$ ) |                                    | $F$    | $\Delta\beta$ |
|--------------------|-----------------|---|------------------------------------|--------|---------------|
|                    |                 | $\Delta g_{ij}/\text{kJ mol}^{-1}$                | $\Delta g_{ji}/\text{kJ mol}^{-1}$ |        |               |
| 25.0               | 1–2             | –2.5216   | 5.0452                             | 0.1790 | 2.6           |
|                    | 1–3             | 12.020  | 6.7120                             |        |               |
|                    | 2–3             | 15.102  | –3.2487                            |        |               |
| 40.0               | 1–2             | –2.7282   | 5.0288                             | 0.3570 | 3.0           |
|                    | 1–3             | 12.666  | 7.0304                             |        |               |
|                    | 2–3             | 15.092  | –3.4147                            |        |               |

sets for each temperature is small. The correlated tie-lines are plotted in Fig. 1(a) and Fig. 1(b), along with the experimental ones. In general, the correlation is quite accurate. However, the major problem of the model is that it can not properly correlate the absence of ionic liquid in the hydrocarbon-rich phase.

### Conclusions

The experimental determination of the LLE of the ternary system (hexane + benzene + [C<sub>2</sub>mim][NTf<sub>2</sub>]) at 25 °C and 40 °C has been carried out. By analysing the data, it has been demonstrated that [C<sub>2</sub>mim][NTf<sub>2</sub>] can be an excellent solvent for liquid extraction processes for the separation of aromatic and aliphatic hydrocarbons. The values of the solute distribution ratio and the selectivity are good, being better than those for sulfolane, which is the conventional solvent of reference for these purposes. The [C<sub>2</sub>mim][NTf<sub>2</sub>] is an ionic liquid with a melting point below room temperature, with a relatively low viscosity, and does not present problems of decomposition or corrosion.<sup>8,11</sup>

As the ionic liquid is present in minute quantities in the equilibrium upper phase, the treatment of the raffinate stream to recover the solvent accompanying the hydrocarbons may be unnecessary. In addition, due to the negligible vapour pressure of the ionic liquids, these solvent recovery operations are easier than when using conventional organic solvents. Therefore, the use of the ionic liquids can lead to major savings in the installation and operational costs of the processes. Also, the economical feasibility of the liquid extraction to perform the separation of aromatics and aliphatics may take place under a wider range of feed conditions than are currently used.

A very small effect of temperature has been observed, the results being slightly better for the lower temperature. Hence, the efficiency of the extraction by [C<sub>2</sub>mim][NTf<sub>2</sub>] is better at room temperature, not requiring energy to keep a higher temperature in the extractor.

The main handicap of [C<sub>2</sub>mim][NTf<sub>2</sub>] towards implementation in real processes might be its current high price; however, this price is expected to critically decrease in the near future as it will be produced on a much larger scale. Moreover, there is plenty of scope to explore other hydrophobic or hydrophilic ionic liquids for this process; there is nothing optimal in the choice of [C<sub>2</sub>mim][NTf<sub>2</sub>]<sup>—</sup>it is simply an exemplar.

## Note added in proof

Since submitting this manuscript, two relevant papers have appeared (ref. 24 and 25). These data complement the results presented here.

## Acknowledgements

HR wants to thank The QUILL Centre for hosting him as a temporary research fellow, and express his gratitude to the Ministerio de Educación y Ciencia (Spain) for the FPI grant with reference BES-2004-5311 under project PPQ2003-01326. We would also like to acknowledge the QUILL Industrial Advisory Board for their support.

## References

- U. Razdan, S. V. Joshi and V. J. Shah, *Curr. Sci.*, 2003, **85**, 761–771.
- A. A. Gaile, G. D. Zalizhevskii, N. N. Gafur, L. V. Semenov, O. M. Varshavskii, N. P. Fedyanin and L. L. Koldobskaya, *Chem. Technol. Fuels Oils*, 2004, **40**, 215–221.
- K. Weissermel and H.-J. Arpe, *Industrial Organic Chemistry*, VCH, New York, USA, 2nd edn, 1993, pp. 316–320.
- R. Wennersten, in *Principles and practices of solvent extraction*, ed. J. Rydberg, C. Musikas and G. R. Choppin, Marcel Dekker, New York, USA, 1992, p. 328.
- D. M. T. Newsham, in *Science and Practice of Liquid–Liquid Extraction*, ed. J. D. Thornton, Clarendon Press, Oxford, UK, 1992, vol. 1, pp. 27–31.
- G. W. Meindersma, A. J. G. Podt and A. B. de Haan, *Fuel Process. Technol.*, 2005, **87**, 59–70.
- N. Deenadayalu, K. C. Ngongo, T. M. Letcher and D. Ramjugernath, *J. Chem. Eng. Data*, 2006, **51**, 988–991.
- Ionic Liquids in Synthesis*, ed. P. Wasserscheid and T. Welton, Wiley-VCH, Weinheim, 2003.
- M. J. Earle, J. M. S. S. Esperança, M. A. Gilea, J. N. Canongia Lopes, L. P. N. Rebelo, J. W. Magee, K. R. Seddon and J. A. Widegren, *Nature*, 2006, **439**, 831–834.
- J. Ranke, K. Mólter, F. Stock, U. Bottin-Weber, J. Poczubutt, J. Hoffmann, B. Ondruschka, J. Filser and B. Jastorff, *Ecotoxicol. Environ. Saf.*, 2004, **28**, 396–404.
- R. P. Swatloski, J. D. Holbrey, S. B. Memon, G. A. Caldwell, K. A. Caldwell and R. D. Rogers, *Chem. Commun.*, 2004, 668–669.
- U. Domańska, A. Pobudkowska and F. Eckert, *Green Chem.*, 2006, **8**, 268–276.
- M. S. Selvan, M. D. McKinley, R. H. Dubois and J. L. Atwood, *J. Chem. Data*, 2000, **45**, 841–845.
- T. M. Letcher and N. Deenadayalu, *J. Chem. Thermodyn.*, 2003, **35**, 67–76.
- T. M. Letcher and P. Reddy, *J. Chem. Thermodyn.*, 2005, **37**, 415–421.
- R. P. Swatloski, J. D. Holbrey and R. D. Rogers, *Green Chem.*, 2003, **5**, 361–363.
- P. Bonhôte, A.-P. Diaz, N. Papageorgiou, K. Kalyanasundaram and M. Grätzel, *Inorg. Chem.*, 1996, **35**, 1168–1178; P. Bonhôte, A.-P. Diaz, M. Armand, N. Papageorgiou, K. Kalyanasundaram and M. Grätzel, *Inorg. Chem.*, 1998, **37**, 166.
- A. Stark, M. J. Torres and K. R. Seddon, *Pure Appl. Chem.*, 2000, **72**, 2275–2287.
- A. Arce, O. Rodríguez and A. Soto, *J. Chem. Eng. Data*, 2004, **49**, 514–517.
- J. Chen, L.-P. Duan, J.-G. Mi, W.-Y. Fei and Z.-C. Li, *Fluid Phase Equilib.*, 2000, **173**, 109–119.
- J. P. Novák, J. Matous and J. Pick, *Liquid–Liquid Equilibria*, Elsevier, Amsterdam, 1987, pp. 128–129.
- H. Renon and J. M. Prausnitz, *AIChE J.*, 1968, **14**, 135–144.
- J. M. Sørensen, doctoral thesis, Danmarks Tekniske Højskole, Lyngby, Denmark, 1980.
- G. W. Meindersma, A. J. G. Podt and A. B. de Haan, *Fluid Phase Equilib.*, 2006, **247**, 158–168.
- G. W. Meindersma, A. Podt and A. B. de Haan, *J. Chem. Eng. Data*, 2006, **51**, 1814–1819.

# Green synthesis of a temperature sensitive hydrogel

Márcio Temtem,<sup>a</sup> Teresa Casimiro,<sup>a</sup> João F. Mano<sup>\*bc</sup> and Ana Aguiar-Ricardo<sup>\*a</sup>

Received 16th March 2006, Accepted 4th October 2006

First published as an Advance Article on the web 27th October 2006

DOI: 10.1039/b603930h

A thermoresponsive hydrogel, poly(*N*-isopropylacrylamide), PNIPAAm, with possible applications in drug delivery, tissue engineering and as smart membranes with tuned permeability, was synthesised in supercritical carbon dioxide. A strategy of solvent-free impregnation/coating of polymeric surfaces with PNIPAAm is also suggested, in order to further extend the applications of membranes or porous bulky systems. In this work, *in situ* synthesis of PNIPAAm within a chitosan scaffold was tested as a proof of concept, in order to produce smart partially-biodegradable scaffolds for tissue engineering applications.

## Introduction

Hydrogels are networks of hydrophilic polymers that have attracted wide research interest as controlled release devices due to their tunable chemical and three-dimensional physical structure, high water content, good mechanical properties, and biocompatibility.<sup>1</sup>

Poly(*N*-isopropylacrylamide), PNIPAAm, is a thermoresponsive hydrogel that has low critical solution temperature (LCST), around 32 °C in an aqueous solution,<sup>2</sup> close to body temperature. It dissolves in water below the LCST and precipitates from the aqueous solution above the LCST due to the disruption of hydrogen bonding with water and the increasing hydrophobic interactions among isopropyl groups. Due to this unique property, PNIPAAm gels have been widely used in biomedical fields, for example, as matrices in protein–ligand recognition, in drug controlled release, in enzyme and cell immobilization and in artificial organs/cell sheet technology.<sup>3</sup>

The preparation of hydrogels from soluble polymers requires typically a cross-linking procedure, that will allow the system to swell water without compromising the integrity of the material. *N,N*-methylenebisacrylamide (MBAM) is the cross-linking agent normally used to prepare PNIPAAm-based hydrogels. The synthesis of polyNIPAM using this cross-linker was first reported by Pelton and Chibante in 1986<sup>4</sup> and since then many publications describing the preparation, characterization and application of temperature-sensitive hydrogels have been reported in the literature.<sup>5</sup>

During the last few years, an effort has been made to modify and improve the properties of PNIPAAm hydrogels. In many attempts the strategies involve the use of organic solvents or toxic additives, that should be then recovered and recycled.<sup>6</sup> In this paper we report the precipitation polymerization of

PNIPAAm in supercritical carbon dioxide (scCO<sub>2</sub>). Our scCO<sub>2</sub>-assisted method to produce PNIPAAm hydrogels presents an enormous advantage when compared with conventional polymerization since there is no need for an intensive drying action before further processing or characterization steps.

The use of scCO<sub>2</sub> as a polymerisation medium offers many advantages over conventional solvents: CO<sub>2</sub> is nontoxic, non-flammable, inexpensive and readily available in high purity from a variety of sources.<sup>7</sup> Since it is a gas at normal pressure by simply reducing the pressure of the system, it is possible to easily separate the solvent from the polymer, leading to highly pure materials<sup>8</sup> ideal for medical applications.

The synthesis of other acrylamides in scCO<sub>2</sub> is already reported in the literature.<sup>9</sup> These polymer syntheses are normally performed in the presence of highly expensive surfactants to emulsify the insoluble monomer in scCO<sub>2</sub>. In our case as the monomer is highly soluble in scCO<sub>2</sub> the polymerization could be performed without any surfactants.

Chitosan is a well known natural polymer that is biodegradable, biocompatible and non-toxic<sup>10</sup> with possible applications in the medical field, including dialysis membranes, contact lenses, antitumor uses, drug delivery controlled-release systems and tissue engineering.

The production of smart partially-biodegradable scaffolds for tissue engineering applications combining the thermoresponsive properties of PNIPAAm, the biocompatible properties of chitosan with the green aspects of polymerizations in scCO<sub>2</sub> is a desired goal.

In this paper we present a new strategy for the polymerization of PNIPAAm that provides new possibilities for the impregnation/coating of these hydrogels in chitosan scaffolds.

## Experimental

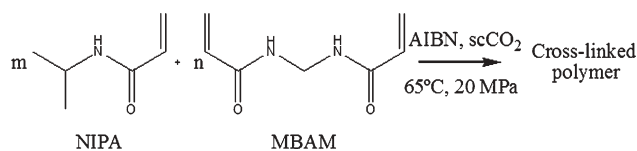
### Materials

*N*-isopropylacrylamide (NIPAAm, 97% purity), *N,N*-methylenebisacrylamide (MBAm, purity ≥ 98%), chitosan (~85% deacetylated, medium molecular weight) and 2,2'-azobis(isobutyronitrile) (AIBN, 98% purity) were purchased from Sigma-Aldrich and used without further purification.

<sup>a</sup>REQUIMTE/CQFB, Departamento de Química, Faculdade de Ciências e Tecnologia, Universidade Nova de Lisboa, 2829-516, Caparica, Portugal. E-mail: aar@dq.fct.unl.pt; Fax: +351 212 948 385; Tel: +351 21 2949648

<sup>b</sup>3B's Research Group—Biomaterials, Biodegradables and Biomimetics, University of Minho, Campus de Gualtar, 4710-057, Braga, Portugal. E-mail: jmano@dep.uminho.pt; Fax: +351 253604492; Tel: +351 253604497

<sup>c</sup>Department of Polymer Engineering, University of Minho, Campus de Azurém, 4810-058, Guimarães, Portugal



Scheme 1

Carbon dioxide was obtained from Air Liquide with 99.998% purity.

### Preparation of PNIPAAm hydrogels

Polymerisation reactions were carried out in a high-pressure apparatus already described elsewhere.<sup>8</sup> In a typical procedure monomer, cross-linking agent (if included), and initiator (2 wt%) are loaded into the high-pressure cell, which is then sealed and nitrogen is added to purge the cell and test leaks. The nitrogen is slowly released and liquid carbon dioxide is loaded into the cell using a high-pressure compressor. The cell is immersed in the water bath and temperature and pressure are allowed to rise to the required experimental conditions. Additional CO<sub>2</sub> may be added to reach the exact desired pressure. The reaction was allowed to proceed for 24 hours under stirring.

The reactions were performed at 65 °C and 20 MPa, according to Scheme 1. At these experimental conditions we have a homogeneous phase with all the reactants completely soluble in the supercritical medium. Different concentrations of cross-linker were tested as summarized in Table 1. Two hours after the beginning of the reaction the mixture turned yellow, then soft orange (Tyndall effect) and within a few minutes white particles of polymer started to precipitate. The resulting polymer was washed with fresh high-pressure CO<sub>2</sub> (65 °C, 20 MPa for one hour) in order to extract the remaining residues of unreacted monomer and cross-linker. When cross-linker was added the polymers conformed closely to the interior of the reaction vessel as a dry, white polymer with a soft consistency. No significant shrinkage was observed upon venting the CO<sub>2</sub>. When no cross-linker was used the polymer precipitated at the bottom of the cell as a fluffy, dry, white, free flowing powder.

### Structural/morphological analysis

The synthesized polymers were analysed by Nuclear Magnetic Resonance (NMR) and Matrix Assisted Laser Desorption/Ionization-Time of Flight Mass Spectrometry (MALDI-TOF MS). NMR spectra were performed in a Bruker equipment (ARX 400 MHz), using deuterated chloroform (CDCl<sub>3</sub>) as solvent and internal reference. MALDI-TOF MS was used to

obtain the molecular weight and it was performed in an AUTOFLEX Bruker using DITHRANOL (1,8,9-anthracenetriol) as matrix. Polymer yield was determined gravimetrically.

Differential scanning calorimetry (DSC) was applied to investigate the thermal features. The LCST of the hydrogel samples was determined in a PerkinElmer DSC 7. The thermal analyses were performed from 15 to 40 °C at 3 °C min<sup>-1</sup> under a dry nitrogen atmosphere (flow rate = 20 mL min<sup>-1</sup>). Calibration for the temperature and energy scale was carried out using a pure indium standard.

Specific surface areas of the networks were determined by adsorption of N<sub>2</sub> according to the BET method. An accelerated surface area and porosimetry system (ASAP 2010 MICROMERITICS) was used under nitrogen flow.

The morphology of hydrogel particles was also evaluated using Scanning Electron Microscopy (SEM) in a Hitachi S-2400, with an accelerating voltage set to 15 kV. Particle size diameters and porosity were obtained by image analysis using SigmaScan Pro (Systat Software Inc.). EasyFit (MathWave Technologies) software was used to fit statistical distributions to our data (Weibull, Lognormal) and perform the Kolmogorov–Smirnov and Anderson–Darling tests to select the more adequate distribution function to each system under study.<sup>11</sup>

### Swelling measurements

Equilibrium hydration or swelling degree ( $W$  (%)) of synthesised samples was determined as defined by eqn (1):

$$\text{Water content } (W(\%)) = \frac{W_t - W_d}{W_d} \times 100 \quad (1)$$

where  $W_d$  is the weight of the dried polymer sample and  $W_t$  is the weight after 24 hours of immersion.

### In situ polymerization inside chitosan scaffolds

PNIPAAm was synthesized inside chitosan scaffolds using scCO<sub>2</sub> assisted polymerizations in order to investigate the feasibility of this technology in the production of smart partially-biodegradable matrices for tissue engineering applications.

Chitosan scaffolds were previously prepared by dissolving medium molecular weight chitosan in 0.2 M acetic acid solution at a concentration of 3 wt%. The solution was then placed in cylindrical silicon moulds, frozen at -80 °C and lyophilized (Telstar-Cryodos -80, Spain) for up to 4 days to completely remove the frozen solvent. Then, the scaffolds were neutralized using a 0.1 M NaOH solution and freeze-dried again.

**Table 1** Effect of cross-linker ratio on the PNIPAAm polymerization in scCO<sub>2</sub>

| Entry | MBAM(wt%) <sup>a</sup> | Yield(%) | LCST/°C | $\Delta H/J \text{ g}^{-1}$ | Surface area/m <sup>2</sup> g <sup>-1</sup> | Polymer morphology                    |
|-------|------------------------|----------|---------|-----------------------------|---|---------------------------------------|
| 1     | 0.0                    | 74.7     | 33.3    | 51                          | 6.1   | Highly aggregated particles           |
| 2     | 1.2                    | 89.6     | 31.7    | 37                          | 10.6  | Defined particles slightly aggregated |
| 3     | 2.4                    | 86.9     | 30.5    | 16                          | 14.3  | Defined particles slightly aggregated |
| 4     | 4.5                    | 94.6     | 30.7    | 10.3                        | 17.3  | Defined particles slightly aggregated |

<sup>a</sup> Weight of MBAM/total weight (NIPAAm, AIBN, MBAM).

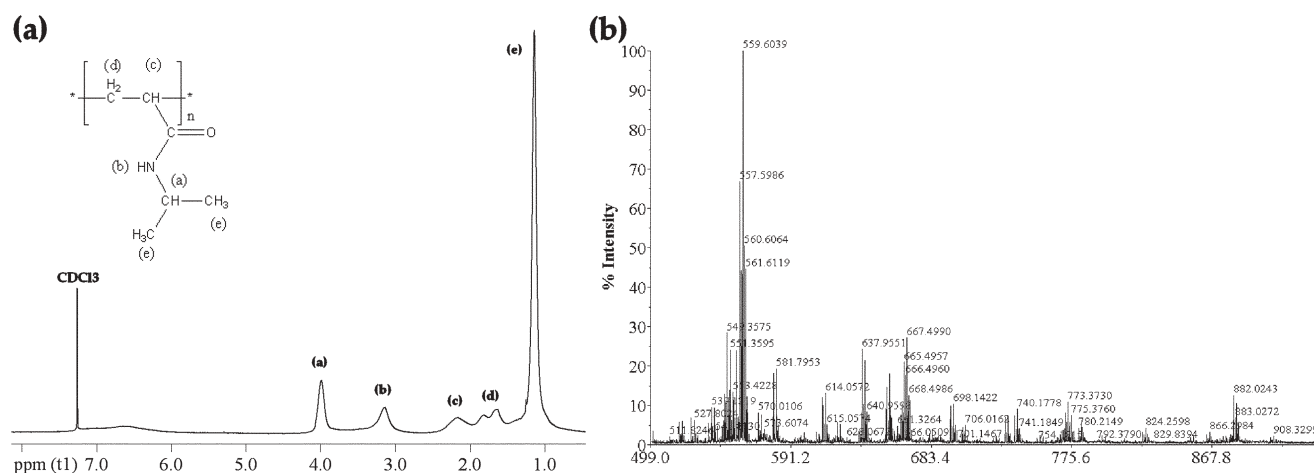


Fig. 1 Characterization of the PNIPAAm hydrogel polymerized without cross-linker: (a) <sup>1</sup>H NMR in CDCl<sub>3</sub>, (b) MALDI-TOF MS spectrum.

For the *in situ* polymerization of PNIPAAm, scaffolds and reactants were placed inside the high pressure vessel and scCO<sub>2</sub> was used as carrier of the monomer/initiator/cross-linker into the porous structures as well as reaction medium. The reaction was performed under the same conditions that were tested in the preparation of PNIPAAm hydrogels.

## Results and discussion

In the absence of cross-linking agent, the precipitation polymerization of PNIPAAm in scCO<sub>2</sub> resulted in low molecular weight polymers (MW = 660) with 75% yield (entry 1 in Table 1). Fig. 1 shows the NMR and MALDI-TOF MS spectra of PNIPAAm synthesised without cross-linker.

The NMR confirmed the structure of PNIPAAm as well as its high purity after the efficient high-pressure CO<sub>2</sub> washing step at the end of the reaction. The NMR and MALDI-TOF MS spectra of the synthesized cross-linked polymers were not used in the discussion due to the low solubility of these hydrogels in the solvents generally used in these techniques, such as chloroform, hexane, acetone and water. By increasing the cross-linker concentration from 1 to 5%, the yield increased up to 95% (entries 2 to 4 in Table 1). This trend might be due to the ability of the cross-linker MBAM to enhance the solubility of the growing polymer in scCO<sub>2</sub> leading to higher yields. Cooper *et al.* observed a similar behaviour in the synthesis of cross-linked polystyrene in scCO<sub>2</sub>.<sup>12a</sup>

In precipitation polymerization,<sup>12</sup> both monomer and initiator are soluble in the continuous phase but as the polymer grows the insoluble polymer chains precipitate and the particles tend to group forming an undefined, agglomerated powder. By increasing the concentration of cross-linker the number of nuclei generated in the reaction increases thus reducing the particle size diameter. Even a small increase of cross-linker (from 1 to 5%) leads to a significant decrease of the particle diameters (from 2.7 to 2.1 μm). PNIPAAm synthesized without cross-linker showed larger particles (5.4 μm), although quite agglomerated (Fig. 2(a)), while when cross-linker was added the particle diameters were significantly reduced (2.1 μm). This trend can be clearly observed by comparing SEM images from Fig. 2 and particle size distributions

from Fig. 5 (see later). The small variation in cross-linker concentration explains the visual similarity between Figs. 2(b), (c) and (d). All samples show some agglomeration which is typical in a precipitation polymerization without the use of a stabiliser. Usually higher cross-linking degree results in less agglomerated polymers since particles are stabilised against coagulation by their cross-linked surfaces rather than by added stabilisers.<sup>12a</sup> This trend is also easily observed in our work. As can be seen in Fig. 2 the sample synthesised in the absence of cross-linker shows a higher degree of agglomeration when compared with the cross-linked samples. It is expected that the morphology of the materials, and their corresponding properties, could be tailored by changing the processing conditions, which makes this strategy a versatile way for preparing thermoresponsive gels.

Fig. 3 shows the DSC thermograms of each sample, which were previously soaked in distilled water for 24 h. An endothermic peak is clearly observed around 32 °C, resulting from the cleavage of the hydrogen bonds between –NH and –C=O groups of PNIPAAm chains and the surrounding water

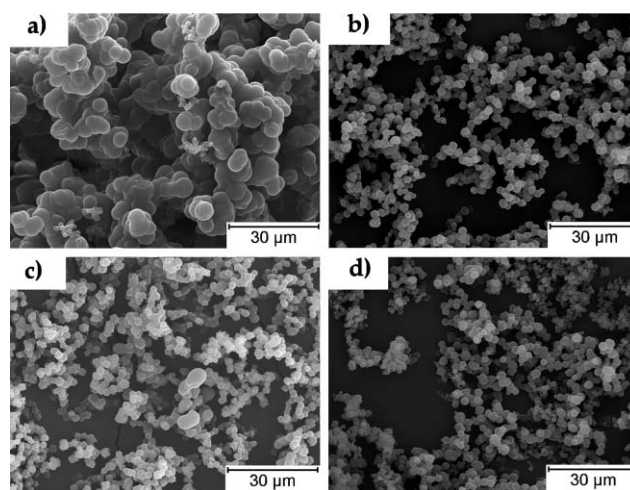
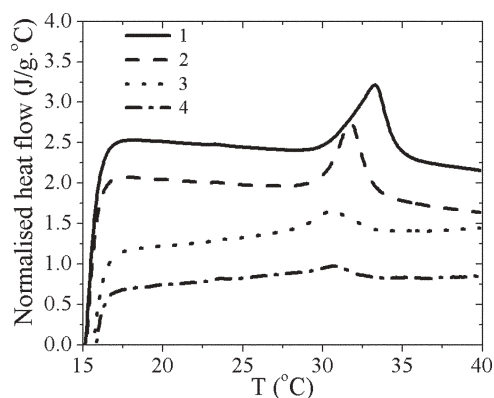


Fig. 2 Scanning electron microscopy images of the hydrogels prepared under different conditions. Samples: (a) 0 wt% MBAM, (b) 1.2 wt% MBAM, (c) 2.4 wt% MBAM, (d) 4.5 wt% MBAM.



**Fig. 3** DSC thermograms of the hydrogels prepared. 1: 0 wt% MBAM; 2: 1.2 wt% MBAM; 3: 2.4 wt% MBAM; 4: 4.5 wt% MBAM.

molecules. The values of the peak temperature (defined as LCST) and endothermic enthalpies ( $\Delta H$ ) are shown in Table 1. For the first three formulations a continuous decrease in the LCST is observed. We can then conclude that the cross-linking influences the phase behaviour of PNIPAAm. The strong variation in the enthalpy clearly suggests that cross-linking highly suppresses the thermoresponsive intensity of such hydrogels, as the cross-linking regions will not participate in this event, and may even repress its occurrence. It should be remarked that for linear polymers (without cross-linker) the enthalpy obtained is of the same order of previous results,<sup>2</sup> where values of  $6.3 \text{ kJ mol}^{-1}$  ( $55.8 \text{ J g}^{-1}$ ) were reported for PNIPAAm with different molecular weight distributions, and recognized to be typical for hydrogen bond interactions.

The swelling degree of a thermoresponsive hydrogel is an important property to be characterised because it will determine properties such as the adsorption and diffusion of solutes through the hydrogel, mechanical properties under wet conditions and water uptake capability. Fig. 4 shows the swelling behaviour, at 25 °C and 37 °C, of the PNIPAAm samples produced in  $\text{scCO}_2$ .

In the swelling process, the water molecules penetrate the dry hydrogel, wetting the polymer chains. They are weakly adsorbed on the hydrophilic polymer chains or are connected with hydrogen bonds to each other, being trapped in the

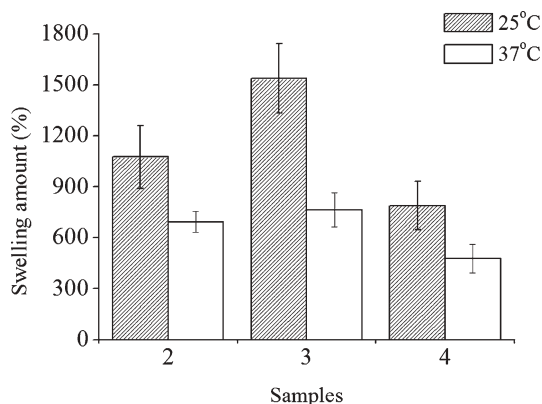


**Fig. 4** Equilibrium swelling at 37 °C and 25 °C for PNIPAAm hydrogels. 2: 1.2 wt% MBAM; 3: 2.4 wt% MBAM; 4: 4.5 wt% MBAM.

hydrophilic polymer matrices. All of these interactions lead the hydrogel to swell well at a temperature lower than the LCST. At temperatures above the LCST, this balance is disturbed, and the interactions among the hydrophobic groups begin to play a dominant role, and so the polymer chains aggregate together. As a result, the entrapped water is squeezed out. In our case 300–700% w/w differences were observed, which indicates that a considerable amount of water is entrapped inside the gel network *via* hydrogen bonds and influenced by the LCST. In all samples the differences in swelling for the two temperatures analysed are statistically significant with 95% confidence. The differences observed for the different samples are due to the influence of the cross-linker in the morphology of the hydrogels. As suggested by the DSC results, the water uptake should be smaller for the highest cross-linked material, being consistent with the data of Fig. 4.

The average particle size, the particle size distribution, and the porosity are also important factors in solute permeation into and out of a hydrogel. In this work the porosity of all hydrogels produced is essentially the same, around 40% even though they present quite different particle diameters and surface areas.

The surface areas obtained by the multipoint BET method (type II) are shown in Table 1. According to the isotherm analysis there is an hysteresis (H3 type) confirming an agglomerated material with slit-pores. These areas are in agreement with the particle size distribution presented in Fig. 5. The hydrogel synthesized without cross-linker has the highest mean diameter (entry 1 in Table 1), and presents the smallest surface area per gram. The particles of the hydrogels produced with different amounts of cross-linker show smaller mean diameters. There is a clear trend between the hydrogels cross-linking and surface area/particles sizes. By increasing the cross-linker concentration a decrease of particles size diameters, as well as an increase in their specific surface areas are observed. This behaviour has been observed by other authors in conventional polymerisation.<sup>13</sup>

This work demonstrates the feasibility for synthesizing thermoresponsive polymers and hydrogels in a  $\text{scCO}_2$  environment. It would be interesting to extend this strategy towards the surface modification or impregnation of previously prepared polymeric systems with a thermoresponsive polymer. This could help in preparing novel smart films, membranes or porous bulky devices with surface properties

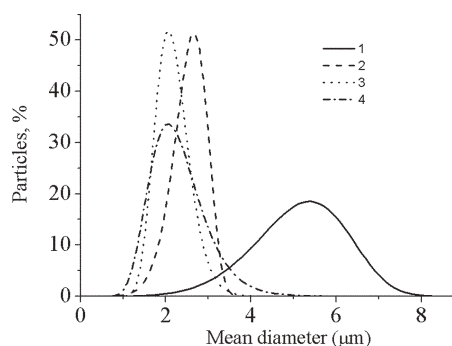


**Fig. 5** Particle size distributions of the different samples. 1: 0 wt% MBAM; 2: 1.2 wt% MBAM; 3: 2.4 wt% MBAM; 4: 4.5 wt% MBAM.

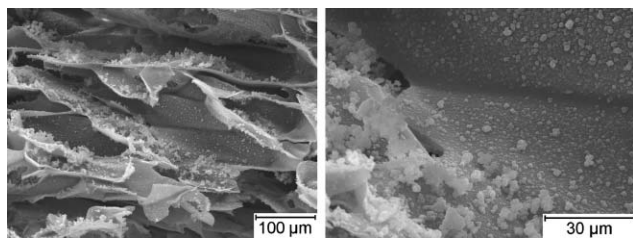


**Fig. 6** SEM pictures of PNIPAAm hydrogel impregnated in a chitosan scaffold.

that could change with temperature. The implementation of such a strategy was tested in this work, where PNIPAAm was impregnated *in situ* within a biodegradable porous structure, made of chitosan, using supercritical fluid technology. Biodegradable foams can be used, for example, in tissue engineering applications where it is required as an adequate non-permanent support for cell adhesion and proliferation prior to implantation in a regenerative medicine context;<sup>14</sup> porous biocompatible and biodegradable polymers have been widely used for this purpose. The incorporation of a fraction (mainly in the surface) of a thermoresponsive polymer could provide other possibilities to the scaffold, including improved or switchable release control of bioactive agent, such as growth factors, or to control cell adhesion/detachment. Porous structures of chitosan can be easily prepared by freeze-drying, where the final structure may be controlled by the processing conditions.<sup>15</sup> PNIPAAm was synthesized within a previously prepared chitosan scaffold. Fig. 6 presents two SEM images of the materials prepared. Such preliminary results clearly show that the hydrogel is uniformly distributed in large amounts inside the pores of the scaffolds.

## Conclusion

In summary, we have developed a novel, simple and green method to synthesise PNIPAAm hydrogels without using organic solvents or any other additives (*e.g.* surfactants). In addition a chitosan scaffold was used as a matrix for the *in situ* polymerisation of NIPA in  $\text{scCO}_2$ . This would allow matrices to be produced with thermoresponsive capability that could be used as porous membranes for advanced purification/separation applications, systems for switchable release of molecules or scaffolds for tissue engineering applications.

## Acknowledgements

We thank Professor Isabel Fonseca and Rui Viegas for help with specific surface area measurements and Professor Eurico

Cabrita for helpful discussions in NMR analysis. The authors also thank the financial support from Fundação para a Ciência e Tecnologia (FCT) through contracts POCTI/35429/QUI/2000, POCTI/FIS/61621/2004, POCTI/EQU/46715/2002, SFRH/BPD/11665/2002, SFRH/BD/16908/2004 and by FEDER and FSE.

## References

- (a) X. Huang and T. L. Lowe, *Biomacromolecules*, 2005, **6**, 2131; (b) R. Langer and N. A. Peppas, *AIChE J.*, 2003, **49**, 2990.
- (a) H. G. Schild, *Prog. Polym. Sci.*, 1992, **17**, 163; (b) V. V. A. Fernandez, N. Tepale, J. C. Sanchez-Diaz, E. Mendizabal, J. E. Puig and J. F. A. Soltero, *Colloid Polym. Sci.*, 2006, **284**, 387.
- (a) T. Okano, N. Yamada, H. Sakai and Y. Sakurai, *J. Biomed. Mater. Res.*, 1993, **27**, 1243; (b) P. S. Stayton, T. Shimoboji, C. Long, A. Chilkoti, G. Chen, J. M. Harris and A. S. Hoffman, *Nature*, 1995, **378**, 472; (c) Y. Qiu and K. Park, *Adv. Drug Delivery Rev.*, 2001, **53**, 321; (d) L. C. Dong and A. S. Hoffman, *J. Controlled Release*, 1986, **4**, 223; (e) R. A. Stile, W. R. Burghardt and K. E. Healy, *Macromolecules*, 1999, **32**, 7370; (f) K.-H. Park and Y. H. Bae, *Biosci., Biotechnol., Biochem.*, 2002, **66**, 1473.
- R. Pelton and P. Chibante, *Colloids Surf.*, 1986, **20**, 247.
- (a) S.-X. Cheng, J.-T. Zhang and R.-X. Zhuo, *Cheng, S., J. Biomed. Mater. Res.*, 2003, **67A**, 96; (b) X. Zhang, Y. Yang, T. Chung and K. Ma, *Langmuir*, 2001, **17**, 6094; (c) R. Zhuo and W. Li, *J. Polym. Sci., Part A: Polym. Chem.*, 2003, **41**, 152; (d) J. Zhang, S. Huang and R. Zhuo, *Macromol. Chem. Phys.*, 2004, **205**, 107; (e) X. Zhang and R. Zhuo, *Eur. Polym. Mater.*, 2000, **36**, 2301.
- (a) X.-Z. Zhang and C.-C. Chu, *J. Mater. Chem.*, 2003, **13**, 2457; (b) D. Kuckling, C. D. Vo, H.-J. P. Adler, A. Völkel and H. Cölfen, *Macromolecules*, 2006, **39**, 1585.
- (a) A. I. Cooper, *J. Mater. Chem.*, 2000, **10**, 207; (b) J. L. Kendall, D. A. Canelas, J. L. Young and J. M. DeSimone, *Chem. Rev.*, 1999, **99**, 543.
- (a) T. Casimiro, A. M. Banet-Osuna, A. M. Ramos, M. Nunes da Ponte and A. Aguiar-Ricardo, *Eur. Polym. J.*, 2005, **41**, 1947.
- F. A. Adamsky and E. J. Beckman, *Macromolecules*, 1994, **27**, 312(a); W. Ye and J. M. DeSimone, *Macromolecules*, 2005, **38**, 2180.
- (a) P. J. VandeVord, H. W. T. Matthew, S. P. DeSilva, L. Mayton, B. Wu and P. H. Wooley, *J. Biomed. Mater. Res.*, 2002, **59**, 585; (b) K. Tuzlakoglu, C. M. Alves, J. F. Mano and R. L. Reis, *Macromol. Biosci.*, 2004, **4**, 811; (c) A. Di Martino, M. Sittinger and M. V. Risbud, *Biomaterials*, 2005, **26**, 5983.
- M. Temtem, T. Casimiro and A. Aguiar-Ricardo, *J. Membr. Sci.*, 2006, **283**, 244.
- (a) A. I. Cooper, W. P. Hems and A. B. Holmes, *Macromolecules*, 1999, **32**, 2156; (b) R. Arshady, *Colloid Polym. Sci.*, 1992, **270**, 717; (c) W. Wang, R. M. T. Griffiths, A. Naylor, M. R. Giles, D. J. Irvine and S. M. Howdle, *Polymer*, 2002, **43**, 6653.
- C. Sayil and O. Okay, *Polym. Bull.*, 2002, **48**, 499.
- (a) M. Chapekar, *J. Biomed. Mater. Res. (Appl. Biomater.)*, 2000, **53**, 617; (b) X. Liu and P. X. Ma, *Ann. Biomed. Eng.*, 2004, **32**, 477; (c) V. Karageorgiou and D. Kaplan, *Biomaterials*, 2005, **26**, 5474.
- S. V. Madihally and H. W. T. Matthew, *Biomaterials*, 1999, **20**, 1133.

# One-step synthesis of *N,N'*-dialkyl-*p*-phenylenediamines†

Luke T. Higham,<sup>a</sup> Katsuya Konno,<sup>b</sup> Janet L. Scott,<sup>a</sup> Christopher R. Strauss\*<sup>c</sup> and Tatsuaki Yamaguchi<sup>b</sup>

Received 30th May 2006, Accepted 18th October 2006

First published as an Advance Article on the web 30th October 2006

DOI: 10.1039/b607632g

Condensation of 1,4-cyclohexanedione with primary alkylamines in the presence of air afforded *N,N'*-dialkyl-*p*-phenylenediamines. Reactions occurred at room temperature and were complete within a few hours, in high atom economy and with water as the major by-product.

## Introduction

In recent investigations into the generation of aromatic species from masked precursors,<sup>1</sup> we discovered a green, multi-component cascade reaction for the preparation of 2- and 4-arylmethyl *N*-substituted and *N,N*-disubstituted anilines.<sup>2</sup> Several known product anilines have pre-existing industrial applications and some of our new compounds have shown interesting biological activities.<sup>3</sup> Consequently, we have extended the scope of our studies into aromatisation to include substituted phenylenediamines such as *N,N'*-dialkyl-*p*-phenylenediamines (**1**).

*p*-Phenylenediamines (**1**) are useful stabilisers for polymers, particularly as antioxidants and antiozonants for rubbers.<sup>4</sup> They also serve as synthetic starting materials for flavins,<sup>5</sup> bis-Tröger's bases,<sup>6</sup> rod-like oligomers, rotaxanes,<sup>7</sup> redox-active macrocycles<sup>8–10</sup> and ladder polymers.<sup>11</sup> Published routes to **1** often involve multiple steps,<sup>11–17</sup> including protection and deprotection, that introduce two additional manipulations and lower the atom economy.<sup>14–16</sup> They do not always show high chemoselectivity.<sup>18–21</sup> Also they may employ potentially hazardous alkylating agents<sup>14,18</sup> or polluting solvents<sup>15,17</sup> and they may generate toxic by-products.<sup>11,17</sup> Moreover, the majority of the syntheses start from *p*-phenylenediamine, which is obtained from benzene in a multi-step process that has low atom economy.<sup>22</sup> Therefore, simpler and greener routes are desirable.

Fifty years ago, Leonard and Sauers reported the two-step synthesis of two *N,N,N',N'*-tetraalkyl-*p*-phenylenediamines by condensation of 1,4-cyclohexanedione (**2**) with secondary amines.<sup>23</sup> A two-step pathway was proposed, involving formation of a bis-enamine intermediate followed by aromatisation through aerial oxidation. Disadvantages included low to moderate yields (13–40%) and the use of benzene, which is now considered as an unacceptable solvent due to its carcinogenicity.<sup>24,25</sup> Nonetheless, the potential for use of air for oxidative aromatisation at room temperature, without the

need for added catalyst, was appealing. Dione **2** can be considered as a green starting material as it is prepared from succinic acid in three steps in good yield.<sup>26</sup> Succinic acid is a renewable resource and may find broad use as a building block for sustainable chemistry.<sup>27</sup> Adaptation of Leonard and Sauers' strategy has been attempted elsewhere with varying success.<sup>28–30</sup> This report, however, discloses the first one-step reactions of dione **2** with primary alkylamines (**3**), in the presence of air for direct, convenient and green preparations of *N,N'*-dialkyl-*p*-phenylenediamines (**1**).

## Results and discussion

*p*-Phenylenediamines **1a–g** were produced by condensation of dione **2** with primary alkylamines **3a–g** in air at room temperature (Table 1). Reactions were conducted in absolute EtOH instead of benzene. Ethanol is greener than many other organic solvents. It has relatively low toxicity and can be produced industrially by fermentation. It is readily recyclable and is both a renewable and a biodegradable resource.<sup>27</sup> Temperatures between ambient and 50 °C were suitable and air was introduced preferably by bubbling through the solution. Reactions proceeded in the absence of light but not

Table 1 Synthesis of *p*-phenylenediamines (**1**)

| Entry                   | R  | Product                | Yield (%) <sup>d</sup> | Lit. yield (%) <sup>d</sup>                                |
|-------------------------|--|------------------------|------------------------|--|
| <b>a</b> <sup>b</sup>   | –CH <sub>2</sub> CH <sub>3</sub>                 | <b>1a</b> <sup>c</sup> | 67                     | 63 <sup>d,11</sup>   |
| <b>b</b>                | –(CH <sub>2</sub> ) <sub>2</sub> CH <sub>3</sub> | <b>1b</b> <sup>c</sup> | 53                     | — <sup>e</sup>   |
| <b>c</b>                | –(CH <sub>2</sub> ) <sub>3</sub> CH <sub>3</sub> | <b>1c</b> <sup>c</sup> | 47                     | 43; <sup>d,16</sup> 59; <sup>d,20</sup> 68 <sup>d,15</sup> |
| <b>d</b>                | –(CH <sub>2</sub> ) <sub>5</sub> CH <sub>3</sub> | <b>1d</b> <sup>c</sup> | 47                     | —  |
| <b>e</b> <sup>f,g</sup> | –(CH <sub>2</sub> ) <sub>7</sub> CH <sub>3</sub> | <b>1e</b> <sup>c</sup> | 62                     | 70 <sup>17</sup>   |
| <b>f</b>                | –CH <sub>2</sub> Ph                              | <b>1f</b> <sup>c</sup> | 56                     | 100 <sup>d,h,10</sup>                                      |
| <b>g</b> <sup>b</sup>   | –(CH <sub>2</sub> ) <sub>2</sub> Ph              | <b>1g</b>              | 57                     | 58 <sup>d,15</sup>   |
| <b>h</b> <sup>i</sup>   | –Ph  | <b>1h</b>              | 43                     | 92 <sup>d,j,31</sup>                                       |

<sup>a</sup> Isolated. <sup>b</sup> Ratio of **2** to **3** was 1 : 4. <sup>c</sup> Dihydrochloride salt. <sup>d</sup> Yield starting from *p*-phenylenediamine. <sup>e</sup> Conversions are given (ref. 14 and 19). <sup>f</sup> Reaction performed at 50 °C. <sup>g</sup> Ratio of **2** to **3e** was 1 : 2.5. <sup>h</sup> Specific method for *N,N'*-diarylmethyl-*p*-phenylenediamines. <sup>i</sup> Reaction performed at reflux. <sup>j</sup> Specific method for *N,N'*-diaryl-*p*-phenylenediamines.

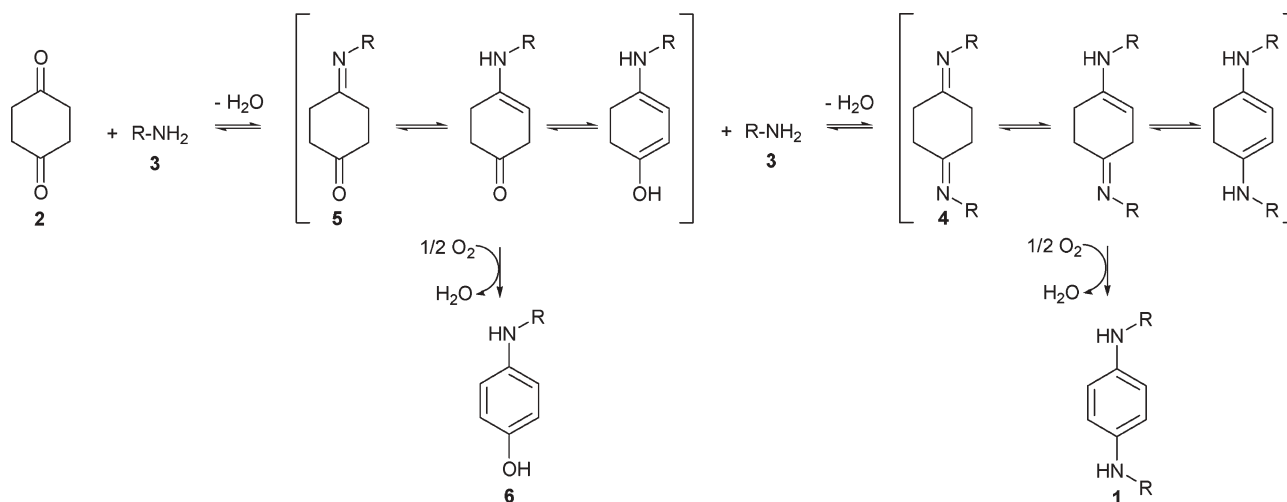
<sup>a</sup>ARC Special Research Centre for Green Chemistry, Monash University, Clayton, Victoria, 3800, Australia

<sup>b</sup>Department of Life and Environmental Sciences, Faculty of Engineering, Chiba Institute of Technology, Tsudanuma, Narashino, Chiba, 275-0016, Japan

<sup>c</sup>CSIRO Molecular and Health Technologies, Private Bag 10, Clayton South, Victoria, 3169, Australia. E-mail: chris.strauss@csiro.au; Fax: +61-3-9545-2446; Tel: +61-3-9545-2183

† Electronic supplementary information (ESI) available: <sup>1</sup>H NMR spectra of compounds **1a–f**·2HCl and **1g**. See DOI: 10.1039/b607632g





**Scheme 1** Proposed pathway for the synthesis of *p*-phenylenediamines (**1**) and by-products.

under anaerobic conditions, presumably by a pathway involving aerial oxidation of putative intermediate diimines, **4a–g** (please see Scheme 1 and Table 1 for **a–g**). Usually a stoichiometric ratio of dione **2** to amine **3** (1 : 2) was employed. Reactions, monitored by GC, GC-MS and  $^1\text{H}$  NMR spectral analysis, typically were completed within 4 h, the conversions generally being greater than 95%. The by-products, which usually comprised 10% or less of the product mixture, included the tentatively identified iminones, **5a–g**, and aminophenols, **6a–g**. In a typical example, the reaction between dione **2** and *n*-propylamine (**3b**) to form *N,N'*-dipropyl-*p*-phenylenediamine (**1b**) is shown in Fig. 1.

The proposed reaction pathway (Scheme 1) involves condensation of dione **2** with alkylamine **3** to give iminone **5**, with the liberation of one molecule of water. Iminone **5** can then undergo aerial oxidation to aminophenol **6** or condensation with another molecule of alkylamine **3** to give diimine **4**, which is then oxidised in the presence of air to give *p*-phenylenediamine **1**. Hence the relative rates with which iminone **5** can be dehydrogenated or condensed with a second molecule of the amine **3**, are critical to the distribution of final products. That diimines **4a–g** were not detected in reactions between **2** and primary alkylamines **3a–g**, suggests that oxidations of **4** were facile. In contrast, evidence for the formation of iminones **5a–g** and aminophenols **6a–g**, albeit as minor products, implies that oxidations of **5** to **6** may have

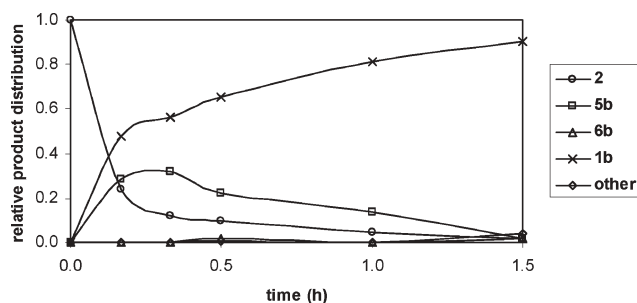


**Fig. 1** Progress of reaction between dione **2** and *n*-propylamine **3b** (1 : 2 ratio) as monitored by GC-MS.

been considerably slower, thereby accounting for the convergence of the process.

The *p*-phenylenediamines **1a–f**, prepared on the 100 mg scale, were usually isolated as their dihydrochloride salts in moderate to good yields that were comparable with those from waste-generating literature methods that had required more steps and less environmentally benign reagents (Table 1). Although produced oxidatively, most of the diamines **1a–h** prepared in this work were sensitive to oxidation.<sup>9,13</sup> This was not surprising in view of the applications for diamines **1a–h** as antioxidants and it implied the need for careful work-up to minimise discrepancies between conversions and isolated yields. When necessary, to limit the extent of decomposition, products were isolated as their dihydrochloride salts from organic solutions of the diamines **1a–h**, which mainly were low melting point solids. It was possible, however, that some loss occurred during work-up and product isolation. The salts were stable and could be stored for months in sealed vials, including in the presence of air.

This work and that of others,<sup>29,30</sup> suggested that the condensation of amines with dione **2** can afford alternative reaction products through relatively subtle changes in conditions. For example, Haga *et al.* found that under acid catalysis, dione **2** with *N*-alkylarylamines or diarylamines in refluxing toluene gave *N*-alkyl-*N*-arylanilines or *N,N*-diarylanilines, respectively.<sup>29</sup> They proposed that an enaminone intermediate underwent dehydrative aromatisation. Up to this point in the present work, acid catalysis had not been employed. When the conditions of Haga *et al.* were used herein, but with a primary amine, *n*-octylamine (**3e**), instead of an *N*-alkylarylamine or a diarylamine, no *N*-*n*-octylaniline was detected. Instead, the present oxidative diamination occurred, with *N,N'*-dioctyl-*p*-phenylenediamine (**1e**) obtained as the major product in 59% yield by GC after 5 h. In the absence of acid, a 62% yield of **1e** had been obtained after 4 h (Table 1). Thus, it was concluded that the process could be conducted in the presence of acid, without any significant effect on the yield.

Recently, Yudina and Bergman obtained 1,4-bis(*p*-methoxyphenyl)phenylenediamine in 13% yield by refluxing a 1 : 2 mixture of dione **2** and *p*-methoxyaniline in benzene for 18 h.<sup>28</sup>

We also have produced *N,N'*-diaryl-*p*-phenylenediamines, but by adaptation of the subject process. A mixture of **2** and aniline (**3h**) in refluxing absolute EtOH for 4 h afforded *N,N'*-diphenyl-*p*-phenylenediamine (**1h**) in 43% yield. The result appeared to be superior to the above literature protocol with regard to reaction time, conditions and yield. This suggests that the approach could supplement a recent high yielding method starting from *p*-phenylenediamine.<sup>31</sup>

## Conclusions

A new method for preparing *N,N'*-dialkyl-*p*-phenylenediamines **1** from the reaction of dione **2** and primary alkylamines **3** is reported. Green aspects included the selection of starting materials, high atom economy, the use of EtOH as a solvent and air at room temperature as an *in situ* oxidant in the absence of added catalyst. The *in situ* multi-step process was performed in one pot, with water as the major by-product and typically, was complete within a few hours.

## Experimental

All solvents, reagents and starting materials were purchased and used without further purification. <sup>1</sup>H and <sup>13</sup>C NMR spectra were recorded on a Bruker Advance DRX 400 spectrometer at 400 and 100 MHz, respectively. Samples were run in CDCl<sub>3</sub> or CD<sub>3</sub>OD and referenced to TMS. *J* values are given in Hz. IR spectra were obtained on neat samples using a Bruker Equinox 55 fitted with a Specac Diamond ATR and MCT detector. Melting points were recorded on a Buchi Melting Point B-545. GC analyses were carried out using a Hewlett Packard Series 5890 GC equipped with a SGE BPX5 fused silica column (25 m × 0.32 mm id, 0.5 μm film thickness). The injector and detector temperatures were 220 and 250 °C, respectively. The oven temperature was programmed as follows: initially 70 °C, increasing to 280 °C at 10 °C min<sup>-1</sup> and holding for 5 min. Helium was the carrier gas (2 mL min<sup>-1</sup>). GC-MS spectra were obtained with a ThermoQuest TRACE DSQ GC-MS using EI with an ionisation energy of 70 eV. The column was a SGE BPX5 (10 m × 0.1 mm id, 0.1 μm film thickness), with a temperature program of 40 °C for 2 min, then heating at 40 °C min<sup>-1</sup> to 300 °C, at which the temperature was held for 2 min. The injector temperature was 250 °C and the transfer line was set to 250 °C. High-purity helium was used as the carrier gas with a flow rate of 0.8 mL min<sup>-1</sup>.

### General procedure for the synthesis of *N,N'*-dialkyl-*p*-phenylenediamines **1a–f**

A mixture of 1,4-cyclohexanedione (**2**, 0.28 g, 2.5 mmol) and the chosen amine **3** (5.0 mmol) in EtOH (99.7%, 25 mL) were stirred in a 50 mL round bottom flask at rt with air bubbling through the solution. After reaction completion (1–4 h), as determined by GC, the EtOH was removed under reduced pressure. The residue was dissolved in a minimal amount of acetone (3–5 mL) and conc. HCl (32%, 10–20 drops) was added to form the dihydrochloride salt. The salt was characterised by mp, <sup>1</sup>H and <sup>13</sup>C NMR spectroscopies, and

IR spectroscopy. The free base was characterised by MS and <sup>1</sup>H NMR spectroscopy.

***N,N'*-Diethyl-*p*-phenylenediamine (**1a**).** A 70% w/w aq solution of ethylamine (**3a**) was used. *m/z* 164 (M<sup>+</sup>, 92%), 149 (100), 135 (52), 106 (16) [lit.,<sup>11</sup> 164 (M<sup>+</sup>)]; δ<sub>H</sub>(CDCl<sub>3</sub>, TMS) 6.56 (4 H, s), 3.08 (6 H, q, *J* 7.1), 1.22 (6 H, t, *J* 7.1) *cf.* lit.<sup>11</sup> **1a**·2HCl: colourless solid; mp 244–246 °C decomp. (from EtOH); ν<sub>max</sub>/cm<sup>-1</sup> 3060, 2965, 2935, 2875, 2605, 2540, 1515, 1475, 1440; δ<sub>H</sub>(CD<sub>3</sub>OD, TMS) 7.62 (4 H, s), 3.46 (4 H, q, *J* 7.2), 1.37 (6 H, t, *J* 7.2); δ<sub>C</sub>(CD<sub>3</sub>OD, TMS) 137.8, 125.0, 47.8, 11.7.

***N,N'*-Dipropyl-*p*-phenylenediamine (**1b**).** *m/z* 192 (M<sup>+</sup>, 56%), 163 (100) [lit.,<sup>14</sup> 192 (M<sup>+</sup>)]; δ<sub>H</sub>(CDCl<sub>3</sub>, TMS) 6.56 (4 H, s), 3.02 (4 H, t, *J* 7.0), 1.61 (4 H, m), 0.98 (6 H, t, *J* 7.4); δ<sub>C</sub>(CDCl<sub>3</sub>) 141.1, 114.9, 47.4, 23.0, 11.8. **1b**·2HCl: colourless solid, mp 239–240 °C decomp. (from EtOH) (lit.,<sup>32</sup> mp 240–241 °C decomp.); ν<sub>max</sub>/cm<sup>-1</sup> 3055, 2970, 2945, 2915, 2880, 2765, 2700, 2650, 2600, 2555, 2505, 2415, 1515, 1475, 1445; δ<sub>H</sub>(CD<sub>3</sub>OD, TMS) 7.54 (4 H, s), 3.34 (4 H, m), 1.76 (4 H, m), 1.05 (6 H, t, *J* 5.8); δ<sub>C</sub>(CD<sub>3</sub>OD, TMS) 138.0, 124.3, 53.8, 21.0, 11.2.

***N,N'*-Dibutyl-*p*-phenylenediamine (**1c**).** *m/z* 220 (M<sup>+</sup>, 54%), 177 (100) [lit.,<sup>14</sup> 220 (M<sup>+</sup>)]; δ<sub>H</sub>(CDCl<sub>3</sub>, TMS) 6.56 (4 H, s), 3.05 (4 H, t, *J* 7.1), 1.58 (4 H, m), 1.41 (4 H, m), 0.94 (6 H, t, *J* 7.3). **1c**·2HCl: colourless solid; mp 247–249 °C decomp. (from EtOH); ν<sub>max</sub>/cm<sup>-1</sup> 3060, 2960, 2935, 2870, 2610, 2530, 2445, 1520, 1475, 1430; δ<sub>H</sub>(CD<sub>3</sub>OD, TMS) 7.75 (4 H, s), 3.43 (4 H, m), 1.75 (4 H, m), 1.48 (4 H, m), 0.99 (6 H, t, *J* 7.4); δ<sub>C</sub>(CD<sub>3</sub>OD, TMS) 138.0, 125.8, 53.4, 29.2, 20.8, 13.9.

***N,N'*-Dihexyl-*p*-phenylenediamine (**1d**).** *m/z* 276 (M<sup>+</sup>, 20%), 205 (100); δ<sub>H</sub>(CDCl<sub>3</sub>, TMS) 6.55 (4 H, s), 3.04 (4 H, t, *J* 7.1), 1.58 (4 H, m), 1.39–1.28 (12 H, m), 0.89 (6 H, t, *J* 6.8). **1d**·2HCl: colourless solid, mp 237–239 °C decomp. (from EtOH); ν<sub>max</sub>/cm<sup>-1</sup> 3060, 3040, 2960, 2930, 2860, 2745, 2650, 2595, 2575, 2515, 2470, 2435, 2405, 1520, 1485, 1470, 1430; δ<sub>H</sub>(CD<sub>3</sub>OD, TMS) 7.67 (4 H, s), 3.40 (4 H, t), 1.74 (4 H, m), 1.44 (4 H, m), 1.35 (8 H, m), 0.92 (6 H, t, *J* 7.0); δ<sub>C</sub>(CD<sub>3</sub>OD, TMS) 138.0, 125.3, 52.9, 32.4, 27.3, 27.2, 23.5, 14.3.

***N,N'*-Dioctyl-*p*-phenylenediamine (**1e**).** *m/z* 332 (M<sup>+</sup>, 100%), 233 (78); δ<sub>H</sub>(CDCl<sub>3</sub>, TMS) 6.55 (4 H, s), 3.03 (4 H, t, *J* 7.0), 1.74 (4 H, m), 1.45–1.30 (20 H, m), 0.89 (6 H, t, *J* 6.8) (*cf.* lit.<sup>17</sup>). **1e**·2HCl: colourless solid; mp 234–236 °C decomp. (from EtOH); ν<sub>max</sub>/cm<sup>-1</sup> 3060, 3040, 2955, 2925, 2855, 2735, 2660, 2610, 2515, 2440, 1520, 1465, 1430; δ<sub>H</sub>(CD<sub>3</sub>OD, TMS) 7.57 (4 H, s), 3.30 (4 H, m), 1.72 (4 H, m), 1.45–1.30 (20 H, m), 0.90 (6 H, t, *J* 6.8); δ<sub>C</sub>(CD<sub>3</sub>OD, TMS) 138.0, 124.5, 52.4, 32.9, 30.3, 30.2, 27.6, 27.5, 23.7, 14.4.

***N,N'*-Dibenzyl-*p*-phenylenediamine (**1f**).** *m/z* 288 (M<sup>+</sup>, 100%), 197 (84), 91 (95); δ<sub>H</sub>(CDCl<sub>3</sub>, TMS) 7.42–7.25 (10 H, m), 6.56 (4 H, s), 4.25 (4 H, s) (*cf.* lit.<sup>10</sup>). **1f**·2HCl: colourless solid; mp 239–241 °C decomp. (from EtOH) (lit.,<sup>33</sup> mp 240–241 °C); δ<sub>H</sub>(CD<sub>3</sub>OD, TMS) 7.37 (10 H, s), 7.09 (4 H, s), 4.47 (4 H, s).

### Synthesis of *N,N'*-diphenethyl-*p*-phenylenediamine (**1g**)

A mixture of 1,4-cyclohexanedione (**2**, 0.28 g, 2.5 mmol) and 2-phenylethanamine (**3g**, 1.21 g, 10.0 mmol) in EtOH (99.7%, 10 mL) were stirred in a 25 mL round bottom flask at rt with air bubbling through the solution for 3 h. After cooling, a solid was collected by filtration and recrystallised from EtOH to give **1g** (0.450 g, 57%) as a colourless solid; mp 127.5–128 °C (lit.,<sup>15</sup> 127–128.5 °C);  $\delta_{\text{H}}$ (CDCl<sub>3</sub>, TMS) 7.32–7.27 (4 H, m), 7.23–7.19 (6 H, m), 6.56 (4 H, br s), 3.49 (2 H, br s), 3.33 (4 H, br m), 2.88 (4 H, t, *J* 7.0);  $\delta_{\text{C}}$ (CDCl<sub>3</sub>, TMS) 148.1, 139.5, 128.8, 128.6, 126.3, 115.2, 46.5, 35.6.

### Synthesis of *N,N'*-diphenyl-*p*-phenylenediamine (**1h**)

A mixture of 1,4-cyclohexanedione (**2**, 0.28 g, 2.5 mmol) and aniline (**3h**, 0.47 g, 5.0 mmol) in EtOH (99.7%, 25 mL) were refluxed in a 50 mL round bottom flask with air bubbling through the solution for 4 h. The solution was cooled to rt and the precipitate was collected by filtration and recrystallised from toluene to give **1h** (0.28 g, 43%) as a brown solid; mp 146–148 °C (lit.,<sup>34</sup> 148–149 °C); *m/z* 260 (M<sup>+</sup>, 100%), 183 (15), 167 (11).

### EI-MS for compounds tentatively identified as iminones (**5**) and aminophenols (**6**)

**4-(Propylimino)cyclohexanone (5b)**. *m/z* 153 (M<sup>+</sup>, 27%), 124 (67), 110 (17), 96 (100).

**4-(Butylimino)cyclohexanone (5c)**. *m/z* 167 (M<sup>+</sup>, 27%), 138 (23), 124 (40), 110 (100), 96 (80).

**4-(Hexylimino)cyclohexanone (5d)**. *m/z* 195 (M<sup>+</sup>, 20%), 138 (100), 124 (50), 110 (60), 96 (76).

**4-(Octylimino)cyclohexanone (5e)**. *m/z* 223 (M<sup>+</sup>, 19%), 166 (86), 152 (56), 138 (56), 124 (70), 110 (71), 96 (100).

**4-(Benzylimino)cyclohexanone (5f)**. *m/z* 201 (M<sup>+</sup>, 23%), 173 (33), 91 (100).

**4-(Phenylimino)cyclohexanone (5h)**. *m/z* 187 (M<sup>+</sup>, 63%), 130 (100), 103 (10), 77 (19).

***p*-Propylaminophenol (6b)**. *m/z* 151 (M<sup>+</sup>, 36%), 122 (100).

***p*-Butylaminophenol (6c)**. *m/z* 165 (M<sup>+</sup>, 33%), 122 (100) [lit.,<sup>35</sup> 165 (M<sup>+</sup>, 84%), 122 (100)].

***p*-Hexylaminophenol (6d)**. *m/z* 193 (M<sup>+</sup>, 30%), 122 (100) [lit.,<sup>35</sup> 193 (M<sup>+</sup>, 30%), 122 (100)].

***p*-Octylaminophenol (6e)**. *m/z* 221 (M<sup>+</sup>, 29%), 122 (100) [lit.,<sup>35</sup> 221 (M<sup>+</sup>, 35%), 122 (100)].

***p*-Benzylaminophenol (6f)**. *m/z* 199 (M<sup>+</sup>, 100%), 122 (10), 108 (28), 91 (68).

***p*-Phenylaminophenol (6h)**. *m/z* 185 (M<sup>+</sup>, 100%).

### Acknowledgements

We thank the Australian Research Council (ARC) for funding this research through the ARC Special Research Centre for Green Chemistry (CGC) and through an Australian Postgraduate Award (to LTH). The CGC is thanked for hosting post-graduate exchange studies (for KK).

### References

- L. T. Higham, U. P. Kreher, C. L. Raston, J. L. Scott and C. R. Strauss, *Org. Lett.*, 2004, **6**, 3261–3264.
- A. E. Rosamilia, J. L. Scott and C. R. Strauss, *Org. Lett.*, 2005, **7**, 1525–1528.
- WO Pat.*, 012 683, 2006; *Chem. Abstr.*, 2006, **144**, 212532.
- M. Braden and A. N. Gent, *J. Appl. Polym. Sci.*, 1962, **4**, 449–455; J. C. Andries, C. K. Rhee, R. W. Smith, D. B. Ross and H. E. Diem, *Rubber Chem. Technol.*, 1979, **52**, 823–837; R. P. Lattimer, R. W. Layer, E. R. Hooser and C. K. Rhee, *Rubber Chem. Technol.*, 1991, **64**, 780–789; G. J. Lake and P. G. Mente, *Polym. Degrad. Stab.*, 1995, **49**, 193–203.
- Y. Yano, M. Nakazato and R. E. Vasquez, *J. Chem. Soc., Chem. Commun.*, 1985, 226–227; F. Yoneda, M. Koga and Y. Yano, *J. Chem. Soc., Perkin Trans. 1*, 1988, **7**, 1813–1817; H. Ohshiro, K. Mitsui, N. Ando, Y. Ohsawa, W. Koizuma, H. Takahashi, S.-I. Kondo, T. Nabeshima and Y. Yano, *J. Am. Chem. Soc.*, 2001, **123**, 2478–2486.
- T. Mas, C. Pardo, F. Salort, J. Elguero and M. R. Torres, *Eur. J. Org. Chem.*, 2004, 1097–1104.
- E. Córdova, R. A. Bissell and A. E. Kaifer, *J. Org. Chem.*, 1995, **60**, 1033–1038.
- US Pat.*, 6 262 258, 2001; *Chem. Abstr.*, 2001, **135**, 92662; X. Liu, A. H. Eisenberg, C. L. Stern and C. A. Mirkin, *Inorg. Chem.*, 2001, **40**, 2940–2941; J. W. Sibert, G. R. Hundt, A. L. Sargent and V. Lynch, *Tetrahedron*, 2005, **61**, 12350–12357.
- H. Takemura, K. Takehara and M. Ata, *Eur. J. Org. Chem.*, 2004, 4936–4941.
- F. C. Krebs and M. Jørgensen, *J. Org. Chem.*, 2002, **67**, 7511–7518.
- K. Oyaizu, F. Mitsuhashi and E. Tsuchida, *Macromol. Chem. Phys.*, 2002, **203**, 1328–1336.
- P. Vourros and K. Biemann, *Org. Mass Spectrom.*, 1969, **2**, 375–386.
- L. Michaelis, M. P. Schubert and S. Granick, *J. Am. Chem. Soc.*, 1939, **61**, 1981–1992.
- N. E. Agafonov, A. V. Dudin, A. A. Preobrazhenskii and V. M. Zhulin, *Russ. Chem. Bull.*, 2003, **52**, 273–275.
- (a) R. Adams and K. A. Schowalter, *J. Am. Chem. Soc.*, 1952, **74**, 2597–2602; (b) for the synthesis of *N,N'*-di(benzenesulfonyl)-*p*-phenylenediamine, see: N. Nagel, H. Bock and P. Eller, *Acta Crystallogr., Sect. B: Struct. Sci.*, 2000, **56**, 234–244.
- J. V. Capinjala, *J. Am. Chem. Soc.*, 1951, **73**, 1849.
- J. Sinnreich, *Synthesis*, 1979, 578–580.
- DE Pat.*, 2 055 208, 1972; *Chem. Abstr.*, 1972, **77**, 61522.
- M. P. Reynolds and H. Greenfield, in *Catalysis of Organic Reactions*, ed. R. E. Malz, Jr, Marcel Dekker, New York, 1996, ch. 30, pp. 343–351.
- J. Horyna and O. Cerny, *Collect. Czech. Chem. Commun.*, 1956, **21**, 906–911.
- CS Pat.*, 87 381, 1957; *Chem. Abstr.*, 1959, **53**, 6827.
- A. I. Vogel, A. R. Tatchell, B. S. Furnis, A. J. Hannaford and P. W. G. Smith, *Vogel's Textbook of Practical Organic Chemistry*, Longman Scientific and Technical, London, 5th edn, 1989.
- N. J. Leonard and R. R. Sauers, *J. Org. Chem.*, 1956, **21**, 1187–1188.
- D. L. Bayliss, C. Chen, A. Jarabek, B. Sonawane and L. Valcovic, *Carcinogenic Effects of Benzene: An Update*, National Center for Environmental Assessment, Washington Office, Washington, DC, 1998, <http://www.epa.gov/ncea/pdfs/benzenef.pdf>.
- P. T. Anastas and J. W. Warner, *Green Chemistry – Theory and Practice*, Oxford University Press, Oxford, New York, 1998.
- A. T. Nielsen and W. R. Carpenter, *Org. Synth.*, 1965, **45**, 25–28.
- H. Danner and R. Braun, *Chem. Soc. Rev.*, 1999, **28**, 395–405.

- 28 L. N. Yudina and J. Bergman, *Tetrahedron*, 2003, **59**, 1265–1275.  
 29 K. Haga, M. Oohashi and R. Kaneko, *Bull. Chem. Soc. Jpn.*, 1984, **57**, 1586–1590; K. Haga, K. Iwaya and R. Kaneko, *Bull. Chem. Soc. Jpn.*, 1986, **59**, 803–807.  
 30 *WO Pat.*, 092 832, 2005; *Chem. Abstr.*, 2005, **143**, 367079.  
 31 S. Kuhl, Y. Fort and R. Schneider, *J. Organomet. Chem.*, 2005, **690**, 6169–6177.  
 32 M. Sekiya, M. Tomie, K. Ito, J. Suzuki, K. Suzuki and Y. Terao, *Chem. Pharm. Bull.*, 1973, **21**, 1625–1631.  
 33 *GB Pat.*, 787 659, 1957; *Chem. Abstr.*, 1958, **52**, 56190.  
 34 D. D. Perrin, W. L. F. Armarego and D. R. Perrin, *Purification of Laboratory Chemicals*, Pergamon, New York, 2nd edn, 1980.  
 35 N. Takahashi, T. Honda and T. Ohba, *Bioorg. Med. Chem.*, 2006, **14**, 409–417.

# Find a SOLUTION

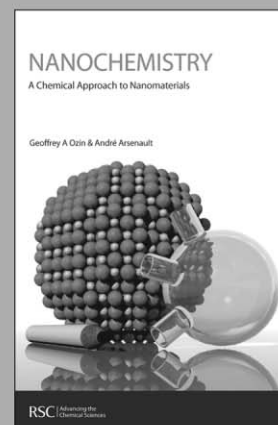
## ... with books from the RSC

Choose from exciting textbooks, research level books or reference books in a wide range of subject areas, including:

- Biological science
- Food and nutrition
- Materials and nanoscience
- Analytical and environmental sciences
- Organic, inorganic and physical chemistry

Look out for 3 new series coming soon ...

- RSC Nanoscience & Nanotechnology Series
- Issues in Toxicology
- RSC Biomolecular Sciences Series



28040542

RSC | Advancing the  
Chemical Sciences

[www.rsc.org/books](http://www.rsc.org/books)

# Novel modified soybean oil containing hydrazino-ester: synthesis and characterization

Atanu Biswas,<sup>\*a</sup> Brajendra K. Sharma,<sup>bc</sup> J. L. Willet,<sup>a</sup> K. Vermillion,<sup>d</sup> Sevim Z. Erhan<sup>b</sup> and H. N. Cheng<sup>\*e</sup>

Received 7th June 2006, Accepted 18th October 2006

First published as an Advance Article on the web 31st October 2006

DOI: 10.1039/b608075h

A novel synthetic approach for chemical modification of vegetable oils is presented. The structural modification is carried out using diethyl azodicarboxylate (DEAD) in the absence of catalyst and solvent. In a microwave oven the reaction can be achieved in 5–15 minutes. The reaction can also proceed using conventional heat, albeit for a longer time. The products are characterized by <sup>1</sup>H, <sup>13</sup>C, and two-dimensional NMR.

## Introduction

There has been a lot of interest in using vegetable oils (particularly soybean oil) as renewable raw materials for new industrial products. It is important to develop a range of relatively facile reactions on vegetable oils in order to facilitate their use. This article represents a step in this direction. The reaction reported is novel and fast, does not require catalyst or solvent, has high yields and is achievable even with a microwave oven. It appears to be a useful reaction that has many potential applications for these oils.

There has been a constant demand for environmentally friendly lubricants. The interest intensified during the last decade due to strict government and environmental regulations.<sup>1</sup> Most of the current lubricants originate from petroleum stock, which is toxic to the environment and difficult to dispose of. Vegetable oils with high oleic content are considered to be potential candidates to substitute conventional mineral oil-based lubricating oils and synthetic esters.<sup>2,3</sup> Vegetable oils are preferred to synthetic fluids because they are renewable resources and potentially cheaper.

Vegetable oils as lubricants are preferred because they are biodegradable and non-toxic, unlike conventional mineral-based oils.<sup>2,4</sup> Apart from these, they have advantages like low volatility, high viscosity index, good boundary lubrication properties, and high solubilizing power for polar contaminants and additive molecules. On the other hand, vegetable oils have poor oxidative stability,<sup>5,6</sup> primarily due to the presence of bis-allylic protons, and are highly susceptible to radical attack

and subsequently undergo oxidative degradation to form polar oxy compounds. This phenomenon may result in insoluble deposits and increases in oil acidity and viscosity, but can be partly mitigated through the use of antioxidants. Vegetable oils can also show poor corrosion protection.<sup>7</sup> Low temperature studies have also shown that most vegetable oils undergo cloudiness, precipitation, poor flow, and solidification at –10 °C upon long-term exposure to cold temperature<sup>8,9</sup> in sharp contrast to mineral oil-based fluids.

In a previous account, Biswas *et al.*<sup>10</sup> reported a method to prepare amino derivatives of soybean oil. Our objective in this work is to explore new pathways to attach nitrogen to vegetable oil. The structural modification is carried out using diethyl azodicarboxylate (DEAD) in the absence of any catalyst and solvent. It has been demonstrated that this reaction is very versatile and can be conducted under different reaction conditions. For example, we can prepare the reaction product using a microwave oven in about 10 minutes, thereby saving a lot of time and energy.

## Experimental

### Microwave-assisted reaction of soybean oil with DEAD

Microwave reactions were carried out using an Ethos<sup>™</sup> MicroSYNTH 1600 Microwave Labstation from Milestone Inc. Reactions were performed in a 50 mL quartz pressure vessel, QRS1550 from Milestone. A mixture of soybean oil 5.32 g (6.2 mmole), 3.1 g of DEAD (18.6 mmole, 3 molar equivalents) were taken into a cross-linked fluoropolymer reactor with a Weflon<sup>™</sup> stir bar and placed in a Milestone Ethos<sup>™</sup> Labstation. Using the Easywave<sup>™</sup> operating software and the fiber-optic temperature probe, the reaction mixture was irradiated with simultaneous magnetic stirring. It took 3 min to reach 120 °C and was held at that temperature for another 10 min. The soybean oil/DEAD adduct was obtained as a viscous, honey-colored oil.

### Conventional thermal synthesis

The same reaction was carried out for 4 hours in a 25 ml round bottom flask with overhead stirrer and a heating mantle as the heat source at 60–120 °C.

<sup>a</sup>Plant Polymer Research Unit, National Center for Agricultural Utilization Research, USDA/Agricultural Research Services, 1815 N. University Street, Peoria, IL, 61604, USA

<sup>b</sup>Food and Industrial Oil Research Unit, National Center for Agricultural Utilization Research, USDA/Agricultural Research Services, 1815 N. University Street, Peoria, IL, 61604, USA

<sup>c</sup>Department of Chemical Engineering, Pennsylvania State University, University Park, PA, 16802, USA

<sup>d</sup>New Crops and Processing Technology Research Unit, National Center for Agricultural Utilization Research, USDA/Agricultural Research Services, 1815 N. University Street, Peoria, IL, 61604, USA

<sup>e</sup>Hercules Incorporated Research Center, 500 Hercules Road, Wilmington, DE, 19808-1599, USA

### Room temperature synthesis in water

A mixture of 5.32 g of soybean oil (6.2 mmole), 3.1 g of DEAD (18.6 mmole, 3 molar equivalents) and 15 ml of water were stirred at room temperature for 3–24 hours. The yellow color of the reaction mixture slowly disappeared and became colorless. Along with the soybean/DEAD adduct, we also obtained white crystals of reduced DEAD (DEADH<sub>2</sub>). The white solid was readily removed to give the soybean/DEAD adduct. If needed, DEADH<sub>2</sub> could be separately crystallized from ethyl acetate–hexane (m.p. 131–133 °C).

### NMR spectroscopy

All <sup>13</sup>C NMR spectra were recorded quantitatively with a Bruker ARX-500 spectrometer (Bruker, Rheinstetten, Germany) at a frequency of 125 MHz and a 5 mm dual probe. The sample solutions were prepared in deuteriochloroform (CDCl<sub>3</sub>, 99.8% D, Cambridge Isotope Laboratories, Inc., Andover, MA, USA). Standard operating conditions were used with 30° pulse angle, 3 seconds between pulses, and <sup>1</sup>H decoupling. Three two-dimensional NMR experiments were run: COSY (correlation spectroscopy), HSQC (heteronuclear single quantum correlation), and HMBC (heteronuclear multiple bond correlation).

### Size exclusion chromatography (SEC)

Molecular weights were measured on a PL-GPC 120 high temperature chromatograph (Polymer Laboratories, Amherst, MA, USA) equipped with autosampler and in-built differential refractometer detector. Two PL gel 3 μm mixed E columns (300 mm × 7.5 mm, Polymer Laboratories) were used in series to resolve the samples. The injection volume was 100 μL. The samples were eluted using a 1.00 mL min<sup>-1</sup> flow rate of THF at 40 °C. The SEC was calibrated using a mixture of linear polystyrene standards (M<sub>n</sub> 1700, 2450, 5050, 7000, 9200, and 10665) obtained from Polymer Laboratories (Amherst, MA, USA), and methyl oleate (M<sub>n</sub> 294.48), methyl linoleate (M<sub>n</sub> 294.48), monoolein (M<sub>n</sub> 353), diolein (M<sub>n</sub> 619.2), and triolein (M<sub>n</sub> 885.4) obtained from Aldrich Chemical (Milwaukee, WI, USA).

### Results and discussion

In this work, we sought a “green” approach to modify vegetable oils that is fast and facile and does not involve any catalysts or solvents. We discovered that soybean oil and DEAD can readily react with each other. Although this work was focused on soybean oil, any vegetable oil with linoleic or linolenic moieties will readily undergo this reaction.

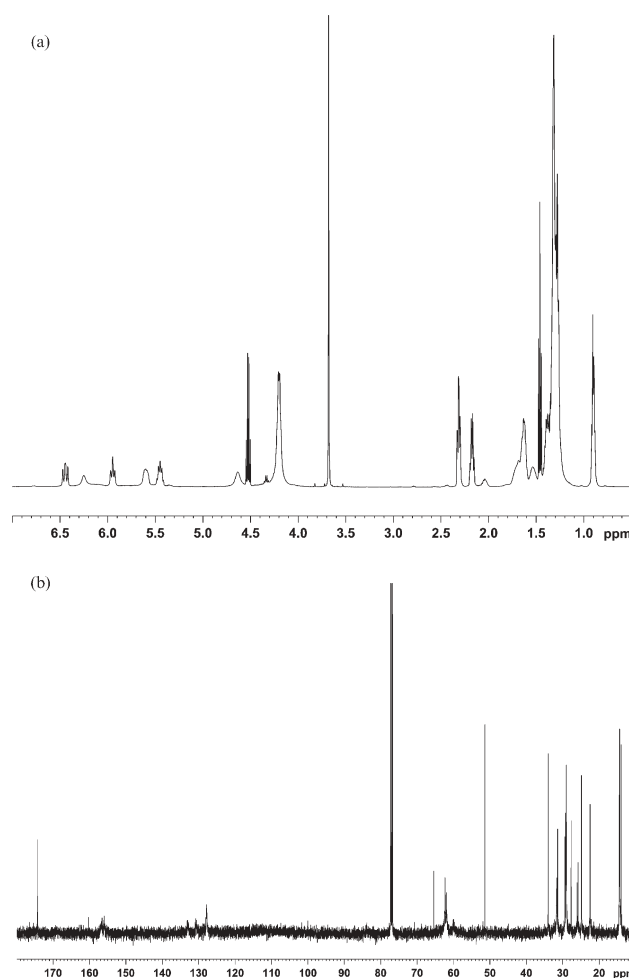


**Fig. 1** (a) <sup>1</sup>H NMR spectrum of the microwave reaction products between methyl linoleate and DEAD. (b) <sup>13</sup>C NMR spectrum of the microwave reaction products between methyl linoleate and DEAD.

### Reactions in a microwave oven

An interesting feature of this reaction is its ability to be carried out in a microwave oven in 5–15 minutes. As far as we know, this is the first report of such a reaction on soybean oil. Some typical reactions are given in Table 1.

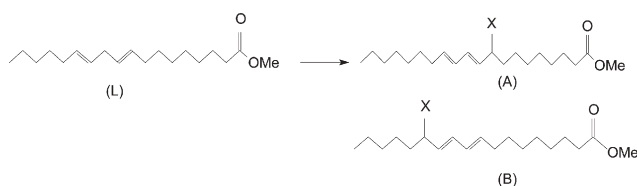
In order to elucidate the reaction mechanism, we also carried out the microwave reaction with methyl linoleate (Table 1). For sample 32-1, the <sup>1</sup>H spectrum is given in Fig. 1a. The spectrum can be assigned mostly to the 1 : 1 ene reaction adduct. The ene reaction is well known and well documented.<sup>11,12</sup> The <sup>13</sup>C NMR spectrum is given in Fig. 1b. To help with interpretation, we obtained the appropriate two-dimensional spectra (COSY, HSQC, and HMBC). The

**Table 1** Microwave reaction of soybean oil and model compounds with DEAD

| Sample     | Reactant     | Molar ratio FA : DEAD | Reaction time/min | Temp/°C | % product         | % ene product <sup>d</sup> |
|------------|--------------|-----------------------|-------------------|---------|-------------------|----------------------------|
| 17865-33-2 | Soybean oil  | 1 : 1.00              | 10                | 115     | 81 <sup>a,c</sup> | 31                         |
| 17865-33-1 | Soybean oil  | 1 : 0.86              | 5                 | 115     | 46 <sup>c</sup>   | 31                         |
| 17865-23-1 | Me linoleate | 1 : 0.80              | 10                | 115     | 82 <sup>d</sup>   | 62                         |
| 17865-32-1 | Me linoleate | 1 : 1.20              | 5                 | 90      | 99 <sup>b,c</sup> | 71                         |

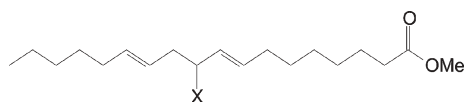
<sup>a</sup> Also contains 15% soybean oil dimer, 4% soybean oil trimer. <sup>b</sup> Also contains 1% methyl linoleate dimer. <sup>c</sup> From SEC. <sup>d</sup> From NMR.

reaction was shown to give two products with the following structures:

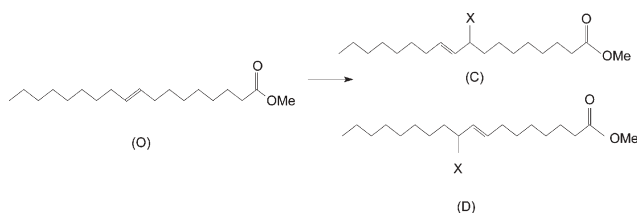


A preliminary structure elucidation was first obtained through literature values on similar materials<sup>13–16</sup> and empirical additive shift rules.<sup>17–19</sup> With the addition of the COSY spectrum, <sup>1</sup>H assignments were positively obtained. From HSQC spectrum, further <sup>13</sup>C and <sup>1</sup>H assignments were made through <sup>13</sup>C–<sup>1</sup>H shift correlation. The assignments were confirmed with the HMBC spectrum. For illustration, the COSY and the HSQC spectra are shown in Fig. 2. The full assignments are summarized in Table 2. It is of interest that despite the spectral complexity, all major peaks are assigned. Note that the peaks next to the point of attachment of DEAD on the linoleate show up as doublet in both <sup>1</sup>H and <sup>13</sup>C spectra due to asymmetry at that point.

In the ene reaction, DEAD can add to the double bond in two ways. It is important to note that only the conjugated structures are observed. The alternative ene reaction products were not found, *e.g.*,

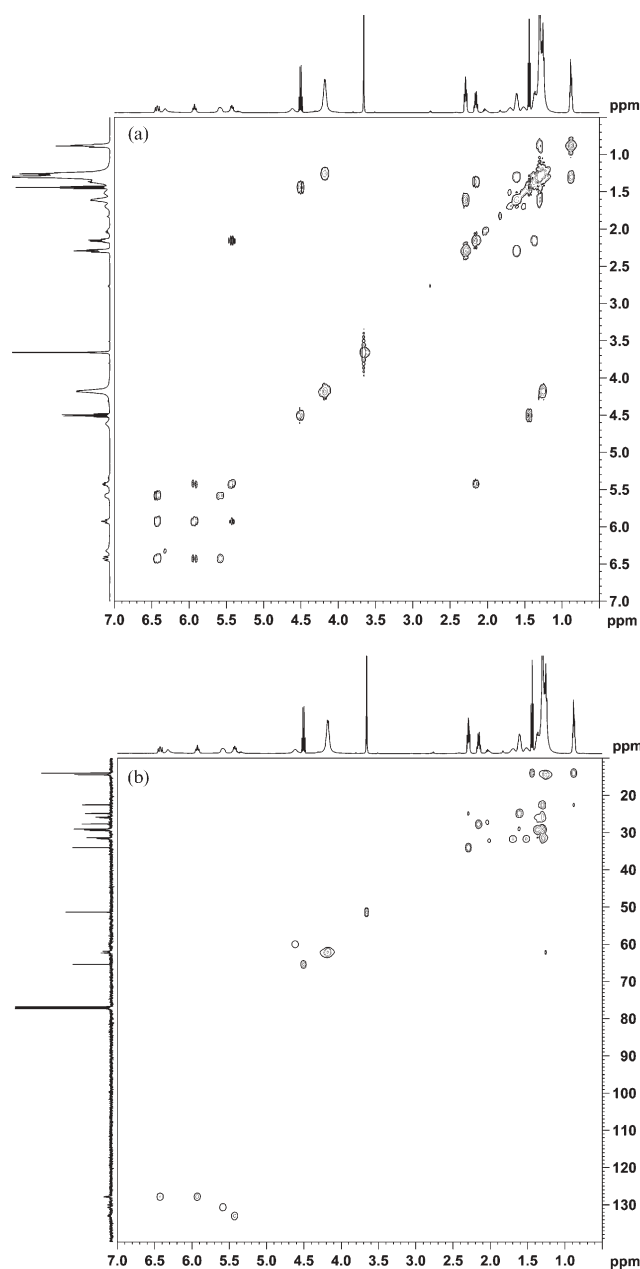


A similar study was done for methyl oleate and DEAD. The reaction was more sluggish, but the reaction products were exactly what we would expect for the ene reaction.



Again, the NMR assignments were made using COSY, HSQC, and HMBC. For convenience, the complete spectral assignments are summarized in Table 2.

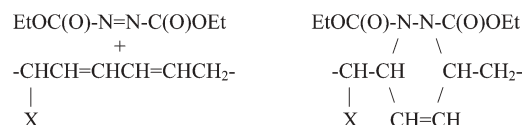
Likewise, the structures of the SBO–DEAD adducts were also elucidated using NMR. Soybean oil contains a distribution of fatty esters, typically about 10% palmitate, 5% stearate, 25% oleate, 51% linoleate, and 7% linolenate. Obviously palmitate and stearate cannot undergo ene reaction. Thus, we would expect the main reactions to occur among linoleate, oleate, (and linolenate) and DEAD. Indeed, the <sup>1</sup>H and <sup>13</sup>C spectra appear to be composites of the linoleate–DEAD and oleate–DEAD adducts (Fig. 3). Accordingly, the same structures shown above for A, B, C, D are also found in the soybean oil–DEAD reaction.



**Fig. 2** (a) <sup>1</sup>H COSY spectrum of the microwave reaction products between methyl linoleate and DEAD. (b) <sup>1</sup>H–<sup>13</sup>C HSQC spectrum of the microwave reaction products between methyl linoleate and DEAD.

Note that in Table 1, the ene reaction products account for only 30–40% of the yield for soybean oil–DEAD. In addition to ene reaction, Diels–Alder reaction occurs with the diene in the fatty acid moiety of the SBO–aza-dicarboxylate ester. Two reactions are shown below.

#### 1. Reaction with DEAD







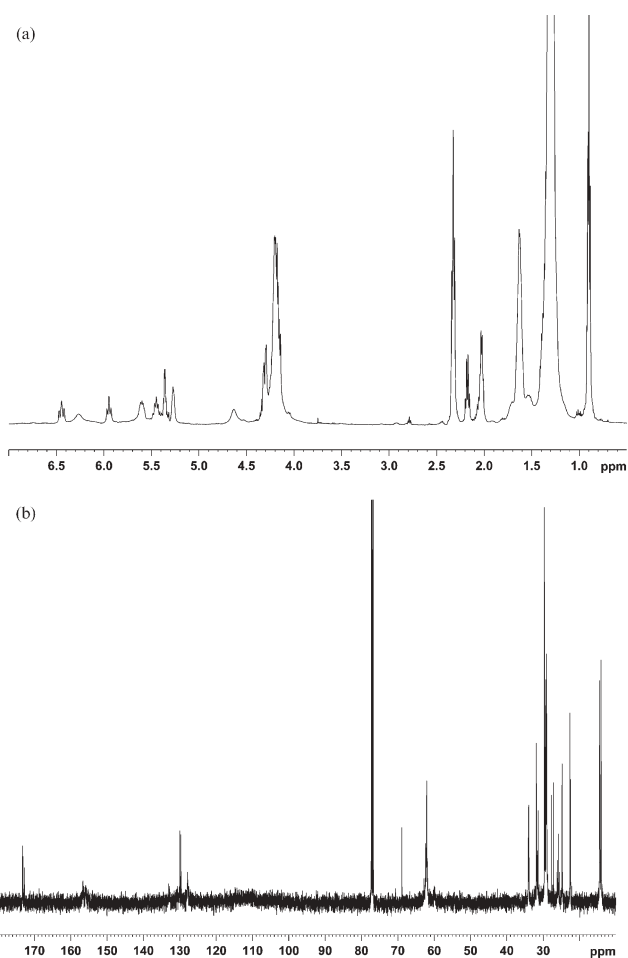


**Fig. 3** (a)  $^1\text{H}$  NMR spectrum of the microwave reaction products between soybean oil and DEAD. (b)  $^{13}\text{C}$  NMR spectrum of the microwave reaction products between soybean oil and DEAD.

**Table 3** Heat treatment of soybean oil with DEAD (4 hours reaction time, 60 °C, under  $\text{N}_2$ )

| Sample    | Molar ratio<br>SBO :<br>DEAD | NMR data                 |                   | SEC data       |                         |                              |
|-----------|------------------------------|--------------------------|-------------------|----------------|-------------------------|------------------------------|
|           |                              | Mole%<br>DEAD<br>reacted | % ene<br>reaction | SBO<br>adducts | SBO<br>dimer<br>adducts | SBO<br>trimer and<br>polymer |
| 17865-3-1 | 1 : 1.0                      | 33                       | 17                | 66             | 17                      | 17                           |
| 17865-4-1 | 1 : 1.7                      | 56                       | 31                |                |                         |                              |
| 17865-8-1 | 1 : 2.0                      | 62                       | 37                | 75             | 13                      | 12                           |
| 17865-9-1 | 1 : 2.5                      | 64                       | 37                |                |                         |                              |
| 17865-7-1 | 1 : 3.0                      | 80                       | 38                | 72             | 17                      | 11                           |

room temperature reaction in detail, and results will be reported in the future.

Following the work of Sharpless,<sup>30</sup> we also tried to react DEAD and soybean oil in water. However, we found that DEAD underwent competing reactions with water and vegetable oil to give both ene product and  $\text{DEADH}_2$ .

Although we could separate the two materials, the yield suffered. The reaction of DEAD with water to give the reduced form ( $\text{DEADH}_2$ ) was known.<sup>31</sup>

## Acknowledgements

The authors wish to thank Janet Berfield for expert technical assistance.

## References

- I. S. Rhee, *NLGI Spokesman*, 1996, **60**(5), 28.
- S. J. Randles and M. Wright, *J. Synth. Lubr.*, 1992, **9**, 145–161.
- S. Asadauskas, J. M. Perez and J. L. Duda, *Lubr. Eng.*, 1996, **52**, 877–882.
- N. S. Battersby, S. E. Pack and R. J. Watkinson, *Chemosphere*, 1998, **24**, 1998–2000.
- R. E. Gapinski, I. E. Joseph and B. D. Layzell, *SAE Tech. Pap. Ser.*, 1994, 941785, pp. 1–9.
- R. Becker and A. Knorr, *Lubr. Sci.*, 1996, **8**, 95–117.
- S. A. Ohkawa, H. Konishi, K. Hatano, K. Tanaka and M. Iwamura, *SAE Tech. Pap. Ser.*, 1995, 951038, pp. 55–63.
- I. S. Rhee, C. Valez and K. Bernewitz, *TARDEC Tech Report 13640*, US Army Tank-Automotive Command Research, Development and Engineering Center, Warren, MI, USA, 1995, 1.
- E. Kassfeldt and D. Goran, Environmentally adapted hydraulic oils, *Wear*, 1997, **207**, 41.
- A. Biswas, A. Adhvaryu, S. H. Gordon, S. Z. Erhan and J. L. Willett, *J. Agric. Food Chem.*, 2005, **53**(24), 9485.
- K. Mikami and M. Shimizu, *Chem. Rev.*, 1992, **92**, 1021.
- S. H. Nahm and H. N. Cheng, *J. Org. Chem.*, 1986, **51**, 5093.
- C. J. Pouchert and J. Behnke, *The Aldrich Library of  $^{13}\text{C}$  and  $^1\text{H}$  FT NMR Spectra*, Aldrich Chemical Co., Inc, 1993.
- J. G. Batchelor, R. J. Cushley and J. H. Prestegard, *J. Org. Chem.*, 1974, **39**, 1698.
- J. Bus, I. Sies and A. Jie, *Chem. Phys. Lipids*, 1976, **17**, 501.
- A. R. Cox, B. Vincent, S. Harley and S. E. Taylor, *Colloids Surf.*, 1999, **146**, 153.
- E. G. Paul and D. M. Grant, *J. Am. Chem. Soc.*, 1964, **86**, 2984.
- E. Pretsch, J. T. Clerc, J. Seibl and W. Simon, *Tables of Spectral Data for Structure Elucidation of Organic Compounds*, Springer, Berlin, 2nd edn, 1989.
- H. N. Cheng and M. A. Bennett, *Anal. Chim. Acta*, 1991, **242**, 43.
- A. Biswas, R. L. Shogren, J. L. Willet, S. Z. Erhan and H. N. Cheng, *Polym. Prepr. (Am. Chem. Soc., Div. Polym. Chem.)*, 2006, **47**(2), 259.
- Z. S. Petrovic, A. Zlatanovic, C. C. Lava and S. Sinadinovic-Fiser, *Eur. J. Lipid Sci. Technol.*, 2002, **104**, 293.
- M. C. Kuo and T. C. Chou, *Ind. Eng. Chem. Res.*, 1987, **26**, 277.
- H. Warth, R. Mulhaupt, B. Hoffmann and S. Lawson, *Angew. Makromol. Chem.*, 2003, **249**, 79.
- P. Tran, K. Seybold, D. Graiver and R. Narayan, *J. Am. Oil Chem. Soc.*, 2005, **82**, 189.
- F. Li, M. V. Hanson and R. C. Larock, *Polymer*, 2001, **42**, 1567.
- S. N. Khot, J. J. Lascala, E. Can, S. S. Morrye, G. I. Williams, G. R. Palmese, S. H. Kusefoglu and R. P. Wool, *J. Appl. Polym. Sci.*, 2001, **82**, 703.
- T. M. Baber, D. Graiver, C. T. Lira and R. Narayan, *Biomacromolecules*, 2005, **6**, 1334.
- U. Biermann and J. O. Metzger, *Angew. Chem., Int. Ed.*, 2000, **39**, 2206.
- H. P. Benecke, B. R. Vijayendran and J. D. Elhard, *U. S. Pat.*, 6 797 753, 2004.
- S. Narayan, J. Muldoon, M. G. Finn, V. V. Fokin, H. C. Kolb and K. B. Sharpless, *Angew. Chem., Int. Ed.*, 2005, **21**, 3157.
- J. C. Kauer, *Org. Synth.*, **CV 4**, 411.

# Ionic liquids *via* reaction of the zwitterionic 1,3-dimethylimidazolium-2-carboxylate with protic acids. Overcoming synthetic limitations and establishing new halide free protocols for the formation of ILs

Marcin Smiglak,<sup>a</sup> John D. Holbrey,<sup>†a</sup> Scott T. Griffin,<sup>a</sup> W. Matthew Reichert,<sup>a</sup> Richard P. Swatloski,<sup>a</sup> Alan R. Katritzky,<sup>\*b</sup> Hongfang Yang,<sup>b</sup> Dazhi Zhang,<sup>b</sup> Kostyantyn Kirichenko<sup>b</sup> and Robin D. Rogers<sup>\*a</sup>

Received 20th July 2006, Accepted 6th November 2006

First published as an Advance Article on the web 5th December 2006

DOI: 10.1039/b610421e

The previously reported preparation of 1,3-dimethylimidazolium salts by the reaction of 1,3-dialkylimidazolium-2-carboxylate zwitterions with protic acids has been reinvestigated in detail, leading to the identification of two competing reactions: isomerisation and decarboxylation. The ability to control both pathways allows this methodology to be used as an effective, green, waste-free approach to readily prepare a wide range of ionic liquids in high yields. Additionally, this reaction protocol opens new possibilities in the formation of other imidazolium salts, whose syntheses were previously either very expensive (due to ion exchange protocols involving metals like Ag) or difficult to achieve (due to multiple extractions and large quantities of hard to remove inorganic by-products).

## Introduction

Ionic liquids (ILs; conventionally defined as organic salts with a melting point below 100 °C<sup>1</sup>) have been extensively investigated in recent years. Their often unique physical and chemical properties, such as potential non-volatility, thermal stability, and large liquid ranges are increasing their potential applications far beyond the initial investigation of IL electrolytes.<sup>2,3</sup> New solvent applications (*e.g.*, electrochemistry,<sup>4-6</sup> separation science,<sup>7-10</sup> chemical synthesis,<sup>11-15</sup> and catalysis<sup>13,16,17</sup>), as well as new materials applications of the ILs themselves (*e.g.*, energetic materials,<sup>18-24</sup> thermal fluids, lubricants, and fuel cell electrolytes<sup>25-27</sup>) are continuously being reported.

This current, growing academic and industrial interest in diverse IL applications and technologies,<sup>1-23,28-32</sup> calls for the development of approaches for the preparation and purification of ILs which are cost/time efficient and at the same time atom efficient and limit the use of hazardous reagents. One such example, the synthesis of 1,3-dialkylimidazolium alkyl sulfates from 1-alkylimidazole with dimethyl or diethyl sulfate, excluding contamination by halides has been described by Holbrey *et al.*<sup>33</sup> and Wasserscheid *et al.*<sup>34</sup>

Unfortunately, most of the current synthetic protocols for the preparation of ILs still struggle with multi-step synthesis, complex purification and, in many cases, formation of undesirable halide-containing by-products. Thus, new synthetic strategies for obtaining imidazolium-based organic salts (IL precursors or ILs themselves) allowing flexible design

capabilities, are still necessary in order to introduce ILs into routine usage.

Since the mid 1980s, there has been considerable interest in the use of dimethyl carbonate (DMC) as a clean methylating agent which could be used as safe replacement of current reagents such as methylhalides, dimethyl sulfate, and phosgene.<sup>35</sup> Additionally, a new and improved synthesis of DMC, developed by Enichem,<sup>36,37</sup> and UBE<sup>38</sup> (catalytic oxidative carbonylation of methanol with oxygen instead of synthesis from phosgene), very low toxicity of this reagent,<sup>39,40</sup> the electrophilic character of DMC,<sup>41</sup> and environmentally benign by-products of the methylation reaction (*i.e.*, MeOH and CO<sub>2</sub>)<sup>41,42</sup> make this an attractive alternative methylating agents in organic synthesis.

As recently reported by several research groups,<sup>43-46</sup> efforts have been made to investigate the properties of DMC as an alkylating agent for the preparation of imidazolium-based organic salts. It was suggested that, when using DMC in reaction with *N*-alkylimidazoles, new halide-free ionic liquids can be formed. According to those reports, alkylation of 1-methylimidazole with DMC, depending on the reaction conditions, resulted in the formation of either 1,3-dimethylimidazolium-2-carboxylate ([1,3-diMIM-2-COO]) (1) or 1,3-dimethylimidazolium-4-carboxylate ([1,3-diMIM-4-COO]) (2). Aresta *et al.*<sup>44</sup> reported simultaneous formation of both products with some selectivity for [1,3-diMIM-2-COO] (1). They also noted that upon heating to 140 °C, complete isomerization of [1,3-diMIM-2-COO] (1) into [1,3-diMIM-4-COO] (2) occurs. These results are consistent with BASF's<sup>47</sup> reported formation of [1,3-diMIM-4-COO] (2) in the reaction of DMC with 1-methylimidazole at 140 °C.

Aresta *et al.*<sup>44</sup> further reported that the reaction of 1,3-dimethylimidazolium-2-carboxylate (1) with tetrafluoroboric acid leads to the formation of two isomeric products: 2-carboxy-1,3-dimethylimidazolium tetrafluoroborate

<sup>a</sup>Center for Green Manufacturing and Department of Chemistry, The University of Alabama, Tuscaloosa, AL, 35487, USA.  
E-mail: rdrogers@bama.ua.edu

<sup>b</sup>Center for Heterocyclic Compounds, Department of Chemistry, University of Florida, Gainesville, FL, 32611, USA.  
E-mail: katritzky@chem.ufl.edu

<sup>†</sup> Present address: The QUILL Research Centre, Queen's University Belfast, Northern Ireland, UK BT9 5AG.

[(2-(COOH)-1,3-diMIM][BF<sub>4</sub>]) (**4b**) and 4-carboxy-1,3-dimethylimidazolium tetrafluoroborate ([4-(COOH)-1,3-diMIM][BF<sub>4</sub>]) (**5b**), depending on the concentration of acid used. Reaction of carboxylate zwitterion salt [1,3-diMIM-2-COO] (**1**) with equimolar acid gave [2-(COOH)-1,3-diMIM][BF<sub>4</sub>] (**4b**), while with excess imidazolium carboxylate ([1,3-diMIM-2-COO]/[HBF<sub>4</sub>] = 1.25 : 1.0) or upon slow addition of the acid to the imidazolium salt, decarboxylation occurred resulting in the formation of 1,3-dimethylimidazolium tetrafluoroborate ([1,3-diMIM][BF<sub>4</sub>]) (**3b**). The treatment of [(2-(COOH)-1,3-diMIM][BF<sub>4</sub>]) (**4b**) with triethylamine also led to decarboxylation to give [1,3-diMIM][BF<sub>4</sub>] (**3b**). In contrast, [4-(COOH)-1,3-diMIM][BF<sub>4</sub>] (**5b**) appeared to be stable under these conditions. The multiple reaction pathways and outcomes, could prevent utilization of these techniques in routine preparation of 1,3-dialkylimidazolium ILs, unless they can be fully understood and controlled.

Louie *et al.*<sup>48,49</sup> have reported the development of protocols for efficiently coupling various diynes with CO<sub>2</sub>, under mild conditions to produce pyrones, *via* utilization of Ni/imidazolylidene complexes. Additionally, Tommasi and Sorrentino<sup>50</sup> recently described aspects of the reactivity of 1,3-dialkylimidazolium-2-carboxylates toward organic substrates (methanol, acetophenone, and benzaldehyde) in the presence of Na<sup>+</sup> and K<sup>+</sup> cations. The authors described the reaction of CO<sub>2</sub> transfer from the 1,3-dialkylimidazolium-2-carboxylates and the formation of new organic carboxylate products.

We had previously proposed<sup>43</sup> that the simple reaction of the 1,3-dialkylimidazolium-2-carboxylate zwitterion with protic acids should yield a variety of halide-free ILs. Here we report the results of investigation of this approach, especially its variable reactivity with acids (as a route to ion-exchange and fast formation of ILs), as well as, the thermal and chemical stability of the products. Our investigation focused on (i) overcoming limitations and difficulties associated with this synthesis, and (ii) the use of this reaction as a protocol to prepare new ILs, or their precursors, *via* both halide and by-product free routes, by utilization of previously mentioned isomeric products: kinetic [2-(COOH)-1,3-diMIM] (**4**) and thermodynamic [4-(COOH)-1,3-diMIM] (**5**) (Table 1).

## Results and discussion

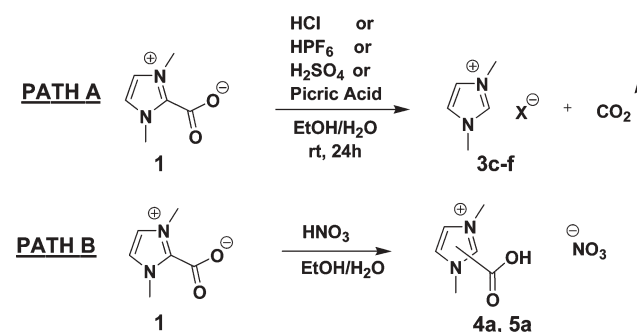
As the starting point for this investigation we repeated the reaction of dimethylcarbonate (DMC) with 1-methylimidazole,<sup>43</sup> and obtained [1,3-diMIM-2-COO] (**1**) in 85% yield as crystalline material. The product was characterized by <sup>1</sup>H and <sup>13</sup>C NMR techniques, and no [1,3-diMIM-4-COO] (**2**) was detected.

A 0.01 mol stirred solution of [1,3-diMIM-2-COO] (**1**) in 50% aqueous ethanol (v/v, 20 mL) was then treated with various acids (HPF<sub>6</sub>, H<sub>2</sub>SO<sub>4</sub>, HCl, HNO<sub>3</sub>, picric acid) *via* dropwise addition of an equimolar amount of the appropriate acid (10 mL of 1 M aqueous solution; ethanolic solution in the case of picric acid), at room temperature. In all cases except one (reaction with HNO<sub>3</sub>) the reaction proceeded as expected (Scheme 1, path A); the zwitterion **1** underwent decarboxylation, leading to the formation of the [1,3-diMIM] salt (**3c-f**) and evolution of gaseous CO<sub>2</sub>. All acids used are considered strong acids with pK<sub>a</sub> < 0, with the exception of picric acid

**Table 1** Investigated components and their abbreviations<sup>a</sup>

| Component number | Component name                        | Component structure | Used component abbreviation |
|------------------|---------------------------------------|---------------------|-----------------------------|
| 1                | 1,3-dimethylimidazolium-2-carboxylate |                     | [1,3-diMIM-2-COO]           |
| 2                | 1,3-dimethylimidazolium-4-carboxylate |                     | [1,3-diMIM-4-COO]           |
| 3                | 1,3-dimethylimidazolium               |                     | [1,3-diMIM]                 |
| 4                | 2-carboxy-1,3-dimethylimidazolium     |                     | [2-(COOH)-1,3-diMIM]        |
| 5                | 4-carboxy-1,3-dimethylimidazolium     |                     | [4-(COOH)-1,3-diMIM]        |

<sup>a</sup> The counter ions used for pairing with the cations include: **a**, nitrate [NO<sub>3</sub>]; **b**, tetrafluoroborate [BF<sub>4</sub>];<sup>44</sup> **c**, hexafluorophosphate [PF<sub>6</sub>]; **d**, chloride [Cl]; **e**, hydrogen sulfate [HSO<sub>4</sub>]; **f**, picrate [Pic].



**Scheme 1** Reactions of [1,3-diMIM-2-COO] (**1**) with different acids. Reaction with nitric acid (depending upon thermal conditions) resulted in the exclusive formation of one of the isomeric [2-(COOH)-1,3-diMIM][NO<sub>3</sub>] (**4a**) or [4-(COOH)-1,3-diMIM][NO<sub>3</sub>] (**5a**).

with pK<sub>a</sub> = 0.3. All salts were characterized by NMR, TGA, and DSC techniques, and the results were compared with the available literature data for known salts (Table 2).

**Table 2** Thermal behavior of 1,3-dimethylimidazolium salts obtained<sup>a</sup>

| Sample                | Compound                       | Mp/°C                         | T <sub>5%dec</sub> /°C |
|-----------------------|--------------------------------|-------------------------------|------------------------|
| <b>3c</b>             | [1,3-diMIM][PF <sub>6</sub> ]  | 67–68 <sup>b</sup>            | 298                    |
| <b>3d</b>             | [1,3-diMIM][Cl]                | 147 (lit ≈ 127) <sup>51</sup> | 202                    |
| <b>3e</b>             | [1,3-diMIM][HSO <sub>4</sub> ] | 98                            | 264                    |
| <b>3f</b>             | [1,3-diMIM][Pic]               | 144 (lit ≈ 151) <sup>52</sup> | 210                    |
| <b>3a<sup>c</sup></b> | [1,3-diMIM][NO <sub>3</sub> ]  | 58                            | 253                    |

<sup>a</sup> Melting points (mp) (°C) were measured from transition onset temperature determined by DSC from the second heating cycle at 5 °C min<sup>-1</sup>, after initially melting and then cooling samples to –100 °C. Decomposition temperatures (T<sub>5%dec</sub>) were determined by TGA from onset to 5 wt% mass loss, heating at 5 °C min<sup>-1</sup> under air. <sup>b</sup> Melting point of **3c** was checked visually using hot stage apparatus due to reported reactivity and catalyzed decomposition of the PF<sub>6</sub> anion-based ionic liquids while in contact with aluminium.<sup>53</sup>

<sup>c</sup> Compound was obtained later in the study as the result of the developed synthetic protocol presented below in the article.

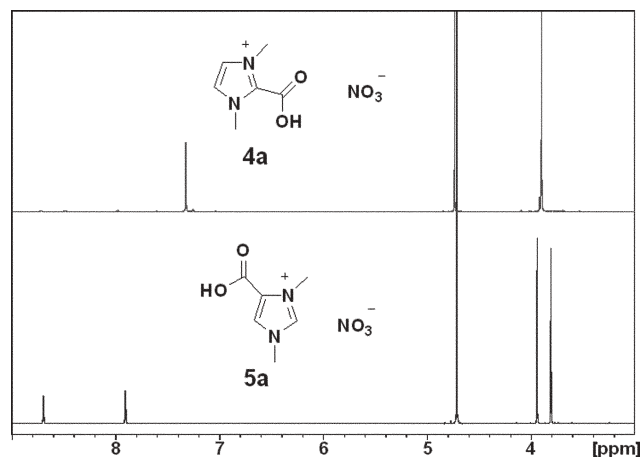


**Fig. 1**  $^1\text{H}$  NMR (360 MHz,  $\text{DMSO-}d_6$ ) evidence for the presence of two distinguishable isomers of carboxy-1,3-dimethylimidazolium nitrates: [2-(COOH)-1,3-diMIM][ $\text{NO}_3^-$ ] (**4a**) and [4-(COOH)-1,3-diMIM][ $\text{NO}_3^-$ ] (**5a**).

Unexpected behavior (Scheme 1, path B) was observed in the reaction with  $\text{HNO}_3$  leading to the formation of different

products, similar to results by Aresta *et al.*<sup>44</sup> Depending on the reaction conditions, the isomeric salts, either [2-(COOH)-1,3-diMIM][ $\text{NO}_3^-$ ] (**4a**) or [4-(COOH)-1,3-diMIM][ $\text{NO}_3^-$ ] (**5a**), were formed with no detectable decarboxylation in contrast to the examples which followed path A. Neither variation of the reaction conditions (concentrations of acid), nor order of addition of the substrates (acid to imidazolium zwitterion or imidazolium zwitterion to acid) resulted in decarboxylation. The structures of both isomers were confirmed by  $^1\text{H}$  (Fig. 1),  $^{13}\text{C}$ , and NOESY NMR, and unambiguously by both single crystal (Fig. 2) and powder X-ray diffraction (Fig. 3).

Single crystals of both isomers were prepared by dissolution of the product in 50% aqueous ethanol (v/v) followed by slow evaporation of the solvents. The crystal structure of [2-(COOH)-1,3-diMIM][ $\text{NO}_3^-$ ] $\cdot\text{H}_2\text{O}$  (**4a** $\cdot\text{H}_2\text{O}$ ) (Fig. 2, top) contains water of crystallization which participates in strong hydrogen bonds with the carboxylic acid group of the cation ( $\text{O2-H2A}\cdots\text{O1W} = 1.48(6) \text{ \AA}$ ,  $170(4)^\circ$ ) and with the anion ( $\text{O1W-H10}\cdots\text{O1}$  at  $1.86(5) \text{ \AA}$ ,  $168(5)^\circ$ , with O1 at  $2-x, 1-y, -z$ ). The structure of [4-(COOH)-1,3-diMIM][ $\text{NO}_3^-$ ] (**5a**) (Fig. 2, bottom) shows the expected conformation for the cation. The closest contact in the structure is between the

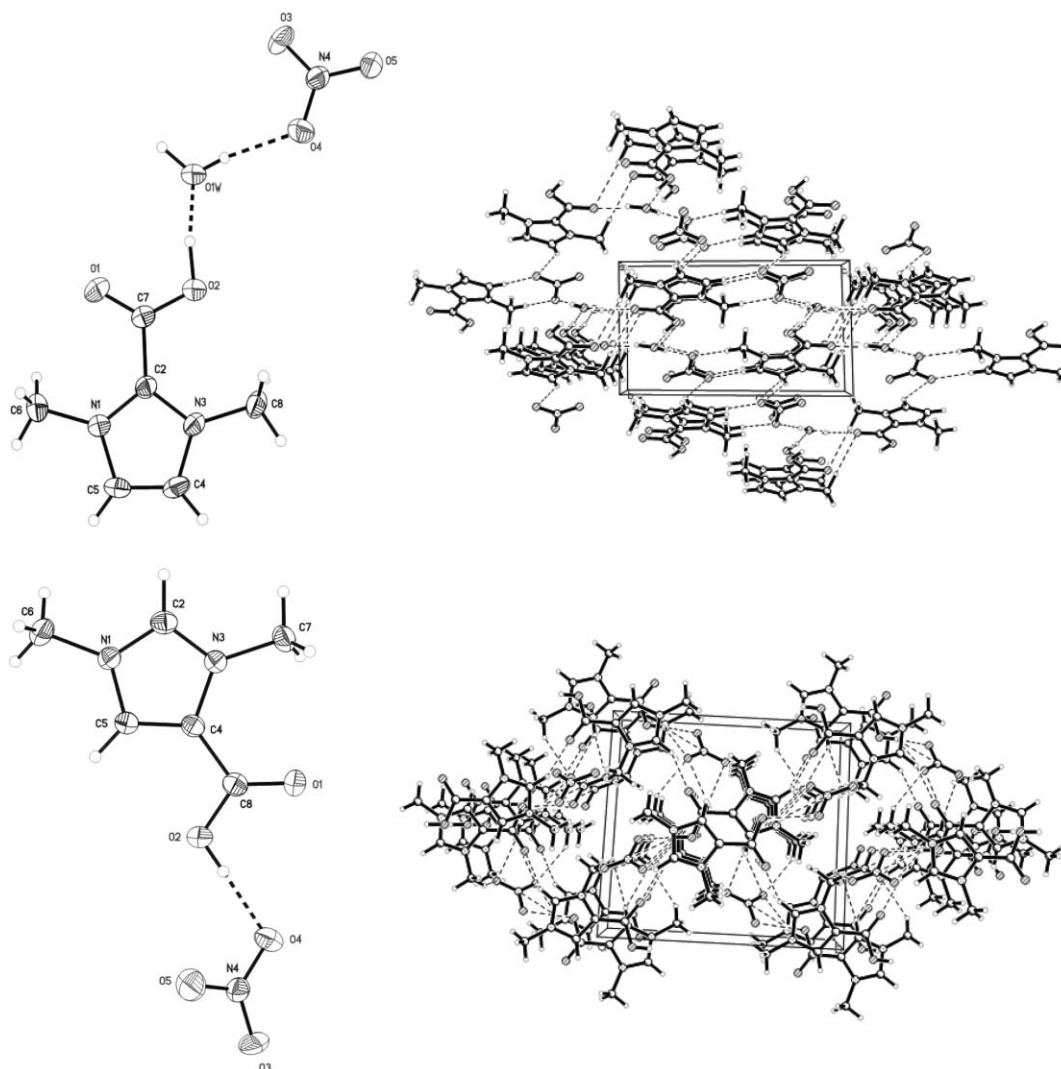


**Fig. 2** ORTEP and packing diagrams of [2-(COOH)-1,3-diMIM][ $\text{NO}_3^-$ ] $\cdot\text{H}_2\text{O}$  (**4a** $\cdot\text{H}_2\text{O}$ ) (top) and [4-(COOH)-1,3-diMIM][ $\text{NO}_3^-$ ] (**5a**) (bottom).

carboxyl group and the anion (O2–H2O···O4 1.79(4) Å, 167(4)°).

To ensure that the single crystal data indeed represented the overall bulk structure, powder X-ray diffraction spectra were obtained. This evidence is supportive of the assumption that the two isomeric carboxy-1,3-dimethylimidazolium nitrates (**4a** and **5a**) can be selectively synthesized. First, the theoretical powder diffraction spectra were generated using the single crystal data for each of the samples {Fig. 3(B) for the [2-(COOH)-1,3-diMIM][NO<sub>3</sub>]·H<sub>2</sub>O (**4a**·H<sub>2</sub>O) isomer, and (D) for the [4-(COOH)-1,3-diMIM][NO<sub>3</sub>] (**5a**) isomer} and these were compared with the experimental spectra {Fig. 3(A) for [2-(COOH)-1,3-diMIM][NO<sub>3</sub>]·H<sub>2</sub>O (**4a**·H<sub>2</sub>O), and (C) for [4-(COOH)-1,3-diMIM][NO<sub>3</sub>] (**5a**)}. The simulated (Fig. 3(D)) and experimental patterns (Fig. 3(C)) for

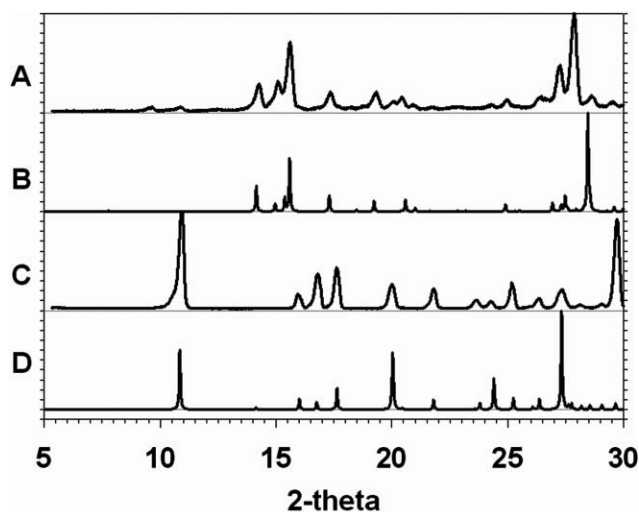


**Fig. 3** Powder X-ray diffraction patterns for isomers of carboxy-1,3-dimethylimidazolium nitrates (**4a**·H<sub>2</sub>O and **5a**) compared with the simulated patterns generated from the single crystal data. (A) Experimental [2-(COOH)-1,3-diMIM][NO<sub>3</sub>]·H<sub>2</sub>O (**4a**·H<sub>2</sub>O); (B) simulated [2-(COOH)-1,3-diMIM][NO<sub>3</sub>]·H<sub>2</sub>O (**4a**·H<sub>2</sub>O); (C) experimental [4-(COOH)-1,3-diMIM][NO<sub>3</sub>] (**5a**); (D) simulated [4-(COOH)-1,3-diMIM][NO<sub>3</sub>] (**5a**).

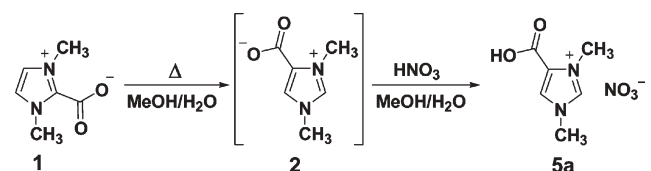
[4-(COOH)-1,3-diMIM][NO<sub>3</sub>] (**5a**) match well, indicating a pure phase. However, a comparison of the simulated (Fig. 3(B)) and experimental spectra (Fig. 3(A)) for [2-(COOH)-1,3-diMIM][NO<sub>3</sub>]·H<sub>2</sub>O (**4a**·H<sub>2</sub>O), while matching reasonably well, reveals the presence of a small amount of [4-(COOH)-1,3-diMIM][NO<sub>3</sub>] (**5a**) in the bulk phase.

### Selective isomer formation

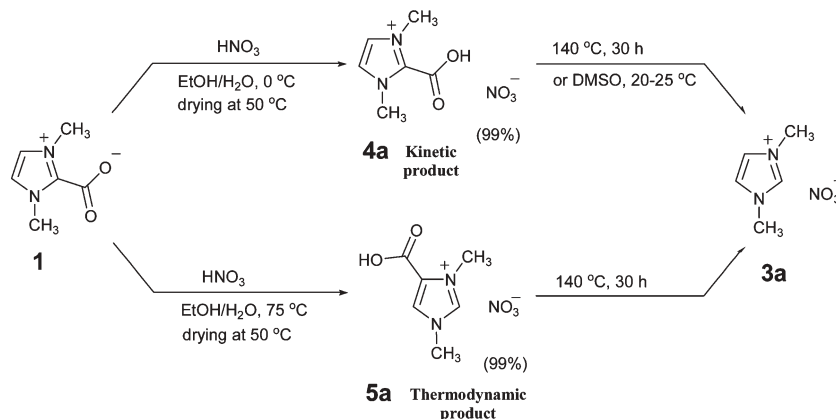
In order to more fully characterize the system, pure [2-(COOH)-1,3-diMIM][NO<sub>3</sub>] (**4a**) and [4-(COOH)-1,3-diMIM][NO<sub>3</sub>] (**5a**) salts were prepared by two different procedures allowing the selective formation of each isomer in high yields and isomeric purity at the appropriate reaction temperature (Scheme 2).

A series of reactions at a constant temperature of ~5 °C including: (i) using various concentrations of nitric acid (from 0.001 M to 0.1 M), (ii) using different ratios of [1,3-diMIM-2-COO] (**1**) and acid (1 : 0.8, 1 : 1, 1 : 1.5, 1 : 3), and (iii) changing the order of addition of substrates, gave exclusively [2-(COOH)-1,3-diMIM][NO<sub>3</sub>] (**4a**). On the other hand, reaction at elevated temperature (>75 °C) produced exclusively [4-(COOH)-1,3-diMIM][NO<sub>3</sub>] (**5a**) (Scheme 2).

From analysis of these results and literature reports,<sup>44</sup> we suggest that the thermal rearrangement of the [1,3-diMIM-2-COO] (**1**) to [1,3-diMIM-4-COO] (**2**) (thermodynamic product) occurs prior to contact with the acid, and this process is immediately followed by the proton transfer from HNO<sub>3</sub> to the zwitterions (**2**) resulting in the formation of [4-(COOH)-1,3-diMIM][NO<sub>3</sub>] (**5a**) (Scheme 3).



**Scheme 3** Thermal rearrangement of [1,3-diMIM-2-COO] (**1**) to [1,3-diMIM-4-COO] (**2**), followed by the addition of acid and proton transfer, resulting in the formation of [4-(COOH)-1,3-diMIM][NO<sub>3</sub>] (**5a**).



**Scheme 2** Formation of [1,3-diMIM][NO<sub>3</sub>] (**3a**) via two distinctive pathways. Top: reaction of [1,3-diMIM-2-COO] (**1**) with HNO<sub>3</sub> at low temperature (kinetic product) and further thermal or DMSO-catalyzed decarboxylation via the [2-(COOH)-1,3-diMIM][NO<sub>3</sub>] intermediate (**4a**). Bottom: reaction of [1,3-diMIM-2-COO] (**1**) with HNO<sub>3</sub> at higher temperature (thermodynamic product) and further thermal decarboxylation of [4-(COOH)-1,3-diMIM][NO<sub>3</sub>] (**5a**).

## Thermal decarboxylation

Having ascertained that control over the formation of the [2-(COOH)-1,3-diMIM][NO<sub>3</sub>] (**4a**) and [4-(COOH)-1,3-diMIM][NO<sub>3</sub>] (**5a**) isomers was possible, we turned our attention to general routes from either isomer to the desired ILs. The thermal stability of **4a** and **5a** was measured on samples taken before re-crystallization and were compared to **1** and **3a** (Table 3, Fig. 4). Both of the isomeric salts (**4a** and **5a**) decompose following a similar two-step decomposition pathway. The first decomposition step (~170–180 °C) is probably the result of the decarboxylation process (and also loss of bound water in the case of [2-(COOH)-1,3-diMIM][NO<sub>3</sub>]·H<sub>2</sub>O (**4a**·H<sub>2</sub>O)), leading to the formation of [1,3-diMIM][NO<sub>3</sub>] (**3a**); which then decomposes on further heating in a second step around 300 °C.

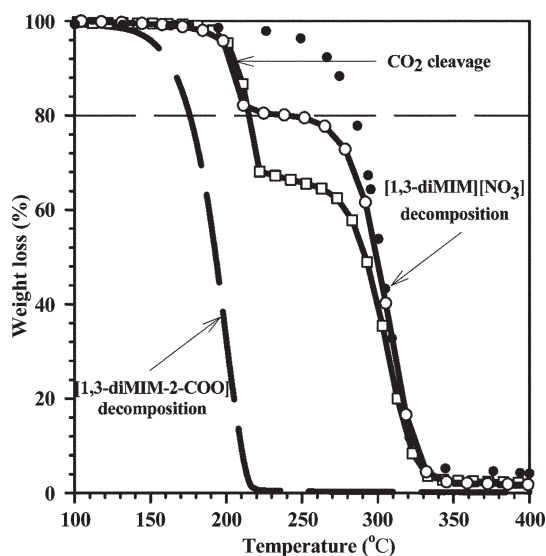


**Fig. 4** Thermal stabilities of analyzed salts determined by TGA with a heating rate of 5 °C min<sup>-1</sup> in the range 50 °C to 400 °C: (---) [1,3-diMIM-2-COO] (**1**); (□) [2-(COOH)-1,3-diMIM][NO<sub>3</sub>]·H<sub>2</sub>O (**4a**·H<sub>2</sub>O), (○) [4-(COOH)-1,3-diMIM][NO<sub>3</sub>] (**5a**); (●) [1,3-diMIM][NO<sub>3</sub>] (**3a**).

**Table 3** Thermal stabilities of analyzed salts<sup>a</sup>

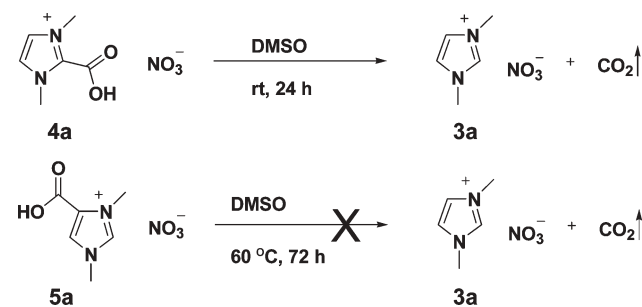
| Sample    | Compound                               | <i>T</i> <sub>5%dec</sub> /°C |                        |
|-----------|--|-------------------------------|------------------------|
|           |  | 1st decomposition step        | 2nd decomposition step |
| <b>1</b>  | [1,3-diMIM-2-COO]                      | 147                           | —                      |
| <b>4a</b> | [2-(COOH)-1,3-diMIM][NO <sub>3</sub> ] | 194                           | 265                    |
| <b>5a</b> | [4-(COOH)-1,3-diMIM][NO <sub>3</sub> ] | 197                           | 275                    |
| <b>3a</b> | [1,3-diMIM][NO <sub>3</sub> ]          | 253                           | —                      |

<sup>a</sup> Decomposition temperatures (*T*<sub>5%dec</sub>) were determined by TGA from onset to 5 wt% mass loss, heating at 5 °C min<sup>-1</sup> under air in the range 50 °C to 400 °C which provides a more realistic representation of thermal stability at elevated temperatures.

This hypothesis is supported by results from heating samples initially to 150 °C, and then maintaining isothermal conditions for 20 h. The <sup>1</sup>H NMR analysis of the product extracted after heating clearly indicated the presence of pure

[1,3-diMIM][NO<sub>3</sub>] (**3a**) in both cases, as a result of thermal decarboxylation at ~140–160 °C. With time, a proton signal corresponding to hydrogens on the respective C2 or C4 carbon of the aromatic ring of **4a** and **5a** was observed to appear and grow, indicating thermal conversion of the 2- or 4-carboxy-1,3-dimethylimidazolium cation (**4** and **5**) to the 1,3-dimethylimidazolium cation (**3**). A strong, single signal in the mass spectrum at 97.07 *m/z* also confirms formation of the [1,3-diMIM][NO<sub>3</sub>] (**3a**) salt.

NMR and mass spectrometry analyses of the residues, recovered from the TGA experiment, after thermal decomposition of 60% of the starting mass of the analyzed sample, also showed the presence of pure [1,3-diMIM][NO<sub>3</sub>] (**3a**). These results suggest the likely initial decarboxylation of products, followed by a retro-S<sub>N</sub>2 reaction (opposite to the formation of 1,3-dialkylimidazolium salts); producing volatile decomposition products, which are evacuated from the sample and therefore not detectable in the residue.



**Scheme 4** Chemically induced decarboxylation of [2-(COOH)-1,3-diMIM][NO<sub>3</sub>] (**4a**).

## DMSO catalyzed decarboxylation

Upon treatment of [2-(COOH)-1,3-diMIM][NO<sub>3</sub>] (**4a**) (but not [4-(COOH)-1,3-diMIM][NO<sub>3</sub>] (**5a**)) with DMSO at room temperature, solvent promoted decarboxylation (similar to, or based on, the Krapcho reaction)<sup>54–59</sup> was observed to give pure [1,3-diMIM][NO<sub>3</sub>] (**3a**) (Scheme 4) with 90% conversion in a matter of hours. The attempts to perform the same reaction in DMF or H<sub>2</sub>O as solvent did not result in formation of desired product at any significant level.

Kinetic studies of the decarboxylation of [2-(COOH)-1,3-diMIM][NO<sub>3</sub>] (**4a**) were conducted by NMR with DMSO-*d*<sub>6</sub> (Fig. 5). The <sup>1</sup>H NMR spectra (acquired after 3, 5, 10, 15, 25, 45, and 60 min and again after 72 h) show that 60% conversion of **4a** to **3a** was reached within 1 h, and complete conversion after 72 h with no evidence for any other impurity or by-product. The <sup>1</sup>H NMR spectra indicated the appearance and gradual increase in relative intensity of the new distinctive signals at 9.04 ppm and 3.86 ppm corresponding to the C-2 proton in the imidazolium ring and to the *N*-CH<sub>3</sub> protons of [1,3-diMIM][NO<sub>3</sub>] (**3a**), respectively, while the intensity of the *N*-CH<sub>3</sub> signal at 4.05 ppm of [2-(COOH)-1,3-diMIM][NO<sub>3</sub>] (**4a**) proportionally decreased (Fig. 5).

Interestingly, the treatment of the [4-(COOH)-1,3-diMIM][NO<sub>3</sub>] (**5a**) isomer does not result in decarboxylation even in DMSO solution for 48 h at 60 °C. From this, we

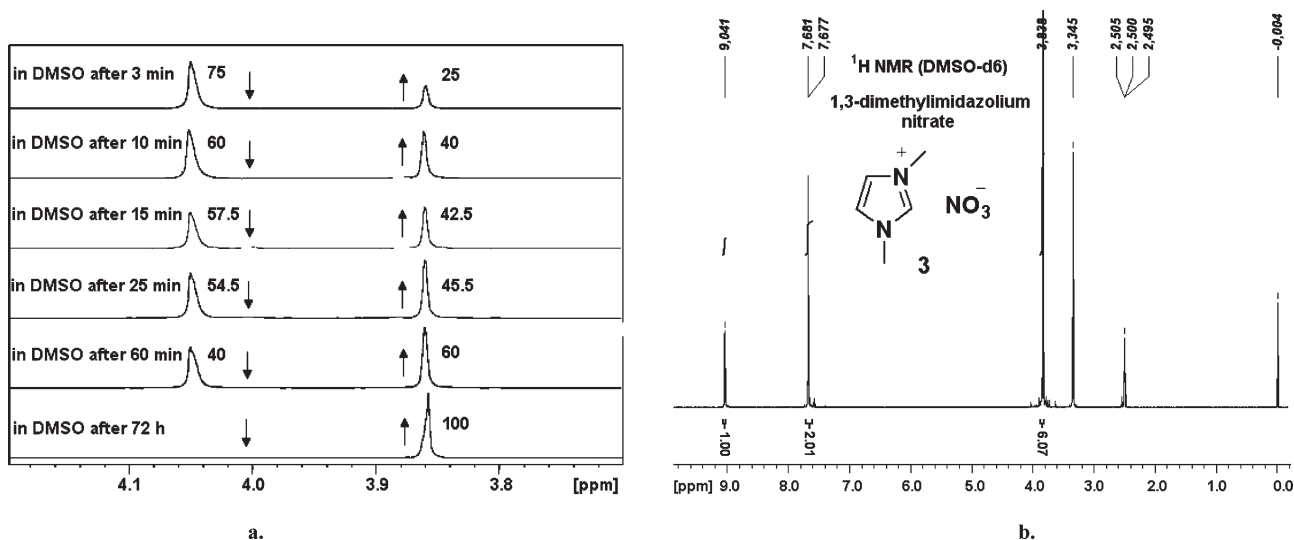


**Fig. 5** (a) Solvent (DMSO) induced decarboxylation of [2-(COOH)-1,3-diMIM][NO<sub>3</sub>] (**4a**) observed by <sup>1</sup>H NMR (360 MHz, DMSO-*d*<sub>6</sub>). (b) The NMR indicates the formation of pure [1,3-diMIM][NO<sub>3</sub>] (**3a**) obtained after performing the decarboxylation reaction of [2-(COOH)-1,3-diMIM][NO<sub>3</sub>] (**4a**) in DMSO at room temperature for 72 h.

confirm the previous conclusion that the 4-carboxy isomer (**5a**) is the more stable (thermodynamic) product and does not undergo decarboxylation for this reason.

It is worth considering the differences between the two solid state structures of the isomeric salts, **4a** and **5a**, as observed in the crystal structures described earlier. The water molecule found in the structure of **4a**, but not in **5a**, is strongly hydrogen-bonded to the carboxylic acid group of the cation. While the presence, or absence, of this hydrate in the crystal form may be due to the crystallization procedure, it is possible that its presence in **4a**·H<sub>2</sub>O reflects a slightly greater acidity of the carboxylic acid group in **4a** compared to **5a**, and that this might account for the differences of reactivity, with the more acidic **4a** being both thermodynamically and chemically more reactive. However, *ab initio* calculations (GAMESS, RHF 6-311 + G(d,p) basis set)<sup>60</sup> of the electrostatic charge distribution about isolated cations do not reveal any differences between the two cations which could support this hypothesis, and the explanation for the differences in reactivity remains unresolved at present.

In a final study to support either the decarboxylation or rearrangement reaction of [2-(COOH)-1,3-diMIM][NO<sub>3</sub>] (**4a**), this isomer was held in aqueous solution for 72 h at room temperature, followed by heating to 60 °C for 12 h. NMR indicated that neither decarboxylation, nor rearrangement to the 4-carboxy isomer (**5a**) takes place under these conditions. Any increase in the concentration of [1,3-diMIM][NO<sub>3</sub>] (**3a**) was below 2%. It appears that the [2-(COOH)-1,3-diMIM][NO<sub>3</sub>] (**4a**) isomer is stable in aqueous media, whereas the decarboxylation reaction occurs quite readily in the polar, aprotic solvent, DMSO.

## Conclusions

Previously reported difficulties with the utilization of the synthesis of halide-free ILs, *via* the reaction of alkylimidazole

with dimethylcarbonate, and further reaction with protic acids were investigated here in detail. A new, improved synthetic protocol for the formation of 1,3-dialkylimidazolium and protic acid (supported by either thermally or chemically induced decarboxylation of carboxy-1,3-dialkylimidazolium intermediate) was designed to overcome these limitations; thus allowing for the wider usage of this technique as a viable route to halide-free, one-pot syntheses of ILs or their precursors. As the results demonstrate, the reaction of [1,3-diMIM-2-COO] (**1**) with protic acid leads to the formation of protonated isomeric 2- and 4-carboxy-1,3-dimethylimidazolium salts (**4a** and **5a**), which previously was a limitation of this protocol for the preparation of pure ILs. Decarboxylation to imidazolium salts can be achieved for *both* isomers *via* thermal decarboxylation heating to 150 °C, and additionally, at room temperature, chemically-induced, DMSO catalyzed decarboxylation is also possible, and occurs only for the [2-(COOH)-1,3-diMIM][NO<sub>3</sub>] (**4a**) isomer. These results support the earlier hypothesis that the [4-(COOH)-1,3-diMIM][NO<sub>3</sub>] salt (**5a**) is the more thermodynamically stable product of the reaction of the zwitterionic substrate with nitric acid.

## Experimental

All reagents were purchased from Sigma-Aldrich (St. Louis, MO) and were used as obtained.

### 1,3-Dimethylimidazolium-2-carboxylate (**1**)

This zwitterion was obtained according to the literature procedure.<sup>43</sup> Colorless crystals of the product, with melting at the decomposition temperature, were obtained in 85% yield and >99% purity. The NMR data were consistent with literature data.<sup>43</sup>

**General procedure for the preparation of 1,3-dimethylimidazolium hexafluorophosphate [PF<sub>6</sub>]<sup>-</sup> (3c), chloride [Cl]<sup>-</sup> (3d), hydrogen sulfate [HSO<sub>4</sub>]<sup>-</sup> (3e), and picrate [Pic]<sup>-</sup> (3f) salts**

All reactions were performed using the same procedure: 0.01 mol of the appropriate acid (HPF<sub>6</sub>, HCl, H<sub>2</sub>SO<sub>4</sub>, picric acid) was dissolved in 10 mL of H<sub>2</sub>O (ethanol in the case of picric acid) and added dropwise, at room temperature, to a stirred solution of 0.01 mol of [1,3-diMIM-2-COO] (1) in 50% aqueous ethanol (v/v, 20 mL). The mixture was stirred for an additional 24 h in closed flask (to avoid inorganic acid evaporation) and the solvent was evaporated on a rotary evaporator under vacuum. All samples were then dried under high vacuum at room temperature. 1,3-Dimethylimidazolium salts (3c–f) were recovered and checked for the presence of starting material using <sup>1</sup>H and <sup>13</sup>C NMR.

**1,3-Dimethylimidazolium hexafluorophosphate (3c)**

White solid, water insoluble, 98% yield, melting point (hot stage apparatus) 67–68 °C, onset for the 5% decomposition  $T_{5\%dec} = 298$  °C;  $\delta_H$  (360 MHz, DMSO-*d*<sub>6</sub>): 3.84 (s, 6H, N-CH<sub>3</sub>), 7.67 (d, 2H, C(4/5)H), 9.01 (s, 1H, C(2)H);  $\delta_C$  (90 MHz, DMSO-*d*<sub>6</sub>): 35.55, 123.34, 136.92.

**1,3-Dimethylimidazolium chloride (3d)**

White solid, very hygroscopic, 99% yield, melting point (DSC) 147 °C, onset for the 5% decomposition  $T_{5\%dec} = 202$  °C;  $\delta_H$  (360 MHz, D<sub>2</sub>O): 3.88 (s, 6H, N-CH<sub>3</sub>), 7.40 (d, 2H, C(4/5)H), 8.64 (s, 1H, C(2)H);  $\delta_H$  (360 MHz, DMSO-*d*<sub>6</sub>): 3.86 (s, 6H, N-CH<sub>3</sub>), 7.75 (d, 2H, C(4/5)H), 9.33 (s, 1H, C(2)H);  $\delta_C$  (90 MHz, DMSO-*d*<sub>6</sub>): 35.63, 123.37, 137.12.

**1,3-Dimethylimidazolium hydrogen sulfate (3e)**

White solid, hygroscopic, 99% yield, melting point (DSC) 98 °C, onset for the 5% decomposition  $T_{5\%dec} = 264$  °C;  $\delta_H$  (360 MHz, D<sub>2</sub>O): 3.84 (s, 6H, N-CH<sub>3</sub>), 7.67 (s, 2H, C(4/5)H), 8.60 (s, 1H, C(2)H);  $\delta_H$  (360 MHz, DMSO-*d*<sub>6</sub>): 3.82 (s, 6H, N-CH<sub>3</sub>), 7.64 (d, 2H, C(4/5)H), 9.00 (s, 1H, C(2)H);  $\delta_C$  (90 MHz, DMSO-*d*<sub>6</sub>): 35.79, 123.56, 136.26.

**1,3-Dimethylimidazolium picrate (3f)**

Yellow solid, 95% yield, melting point (DSC) 144 °C, onset for the 5% decomposition  $T_{5\%dec} = 210$  °C;  $\delta_H$  (360 MHz, D<sub>2</sub>O): 3.87 (s, 6H, N-CH<sub>3</sub>), 7.39 (s, 2H, C(4/5)H), 8.62 (s, 1H, C(2)H), 8.95 (s, 2H, picrate);  $\delta_H$  (360 MHz, DMSO-*d*<sub>6</sub>): 3.84 (s, 6H, N-CH<sub>3</sub>), 7.67 (d, 2H, C(4/5)H), 8.59 (s, 2H, picrate), 9.03 (s, 1H, C(2)H);  $\delta_C$  (90 MHz, DMSO-*d*<sub>6</sub>): 35.57, 123.35, 124.05, 125.11, 136.95, 141.75, 160.71.

**2-Carboxy-1,3-dimethylimidazolium nitrate (4a)**

To a solution of [1,3-diMIM-2-COO] (1) (0.01 mol) dissolved in 20 mL of a 50% aqueous ethanol (v/v), 5.15 mL of 2 M HNO<sub>3</sub> (0.0103 mol) was added dropwise. The reaction mixture was stirred at ~10 °C for 24 h. The product crystallized during slow solvent evaporation at room temperature and under atmospheric pressure, as colorless crystals. The product melts

at the first decomposition temperature (~200 °C). Onset for the 5% decomposition  $T_{5\%dec} = 194$  °C;  $\delta_H$  (360 MHz, D<sub>2</sub>O): 3.99 (s, 6H, N-CH<sub>3</sub>), 7.39 (s, 2H, C(4/5)).

Note: changes in the order of added substrates, as well as, different concentrations of acid did not influence the final product. The evaporation of the solvent under vacuum does not cause isomerization of [2-(COOH)-1,3-diMIM][NO<sub>3</sub>] (4a) to [4-(COOH)-1,3-diMIM][NO<sub>3</sub>] (5a).

**4-Carboxy-1,3-dimethylimidazolium nitrate (5a)**

To a solution of [1,3-diMIM-2-COO] (1) (0.01 mol) in 20 mL of a 50% aqueous ethanol (v/v), at 75 °C, was added dropwise 5.15 mL of 2 M HNO<sub>3</sub> (0.0103 mol). The reaction mixture was stirred at ~10 °C for 24 h and the solvent was removed under vacuum without heating. The product crystallized during slow solvent evaporation as white crystals. The product melts at the first decomposition step temperature (~200 °C). Onset for the 5% decomposition  $T_{5\%dec} = 197$  °C;  $\delta_H$  (360 MHz, D<sub>2</sub>O): 3.90 (s, 3H, N1-CH<sub>3</sub>), 4.04 (s, 3H, N3-CH<sub>3</sub>), 8.00 (d, 1H, C(5)H), 8.79 (s, 1H, C(2)H);  $\delta_H$  (360 MHz, DMSO-*d*<sub>6</sub>): 3.86 (s, 3H, N1-CH<sub>3</sub>), 3.98 (s, 3H, N3-CH<sub>3</sub>), 8.38 (d, 1H, C(5)H), 9.28 (s, 1H, C(2)H), 14.24 (broad, 1H, COOH);  $\delta_C$  (90 MHz, DMSO-*d*<sub>6</sub>): 30.66, 35.94, 124.66, 129.10, 140.52, 158.95. Additionally, NOE NMR confirmed the structure of this isomer.

**1,3-Dimethylimidazolium nitrate (3a)**

**Via thermal decarboxylation.** 3.00 mmol of either [2-(COOH)-1,3-diMIM][NO<sub>3</sub>] (4a) or [4-(COOH)-1,3-diMIM][NO<sub>3</sub>] (5a) was placed on a Petri dish and heated at 150 °C in an oven for 20 h. The same experiment was performed using small samples controlled in a TGA. The residual, viscous, semi-solid product was analyzed by NMR; confirming the structure as [1,3-diMIM][NO<sub>3</sub>] (3a).

**Via chemical decarboxylation.** 50 mg of [2-(COOH)-1,3-diMIM][NO<sub>3</sub>] (4a) was placed in an NMR tube, 0.8 mL of DMSO-*d*<sub>6</sub> was added at room temperature, and the decarboxylation reaction was followed by NMR. The pure product, [1,3-diMIM][NO<sub>3</sub>] (3a), was obtained after 72 h. The same reaction performed in DMF-*d*<sub>7</sub> or D<sub>2</sub>O did not progress to any significant level. Product was recovered as white solid, 98% yield, with melting point (DSC) 58 °C, and onset for the 5% decomposition  $T_{5\%dec} = 253$  °C;  $\delta_H$  (360 MHz, D<sub>2</sub>O): 3.84 (s, 6H, N-CH<sub>3</sub>), 7.36 (d, 2H, C(4/5)H), 8.59 (s, 1H, C(2)H);  $\delta_H$  (360 MHz, DMSO-*d*<sub>6</sub>): 3.84 (s, 6H, N-CH<sub>3</sub>), 7.68 (d, 2H, C(4/5)H), 9.05 (s, 1H, C(2)H);  $\delta_C$  (90 MHz, DMSO-*d*<sub>6</sub>): 35.58, 123.37, 136.97.

**Analyses**

**NMR analyses.** NMR spectra were obtained in DMSO-*d*<sub>6</sub> or D<sub>2</sub>O with TMS or residual hydrogen signals in the deuterated solvent used as the internal standard for <sup>1</sup>H (360 MHz) and for <sup>13</sup>C (90 MHz).

**Melting point analyses.** Melting points of the isolated salts were determined by differential scanning calorimetry (DSC)



using a TA Instruments model 2920 Modulated DSC (New Castle, DE) cooled with a liquid nitrogen cryostat. The calorimeter was calibrated for temperature and cell constants using indium (melting point 156.61 °C,  $H = 28.71 \text{ J g}^{-1}$ ). Data were collected at constant atmospheric pressure, using samples between 5–15 mg in aluminium sample pans (with the exception of the [1,3-diMIM][PF<sub>6</sub>]<sup>-</sup> salt, whose melting point was checked visually due to reported reactivity and catalyzed decomposition of the PF<sub>6</sub><sup>-</sup> anion-based materials while in contact with aluminium<sup>53</sup>). Experiments were performed heating at 5 °C min<sup>-1</sup>. The DSC was adjusted so that zero heat flow was between 0 and -0.5 mW, and the baseline drift was less than 0.1 mW over the temperature range 0–180 °C. An empty sample pan was used as reference.

**Thermal stability analyses.** Decomposition temperatures were measured in the dynamic heating regime using a TGA 2950 TA instrument under helium atmosphere. Samples between 2–10 mg were heated from 40–500 °C under constant heating at 5 °C min<sup>-1</sup>. For the thermal decarboxylation studies the samples were heated up to 150 °C with the heating rate set at 5 °C min<sup>-1</sup>. At that point, the instrument held the temperature at a constant level for an additional 20 h.

**X-Ray crystallographic studies.** Samples were recrystallized from ethanol–water, and single crystals were selected, mounted on fibers, and transferred to the goniometer. The crystals were cooled to -100 °C with a stream of nitrogen gas and data was collected on a Siemens SMART diffractometer with a CCD area detector, using graphite monochromated MoK $\alpha$  radiation. The SHELXTL software, version 5, was used for solution and refinement.<sup>61</sup> Absorption corrections were made with SADABS.<sup>62</sup> Each structure was refined by full-matrix least-squares on  $F^2$ .

**[2-(COOH)-1,3-diMIM][NO<sub>3</sub>]·H<sub>2</sub>O (4a·H<sub>2</sub>O).** C<sub>6</sub>H<sub>11</sub>N<sub>3</sub>O<sub>6</sub>,  $M = 221.18$ , triclinic,  $P\bar{1}$ ,  $a = 6.430(4)$ ,  $b = 6.715(4)$ ,  $c = 11.544(7) \text{ \AA}$ ,  $\alpha = 87.486(12)$ ,  $\beta = 80.110(12)$ ,  $\gamma = 80.82(1)^\circ$ ,  $V = 484.6(5) \text{ \AA}^3$ ,  $Z = 2$ ,  $T = 173(2) \text{ K}$ ,  $d_{\text{cal}} = 1.516 \text{ g cm}^{-3}$ , 1913 reflections collected, 1303 independent reflections ( $R_{\text{int}} = 0.0389$ ),  $R_1 = 0.0539$ ,  $wR_2 = 0.1394$  [ $I > 2\sigma(I)$ ].

**[4-(COOH)-1,3-diMIM][NO<sub>3</sub>] (5a).** C<sub>6</sub>H<sub>9</sub>N<sub>3</sub>O<sub>5</sub>,  $M = 203.16$ , monoclinic,  $P2_1/m$ ,  $a = 6.628(2)$ ,  $b = 11.910(4)$ ,  $c = 11.538(4) \text{ \AA}$ ,  $\beta = 104.508(7)^\circ$ ,  $V = 881.7(5) \text{ \AA}^3$ ,  $Z = 4$ ,  $T = 173(2) \text{ K}$ ,  $d_{\text{cal}} = 1.531 \text{ g cm}^{-3}$ , 3851 reflections collected, 1264 independent reflections ( $R_{\text{int}} = 0.0315$ ),  $R_1 = 0.0448$ ,  $wR_2 = 0.1004$  [ $I > 2\sigma(I)$ ].

CCDC reference numbers 605759 and 605760. For crystallographic data in CIF or other electronic format see DOI: 10.1039/b610421e.

**Powder X-ray crystallographic studies.** Bulk sample compositions were investigated using a Rigaku Powder Diffractometer (Woodlands, TX) at 25 °C with CuK $\alpha$  ( $\lambda = 1.5418 \text{ \AA}$ ) radiation in the  $2\theta$  range 5.00–30.00°. Spectra were taken at 0.01° steps at intervals of 0.2 s per step.

## Acknowledgements

This research was supported by the Air Force Office of Scientific Research (grant F49620-03-1-0357).

## References

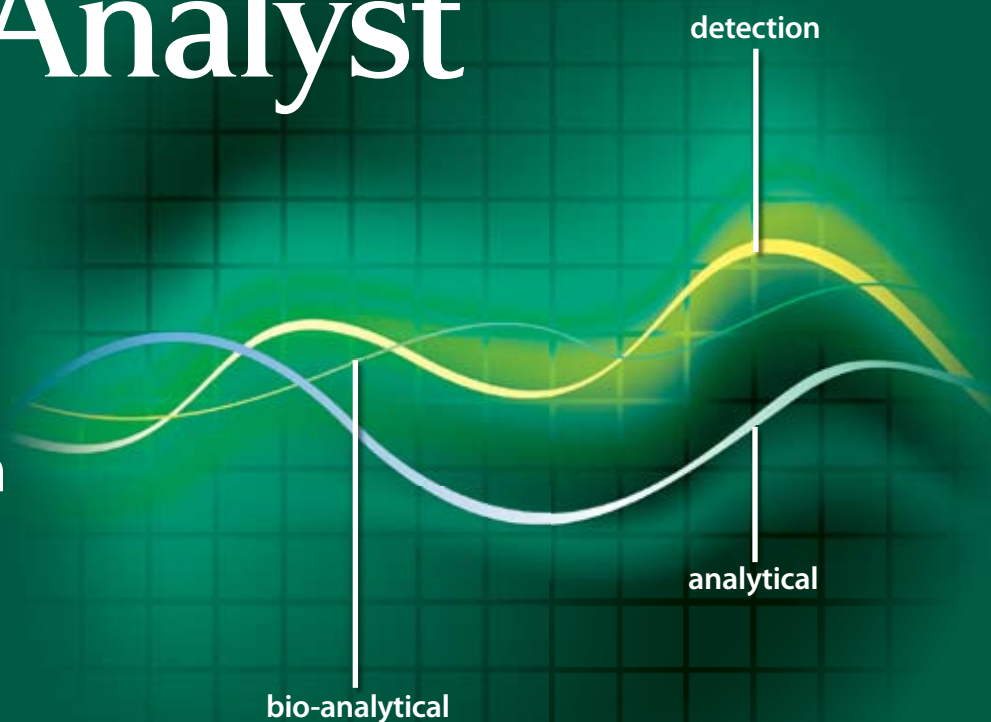
- P. Wasserscheid and W. Keim, *Angew. Chem., Int. Ed.*, 2000, **39**, 3773.
- T. Welton, *Chem. Rev.*, 1999, **99**, 2071.
- J. Dupont, R. F. de Souza and P. A. Z. Suarez, *Chem. Rev.*, 2002, **102**, 3667.
- S. Zein El Abedin, H. K. Farag, E. M. Moustafa, U. Welz-Biermann and F. Endres, *Phys. Chem. Chem. Phys.*, 2005, **7**, 2333.
- P. Wang, S. M. Zakeeruddin, I. Exnarb and M. Grätzel, *Chem. Commun.*, 2002, 2972.
- T. Sato, G. Masuda, M. Kotani and S. Iizuka, *PCT Int. Appl.*, 2004019356, 2004; *Chem. Abstr.*, 2004, **140**, 245004.
- A. E. Visser, R. P. Swatloski, W. M. Reichert, S. T. Griffin and R. D. Rogers, *Ind. Eng. Chem. Res.*, 2000, **39**, 3596.
- A. E. Visser, R. P. Swatloski, W. M. Reichert, R. Mayton, S. Sheff, A. Wierzbicki, J. H. Davis, Jr. and R. D. Rogers, *Chem. Commun.*, 2001, 135.
- S. Dai, Y. H. Ju and C. E. Barnes, *J. Chem. Soc., Dalton Trans.*, 1999, 1201.
- P. Wasserscheid, A. Boesmann, A. Jess, L. Datsevitch, C. Schmitz and A. Lauter, *PCT Int. Appl.*, 2003037835, 2003; *Chem. Abstr.*, 2003, **138**, 370660.
- C. Chiappe and D. Pieraccini, *ARKIVOC*, 2002, **11**, 249.
- L. Kiss, T. Kurtán, S. Antus and H. Brunner, *ARKIVOC*, 2003, **5**, 69.
- T. Welton, *Coord. Chem. Rev.*, 2004, **248**, 2459.
- J. Mo, L. Xu and J. Xiao, *J. Am. Chem. Soc.*, 2005, **127**, 751.
- J. Ding, V. Desikan, X. Han, T. L. Xiao, R. Ding, W. S. Jenks and D. W. Armstrong, *Org. Lett.*, 2005, **7**, 335.
- C. M. Gordon, *Appl. Catal., A*, 2001, **222**, 101.
- H. Olivier-Bourbigou and L. Magna, *J. Mol. Catal. A: Chem.*, 2002, **182–183**, 419.
- G. Drake, T. Hawkins, A. Brand, L. Hall, M. McKay, A. Vij and I. Ismail, *Propellants, Explos., Pyrotech.*, 2003, **28**, 174.
- A. R. Katritzky, S. Singh, K. Kirichenko, J. D. Holbrey, M. Smiglak, W. M. Reichert and R. D. Rogers, *Chem. Commun.*, 2005, 868.
- A. R. Katritzky, H. Yang, D. Zhang, K. Kirichenko, M. Smiglak, J. D. Holbrey, W. M. Reichert and R. D. Rogers, *New J. Chem.*, 2006, **30**, 349.
- H. Xue, B. Twamley and J. M. Shreeve, *J. Mater. Chem.*, 2005, **15**, 3459.
- C. Ye, J. Xiao, B. Twamley and J. M. Shreeve, *Chem. Commun.*, 2005, 2750.
- H. Xue, Y. Gao, B. Twamley and J. M. Shreeve, *Inorg. Chem.*, 2005, **44**, 5068.
- H. Xue and J. M. Shreeve, *Adv. Mater.*, 2005, **17**, 2142.
- Q. Lu, H. Wang, C. Ye, W. Liu and Q. Xue, *Tribol. Int.*, 2004, **37**, 547.
- Z. Mu, W. Liu, S. Zhang and F. Zhouy, *Chem. Lett.*, 2004, **33**, 524.
- C. Ye, W. Liu, Y. Chen and L. Yu, *Chem. Commun.*, 2001, 2244.
- M. T. Carter, C. L. Hussey, S. K. D. Strubinger and R. A. Osteryoung, *Inorg. Chem.*, 1991, **30**, 1149.
- J. D. Holbrey and K. R. Seddon, *Clean Prod. Process.*, 1999, **1**, 223.
- R. Sheldon, *Chem. Commun.*, 2001, 2399.
- K. N. Marsh, J. A. Boxall and R. Lichtenthaler, *Fluid Phase Equilib.*, 2004, **219**, 93.
- S. A. Forsyth, J. M. Pringle and D. R. MacFarlane, *Aust. J. Chem.*, 2004, **57**, 113.
- J. D. Holbrey, W. M. Reichert, R. P. Swatloski, G. A. Broker, W. R. Pitner, K. R. Seddon and R. D. Rogers, *Green Chem.*, 2002, **4**, 407.
- P. Wasserscheid, R. van Hal, A. Bosmann, J. Esser and A. Jess, New ionic liquids based on alkylsulfate and alkyl oligoether sulfate anions: synthesis and applications, in *Ionic Liquids as Green Solvents*, ed. R. D. Rogers and K. R. Seddon, American Chemical Society Symposium Series 856, Washington, DC, USA, 2003, p. 57.

- 35 P. Tundo and M. Selva, *Acc. Chem. Res.*, 2002, **35**, 706.
- 36 U. Romano, F. Rivetti and N. Di Muzio, *U.S. Pat.*, 4318862, 1979; U. Romano, F. Rivetti and N. Di Muzio, *Chem. Abstr.*, 1981, **95**, 80141w.
- 37 F. Rivetti, U. Romano and D. Delle Donne, Dimethylcarbonate and its production technology, in *Green Chemistry: Designing Chemistry for the Environment*, ed. P. Anastas and T. C. Williamson, American Chemical Society Symposium Series 626, Washington, DC, USA, 1996, p. 70.
- 38 K. Nishira, K. Mizutane and S. Tanaka, UBE Industries, Japan, *U.S. Pat.*, 5162563, 1992.
- 39 F. Rivetti, Dimethylcarbonate: an answer to the need for safe chemicals, in *Green Chemistry: Challenging Perspectives*, ed. P. Tundo and P. Anastas, Oxford University Press, Oxford, UK, 2000, p. 201.
- 40 *Registry of Toxic Effects of Chemical Substances*, ed. D. V. Sweet, U.S. GPO, Washington, DC, USA, 1986, **vol. 2**, p. 186.
- 41 P. Tundo, L. Rossi and A. Loris, *J. Org. Chem.*, 2005, **70**, 2219.
- 42 F. Trotta, P. Tundo and G. Moraglio, *J. Org. Chem.*, 1987, **52**, 1300.
- 43 J. D. Holbrey, W. M. Reichert, I. Tkatchenko, E. Bouajila, O. Walter, I. Tommasi and R. D. Rogers, *Chem. Commun.*, 2003, 28.
- 44 M. Aresta, I. Tkatchenko and I. Tommasi, Unexpected synthesis of 1,3-dialkylimidazolium-2-carboxylate, in *Ionic Liquids as Green Solvents*, R. D. Rogers and K. R. Seddon, American Chemical Society Symposium Series 856, Washington, DC, USA, 2002, 93.
- 45 S. Mori, K. Ida and M. Ue, Mitsubishi Chemical Co, Ltd, *U.S. Pat.*, 4892944, 1990.
- 46 M. Ue, M. Takeda, T. Takahashi and M. Takehara, *U.S. Pat.*, 5856513, 1997.
- 47 J. Fisher, W. Siegel, V. Bomm, M. Fisher and K. Munding, *U.S. Pat.*, 6175019, 1999.
- 48 J. Louie, J. E. Gibby, M. V. Farnworth and T. N. Tekavec, *J. Am. Chem. Soc.*, 2002, **124**, 15188.
- 49 T. N. Tekavec, A. M. Arif and J. Louie, *Tetrahedron*, 2004, **60**, 7431.
- 50 I. Tommasi and F. Sorrentino, *Tetrahedron Lett.*, 2005, **46**, 2141.
- 51 J. S. Wilkes, J. A. Levisky, R. A. Wilson and C. L. Hussey, *Inorg. Chem.*, 1982, **21**, 1263.
- 52 D. W. Karkhanis and L. Field, *Phosphorus Sulfur*, 1985, **22**, 49.
- 53 H. L. Ngo, K. LeCompte, L. Hargens and A. B. McEwen, *Thermochim. Acta*, 2000, **357–358**, 97.
- 54 A. P. Krapcho, G. A. Glynn and B. J. Grenon, *Tetrahedron Lett.*, 1967, **8**, 215.
- 55 A. P. Krapcho, J. F. Weimaster, J. M. Eldridge, E. G. E. Jahngen, A. J. Lovey and W. P. Stephens, *J. Org. Chem.*, 1978, **43**, 138.
- 56 A. M. Bernard, G. Cerioni and P. P. Piras, *Tetrahedron*, 1990, **46**, 3929.
- 57 P. J. Gilligan and P. J. Krenitsky, *Tetrahedron Lett.*, 1994, **35**, 3441.
- 58 A. P. Krapcho, *Synthesis*, 1982, **10**, 805.
- 59 A. P. Krapcho, *Synthesis*, 1982, **11**, 893.
- 60 M. W. Schmidt, K. K. Balsrige, J. A. Boatz, S. T. Elbert, M. S. Gordon, J. H. Jensen, S. Koseki, M. Matsunaga, K. A. Nguyen, S. J. Su, T. L. Windus, M. Dupuis and J. A. Montgomery, *J. Comput. Chem.*, 1993, **14**, 1347.
- 61 G. M. Sheldrick, *SHELXTL, version 5.05*, Siemens Analytical X-Ray Instruments Inc., Madison, WI, USA, 1996.
- 62 G. M. Sheldrick, *Program for Semiempirical Absorption Correction of Area Detector Data*, University of Göttingen, Germany, 1996.

Downloaded on 10 November 2010  
Published on 05 December 2006 on http://pubs.rsc.org | doi:10.1039/B610421E

# The Analyst

Not just an  
analytical  
chemistry  
journal



## Call for Communications

**For fast publication of your communications look no further than *The Analyst*... the leading analytical science journal for communications.**

**'I am extremely pleased with the effective, professional and rapid handling of our Communication. This is exactly why I picked *The Analyst* for submission!**

Professor Joseph Wang,  
Arizona State University, USA

*The Analyst* communications report on preliminary research findings that are highly original in nature, of immediate interest and are likely to have a high impact in their field. The key aim is to present research on innovative chemical concepts with important analytical implications.

Benefits of publishing a Communication in *The Analyst* include:

- High impact
- Short times to publication (typically 50 days from receipt)
- High profile (within the journal and widely promoted)

**Submit your work today!**

RSC Publishing

[www.rsc.org/analyst/communications](http://www.rsc.org/analyst/communications)

Registered Charity Number 207890

# RSC eBook Collection

Access and download existing and new books from the RSC

- **Comprehensive:** covering all areas of the chemical sciences
- **Fully searchable:** advance search and filter options
- **Wide ranging:** from research level monograph to popular science book

See for yourself –  
go online to search  
the collection and  
read selected  
chapters  
for free!



Registered Charity Number 207890

20100654

RSCPublishing

[www.rsc.org/ebooks](http://www.rsc.org/ebooks)